

**UNIVERSIDAD AUTÓNOMA DE NUEVO LEÓN**

**FACULTAD DE CIENCIAS QUÍMICAS**



**Isolation, structural characterization and assessment of the  
antibacterial activity of constituents of *Solanum chrysotrichum*  
Schldl., determination of enhancement of antibacterial activity of  
sapogenins by derivatization of diosgenin**

**By**

**MSc GUILLERMO NÚÑEZ MOJICA**

**As a partial requirement to obtain the degree of Doctor in Science  
with Orientation in Pharmacy**

**November 2020**

**Dedicated to**

**My parents  
Guillermo Núñez Fonseca  
Olga Mojica Rodríguez**

## ACKNOWLEDGEMENTS

**Dra. María Del Rayo Camacho Corona**  
**Facultad de Ciencias Químicas, UANL**

For implementation of logistic, resource management and academic and moral support regarding the phytochemical part of the project.

**Dra. Elvira Garza González**  
**Servicio de Gastroenterología,**  
**Hospital Universitario Dr. José Eleuterio González.**

For implementation of logistic, resource management and academic and moral support regarding the *in vitro* antibacterial activity assays

**Prof. Pascal Marchand**  
**Université de Nantes, Cibles et Médicaments des Infections et du Cancer**  
For implementation of logistic, resource management and academic and moral support regarding the synthesis of aminoether derivatives

**Marc-Antoine Bazin**  
**Université de Nantes, Cibles et Médicaments des Infections et du Cancer**  
For the support regarding the synthesis of aminoether derivatives

**Tutorial committe**  
**Dra. Susana Thelma López Cortina**  
**Dra. María del Rosario González González**  
**Dr. Omar González Santiago**  
**Facultad de Ciencias Químicas, UANL**  
For their contributions in the logistics, organization and correction of the thesis project through tutorial meetings and departmental seminars.

**Dra. Verónica Mayela Rivas Galindo**  
**Departamento de Química Analítica, Facultad de Medicina, UANL.**  
For performing the NMR spectroscopy which was used for the present project

**Biologist, MC Mauricio González Ferrara**  
**Pacalli, la casa de las hierbas**  
For providing the plant *Solanum chrysotrichum* Schldl

**Dra. Laura P. Álvarez Berber**  
**Universidad Autónoma del Estado de Morelos, Centro de Investigaciones Químicas**

For performing the GC/MS analysis of the organic extracts and the contributions in the logistics, organization and correction of the thesis project through tutorial meetings.

**Prof. Olivier Grovel**  
**Université de Nantes, Corsaire ThalassOMICS Metabolomics**  
For performing the HRMSESI spectrometry of all the saponins and acetylated derivatives.

**Marie-Renée Nourrisson**  
**Université de Nantes, Cibles et Médicaments des Infections et du Cancer**  
For the technical support regarding the synthesis of aminoether derivatives

**Thiefaine Jérôme**  
**Université de Nantes, Cibles et Médicaments des Infections et du Cancer**  
For the technical support regarding the synthesis of aminoether derivatives



**Universidad Autónoma de Nuevo León**  
**Facultad de Ciencias Químicas**  
**and**  
**Laboratorio de Química Farmacéutica**

For providing laboratory facilities, services and infrastructure for the development of the doctoral thesis project (FARDC-93765-MRCC-18/01)



UNIVERSITÉ DE NANTES  
UFR DE SCIENCES PHARMACEUTIQUES  
ET BIOLOGIQUES

**Université de Nantes**  
**Cibles et Médicaments des Infections et du Cancer**

For providing laboratory facilities, services and infrastructure for the development of the doctoral thesis project



**Universidad Autónoma de Nuevo León**

For providing scholarship for travel expenses for the doctoral thesis project



For providing the scholarship 700603 to the doctoral candidate  
MC Guillermo Núñez Mojica

**Isolation, structural characterization and assessment of the antibacterial activity of constituents of *Solanum chrysotrichum* Schldl., determination of enhancement of antibacterial activity of sapogenins by derivatization of diosgenin**

**Thesis approval:**



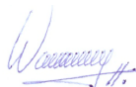
---

**Dra. María del Rayo Camacho corona  
President**



---

**Dra. María del Rosario González González  
Secretary**



---

**Dra. Susana T. López Cortina  
First vocal**



---

**Dr. Omar González Santiago  
Second Vocal**



---

**Dra. Laura Patricia Álvarez Berber  
Third Vocal**

---

**Dra. María Elena Cantú Cárdenas  
Postgraduate School Subdirector**

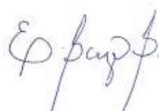
**Isolation, structural characterization and assessment of the antibacterial activity of constituents of *Solanum chrysotrichum* Schldl., determination of enhancement of antibacterial activity of sapogenins by derivatization of diosgenin**

**Thesis review and approval:**



---

**Dra. María del Rayo Camacho corona**  
**Thesis director**



---

**Dra. Elvira Garza González**  
**Thesis Co-director**



---

**Prof. Pascal Marchand**  
**External Thesis Co-director**



---

**Dra. Susana T. López Cortina**  
**Tutorial committee member**




---

**Dra. María del Rosario González González**  
**Tutorial committee member**



---

**Dr. Omar González Santiago**  
**Tutorial committee member**



---

**Dra. Laura Patricia Álvarez Berber**  
**External tutorial committee member**

## RESUMEN

MC Guillermo Núñez Mojica  
Universidad Autónoma de Nuevo León  
Facultad de Ciencias Químicas

Fecha de graduación:  
26/04/2021

Université de Nantes  
UFR des Sciences Pharmaceutiques et Biologiques

**Título del proyecto: Isolation, structural characterization and assessment of the antibacterial activity of constituents of *Solanum chrysotrichum* Schldl., determination of enhancement of antibacterial activity of sapogenins by derivatization of diosgenin**

**Número de páginas: 185**

**Candidato a obtener el grado de  
Doctor en Ciencias con Orientación  
en Farmacia**

**Área de estudio: Farmacia**

### **Propósito y Método de estudio:**

El desarrollo y administración de antibióticos es un punto culminante en la medicina moderna, sin embargo, la farmacorresistencia de los microorganismos patógenos amenaza con reducir los avances logrados hasta la fecha a una solución temporal, dada la tendencia observada de que a mayor variedad de antibióticos que utilizamos, mayor el número de microorganismos que se vuelven resistentes a ellos. Como consecuencia, los tratamientos antimicrobianos se vuelven más complicados, menos efectivos y más costosos, por lo que en algunos casos es posible que no se disponga de un tratamiento eficaz. La farmacorresistencia tiene importantes repercusiones económicas para la industria farmacéutica, y la falta de antibióticos en la fase de aprobación aumenta la relevancia de la farmacorresistencia como un tema prioritario para la salud mundial. Para controlar la crisis de resistencia a los medicamentos, la Organización Mundial de la Salud (OMS) promovió la investigación para el descubrimiento de nuevos medicamentos mediante la introducción de su Sistema Global de Vigilancia de la Resistencia a los Antimicrobianos (GLASS por sus siglas en inglés) en 2015, a través del cual se fomenta la investigación para el descubrimiento de nuevos fármacos contra las bacterias farmacorresistentes de mayor importancia clínica documentadas en la lista global de bacterias farmacorresistentes (*Acinetobacter* spp., *Pseudomonas aeruginosa*, *Escherichia coli*, *Klebsiella pneumoniae*, *Enterobacter* spp, *Serratia* spp, *Providencia* spp. *Morganella* spp, *Neisseria gonorrhoeae*, *Salmonella* spp.,



*Shigella* spp, *Enterococcus faesium*, *Staphylococcus aureus*, *Helycobacter pilory*, *Campylobacter* spp, *Streptococcus pneumoniae* and *Haemophylus influenzae*).

El descubrimiento de nuevos compuestos para tratar las infecciones por bacterias farmacorresistentes antes mencionadas es imperativo para evitar el creciente problema, por lo que la exploración de nuevas fuentes de antibióticos debe ser una tarea prioritaria para la investigación.

Como agravante del problema, la bacteria *Mycobacterium tuberculosis* continúa desarrollando resistencia a los principales fármacos antituberculosos de primera y segunda línea, este hecho es importante debido a que la tuberculosis es la novena causa de muerte a nivel mundial, según los datos más recientes de la Organización Mundial de la Salud. Los datos epidemiológicos sobre la tuberculosis son alarmantes, con 10 millones de personas infectadas a nivel mundial siendo 558,000 casos resistentes a rifampicina (TB-RR), de los cuales el 82% de los casos TB-RR presentaron multiresistencia (TB-MDR), siendo el 8.5% extremadamente resistentes a los medicamentos (XDR-TB). Adicionalmente, se documentaron 1.3 millones de muertes por tuberculosis entre pacientes con VIH- y 0.3 millones entre pacientes VIH+ en todo el mundo. Los datos anteriores proporcionan una fuerte evidencia de que la resistencia a los medicamentos debe considerarse el mayor desafío a enfrentar por las instituciones de salud, por lo que, si no se encuentran nuevos medicamentos antibacterianos efectivos, existe un alto riesgo de un impacto negativo severo en la calidad de vida de la población mundial.

Para colaborar en la búsqueda de una solución contra las infecciones bacterianas farmacorresistentes, en el presente trabajo se descubrieron nuevos agentes antibacterianos mediante la realización de un estudio fitoquímico utilizando la planta *Solanum chrysotrichum* Schldl, que es un espécimen vegetal muy utilizado en la medicina tradicional mexicana. El enfoque de esta investigación se basa en el hecho de que las plantas son el principal recurso en la medicina tradicional, y según la OMS, el 80% de las personas a nivel mundial utilizan plantas para el tratamiento de enfermedades, siendo actualmente utilizadas como medicamentos 119 entidades químicas derivadas de 90 especies de las plantas, y de estas, el 74% se descubrieron como resultado del aislamiento de principios activos de plantas utilizadas en la medicina tradicional. Actualmente, entre el 25 y el 28% de todas las drogas son productos naturales o derivados semisintéticos obtenidos de plantas superiores, lo que es un indicio del enorme potencial de las plantas medicinales. Sobre esta base, la exploración fitoquímica y farmacológica de plantas medicinales con antecedentes etnomédicos puede ser un área prometedora y potencialmente fructífera en la búsqueda de nuevas moléculas activas. Con base en el argumento anterior, es justificable y racional recurrir a las plantas medicinales en la búsqueda de soluciones contra las infecciones bacterianas resistentes a los medicamentos.

### **Conclusiones y Contribuciones:**

A partir de las partes aéreas de *Solanum chrysotrichum* Schldl se prepararon el extracto hexánico, diclorometanoico, metanólico y acuoso. Se realizó análisis por GC/MS de los extractos hexánico y diclorometanoico, el extracto hexánico estuvo compuesto principalmente por los alcanos tritriacontano (44.505%) y dotriacontano (32.811%). El extracto diclorometanoico estuvo compuesto principalmente por los alcanos tritriacontano (38.177%), hexatriacontano (27.195%) y el alcohol

diterpénico fitol (20.992%). El extracto metanólico se sometió a cromatografía en columna de gel de sílice de la cual fueron obtenidas nueve fracciones (A-I). A partir de la fracción B se obtuvo ácido salicílico (SC10) y el esteroil glicosilado campesterol- $\beta$ -D-glucopiranosido (SC7B). De las fracciones C y D se obtuvo una mezcla de tres saponinas esteroidales (SC5), dicha mezcla fue acetilada y sometida a cromatografía en columna para obtener las nuevas saponinas acetiladas 2'',3'',5''-triacetoxi-6- $\alpha$ -O- $\alpha$ -L-ramnopiranosil-(1 $\rightarrow$ 3)-2',4'-diacetoxi- $\beta$ -D-quinovopiranosil-(25S)-5 $\alpha$ -espirostan-3 $\beta$ -acetato (SC5AcA) y 2'',3'',5''-triacetoxi-6- $\alpha$ -O- $\alpha$ -L-ramnopiranosil-(1 $\rightarrow$ 3)-2',4'-diacetoxi- $\beta$ -D-quinovopiranosil-(23R,25S)-5 $\alpha$ -espirostan-3 $\beta$ ,23 $\beta$ -acetato (SC5AcB) y la saponina previamente reportada 2'',3'',5''-triacetoxi-6- $\alpha$ -O- $\beta$ -D-xilopyranosil-(1 $\rightarrow$ 3)-2',4'-diacetoxi- $\beta$ -D-quinovopiranosil-(23R,25S)-5 $\alpha$ -espirostan-3 $\beta$ ,23 $\beta$ -acetato (SC5AcC). Cada saponina acetilada fue sometida a saponificación usando KOH etanólico, obteniéndose como resultado las dos nuevas saponinas 6- $\alpha$ -O- $\alpha$ -L-ramnopiranosil-(1 $\rightarrow$ 3)- $\beta$ -D-quinovopiranosil-(25S)-5 $\alpha$ -espirostan-3 $\beta$ -ol (SC5A) y 6- $\alpha$ -O- $\alpha$ -L-ramnopiranosil-(1 $\rightarrow$ 3)- $\beta$ -D-quinovopiranosil-(23R,25S)-5 $\alpha$ -espirostan-3 $\beta$ ,23 $\beta$ -ol (SC5B) y la saponina conocida 6- $\alpha$ -O- $\beta$ -D-xilopiranosil-(1 $\rightarrow$ 3)- $\beta$ -D-quinovopiranosil-(23R,25S)-5 $\alpha$ -espirostan-3 $\beta$ ,23 $\beta$ -ol (SC5C) previamente aislada de *Solanum hispidum*. De la fracción D se obtuvo el flavonol glicosilado 3'-O-metilquercetina-3-O- $\beta$ -D-glucopiranosido (SC11). Todos los compuestos aislados del extracto metanólico se caracterizaron estructuralmente mediante análisis de datos espectroscópicos (RMN 1D y 2D) y espectrométricos (HRMSESI). Se intentó la hidrólisis ácida de la saponina SC5B con el fin de obtener su correspondiente aglicona para luego derivatizarla y sintetizar derivados aminoéter, pero no fue posible obtener el producto de hidrólisis. Como alternativa, se obtuvo diosgenina de fuentes comerciales con el fin de ser utilizada como material de partida para la preparación de los derivados. Se prepararon nueve derivados aminoéter de diosgenina (DIO-01 a DIO-09) y se caracterizaron mediante análisis de datos espectroscópicos. Se evaluó la actividad antibacteriana de extractos, compuestos, derivados acetilados y derivados del aminoéter de diosgenina frente a bacterias gram negativas. (Resistente a Carbapenem (RC) *Acinetobacter baumannii* (12-666), Betalactamasa positiva de espectro extendido (BLEE) *Escherichia coli* (14-2081), (RC) *Pseudomonas aeruginosa* (13-1391), Carbapenem y cefalosporinas de resistencia extendida (CCR) *Klebsiella pneumoniae* NDM-1 positiva (14-3335), (BLEE) *Klebsiella pneumoniae* (14-2081), bacterias gram positivas (Resistente a meticilina (RM) *Staphylococcus aureus* (MRSA, 14-2095), Resistente a Linezolid (RL) *Staphylococcus epidermidis* (14-583) y Resistente a Vancomicina (RV) *Enterococcus faecium* (10-984)), y dos cepas de *Mycobacterium tuberculosis*, la cepa sensible H37Rv y la cepa multifarmacorresistente G122. Los extractos orgánicos (hexánico, diclorometanólico y metanólico) mostraron actividad antibacteriana contra (RC) *Acinetobacter baumannii* (CMI: 125  $\mu$ g/mL) y (RC) *Pseudomonas aeruginosa* (CMI: 250  $\mu$ g/mL). La saponina esteroil SC5C fue el único compuesto aislado del extracto metanólico que mostró actividad antibacteriana, siendo activo contra las tres bacterias gram positivas ensayadas, con un valor de CMI de 12.5  $\mu$ g/mL, siendo tan activa como el levofloxacin contra (RL) *S. epidermidis*. Los derivados aminoéter de diosgenina DIO-02 y DIO-09 fueron los únicos derivados que mostraron actividad

antibacteriana, siendo DIO-02 activo solo contra (RM) *S. aureus* (CMI 50 µg/mL) y DIO-09 contra las tres cepas gram positivas ensayadas (CMI 12.5-25 µg/ml) siendo dos veces menos activo que el levofloxacino. La actividad antimycobacteriana fue observada solo en el extracto de hexanico contra ambas cepas de *M. tuberculosis*, con un valor de CMI de 250 µg/ml. Este proyecto representa el primer reporte de buena actividad antibacteriana de extractos orgánicos de *S. chysotrichum*, el primer reporte de actividad antimycobacteriana para del extracto hexánico de *S. chysotrichum*, el primer reporte de actividad antibacteriana de la saponina SC5C, y el primer reporte de nueve nuevos derivados aminoéter de diosgenina, mostrando actividad antibacterial los compuestos DIO-02 y DIO-09.

## ABSTRACT

MSc Guillermo Núñez Mojica

Grade evaluation date:

Universidad Autónoma de Nuevo León  
Facultad de Ciencias Química

26/04/2021

Université de Nantes  
UFR des Sciences Pharmaceutiques et Biologiques

**Project title: Isolation, structural characterization and assessment of the antibacterial activity of constituents of *Solanum chrysotrichum* Schldl., determination of enhancement of antibacterial activity of sapogenins by derivatization of diosgenin**

Number of pages: 185

Candidate for the grade of Doctor in  
Science with orientation in Pharmacy

**Study discipline: Pharmacy**

### **Purpose and method of study:**

The development and ministration of antibiotics is a high-point in modern medicine, however, drug-resistance of pathogenic microorganisms threaten to reduce advances achieved to date to a temporary solution, given the observed trend that the greater the variety of antibiotics we use, the greater the number of microorganisms that become resistant to them. As a consequence, antimicrobial treatments become more complicated, less effective and costlier and in some extreme cases of drug-resistant infections, no effective treatment may be available. Drug-resistance has major economic impact implications for the pharmaceutical industry, and the lack of antibiotics currently in the approval phase increase the relevance of drug-resistance as a priority issue for the world heath. In order to control the drug-resistance crisis, the World Health Organization (WHO) encourage the drug-discovery research by introducing its Global Antimicrobial Resistance Surveillance System (GLASS) in 2015, through which are targeted for research the most clinically important drug-resistant bacteria of the Global Priority List of Antibiotic-resistant Bacteria (*Acinetobacter* spp., *Pseudomonas aeruogiosa*, *Escherichia coli*, *Klebsiella pneumoniae*, *Enterobacter* spp, *Serratia* spp, *Prividencia* spp, *Morganella* spp, *Neisseria gonorrhoeae*, *Salmonella* spp., *Shigella* spp, *Enterococcus faesium*, *Staphylococcus aureus*, *Helycobacter pilory*, *Campylobacter* spp, *Streptococcus pneumoniae* and *Haemophylus influenzae*). The discovery of novel compounds to treat the aforementioned drug-resistant bacteria is imperative to avoid the ever-growing problem of bacterial infections, so the exploration of new sources of antibiotics must be a priority task for research.

As an additional crisis, the bacteria *Mycobacterium tuberculosis* continues to develop resistance to the main first and second-line anti-tubercular drugs, this fact is important due to tuberculosis being the ninth cause of death globally. The World Health Organization most recent epidemiological data about tuberculosis is alarming, with 10 million people infected on a global level being 558,000 cases resistant to rifampicin (RR-TB), from which the 82% of RR-TB cases presented multidrug-resistance (MDR-TB) and the 8.5 % were extremely drug-resistant (XDR-TB). There were 1.3 million deaths among HIV- patients and 0.3 million deaths among HIV+ positive patients from tuberculosis globally. The above data provide strong evidence that drug resistance should be considered the biggest challenge the health institutions has to face, so then, if new effective antibacterial drugs are not found, there is a high risk of a severe negative impact on quality of life for the world population.

To collaborate to find a solution against the drug resistance bacterial infections, new antibacterial agents were discovered in the present work, by conducting a phytochemical study using the plant *Solanum chrysotrichum* Schldl, a vegetal specimen widely used in Mexican traditional medicine. The approach for this research is based on the fact that plants are the main resource in traditional medicine. According to the WHO, 80% of people globally use plants for treatment of diseases, being currently used as drugs 119 chemical entities derived from 90 species of plants, and of these 74% were discovered as a result of the isolation of active principles of plants used in traditional medicine. Currently 25-28% of all drugs are natural products or semi-synthetic derivatives obtained from higher plants, which is a sign of medicinal plants vast potential. On this basis, phytochemical and pharmacological exploration of medicinal plants with ethnomedical backgrounds can be seen as a promising and potentially fruitful area in the search for new active molecules. Therefore, it is justifiable and rational to look to medicinal plants in the search for solutions against drug-resistant bacterial infections.

### **Conclusions and Contributions:**

From grounded and dried aerial parts of *Solanum chrysotrichum* Schldl were prepared the hexane extract, dichloromethane extract, methanol extract and aqueous extract. Analysis by GC/MS was conducted for the hexane and dichloromethane extracts, being the hexane extract composed mainly of the alkanes tritriacontane (44.505 %) and dotriacontane (32.811 %), the dichloromethane extract was composed mainly of the alkanes tritriacontane (38.177 %), hexatriacontane (27.195 %), and the diterpenic alcohol phytol (20.992 %). The methanol extract was subjected to silica gel column chromatography yielding nine fractions (A-I). From B fraction was obtained salicylic acid (SC10) and the glycosylated sterol campesterol- $\beta$ -D-glucopyranoside (SC7B). From C and D fractions were obtained a mixture of three steroidal saponins (SC5) which were subjected to acetylation, subsequently column chromatography was performed to obtain the new acetylated saponins 2'',3'',5''-triacetoxo-6- $\alpha$ -O- $\alpha$ -L-rhamnopyranosyl-(1 $\rightarrow$ 3)-2',4'-diacetoxo- $\beta$ -D-quinovopyranosyl-(25S)-5 $\alpha$ -spirostan-3 $\beta$ -acetate (SC5AcA) and 2'',3'',5''-triacetoxo-6- $\alpha$ -O- $\alpha$ -L-rhamnopyranosyl-(1 $\rightarrow$ 3)-2',4'-diacetoxo- $\beta$ -D-

quinovopyranosyl-(23R,25S)-5 $\alpha$ -spirostan-3 $\beta$ ,23 $\beta$ -acetate (SC5AcB) and the known 2'',3'',5''-triacetoxyl-6- $\alpha$ -O- $\beta$ -D-xylopyranosyl-(1 $\rightarrow$ 3)-2',4'-diacetoxyl- $\beta$ -D-quinovopyranosyl-(23R,25S)-5 $\alpha$ -spirostan-3 $\beta$ ,23 $\beta$ -acetate (SC5AcC). Each acetylated saponin was subjected to saponification using ethanolic KOH obtaining as result the two new steroidal saponins 6- $\alpha$ -O- $\alpha$ -L-rhamnopyranosyl-(1 $\rightarrow$ 3)- $\beta$ -D-quinovopyranosyl-(25S)-5 $\alpha$ -spirostan-3 $\beta$ -ol (SC5A) and 6- $\alpha$ -O- $\alpha$ -L-rhamnopyranosyl-(1 $\rightarrow$ 3)- $\beta$ -D-quinovopyranosyl-(23R,25S)-5 $\alpha$ -spirostan-3 $\beta$ ,23 $\beta$ -ol (SC5B) and the known 6- $\alpha$ -O- $\beta$ -D-xylopyranosyl-(1 $\rightarrow$ 3)- $\beta$ -D-quinovopyranosyl-(23R,25S)-5 $\alpha$ -spirostan-3 $\beta$ ,23 $\beta$ -ol (SC5C) previously isolated from *Solanum hispidum*. From fraction D was obtained the glycosidated flavonol 3'-O-methylquercetin-3-O- $\beta$ -D-glucopyranoside (SC11). All the isolated compounds from the methanol extract were structurally characterized by analysis of spectroscopic (1D and 2D NMR) and spectrometric (HRMSESI) data. Acid hydrolysis of the saponin SC5B was attempted in order to obtain its corresponding aglycone to be further derivatized to synthesize aminoether derivatives, but it was not possible to obtain the hydrolysis product, so as an alternative, diosgenin was obtained from commercial sources in order to be used as starting material for the preparation of the derivatives. Nine diosgenin aminoether derivatives were prepared (DIO-01 to DIO-09) and characterized by analysis of spectroscopic data. The antibacterial activity of extracts, compounds, acetylated derivatives and diosgenin aminoether derivatives was assessed against gram-negative bacteria (carbapenem-resistant (CR) *Acinetobacter baumannii* (12-666), extended spectrum  $\beta$ -lactamase-positive (ESBL) *Escherichia coli* (14-2081), (CR) *Pseudomonas aeruginosa* (13-1391), carbapenem and broad spectrum cephalosporins-resistant (CCR) *Klebsiella pneumoniae* NDM-1 positive (14-3335), ESBL *Klebsiella pneumoniae* (14-2081)), gram-positive bacteria (methicillin-resistant (MR) *Staphylococcus aureus* (MRSA, 14-2095), linezolid-resistant (LR) *Staphylococcus epidermidis* (14-583) and vancomycin-resistant (VR) *Enterococcus faecium* (10-984)), and two strains of *Mycobacterium tuberculosis*, the sensitive strains H37Rv and the multidrug-resistant strain G122. The organic extracts (hexane, dichlorometane and methanol) showed antibacterial activity against (CR) *Acinetobacter baumannii* (MIC: 125  $\mu$ g/mL) and (CR) *Pseudomonas aeruginosa* (MIC: 250  $\mu$ g/mL). The known steroidal saponin SC5C was the only compound isolated from the methanol extract that showed antibacterial activity, being active against the three gram-positive bacteria tested with a MIC value of 12.5  $\mu$ g/mL, being as active as levofloxacin against (LR) *S. epidermidis*. The diosgenin aminoether derivatives DIO-02 and DIO-09 were the only derivatives that showed antibacterial activity, being DIO-02 active only against (MR) *S. aureus* (MIC 50  $\mu$ g/mL), and DIO-09 against the three gram-positive bacteria tested (MIC 12.5-25  $\mu$ g/mL) being two-fold less active than levofloxacin. Antimycobacterial activity was displayed only by the hexane extract against both *M. tuberculosis* strains with a MIC value of 250  $\mu$ g/mL. This project represents the first report of good antibacterial activity for organic extracts of *S. chrysotrichum*, the first report of antimycobacterial activity for the hexane extract of *S. chrysotrichum*, the first report of antibacterial activity for the known saponin SC5C, and the first report of nine new diosgenin aminoether derivatives, possessing the compounds DIO-02 and DIO-09 antibacterial activity.

# RÉSUMÉ

MSc Guillermo Núñez Mojica

Date de l'examen:

Universidad Autónoma de Nuevo León  
Facultad de Ciencias Químicas

26/04/2021

Université de Nantes  
UFR des Sciences Pharmaceutiques et Biologiques

**Titre du projet: Isolation, structural characterization and assessment of the antibacterial activity of constituents of *Solanum chrysotrichum* Schldl., determination of enhancement of antibacterial activity of sapogenins by derivatization of diosgenin**

Nombre de pages: 185

Candidat au grade de Docteur en  
Science avec Orientation en Pharmacie

**Discipline d'étude : Pharmacie**

## **Objectif et méthode d'étude :**

Le développement et l'administration d'antibiotiques constituent une approche majeure de la médecine moderne. Cependant, la résistance aux médicaments des micro-organismes pathogènes menace de réduire les progrès réalisés à ce jour à une solution temporaire. Par ailleurs, la tendance observée est la suivante : plus la variété d'antibiotiques que nous utilisons est grande, plus le nombre de micro-organismes résistants augmente. En conséquence, les traitements antimicrobiens deviennent plus compliqués, moins efficaces et plus coûteux et, dans certains cas extrêmes d'infections résistantes aux médicaments, aucun traitement efficace ne peut être disponible. La résistance aux médicaments a des implications économiques majeures pour l'industrie pharmaceutique, et le manque d'antibiotiques actuellement en phase d'approbation augmente la pertinence de la résistance aux médicaments en tant que problème prioritaire pour la santé mondiale. Afin de contrôler la crise de la résistance aux médicaments, l'Organisation Mondiale de la Santé (OMS) encourage la recherche sur la découverte de médicaments en introduisant son « système mondial de surveillance de la résistance aux antimicrobiens » (GLASS pour son acronyme en anglais) en 2015, à travers lequel sont ciblés pour la recherche les pharmacorésistants les plus cliniquement importants. Les bactéries de la liste prioritaire mondiale des bactéries résistantes aux antibiotiques sont *Acinetobacter* spp., *Pseudomonas aeruginosa*, *Escherichia coli*, *Klebsiella pneumoniae*, *Enterobacter* spp, *Serratia* spp, *Providencia* spp, *Morganella* spp, *Neisseria gonorrhoeae*, *Salmonella* spp., *Shigella* spp, *Enterococcus faesium*, *Staphylococcus aureus*, *Helycobacter pilory*, *Campylobacter*

spp, *Streptococcus pneumoniae* and *Haemophilus influenzae*). La découverte de nouveaux composés pour traiter les bactéries résistantes aux médicaments mentionnés précédemment est impérative pour éviter le problème toujours croissant des infections bactériennes, de sorte que l'exploration de nouvelles sources d'antibiotiques doit être une tâche prioritaire de la recherche.

En tant que facteur aggravant, la bactérie *Mycobacterium tuberculosis* continue de développer une résistance aux principaux médicaments antituberculeux de première et de deuxième intention. Ce fait est important car la tuberculose est la neuvième cause de décès dans le monde, et selon l'Organisation Mondiale de la Santé, les données épidémiologiques récentes sur la tuberculose sont alarmantes, avec 10 millions de personnes infectées au niveau mondial, soit 558000 cas résistants à la rifampicine (RR-TB), dont 82% des cas de RR-TB présentaient une multirésistance (MDR-TB) et les 8,5 % étaient extrêmement résistants aux médicaments (XDR-TB). Il y a eu 1,3 million de décès parmi les patients séropositifs et 0,3 million parmi les patients séropositifs atteints de tuberculose dans le monde. Les données ci-dessus fournissent des preuves solides que la résistance aux médicaments devrait être considérée comme le plus grand défi auquel les établissements de santé doivent faire face, donc si de nouveaux médicaments antibactériens efficaces ne sont pas trouvés, il y a un risque élevé d'un impact négatif grave sur la qualité de vie pour les populations mondiales.

Afin de collaborer pour trouver une solution contre les infections bactériennes pharmacorésistantes, de nouveaux agents antibactériens ont été découverts dans le présent travail, en menant une étude phytochimique à l'aide de la plante *Solanum chrysotrichum* Schldl, un spécimen végétal largement utilisé en médecine traditionnelle mexicaine. L'approche de cette recherche est basée sur le fait que les plantes sont la principale ressource de la médecine traditionnelle, et selon l'OMS, 80% des personnes dans le monde utilisent des plantes pour le traitement des maladies. Actuellement utilisées comme médicaments, 119 entités chimiques sont dérivées de 90 espèces des plantes, dont 74% ont été découvertes à la suite de l'isolement de principes actifs de plantes utilisées en médecine traditionnelle. Actuellement, 25 à 28% de tous les médicaments sont des produits naturels ou des dérivés semi-synthétiques obtenus à partir de plantes supérieures, ce qui est un signe du vaste potentiel des plantes médicinales. Sur cette base, l'exploration phytochimique et pharmacologique des plantes médicinales d'origine ethnomédicale peut être considérée comme un domaine prometteur et potentiellement fructueux dans la recherche de nouvelles molécules actives. Ainsi, il est justifié et rationnel de se tourner vers les plantes médicinales dans la recherche de solutions contre les infections bactériennes résistantes aux médicaments.

### **Conclusions et contributions :**

A partir de parties aériennes broyées et séchées de *Solanum chrysotrichum* Schldl, ont été préparés : l'extrait d'hexane, l'extrait de dichlorométhane, l'extrait de méthanol et l'extrait aqueux. Une analyse par GC / MS a été réalisée pour les extraits hexane et dichlorométhane. L'extrait hexane était composé principalement des alcanes tritriacontane (44.50%) et dotriacontane (32.81%), l'extrait de dichlorométhane était composé principalement des alcanes tritriacontane (38.18%), hexatriacontane (27.19%) et de l'alcool diterpénique phytol (20.99%). L'extrait au



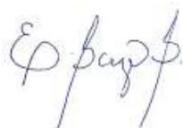
méthanol a été soumis à une chromatographie sur colonne de gel de silice pour donner neuf fractions (A-I). A partir de la fraction B, on a obtenu l'acide salicylique (SC10) et le stérol campestérol- $\beta$ -D-glucopyranoside glycosylé (SC7B). A partir des fractions C et D, on a obtenu un mélange de trois saponines stéroïdiennes (SC5) qui ont été soumises à une acétylation, puis une chromatographie sur colonne a été réalisée pour obtenir les nouvelles saponines acétylées. 2'',3'',5''-triacetoxy-6- $\alpha$ -O- $\alpha$ -L-rhamnopyranosyl-(1 $\rightarrow$ 3)-2',4'-diacetoxy- $\beta$ -D-quinovopyranosyl-(25S)-5 $\alpha$ -spirostan-3 $\beta$ -acetate (SC5AcA) et 2'',3'',5''-triacetoxy-6- $\alpha$ -O- $\alpha$ -L-rhamnopyranosyl-(1 $\rightarrow$ 3)-2',4'-diacetoxy- $\beta$ -D-quinovopyranosyl-(23R,25S)-5 $\alpha$ -spirostan-3 $\beta$ ,23 $\beta$ -acetate (SC5AcB) et le 2'',3'',5''-triacetoxy-6- $\alpha$ -O- $\beta$ -D-xylopyranosyl-(1 $\rightarrow$ 3)-2',4'-diacetoxy- $\beta$ -D-quinovopyranosyl-(23R,25S)-5 $\alpha$ -spirostan-3 $\beta$ ,23 $\beta$ -acetate (SC5AcC) connu. Chaque saponine acétylée a été soumise à une saponification à l'aide de KOH éthanolique, obtenant ainsi les deux nouvelles saponines stéroïdiennes 6- $\alpha$ -O- $\alpha$ -L-rhamnopyranosyl-(1 $\rightarrow$ 3)- $\beta$ -D-quinovopyranosyl-(25S)-5 $\alpha$ -spirostan-3 $\beta$ -ol (SC5A) et 6- $\alpha$ -O- $\alpha$ -L-rhamnopyranosyl-(1 $\rightarrow$ 3)- $\beta$ -D-quinovopyranosyl-(23R,25S)-5 $\alpha$ -spirostan-3 $\beta$ ,23 $\beta$ -ol (SC5B) et le 6- $\alpha$ -O- $\beta$ -D-xylopyranosyl-(1 $\rightarrow$ 3)- $\beta$ -D-quinovopyranosyl-(23R,25S)-5 $\alpha$ -spirostan-3 $\beta$ ,23 $\beta$ -ol (SC5C) connu et précédemment isolé de *Solanun hispidum*. A partir de la fraction D, on a obtenu le flavonol glycosidé 3'-O-méthyl-quercétine-3-O- $\beta$ -D-glucopyranoside (SC11). Tous les composés isolés de l'extrait de méthanol ont été caractérisés structurellement par l'analyse des données spectroscopiques (RMN 1D et 2D) et spectrométriques (HRMS-ESI). Une hydrolyse acide de la saponine SC5B a été tentée afin d'obtenir son aglycone correspondant à dériver pour synthétiser des dérivés d'aminoéther. Malheureusement, il n'a pas été possible d'obtenir le produit d'hydrolyse, de sorte qu'en alternative, la diosgénine a été obtenue à partir de sources commerciales afin d'être utilisée comme matière de départ pour la préparation des dérivés. Neuf dérivés d'aminoéther de diosgénine ont été préparés (DIO-01 à DIO-09) et caractérisés par analyse des données spectroscopiques. L'activité antibactérienne des extraits, des composés, des dérivés acétylés et des dérivés de diosgénine aminoether a été évaluée contre les bactéries à gram négatif (carbapenem-resistant (CR) *Acinetobacter baumannii* (12-666), extended spectrum  $\beta$ -lactamase-positive (ESBL) *Escherichia coli* (14-2081), (CR) *Pseudomonas aeruginosa* (13-1391), carbapenem and broad spectrum cephalosporins-resistant (CCR) *Klebsiella pneumoniae* NDM-1 positive (14-3335), ESBL *Klebsiella pneumoniae* (14-2081)), et à gram positif (methicillin-resistant (MR) *Staphylococcus aureus* (MRSA, 14-2095), linezolid-resistant (LR) *Staphylococcus epidermidis* (14-583) et vancomycin-resistant (VR) *Enterococcus faecium* (10-984)), et deux souches de *Mycobacterium tuberculosis*, les souches sensibles H37Rv et la souche multirésistante G122. Les extraits organiques (hexane, dichlorométhane et méthanol) ont montré une activité antibactérienne contre (CR) *Acinetobacter baumannii* (CMI : 125  $\mu$ g/mL) et (CR) *Pseudomonas aeruginosa* (CMI : 250  $\mu$ g/mL). La saponine stéroïdienne SC5C connue était le seul composé isolé de l'extrait de méthanol qui présentait une activité antibactérienne, étant active contre les trois bactéries gram-positives testées avec une valeur CMI de 12.5  $\mu$ g/mL, et étant aussi active que la lévofloxacine de référence contre (LR) *S. epidermidis*. Les dérivés de diosgénine aminoéther DIO-02 et DIO-09 étaient les seuls dérivés qui ont montré une activité

antibactérienne, avec DIO-02 actif uniquement contre (MR) *S. aureus* (MIC : 50 µg/mL) et DIO-09 actif contre les trois bactéries à gram positif testées (CMI : 12.5-25 µg/mL), soit deux fois moins actives que la lévofloxacine. L'activité antimycobactérienne n'a été détectée que pour l'extrait d'hexane contre les deux souches de *M. tuberculosis* avec une valeur CMI de 250 µg/mL. Ce projet représente le premier rapport de bonnes activités antibactériennes pour les extraits organiques de *S.chysotrichum*, le premier rapport d'activité antimycobactérienne pour l'extrait d'hexane de *S. chrysotrichum*, et le premier rapport d'activité antibactérienne pour la saponine connue SC5C. Par ailleurs, neuf nouveaux dérivés de diosgénine aminoether ont été décrits, dont deux (DIO-02 et DIO-09) possèdent des activités antibactériennes prometteuses.



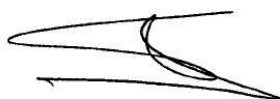
---

**Dra. María del Rayo Camacho corona**  
Thesis director



---

**Dra. Elvira Garza González**  
Thesis Co-director



---

**Prof. Pascal Marchand**  
External Thesis Co-director

## INDEX

Chapter	Page
1. INTRODUCTION	1
1.1. Epidemiology of drug resistant bacteria	1
1.2. Plants as a potential source of new drugs	3
2. BACKGROUND	5
2.1. Overview of the genus <i>Solanum</i>	5
2.2. Ethnomedical uses of various species of the genus <i>Solanum</i>	5
2.3. Chemistry and pharmacology of the constituents of the genus <i>Solanum</i>	7
2.3.1. Antimicrobial activity	7
3. HYPOTHESIS AND GENERAL AIM	10
3.1. Hypothesis	10
3.2. General Aim	10
3.2.1. Specific aims	10
4. MATERIAL AND METHODS	12
4.1. Materials and reagents	12
4.1.1. Equipment used in the experimental procedures	13
4.2. Methods	14
4.2.1. Phytochemistry	14
4.2.1.1. Extracts preparation	15
4.2.1.2. Fractionation by column chromatography of the methanol extract of <i>S. chrysotrichum</i>	15
4.2.1.3. Isolation and purification of phytocompounds of methanol extract of <i>S. chrysotrichum</i>	16
4.2.2. Acetylation of SC5 mixture	18
4.2.3. Saponification of acetylated derivatives	19
4.2.4. Acid hydrolysis of steroidal saponin SC5B	19
4.2.5. Synthesis of diosgenin aminoethers derivatives by Williamson ether synthesis reaction	21
4.2.5.1. Synthesis of derivative DIO-01	22
4.2.5.2. Synthesis of derivative DIO-02	23
4.2.5.3. Synthesis of derivative DIO-03	25
4.2.5.4. Synthesis of derivative DIO-04	27
4.2.5.5. Synthesis of derivative DIO-05	28
4.2.5.6. Synthesis of derivative DIO-06	30
4.2.5.7. Synthesis of derivative DIO-07	31
4.2.5.8. Synthesis of derivative DIO-08	33
4.2.5.9. Synthesis of derivative DIO-09	35
4.2.6. Structural characterization of compounds	36
4.2.7. Biological assays	36
4.2.7.1. Microdilution method for the determination of antibacterial activity against clinical isolates of drug-	36

resistant bacteria	
4.2.7.2. Alamar blue method for the determination of antibacterial activity against sensitive and drug-resistant <i>Mycobacterium tuberculosis</i>	38
4.2.8. Disposal of waste	41
5. RESULTS AND DISCUSSION	42
5.1. Structural elucidation of some compounds isolated from the methanol extract of <i>S. chrysotrichum</i>	42
5.1.1. Physical and spectroscopic data of salicylic acid (SC10)	42
5.1.1.1. Structural elucidation of salicylic acid (SC10)	43
5.1.2. Physical and spectroscopic data of campesterol- $\beta$ -D-glucopyranoside (SC7B)	52
5.1.2.1. Structural elucidation of 2',3',4',5'-tetraacetoxy- campesterol- $\beta$ -D glucopyranoside (SC7BAc)	53
5.1.3. Physical and spectroscopic data of 2'',3'',5''-triacetoxy-6- $\alpha$ -O- $\alpha$ -L-rhamnopyranosyl-(1-3)-2',4'-diacetoxy- $\beta$ -quinovopyranosyl-(25S)-5 $\alpha$ -spirostan-3 $\beta$ -acetate (SC5AcA)	61
5.1.3.1. Structural elucidation of 2'',3'',5''-triacetoxy-6- $\alpha$ -O- $\alpha$ -L-rhamnopyranosyl-(1-3)-2',4'-diacetoxy- $\beta$ -quinovopyranosyl-(25S)-5 $\alpha$ -spirostan-3 $\beta$ -acetate (SC5AcA)	62
5.1.4. Physical and spectrometric data of 6- $\alpha$ -O- $\alpha$ -L-rhamnopyranosyl-(1 $\rightarrow$ 3)- $\beta$ -D-quinovopyranosyl-(25S)-5 $\alpha$ -spirostan-3 $\beta$ -ol (SC5A)	71
5.1.5. Physical and spectrometric data of 2'',3'',5''-triacetoxy-6- $\alpha$ -O- $\alpha$ -L-rhamnopyranosyl-(1 $\rightarrow$ 3)-2',4'-diacetoxy- $\beta$ -D-quinovopyranosyl-(23R,25S)-5 $\alpha$ -spirostan-3 $\beta$ ,23 $\beta$ -acetate (SC5AcB)	72
5.1.5.1. Structural elucidation of 2'',3'',5''-triacetoxy-6- $\alpha$ -O- $\alpha$ -L-rhamnopyranosyl-(1 $\rightarrow$ 3)-2',4'-diacetoxy- $\beta$ -D-quinovopyranosyl-(23R,25S)-5 $\alpha$ -spirostan-3 $\beta$ ,23 $\beta$ -acetate (SC5AcB)	73
5.1.6. Physical and spectrometric data of 6- $\alpha$ -O- $\alpha$ -L-rhamnopyranosyl-(1 $\rightarrow$ 3)- $\beta$ -D-quinovopyranosyl-(23R,25S)-5 $\alpha$ -spirostan-3 $\beta$ ,23 $\beta$ -ol (SC5B)	82
5.1.7. Physical, spectroscopic and spectrometric data of 2'',3'',5''-triacetoxy-6- $\alpha$ -O- $\beta$ -D-xylopyranosyl-(1 $\rightarrow$ 3)-2',4'-diacetoxy- $\beta$ -D-quinovopyranosyl-(23R,25S)-5 $\alpha$ -spirostan-3 $\beta$ ,23 $\beta$ -acetate (SC5AcC)	83
5.1.7.1. Structural elucidation of 2'',3'',5''-triacetoxy-6- $\alpha$ -O- $\beta$ -D-xylopyranosyl-(1 $\rightarrow$ 3)-2',4'-diacetoxy- $\beta$ -D-quinovopyranosyl-(23R,25S)-5 $\alpha$ -spirostan-3 $\beta$ ,23 $\beta$ -acetate (SC5AcC)	84
5.1.8. Physical and spectrometric data of 6- $\alpha$ -O- $\beta$ -D-xylopyranosyl-(1 $\rightarrow$ 3)- $\beta$ -D-quinovopyranosyl-(23R,25S)-5 $\alpha$ -spirostan-3 $\beta$ ,23 $\beta$ -ol (SC5C)	92

5.1.9. Physical and spectroscopic data of 3'-O-methyl-quercetin-3-O- $\beta$ -D-glucopyranoside (SC11)	93
5.1.9.1. Structural elucidation of 3'-O-methyl-quercetin-3-O- $\beta$ -D-glucopyranoside (SC11)	94
5.2. Analysis of the hexane and dichloromethane extracts of <i>S. chrysotrichum</i>	104
5.3. Antibacterial activity of organic and aqueous extracts of <i>S.</i> <i>chrysotrichum</i>	106
5.4. Antibacterial and antimycobacterial activity of isolated compounds from the methanol extract <i>S. chrysotrichum</i> and acetylated derivatives	111
5.5. Acid hydrolysis of steroidal saponin SC5B	116
5.6. Physical constants and yields of diosgenin aminoether derivatives	117
5.7. Structural elucidation of diosgenin aminoether derivatives	118
5.7.1. Structural elucidation of DIO-01	119
5.7.2. Structural elucidation of DIO-02	125
5.7.3. Structural elucidation of DIO-03	129
5.7.4. Structural elucidation of DIO-04	133
5.7.5. Structural elucidation of DIO-05	137
5.7.6. Structural elucidation of DIO-06	142
5.7.7. Structural elucidation of DIO-07	146
5.7.8. Structural elucidation of DIO-08	150
5.7.9. Structural elucidation of DIO-09	154
5.5. Antibacterial activity of diosgenin aminoether derivatives	158
6. CONCLUSIONS	163
7. PERSPECTIVES	167
8. REFERENCES	168
APPENDIX A: Mass spectrums of steroidal saponins SC5A, SC5B and SC5C and its corresponding acetylated derivatives SC5AcA, SC5AcB and SC5AcC	179
APPENDIX B: Certificate of attendance as oral communicator in the Journée Recherche 2019 at the Université de Nantes	183
APPENDIX C: Certificate of attendance as oral communicator in the Young Research Fellow Meeting 2020 at the Université de Caen Normandie	184
APPENDIX D: Front page of the publication derived of the thesis work	185

## FIGURE INDEX

Figure	Page
1. Antibacterial steroidal alkaloids isolated from <i>S. leucocarpum</i>	8
2. Antibacterial tomatidine isolated from <i>S. nigrum</i>	9
3. Aminoalkyl halide modulations used for the synthesis of diosgenin amioether derivatives	21
4. Salicylic acid (SC10)	42
5. FT-IR spectrum of salicylic acid (SC10)	46
6. <sup>1</sup> H NMR spectrum (400 MHz, CDCl <sub>3</sub> ) of salicylic acid (SC10)	47
7. COSY NMR spectrum (400 MHz, CDCl <sub>3</sub> ) of salicylic acid (SC10)	48
8. <sup>13</sup> C NMR spectrum (100 MHz, CDCl <sub>3</sub> ) of salicylic acid (SC10)	49
9. HSQC NMR spectrum (400 MHz, CDCl <sub>3</sub> ) of salicylic acid (SC10)	50
10. HMBC NMR spectrum (400 MHz, CDCl <sub>3</sub> ) of of salicylic acid (SC10)	51
11. β-campesterol-D-glucoside (SC7B)	52
12. 2',3',4',5'-tetraacetoxy- campesterol- β-D-glucopyranoside (SC7Ac)	53
13. <sup>1</sup> H NMR spectrum (400 MHz, CDCl <sub>3</sub> ) of 2',3',4',5'-tetraacetoxy- campesterol- β-D-glucoside (SC7BAc)	57
14. <sup>13</sup> C NMR spectrum (100 MHz, CDCl <sub>3</sub> ) of 2',3',4',5'-tetraacetoxy- campesterol- β-D-glucoside (SC7BAc)	58
15. HSQC spectrum (400 MHz, CDCl <sub>3</sub> ) of 2',3',4',5'-tetraacetoxy- campesterol- β-D-glucoside (SC7BAc)	59
16. HMBC spectrum (400 MHz, CDCl <sub>3</sub> ) of 2',3',4',5'-tetraacetoxy- campesterol- β-D-glucoside (SC7BAc)	60
17. 2'',3'',5''-triacetoxy-6-α-O- α-L-rhamnopyranosyl-(1→3)-2',4'-diacetoxy-β-D-quinovopyranosyl-(25S)-5α-spirostan-3β-acetate (SC5AcA)	61
18. <sup>1</sup> H NMR spectrum (400 MHz, CDCl <sub>3</sub> ) of 2'',3'',5''-triacetoxy-6-α-O-α-L-rhamnopyranosyl-(1→3)-2',4'-diacetoxy-β-D-quinovopyranosyl-(25S)-5α-spirostan-3β-acetate (SC5AcA)	66
19. <sup>13</sup> C NMR spectrum (100 MHz, CDCl <sub>3</sub> ) of 2'',3'',5''-triacetoxy-6-α-O-α-L-rhamnopyranosyl-(1→3)-2',4'-diacetoxy-β-D-quinovopyranosyl-(25S)-5α-spirostan-3β-acetate (SC5AcA)	67
20. HSQC partial spectrum (400 MHz, CDCl <sub>3</sub> ) of 2'',3'',5''-triacetoxy-6-α-O-α-L-rhamnopyranosyl-(1→3)-2',4'-diacetoxy-β-D-quinovopyranosyl-(25S)-5α-spirostan-3β-acetate (SC5AcA)	68
21. HMBC partial spectrum (400 MHz, CDCl <sub>3</sub> ) of 2'',3'',5''-triacetoxy-6-α-O-α-L-rhamnopyranosyl-(1→3)-2',4'-diacetoxy-β-D-quinovopyranosyl-(25S)-5α-spirostan-3β-acetate (SC5AcA)	69
22. COSY partial spectrum (400 MHz, CDCl <sub>3</sub> ) of 2'',3'',5''-triacetoxy-6-α-O-α-L-rhamnopyranosyl-(1→3)-2',4'-diacetoxy-β-D-quinovopyranosyl-(25S)-5α-spirostan-3β-acetate (SC5AcA)	70
23. 6-α-O-α-L-rhamnopyranosyl-(1→3)-β-D-quinovopyranosyl-(25S)-5α-	71

spirostan-3 $\beta$ -ol (SC5A)	
24. 2'',3'',5''-triacetoxo-6- $\alpha$ -O- $\alpha$ -L-rhamnopyranosyl-(1 $\rightarrow$ 3)-2',4'-diacetoxo- $\beta$ -D-quinovopyranosyl-(23R,25S)-5 $\alpha$ -spirostan-3 $\beta$ ,23 $\beta$ -acetate (SC5AcB)	72
25. <sup>1</sup> H NMR spectrum (400 MHz, CDCl <sub>3</sub> ) of 2'',3'',5''-triacetoxo-6- $\alpha$ -O- $\alpha$ -L-rhamnopyranosyl-(1 $\rightarrow$ 3)-2',4'-diacetoxo- $\beta$ -D-quinovopyranosyl-(23R,25S)-5 $\alpha$ -spirostan-3 $\beta$ ,23 $\beta$ -acetate (SC5AcB)	77
26. <sup>13</sup> C NMR spectrum (400 MHz, CDCl <sub>3</sub> ) of 2'',3'',5''-triacetoxo-6- $\alpha$ -O- $\alpha$ -L-rhamnopyranosyl-(1 $\rightarrow$ 3)-2',4'-diacetoxo- $\beta$ -D-quinovopyranosyl-(23R,25S)-5 $\alpha$ -spirostan-3 $\beta$ ,23 $\beta$ -acetate (SC5AcB)	78
27. HSQC spectrum (400 MHz, CDCl <sub>3</sub> ) of 2'',3'',5''-triacetoxo-6- $\alpha$ -O- $\alpha$ -L-rhamnopyranosyl-(1 $\rightarrow$ 3)-2',4'-diacetoxo- $\beta$ -D-quinovopyranosyl-(23R,25S)-5 $\alpha$ -spirostan-3 $\beta$ ,23 $\beta$ -acetate (SC5AcB)	79
28. HMBC partial spectrum (400 MHz, CDCl <sub>3</sub> ) of 2'',3'',5''-triacetoxo-6- $\alpha$ -O- $\alpha$ -L-rhamnopyranosyl-(1 $\rightarrow$ 3)-2',4'-diacetoxo- $\beta$ -D-quinovopyranosyl-(23R,25S)-5 $\alpha$ -spirostan-3 $\beta$ ,23 $\beta$ -acetate (SC5AcB)	80
29. COSY partial spectrum (400 MHz, CDCl <sub>3</sub> ) of 2'',3'',5''-triacetoxo-6- $\alpha$ -O- $\alpha$ -L-rhamnopyranosyl-(1 $\rightarrow$ 3)-2',4'-diacetoxo- $\beta$ -D-quinovopyranosyl-(23R,25S)-5 $\alpha$ -spirostan-3 $\beta$ ,23 $\beta$ -acetate (SC5AcB)	81
30. 6- $\alpha$ -O- $\alpha$ -L-rhamnopyranosyl-(1 $\rightarrow$ 3)- $\beta$ -D-quinovopyranosyl-(23R,25S)-5 $\alpha$ -spirostan-3 $\beta$ ,23 $\beta$ -ol (SC5B)	82
31. 2'',3'',5''-triacetoxo-6- $\alpha$ -O- $\beta$ -D-xylopyranosyl-(1 $\rightarrow$ 3)-2',4'-diacetoxo- $\beta$ -D-quinovopyranosyl-(23R,25S)-5 $\alpha$ -spirostan-3 $\beta$ ,23 $\beta$ -acetate (SC5AcC)	83
32. <sup>1</sup> H NMR spectrum (400 MHz, CDCl <sub>3</sub> ) of 2'',3'',5''-triacetoxo-6- $\alpha$ -O- $\beta$ -D-xylopyranosyl-(1 $\rightarrow$ 3)-2',4'-diacetoxo- $\beta$ -D-quinovopyranosyl-(23R,25S)-5 $\alpha$ -spirostan-3 $\beta$ ,23 $\beta$ -acetate (SC5AcC)	87
33. <sup>13</sup> C NMR spectrum (100 MHz, CDCl <sub>3</sub> ) of 2'',3'',5''-triacetoxo-6- $\alpha$ -O- $\beta$ -D-xylopyranosyl-(1 $\rightarrow$ 3)-2',4'-diacetoxo- $\beta$ -D-quinovopyranosyl-(23R,25S)-5 $\alpha$ -spirostan-3 $\beta$ ,23 $\beta$ -acetate (SC5AcC)	88
34. HSQC spectrum (400 MHz, CDCl <sub>3</sub> ) of 2'',3'',5''-triacetoxo-6- $\alpha$ -O- $\beta$ -D-xylopyranosyl-(1 $\rightarrow$ 3)-2',4'-diacetoxo- $\beta$ -D-quinovopyranosyl-(23R,25S)-5 $\alpha$ -spirostan-3 $\beta$ ,23 $\beta$ -acetate (SC5AcC)	89
35. HMBC spectrum (400 MHz, CDCl <sub>3</sub> ) of 2'',3'',5''-triacetoxo-6- $\alpha$ -O- $\beta$ -D-xylopyranosyl-(1 $\rightarrow$ 3)-2',4'-diacetoxo- $\beta$ -D-quinovopyranosyl-(23R,25S)-5 $\alpha$ -spirostan-3 $\beta$ ,23 $\beta$ -acetate (SC5AcC)	90
36. COSY spectrum (400 MHz, CDCl <sub>3</sub> ) of 2'',3'',5''-triacetoxo-6- $\alpha$ -O- $\beta$ -D-xylopyranosyl-(1 $\rightarrow$ 3)-2',4'-diacetoxo- $\beta$ -D-quinovopyranosyl-(23R,25S)-5 $\alpha$ -spirostan-3 $\beta$ ,23 $\beta$ -acetate (SC5AcC)	91
37. 6- $\alpha$ -O- $\beta$ -D-xylopyranosyl-(1 $\rightarrow$ 3)- $\beta$ -D-quinovopyranosyl-(23R,25S)-5 $\alpha$ -spirostan-3 $\beta$ ,23 $\beta$ -ol (SC5C)	92
38. 3'-O-methyl-quercetin-3-O- $\beta$ -D-glucopyranoside (SC11)	93
39. <sup>1</sup> H NMR (400 MHz, CD <sub>3</sub> OD) spectrum of 3'-O-methyl-quercetin-3-O- $\beta$ -D-glucopyranoside (SC11)	97
40. <sup>1</sup> H NMR (400 MHz, DMSO) spectrum of 3'-O-methyl-quercetin-3-O- $\beta$ -D-glucopyranoside (SC11)	98

41. <sup>13</sup> C NMR (100 MHz, CD <sub>3</sub> OD) spectrum of 3'-O-methyl-quercetin-3-O-β-D-glucopyranoside (SC11)	99
42. HSQC NMR (400 MHz, CD <sub>3</sub> OD) spectrum of 3'-O-methyl-quercetin-3-O-β-D-glucopyranoside (SC11)	100
43. HMBC NMR (400 MHz, CD <sub>3</sub> OD) spectrum of 3'-O-methyl-quercetin-3-O-β-D-glucopyranoside (SC11)	101
44. COSY NMR (400 MHz, CD <sub>3</sub> OD) spectrum of 3'-O-methyl-quercetin-3-O-β-D-glucopyranoside (SC11)	102
45. NOESY NMR (400 MHz, CD <sub>3</sub> OD) spectrum of 3'-O-methyl-quercetin-3-O-β-D-glucopyranoside (SC11)	103
46. Chemical structure and antibacterial activities comparison of some steroidal saponins from <i>S. chrysotrichum</i> and acetylated derivative SC5AcC	113
47. Chemical structure of diosgenin	117
48. <sup>1</sup> H NMR (400 MHz, CDCl <sub>3</sub> ) spectrum of diosgenin	119
49. aminoether derivative DIO-01	119
50. <sup>1</sup> H NMR (400 MHz, CDCl <sub>3</sub> ) spectrum of DIO-01	123
51. <sup>13</sup> C NMR (100 MHz, CDCl <sub>3</sub> ) spectrum of DIO-01	124
52. aminoether derivative DIO-02	125
53. <sup>1</sup> H NMR (400 MHz, CDCl <sub>3</sub> ) spectrum of DIO-02	127
54. <sup>13</sup> C NMR (100 MHz, CDCl <sub>3</sub> ) spectrum of DIO-02	128
55. aminoether derivative DIO-03	129
56. <sup>1</sup> H NMR (400 MHz, CDCl <sub>3</sub> ) spectrum of DIO-03	131
57. <sup>13</sup> C NMR (100 MHz, CDCl <sub>3</sub> ) spectrum of DIO-03	132
58. aminoether derivative DIO-04	133
59. <sup>1</sup> H NMR (400 MHz, CDCl <sub>3</sub> ) spectrum of DIO-04	135
60. <sup>13</sup> C NMR (100 MHz, CDCl <sub>3</sub> ) spectrum of DIO-04	136
61. aminoether derivative DIO-05	137
62. <sup>1</sup> H NMR (400 MHz, CDCl <sub>3</sub> ) spectrum of DIO-05	140
63. <sup>13</sup> C NMR (100 MHz, CDCl <sub>3</sub> ) spectrum of DIO-05	141
64. aminoether derivative DIO-06	142
65. <sup>1</sup> H NMR (400 MHz, CDCl <sub>3</sub> ) spectrum of DIO-06	144
66. <sup>13</sup> C NMR (100 MHz, CDCl <sub>3</sub> ) spectrum of DIO-06	145
67. aminoether derivative DIO-07	146
68. <sup>1</sup> H NMR (400 MHz, CDCl <sub>3</sub> ) spectrum of DIO-07	148
69. <sup>13</sup> C NMR (100 MHz, CDCl <sub>3</sub> ) spectrum of DIO-07	149
70. aminoether derivative DIO-08	150
71. <sup>1</sup> H NMR (400 MHz, CDCl <sub>3</sub> ) spectrum of DIO-08	152
72. <sup>13</sup> C NMR (100 MHz, CDCl <sub>3</sub> ) spectrum of DIO-08	153
73. aminoether derivative DIO-09	154
74. <sup>1</sup> H NMR (400 MHz, CDCl <sub>3</sub> ) spectrum of DIO-09	156
75. <sup>13</sup> C NMR (100 MHz, CDCl <sub>3</sub> ) spectrum of DIO-09	157
76. Active derivatives DIO-02 and DIO-09	159
77. Triazolyl diosgenin derivative	161
78. Lignan aminoether derivatives <i>meso-26</i> and <i>meso-27</i>	162



## TABLE INDEX

Table	Page
1. Organic and aqueous extracts of <i>S. chrysotrichum</i>	15
2. Pooled fractions of methanol extract of <i>S. chrysotrichum</i>	16
3. $^{13}\text{C}$ NMR and $^1\text{H}$ NMR of SC7BAC and reference compound <sup>35</sup>	56
4. $^{13}\text{C}$ NMR and $^1\text{H}$ NMR constants for SC5AcA and reference compound 5a <sup>23</sup>	65
5. $^{13}\text{C}$ NMR and $^1\text{H}$ NMR data for SC5AcB and reference compound 6a <sup>23</sup>	76
6. $^{13}\text{C}$ NMR and $^1\text{H}$ NMR data for SC5AcC and reference compound 3a <sup>21</sup>	86
7. GC-MS analysis of <i>S. chrysotrichum</i> hexane extract	104
8. GC-MS analysis of <i>S. chrysotrichum</i> dichloromethane extract	105
9. Antibacterial and antimycobacterial activities of extracts of <i>S. chrysotrichum</i>	110
10. Antibacterial and antimycobacterial activities of compounds from <i>S. chrysotrichum</i> and acetylated derivatives	114
11. Physical constants and yields of diosgenin aminoether derivatives	117
12. $^1\text{H}$ and $^{13}\text{C}$ NMR spectroscopic constants of diosgenin	118
13. Antibacterial and antimycobacterial activities of diosgenin aminoether Derivatives	160

## SCHEME INDEX

<b>Scheme</b>	<b>Page</b>
1. Acetylation reaction of the steroidal saponin mixture SC5	18
2. Saponification reaction of acetylated saponins	19
3. Acid hydrolysis of steroidal saponin SC5B	20
4. Williamson ether synthesis	21
5. Synthesis of aminoether derivative DIO-01	22
6. Synthesis of aminoether derivative DIO-02	24
7. Synthesis of aminoether derivative DIO-03	26
8. Synthesis of aminoether derivative DIO-04	27
9. Synthesis of aminoether derivative DIO-05	29
10. Synthesis of aminoether derivative DIO-06	30
11. Synthesis of aminoether derivative DIO-07	32
12. Synthesis of aminoether derivative DIO-08	34
13. Synthesis of aminoether derivative DIO-09	35

## LIST OF ABBREVIATIONS

°C: celcius grades

μL: microliters

μg: micrograms

<sup>13</sup>C: thirteen

<sup>1</sup>H: proton

EtOAc: ethyl acetate

CC: column chromatography

TLC: thin layer chromatography

LLP: liquid-liquid partition

CDCl<sub>3</sub>: deuterated chloroform

MIC: minimun inhibitory concentration

PPC: preparative plate chromatography

PPM: parts per million

DMSO: dimethyl sulfoxide

DMF: dimethylformamide

XDR: extremely drug resistant

SP: stationary phase

MP: mobile phase

MDR: multidrug resistant

g: gram

h: hour

LVF: levofloxacin

mg: miligram

mL: milliliter

N.D.: not determined

OADC: oleic acid, albumin, dextrose y catalase

WHO: world health organization

M.P.: melting point

CR: carbapenem resistant

CCR: resistant to carbapenen and cephalosporin

LR: linezolid resistant

NMR: nuclear magnetic resonance

VR: vancomycin resistant

TB: tuberculosis

XFR-TB: extremely drug resistant tuberculosis

MDR-TB: multidrug resistant tuberculosis

RR-TB: rifampicin resistant tuberculosis

TMS: tetrametilsilane

# 1. INTRODUCTION

## 1.1. Epidemiology of drug resistant bacteria

Life expectancy in today's society is far higher than in past centuries, mainly because infections that were deadly in the past are now curable thanks to the discovery of antibiotics. The era of antibiotics is a high-point in modern medicine. However, drug resistance developed by pathogenic microorganisms and the lack of attention, monitoring and preventive measures to control this problem, threaten to reduce advances achieved to date to a temporary solution, given the observed trend that the greater the variety of antibiotics we use, the greater the number of microorganisms that become resistant to them. As a consequence, antimicrobial treatments become more complicated, less effective and costlier. In some extreme cases of drug resistance, no effective treatment may be available<sup>1</sup>.

Drug resistance has major economic impact implications for the pharmaceutical industry, considering that ineffective antibiotics lose commercial value. Replacing obsolete antibiotics must be a key priority for the industry, especially considering that no new class of antibacterial agents has been discovered since 1987. Furthermore, the lack of antibiotics currently in the approval phase increase the relevance of drug resistance as a priority issue for the world health<sup>2</sup>. In response to this problem, the World Health Organization (WHO) introduced its Global Antimicrobial Resistance Surveillance System (GLASS) in 2015, through which

epidemiological information about the most clinically important drug-resistant bacteria is reported (*Acinetobacter* spp., *Pseudomonas aureogiosa*, *Escherichia coli*, *Klebsiella pneumoniae*, *Enterobacter* spp, *Serratia* spp, *Prividencia* spp, *Morganella* spp, *Neisseria gonorrhoeae*, *Salmonella* spp., *Shigella* spp, *Enterococcus faesium*, *Staphylococcus aureus*, *Helycobacter pilory*, *Campylobacter* spp, *Streptococcus pneumoniae* and *Haemophylus influenzae*, as listed in the WHO's Global Priority List of Antibiotic-resistant Bacteria to Guide Research, Discovery, and Development of New Antibiotics 2017). The epidemiological information was gathered from 42 countries in the period 2016 to 2017<sup>3,4</sup>.

As an aggravator of the problem, the bacteria *Mycobacterium tuberculosis*, the causal agent of tuberculosis, continues to develop resistance to the main first and second-line anti-tubercular drugs. To lessen this problem is of crucial importance considering that tuberculosis is the ninth cause of death globally. The WHO's 2019 epidemiological data about tuberculosis is alarming, with 10 million people infected on a global level being 465,000 cases resistant to rifampicin (RR-TB), from which the 78% of RR-TB cases presented multidrug-resistance (MDR-TB). In 2019 there were 1.2 million deaths among HIV- patients and 208,000 deaths among HIV+ positive patients from tuberculosis globally. In Mexico in the year 2018, 23,520 tuberculosis cases were reported and 2,970 deaths from the disease<sup>5</sup>.

It is relevant to point out that the incidence of TB is increasing in Mexico, being a country that has not implemented the GLASS system. As such, global measures aimed at combating drug resistance are not implemented on a local level. Active epidemiological surveillance is carried out in hospitals and health centers, with the most recent data reported by the health ministry in weekly bulletins. However, this data does not include information about the drug resistance of microorganisms, and surveillance protocols are not applied in all health centers in the country. It is important that Mexico implements preventive measures to detect and combat resistant bacteria. The above data provide strong evidence that drug resistance should be considered the biggest challenge the health sector has faced, given that, if new, effective antibacterial drugs are not found, there is a risk of a severe negative impact on quality of life.

## **1.2. Plants as a potential source of new drugs**

Plants are the main resource in traditional medicine. According to the WHO, 80% of people globally use plants for treatment of diseases. Currently, 119 chemical entities derived from 90 species of plants are in use as drugs in more than one country. Of these, 74% were discovered as a result of the isolation of active principles of plants used in traditional medicine. This shows the great importance of ethnomedicine in the discovery of new drugs<sup>6</sup>. In an industrial context, many drugs with high pharmacological value such as vincristine, vinblastine or taxol (anticancer drugs) have been obtained from natural sources, and have good anticancer activities without being modified. However, the preferred approach in

the industry is to search for active molecules with an ethnomedical background for use as lead compounds for the semi-synthesis of new drugs, in order to improve their biological activity and secure patent rights<sup>7</sup>. Currently 25-28% of all drugs are natural products or semi-synthetic derivatives obtained from higher plants, which is a sign of medicinal plants' vast potential. Examples include Arteether (artemotil), an antimalarial sesquiterpene lactone isolated from *Artemisia annua*, galantamine (Reminyl), an alkaloid isolated from *Galanthus woronowii* and used in Alzheimer's disease, apomorphine chloride (Apokyn), extracted from *Papaver somniferum* L. and used to treat Parkinson's disease, and the aforementioned anticancer drugs<sup>8</sup>. In addition, many molecules extracted from plants have interesting antimicrobial activity. These include gallic acid, active against *S. aureus* and extracted from *Lawsonia inermis*, Glabrol, active against *S. aureus* and *M. tuberculosis* and isolated from *Glycyrrhiza glabra*, and nordihydroguaiaretic acid, active against cutaneous bacteria and isolated from *Larrea tridentata*<sup>9</sup>.

On this basis, phytochemical and pharmacological exploration of medicinal plants with ethnomedical backgrounds can be seen as a promising and potentially fruitful area in the search for new active molecules. As such, it is justifiable and rational to look to medicinal plants in the search for solutions to the range of diseases that affect today's society.



## 2. BACKGROUND

### 2.1. Overview of the genus *Solanum*

Solanaceas comprise a variety of plant species with a wide range of medicinal and nutritional properties. The most cultivated examples include the potato (*Solanum tuberosum* L.) and eggplant (*S. melongena* L.), as well as the ornamental species *S. jasminoides* Paxton and the “gloria” (*S. dulcamaroides* Dunal)<sup>10</sup>. Members of the *Solanum* genus can be herbaceous plants, shrubs, trees and even climbers. Some species are spiny with hairs, which are often stellate or branched; their leaves are alternate, and often organized in pairs, one being bigger than the other, whole or pinnate, sometimes with pseudo-stipules; their inflorescences are generally of cymose type, although sometimes umbelliferous or racemose, terminal or axillary, or leaf-opposed or often intermodal; the calyx can be campanulated or often lobed, with rotaceous or subrotaceous corolla, deeply parted, white, purple, blue or yellow; with 3 or 5 stamens, sometimes uneven, with generally connivent anthers, dehiscent essentially by terminal pores; ovules almost always bilocular; their fruits are berry-shaped and seeds generally numerous and compressed<sup>10</sup>.

### 2.2. Ethnomedical uses of various species of the genus *Solanum*

Medicinal plants have played a fundamental role in the development of the pharmaceutical industry as a source of new biologically active molecules. Many

plant-based remedies have been passed down in the form of ancestral knowledge in different cultures and ethnic groups, and these have been used as background in the search for new therapeutic compounds. Plants of the *Solanum* genus are widely used for their nutritional and medicinal properties, especially in developing countries such as Ethiopia, where ethnomedicine is often the only resource available to treat disease, with 80% of the population resorting to plants as their only treatment. Some *Solanaceas* used in the region, such as *S. hastifolium* Hochst. ex Dunal in DC., *S. incanum* L. and *S. marginatum* L.f., are bushes which, depending on the part used, can reduce problems such as abdominal pain, cutaneous infections (cutaneous anthrax) and parasite infections (ascariasis)<sup>11</sup>. In addition, in Ghana, leaves and fruits of *S. torvum* Sw. are used as a treatment for tuberculosis (TB), and according to studies conducted by Mwanzia *et al.* 2016 and Mohamad *et al.* 2011, aqueous methanol and ethanolic extracts (8:2) have anti-TB activity in the MIC range of 1600 to 1250 µg/mL<sup>12,13</sup>. Consequently, plants from the genus *Solanum* could be good prospects in the search for new anti-TB agents.

Mexico's ethnomedical background also includes the use of plants from the *Solanum* genus. As reported by Lozoya *et al.* 1992, 200 communities in rural Chiapas State described *S. chrysotrichum* Schldl or "Sosa" as a remedy for topical mycosis such as athlete's foot (*Tinea pedis*). This has been backed up through a clinical study, in which applying methanol extract of the plant as a topical formula in patients with athlete's foot resulted in the eradication of the infection in 45% of patients in 4 weeks, with the extract proving as effective as

commercial miconazole formulas<sup>14</sup>. In addition, a clinical study involving 101 women by Herrera-Arellano *et al.* 2009, showed vaginal suppositories containing 1.89 mg of methanol extract of *S. chrysotrichum* Schldl clinically cured 57.14% of patients with *Candida albicans*, a clinical effectiveness similar to that of ketoconazole, confirming the plant's ethnomedical use as an antimycotic<sup>15</sup>.

As well as its antimycotic activity, aqueous and ethanolic extracts of *S. chrysotrichum* Schldl showed anticancer activity, as reported by Aguilar-Santamaría *et al.* 2013, with cytotoxic activity against the KB cell line (nasopharyngeal cancer). As such, *S. chrysotrichum* Schldl should be considered a potential source of anticancer drugs, while the *Solanum* genus as a whole as a potential can be seen as a source of antibacterial, antifungal and anti-TB compounds<sup>16</sup>.

## **2.3. Chemistry and pharmacology of the constituents of the genus**

### ***Solanum***

#### **2.3.1. Antimicrobial activity**

Antimicrobial activity of alkaloids from the genus *Solanum*, and particularly antibacterial and antifungal activity, has been studied principally through *in vitro* evaluation of diverse extracts. There is a solid background in respect of the activity of alkaloids in their pure form, as reported by Niño *et al.*, 2009, who evaluated some alkaloids of *S. leucocarpum* (figure 1) using diffusion in agar,

against *Bacillus subtilis* (ATCC No. 21556), *E. coli* (ATCC No. 9637), *K. pneumoniae* (ATCC No. 10031), *Pseudomonas aeruginosa* (ATCC No. 27853) and *S. aureus* (ATCC No. 6538). Strong activity was observed against *S. aureus* with the compounds demisidine (MIC: 250 µg /mL), dihydrocongestidine (MIC: 125 µg /mL) and solasodine (MIC: 62.5 µg /mL)<sup>17</sup>.

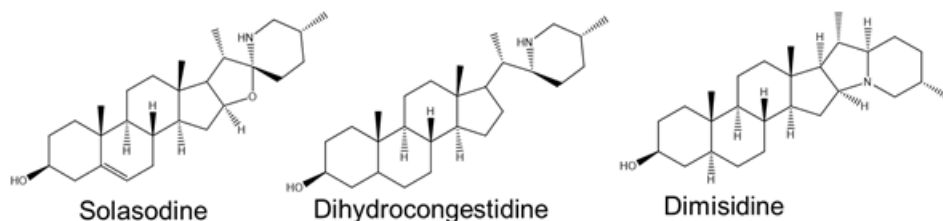


**Figure 1:** Antibacterial steroidal alkaloids isolated from *Solanum leucocarpum*

Additionally, Chagnon *et al.* 2014 reported the antimicrobial and synergistic activity of the alkaloid tomatidine (figure 2) obtained from *S. nigrum*. This compound, when tested using microdilution methods, showed a MIC greater of 64 µg/mL against *S. aureus* (ATCC No. 29213). This value which may not be very promising itself, but when administered in conjunction with the aminoglycoside gentamicin, a marked synergy was observed, with gentamicin becoming 8 times more potent when applied with the alkaloid (MIC: 0.06 µg/mL). On this basis, alkaloids from the genus *Solanum* can be useful for the reactivation of antibiotics that have lost their effectiveness as a result of drug resistance<sup>18</sup>.

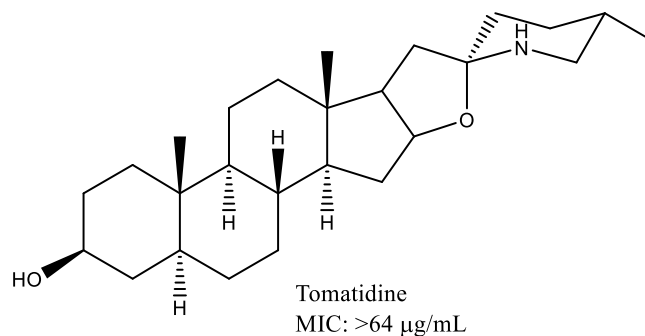


**Figure 2:** Antibacterial tomatidine isolated from *S. nigrum*

As well as antibacterial activity, the antiprotozoal activity of some alkaloids from the genus *Solanum* has been evaluated. For example, Moreira *et al.* 2013 showed the trypanocidal activity of the glycoalkaloid solamargine obtained from *S. palinacanthum*, with a median inhibitory concentration ( $IC_{50} = 15.3 \mu\text{g/mL}$ ) close to that of the positive control benznidazole ( $IC_{50} = 9 \mu\text{g/mL}$ ), a drug used to treat trypanosomiasis or Chagas disease. This shows that glycoalkaloids from the genus *Solanum* could be a good option for the development of antiprotozoal drugs<sup>19</sup>. The preceding background shows the importance of the isolation and characterization of natural products from the genus *Solanum*. In addition, there are few reports referring to antibacterial activity against drug-resistant clinical isolates of natural products from plants of the genus *Solanum*, and it is important to point out that such phytocompounds have not been tested as pure compounds against *M. tuberculosis*, displaying great potential for the assessing of their antimicrobial activity. On this basis, it can be asserted that backing up any hypothesis relating to the biological activity of these compounds is of vital importance, and that the possible mechanisms of action involved should be examined based on evidence. Chemical computational testing could be a viable

option for the prediction of mechanisms of action for the natural products of the plants of genus *Solanum*.

### **3. HYPOTHESIS AND GENERAL AIM**

#### **3.1. Hypotesis**

*S. chrysotrichum* Schldl possesses at least one compound as active as levofloxacin against clinical isolates of drug-resistant bacteria or against *M. tuberculosis*.

#### **3.2. General Aim**

To isolate and structurally characterize compounds from the leaves of *S. chrysotrichum* Schldl, synthesize ten semi-synthetic derivatives using sapogenins as starting material, and evaluate the antibacterial activity for all the compounds and derivatives.

##### **3.2.1. Specific aims**

1. Bibliographic research of the plant species to be studied (*S. chrysotrichum*)
2. To prepare organic and aqueous extracts
3. To isolate and purify the compounds of the methanol extract

4. To analyze by GC/MS the hexane and dichloromethane extracts
5. To structurally characterize the isolated compounds
6. To determine the antibacterial activity of extracts and compounds
7. To obtain 10 semi-synthetic derivatives using diosgenin as starting material
8. To determine the antibacterial activity of diosgenin derivatives

## 4. MATERIAL AND METHODS

### 4.1. Materials and reagents

Silica gel (0.040-0.063 mm; EMD chemical inc.) was used as the stationary phase (SP) in column chromatography (CC). Biotage SNAP cartridge (KP-Sil 10g, 50  $\mu$ m irregular silica) and Biotage SNAP Ultra C18 cartridge (12g, 25  $\mu$ m spherical silica) were used on flash column chromatography (Biotage Isolera One Flash Chromatography System). Preparative plate chromatography (PPC) and thin layer chromatography (TLC) were performed using 20 X 20 cm silica gel 60 F-254 plates (Fluka analytical and Merk). The solvents (MERCK, USA) used for the experimental procedures were methanol (CH<sub>3</sub>OH; 99.99%), butanol (BuOH); 99.99%), acetone (99.99%), ethyl acetate (EtOAc; 99.99%), chloroform (CHCl<sub>3</sub>; 98.85%), dichloromethane (CH<sub>2</sub>Cl<sub>2</sub>; 98.85%) and n-hexane (98.99%). For the acetylation reactions, acetic anhydride (Sigma Aldrich), pyridine (Sigma Aldrich) and DMF (Sigma Aldrich) were used. All the aminoalkyl chlorhydrates modulations used for the Williamson ether synthesis were obtained in Sigma Aldrich and were: 2-Chloro-N,N-dimethylethylamine hydrochloride, 1-(2-Chloroethyl)piperidine hydrochloride, 1-(3-Chloropropyl)piperidine monohydrochloride, 1-(2-Chloroethyl)pyrrolidine hydrochloride, 2-(Chloromethyl)-1-ethylpyrrolidine hydrochloride, N-(2-Chloroethyl)dibenzylamine hydrochloride, 2-(2-Chloroethyl)-1,2,3,4-tetrahydroisoquinoline hydrochloride, 4-(2-Chloroethyl)morpholine hydrochloride, and 2-Chloro-N,N-diethylethylamine hydrochloride. Antibacterial and antimycobacterial activity assays were performed using sterile 96 well microplates



with lid (Corning Costar, New York), Mueller Hinton broth (Becton Dickinson, Franklin Lakes, NJ), Middlebrook 7H9 broth (Becton Dickinson, Franklin Lakes, NJ) and Lowenstein Jensen solid medium (Becton Dickinson, Franklin Lakes, NJ). Oleic acid, albumin, dextrose, and catalase (OADC, Becton Dickinson, Franklin Lakes, NJ) was used as enrichment nutrients for the Middlebrook 7H9 broth. Tween 80 (Sigma Aldrich, St Louis, MO), glycerol (Sigma Aldrich, St Louis, MO), and Alamar blue (Biotum, Hayward, CA) were used during the assays, and the antibiotics streptomycin, levofloxacin, rifampicin, isoniazid y ethambutol (Sigma Aldrich, St Louis, MO) were used as controls. The solvents used were dimethylsulfoxide (DMSO) (J.T.Baker, USA) and deionized water.

#### **4.1.1. Equipment used in the experimental procedures**

The vacuum destilation of extracts and samples was performed in a Buchi R300 rotary evaporator. The weight of samples was obtained in a Sartorius B1205 analytical balance; the melting points were determined in a Fisher-Johns apparatus. The flash chromatography was performed in a Biotage Isolera one flash chromatography system. The gas chromatography was performed in an Agilent 6890 chromatography system using a the mass detector IE (70eV) Agilent 5973N and the column HP-5MS (30m x 0.250mm x 0.25m  $\mu$ M). The NMR spectra were recorded on a Bruker NMR400 at 400 MHz for  $^1\text{H}$  NMR,  $^1\text{H}$ - $^1\text{H}$  COSY, NOESY, HSQC, HMBC, and 100 MHz for  $^{13}\text{C}$  NMR and  $^{13}\text{C}$  DEPT using the solvents  $\text{CDCl}_3$ ,  $\text{CD}_3\text{OD}$ , and DMSO. Chemical shifts are reported in ppm relative to TMS. The biological assays

were performed on a level II laminar flow cabinet BSC110011B2-X Biobase and Edgegard using pipettes Biopette A BP1000, BP200 and multichannel pipette VWR. All the consumable resources were sterilized on laboratory autoclave Tuttnauer.

## **4.2. Methods**

The phytochemical work was performed in the laboratorio de química farmacéutica, División de Estudios de Posgrado, Facultad de Ciencias Químicas, Universidad Autónoma de Nuevo León. The synthesis of aminoether derivatives was performed in the Cibles et Médicaments des Infections et du Cancer facilities of the university of Nantes. The biological assays were performed in the Laboratorio de Gastroenterología, Hospital universitario Dr. José Eleuterio González, Universidad Autónoma de Nuevo León.

### **4.2.1. Phytochemistry**

**Vegetal material:** Leaves of *Solanum chrysotrichum* Schldl (1285.0 g dry weight) were collected in Rayones, Nuevo León, México on September 2018 and identified by biologist MSc. Mauricio González-Ferrara. A voucher specimen was stored in the botanic department of Facultad de Biología, Universidad Autónoma de Nuevo León. Voucher specimens (code number: 030242).

#### 4.2.1.1. Extracts preparation

Dried and grounded vegetal material (1285 g) was extracted sequentially by maceration with n-hexane (8 L for 48 h), dichloromethane (8 L for 48 h), methanol (8 L x 3 for 48 h each) and distilled water (8 L for 24 h) to obtain four extracts (Table 1).

**Table 1. Organic and aqueous extracts of *S. chrysotrichum***

Extract	Weight (g)	Yield (%)
Hexane	11	0.85
Dichloromethane	14.4	1.12
Methanol	223	17.35
Aqueous	58	4.51

The hexane and dichloromethane extracts were obtained in order to degrease the plant material. The methanol extract was obtained using a more extensive extraction process because it contains the compounds that exhibit biological activities (antimicrobial and cytotoxic) according to the literature of *genus Solanum*<sup>20</sup>. The composition of the hexane and dichloromethane extracts was analyzed by GC-MS. The methanol extract was subjected to fractionation by column chromatography (CC).

#### 4.2.1.2. Fractionation by column chromatography of the methanol extract of *S. chrysotrichum*

Methanol extract (223 g) was subjected to silica gel CC eluted with a gradient of ethyl acetate/methanol/water, yielding 224 fractions of 400 mL each. Fractions were

analyzed by TLC and observed under UV light (254 and 365 nm) and then sprayed with ceric sulfate. Fractions were pooled according to their TLC pattern into nine fractions (Table 2).

**Table 2. Pooled fractions of methanol extract of *S. chrysotrichum***

<b>Fraction Code</b>	<b>Pooled Fraction</b>	<b>Mobile phase Column chromatography</b>
<b>A</b>	1-25	EtOAc/CH <sub>3</sub> OH (95:5)
<b>B</b>	26-50	EtOAc/CH <sub>3</sub> OH (75:25)
<b>C</b>	51-65	EtOAc/CH <sub>3</sub> OH (65:35)
<b>D</b>	66-128	EtOAc/CH <sub>3</sub> OH (20:80)
<b>E</b>	129-144	EtOAc/CH <sub>3</sub> OH (10:90)
<b>F</b>	145-157	CH <sub>3</sub> OH (100)
<b>G</b>	158-184	CH <sub>3</sub> OH /H <sub>2</sub> O (85:15)
<b>H</b>	185-216	CH <sub>3</sub> OH /H <sub>2</sub> O (75:25)
<b>I</b>	217-224	H <sub>2</sub> O (100)

#### **4.2.1.3. Isolation and purification of compounds from *S. chrysotrichum* methanol extract**

Fraction A (1-6, n-hexane 100%) was not used for the isolation due to the lack of compounds of interest because when analyzed by TLC, only colorants and minority fatty acids were identified.

**Isolation and purification of campesterol- $\beta$ -D-glucoside (SC7B):** Fraction B (6.64 g) was dissolved in hot acetone (35 °C) and then cooled at 4 °C yielding a white solid (98 mg) which was separated by filtration; the liquid mother was distilled in vacuum yielding 5.66 g. On the other hand, the white solid was subjected to preparative TLC chromatography eluted with CHCl<sub>3</sub>/BuOH (6:4) yielding 34.8 mg of

a white solid, then this solid was subjected to silica gel (CC) eluted with a gradient of  $\text{CHCl}_3/\text{BuOH}$ , from subfraction (sf) 36-65 ( $\text{CHCl}_3/\text{BuOH}$  85:15) a white solid SC7B (10.7 mg, 0.000778 %) was obtained.

**Isolation and purification of Salicylic acid (SC10):** The liquid mother obtained above (5.66 g) was subjected to three sequential silica gel CCs eluted the first with  $\text{CHCl}_3/\text{acetone}$ , the second with n-hexane/acetone and the third with  $\text{CHCl}_3/\text{CH}_3\text{O}$ . From the last column was obtained SC10 (11 mg) as colorless crystals.

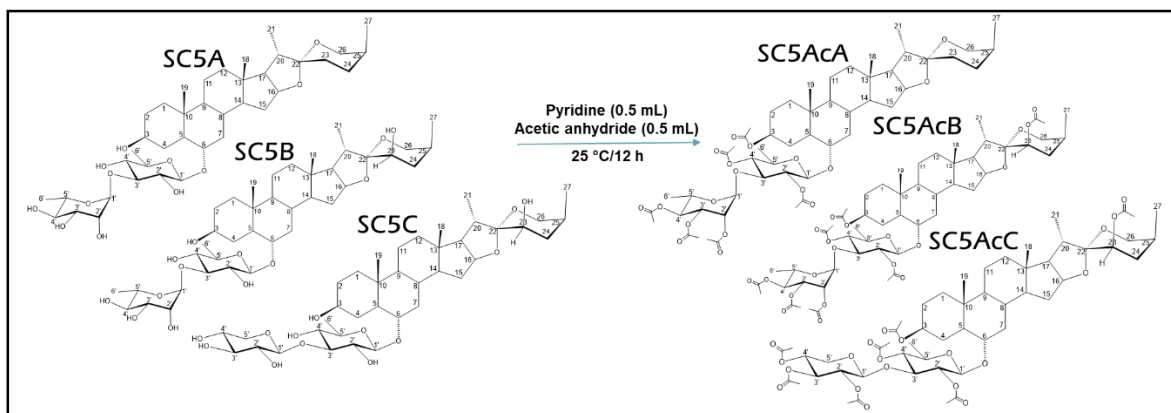
**Isolation and purification of steroidal saponins mixture (SC5):** Fraction C (10.5 g) was dissolved in hot acetone (35 °C) and then cooled at 4 °C yielding a yellowish suspension and the liquid mother which was distilled *in vaccum* (9.28 g). The yellowish suspension was filtered and a white solid was obtained (1.4 g), such solid was indexed as SC5 and was constituted by three steroidal saponins. The dried liquid mother (9.28 g) was subjected to silica gel CC eluted with  $\text{AcOEt}/\text{CH}_3\text{OH}$ . The sf: 79-97 (1.375 g,  $\text{AcOEt}/\text{CH}_3\text{OH}$  85:15) was further precipitated with acetone yielding 1.3 g of SC5. Fraction D (70 g) was subjected to silica gel CC eluted with a gradient of  $\text{AcOEt}/\text{CH}_3\text{OH}$ ; the sf: 41-52 (2.9 g,  $\text{EtOAc}/\text{CH}_3\text{OH}$  80: 20) was further treated with acetone yielding 2.87 g of SC5.

**Isolation and purification of 3'-O-methyl-quercetin-3-O- $\beta$ -D-glucopyranoside (SC11):** Fraction D (70 g) was subjected to silica gel CC the sf: 21-28 (312.5 mg,  $\text{AcOEt}/\text{CH}_3\text{OH}$  9:1) which was treated with liquid-liquid partition (LLP) using  $\text{H}_2\text{O}/\text{AcOEt}$ , then the dried organic phase (194 mg) was subjected to CC eluted with

a gradient of  $\text{CHCl}_3/\text{CH}_3\text{OH}$  yielding the sf: 76-90 (42 mg,  $\text{CHCl}_3/\text{CH}_3\text{OH}$  9:1) which was subjected to preparative plate chromatography (PPC) eluted with  $\text{AcOEt}/\text{CH}_3\text{OH}/\text{H}_2\text{O}$  11:2:2 yielding a yellow resin indexed as SC11 (5 mg).

#### 4.2.2. Acetylation of SC5 mixture

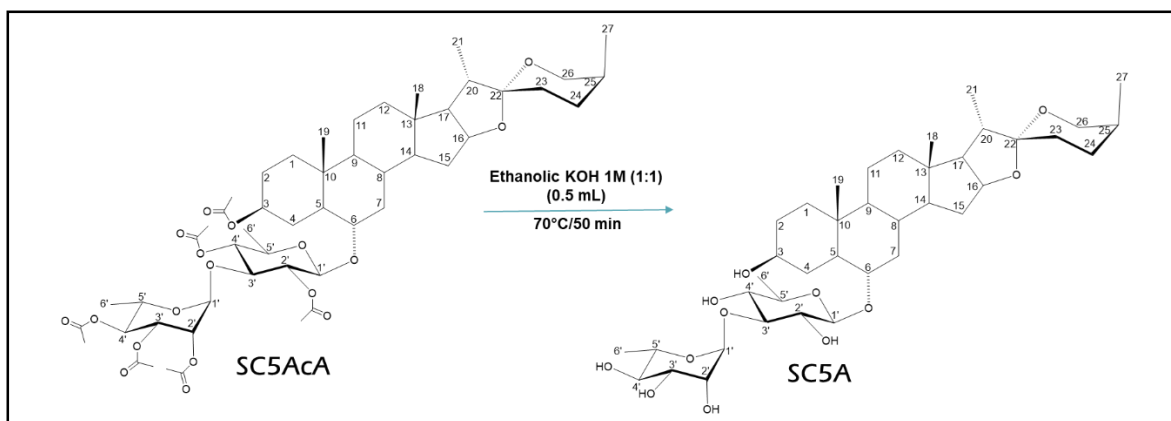
The saponin mixture SC5 (90 mg) was acetylated with pyridine (0.5 mL) as catalyzer and acetic anhydride (0.5 mL) as acetylating agent (scheme 1)<sup>21</sup>. After 24 h at room temperature (25 °C), the reaction mixture was subjected to liquid-liquid partition (LLP) using EtOAc and HCl 10% to remove the pyridine, the organic phase was concentrated *in vacuo*. The organic phase was subjected to silica gel CC eluting with a gradient of hexane/acetone yielding the acetylated products **SC5AcA** (10 mg, sf: 133-153, hexane/acetone 82:18), **SC5AcB** (75 mg, sf: 173-176, n-hexane/acetone 82:18), and **SC5AcC** (10 mg, sf: 200-228, n-hexane/acetone 82:18) as acetylated steroidal saponins. The reaction was repeated with a bigger quantity of starting material depending on the requirements of the acetylated derivative to be used in further procedures.



**Scheme 1.** Acetylation reaction of the steroidal saponin mixture SC5

### 4.2.3. Saponification of acetylated derivatives

Each acetylated derivative (10 mg) was subjected to a saponification reaction (scheme 2), dissolving in 0.5 mL of ethanolic KOH 1M (1:1), then the solution was heated at 70 °C for 50 min<sup>22</sup>. Then LLP was performed for the crude of reaction with EtOAc/H<sub>2</sub>O, the organic phase was dried with anhydrous sodium sulfate and concentrated in vacuum yielding 8.4 mg of each saponification products, the steroidal saponins **SC5A**, **SC5B** and **SC5C**. The reaction was repeated with a bigger quantity of starting material depending on the requirements of the saponin to be used in further procedures.

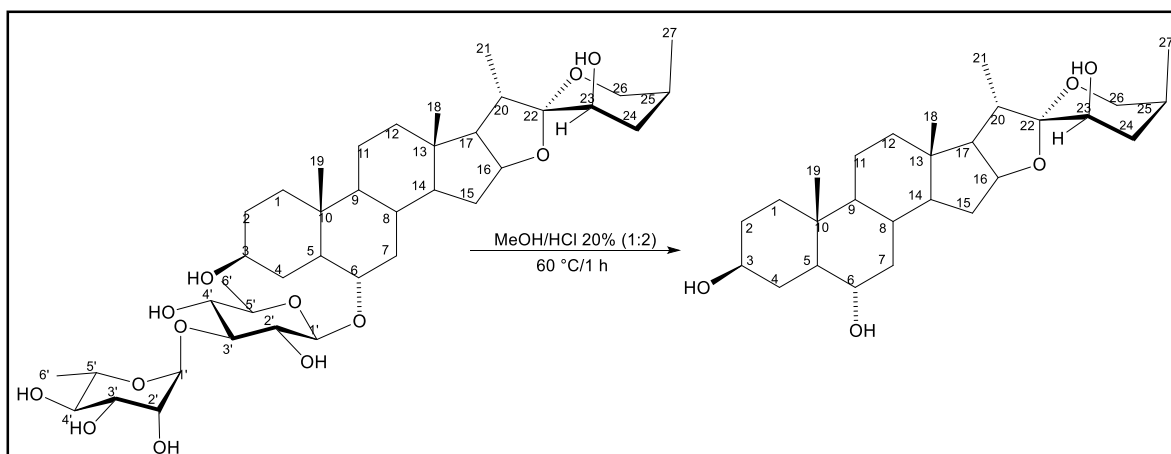


**Scheme 2.** Saponification reaction for acetylated saponins

### 4.2.4. Acid hydrolysis of steroidal saponin SC5B

The steroidal saponin SC5B was subjected to acid hydrolysis using the conditions proposed by Zamilpa *et al.*, 2002<sup>23</sup>, but the attempt was unrewarded and the starting material was recovered completely. The steroidal saponin SC5B was therefore

subjected to acid hydrolysis by modifying the acid hydrolysis conditions proposed by Tava *et al.*, 2017<sup>24</sup> (scheme 3). The reaction was attempted five times, using 500 mg of SC5B each time, hydrolyzing with 40 mL of hydroalcoholic solution composed by CH<sub>3</sub>OH/HCl 20% (1:2), and applying stirring and reflux under 60 °C for 1 h. After the reaction time was completed, the reaction mixture was neutralized at pH 7 with NH<sub>4</sub>OH (26%), afterward the crude of reaction was distilled *in vacuum* and subjected to LLP using EtOAc as organic phase. The organic phase was concentrated and analyzed by TLC observing a mixture of two compounds from which one of them is the aglycone of SC5B. Unfortunately, the hydrolysis products had similar R<sub>F</sub> in the TLC and conventional chromatographic methods were not efficient to obtain the pure compounds. Therefore, the hydrolysis products were acetylated in order to better resolve the components of the mixture; however the sample was not separated when chromatographic methods were applied. The aglycone of SC5B remained in mixture with its corresponding artefacts.

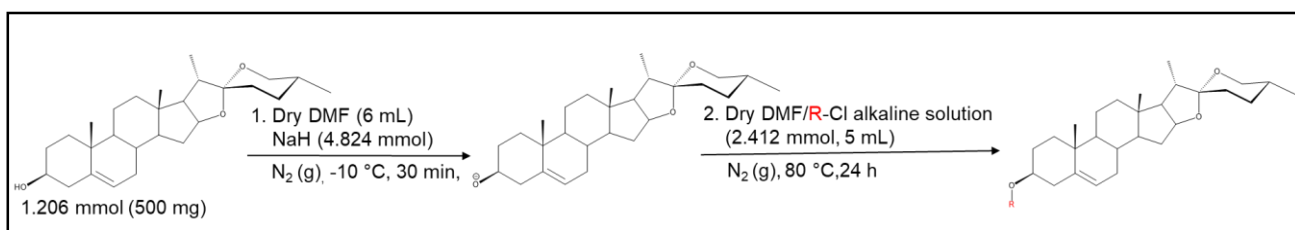


**Scheme 3.** Acid hydrolysis of steroidal saponin SC5B



#### 4.2.5. Synthesis of diosgenin aminoethers derivatives by Williamson ether synthesis reaction

Using diosgenin as starting material (Alfa Aesar, Thermo Fischer Scientific) nine aminoether derivatives were synthesized applying the procedure for the Williamson ether synthesis (scheme 4)<sup>25</sup>. The procedure consisted in prepare the corresponding alkali metal alkoxide of diosgenin by reacting the starting material with a strong base such as NaH, KH, LHMDS or LDA; the solvent used could be a dipolar aprotic solvent such as DMF or DMSO. As final step, the aminoalkyl halide (figure 3) is added to the reaction mixture in order to undergo SN2 reaction for the formation of the aminoether product.



**Scheme 4.** Williamson ether synthesis

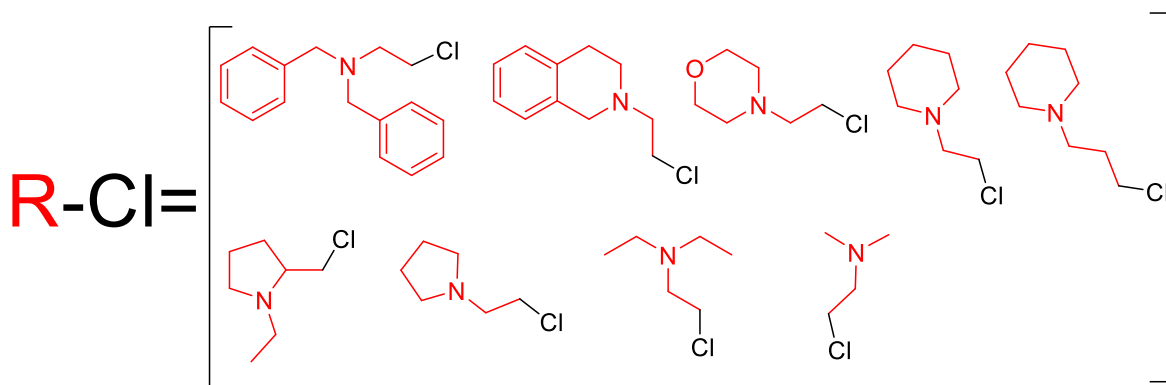
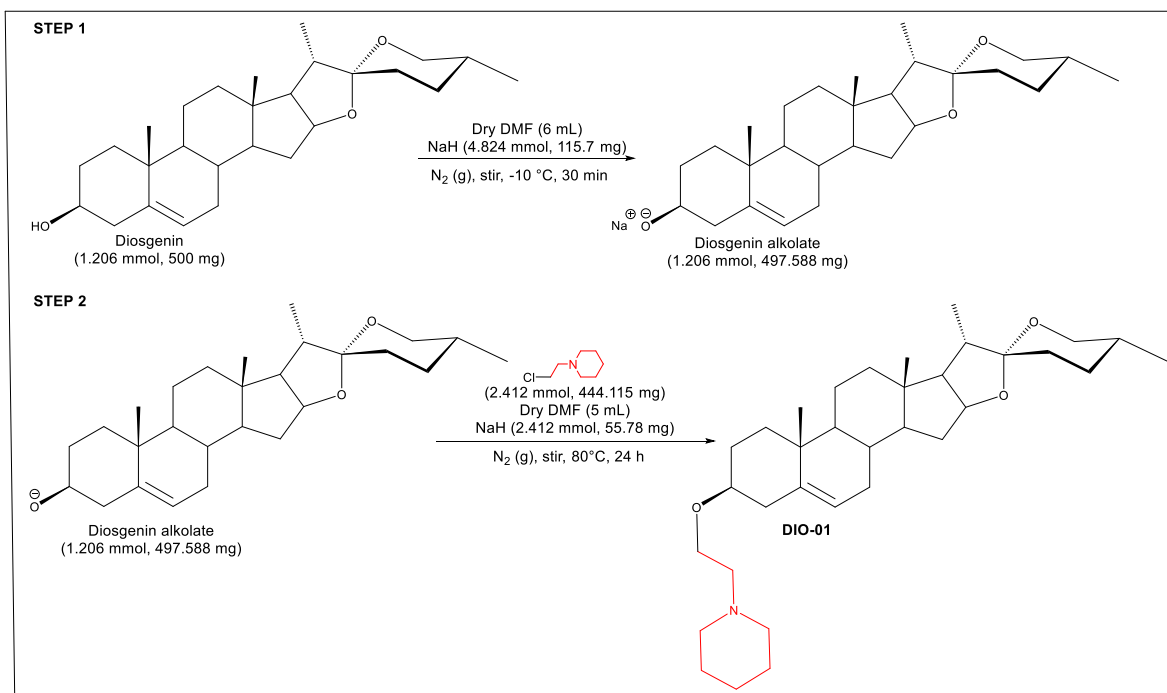


**Figure 3.** Aminoalkyl halide modulations used for the synthesis of diosgenin aminoether derivatives

#### 4.2.5.1. Synthesis of derivative DIO-01

The step one of the reaction consisted in add solid NaH (4.824 mmol, 115.7 mg) at -10 °C under N<sub>2</sub> atmosphere to a solution of dry DMF (6 mL) containing the starting material diosgenin (1.206 mmol, 500 mg), the mixture was stirred for 30 min and afterward, the step two consisted in heat at 80 °C to subsequently add by dropwise a solution of dry DMF (5 mL) containing the aminoalkyl halide modulation 1-(2-chloroethyl)piperidine hydrochloride (2.412 mmol, 444.115 mg) and NaH (2.412 mmol, 55.7 mg). The reaction was stirred for 24 h at 80 °C under N<sub>2</sub> atmosphere (scheme 5). The reaction was monitored every 3 h by thin layer chromatography (TLC) eluting with the gradient CHCl<sub>3</sub>/CH<sub>3</sub>OH 9:1, the product showed considerable higher polarity than the starting material and the minority side products.



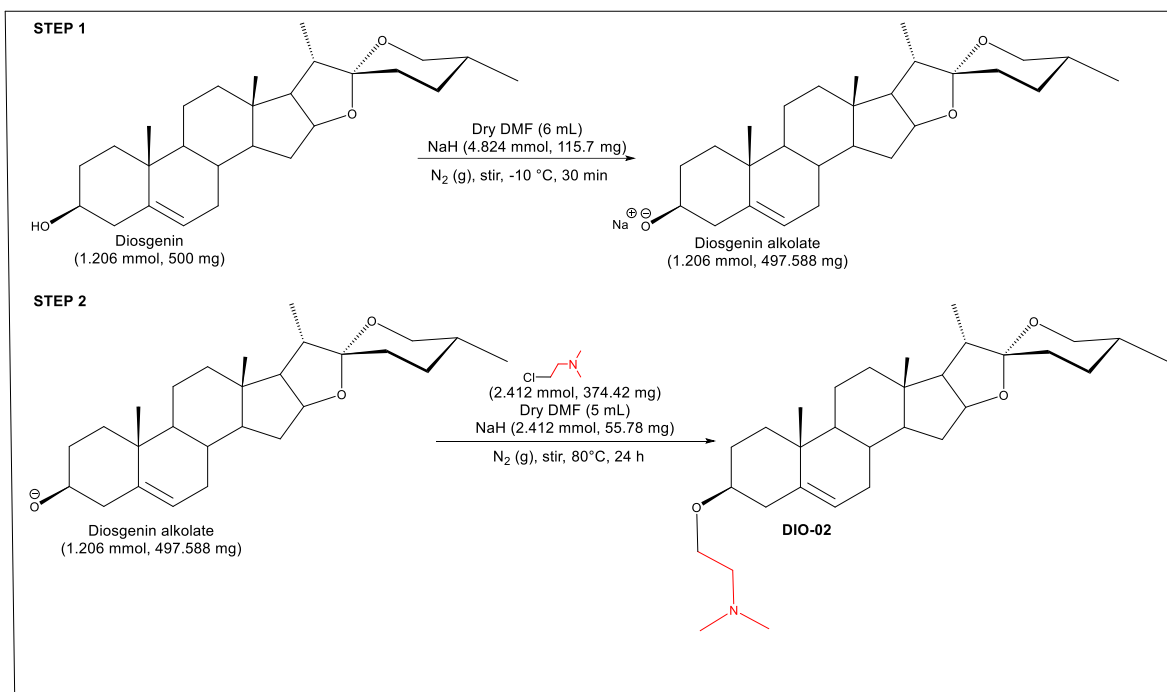
**Scheme 5.** Synthesis of aminoether derivative DIO-01

After the reaction time was completed, the crude of reaction was diluted in 50 mL of EtOAc and liquid-liquid partition (LLP) was performed consecutively with 50 mL of H<sub>2</sub>O, HCl 1M, K<sub>2</sub>CO<sub>3</sub> 50% and Brine. After the four partitions, the organic phase was dried using sodium sulfate and concentrated to dryness in vacuum. Flash column chromatography (FCC) was performed using a silica gel BUCHI flash cartridge (12 g, 15-40 μm particle size, 17 mL column volume) eluting with a gradient of cyclohexane/EtOAc/CH<sub>3</sub>OH increasing the polarity by 5% until cyclohexane/EtOAc 70:30 was reached, then the gradient was changed to CH<sub>3</sub>OH 100% and eluted until product detection by electroevaporative light-scattering detection (ELSD) stopped. The pure product of reaction **DIO-01** was obtained as the fraction 25-26 (fraction volume: 20 mL, faction polarity: CH<sub>3</sub>OH 100%, fraction dry weight: 275 mg).

#### 4.2.5.2. Synthesis of derivative DIO-02

The step one of the reaction consisted in add solid NaH (4.824 mmol, 115.7 mg) at -10 °C under N<sub>2</sub> atmosphere to a solution of dry DMF (6 mL) containing the starting material diosgenin (1.206 mmol, 500 mg), the mixture was stirred for 30 min and afterward, the step two consisted in heat at 80 °C to subsequently add by dropwise a solution of dry DMF (5 mL) containing the aminoalkyl halide modulation 2-chloro-N,N-dimethylethylamine hydrochloride (2.412 mmol, 374.42 mg) and NaH (2.412 mmol, 55.7 mg). The reaction was stirred for 24 h at 80 °C under N<sub>2</sub> atmosphere (scheme 6). The reaction was monitored every 3 h by thin layer chromatography

(TLC) eluting with the gradient  $\text{CHCl}_3/\text{CH}_3\text{OH}$  9:1, the product showed considerable higher polarity than the starting material and the minority side products.



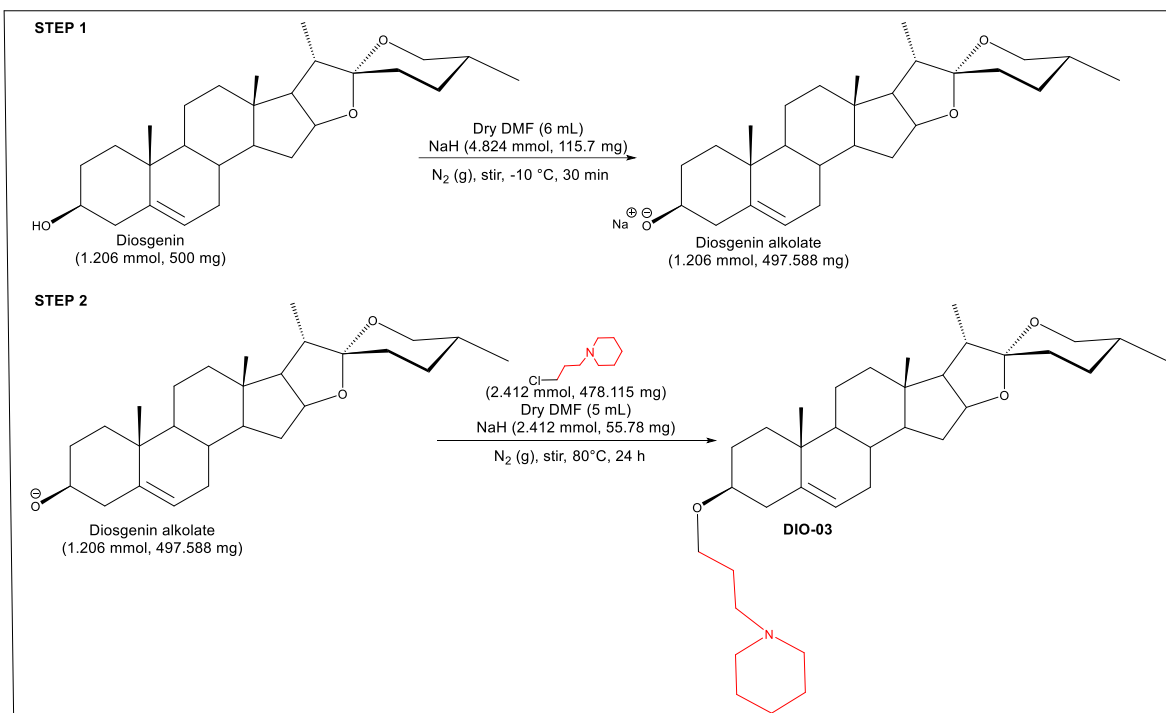
**Scheme 6.** Synthesis of aminoether derivative DIO-02

After the reaction time was completed, the crude of reaction was diluted in 50 mL of EtOAc and liquid-liquid partition (LLP) was performed consecutively with 50 mL of  $\text{H}_2\text{O}$ , HCl 1M,  $\text{K}_2\text{CO}_3$  50% and Brine. After the four partitions, the organic phase was dried using sodium sulfate and concentrated to dryness in vacuum. Flash column chromatography (FCC) was performed using a silica gel BUCHI flash cartridge (12 g, 15-40  $\mu\text{m}$  particle size, 17 mL column volume) eluting with a gradient of cyclohexane/EtOAc/  $\text{CH}_3\text{OH}$  increasing the polarity by 5% until cyclohexane/EtOAc 70:30 was reached, then the gradient was changed to  $\text{CH}_3\text{OH}$  100% and eluted until product detection by electroevaporative light-scattering detection (ELSD) stopped.

The pure product of reaction **DIO-02** was obtained as the fraction 37-47 (fraction volume: 20 mL, fraction polarity: CH<sub>3</sub>OH 100%, fraction dry weight: 128.8 mg).

#### **4.2.5.3. Synthesis of derivative DIO-03**

The step one of the reaction consisted in add solid NaH (4.824 mmol, 115.7 mg) at -10 °C under N<sub>2</sub> atmosphere to a solution of dry DMF (6 mL) containing the starting material diosgenin (1.206 mmol, 500 mg), the mixture was stirred for 30 min and afterward, the step two consisted in heat at 80 °C to subsequently add by dropwise a solution of dry DMF (5 mL) containing the aminoalkyl halide modulation 1-(3-cholopropyl)piperidine hydrochloride (2.412 mmol, 478 mg) and NaH (2.412 mmol, 55.7 mg). The reaction was stirred for 24 h at 80 °C under N<sub>2</sub> atmosphere (scheme 7). The reaction was monitored every 3 h by thin layer chromatography (TLC) eluting with the gradient CHCl<sub>3</sub>/CH<sub>3</sub>OH 9:1, the product showed considerable higher polarity than the starting material and the minority side products.

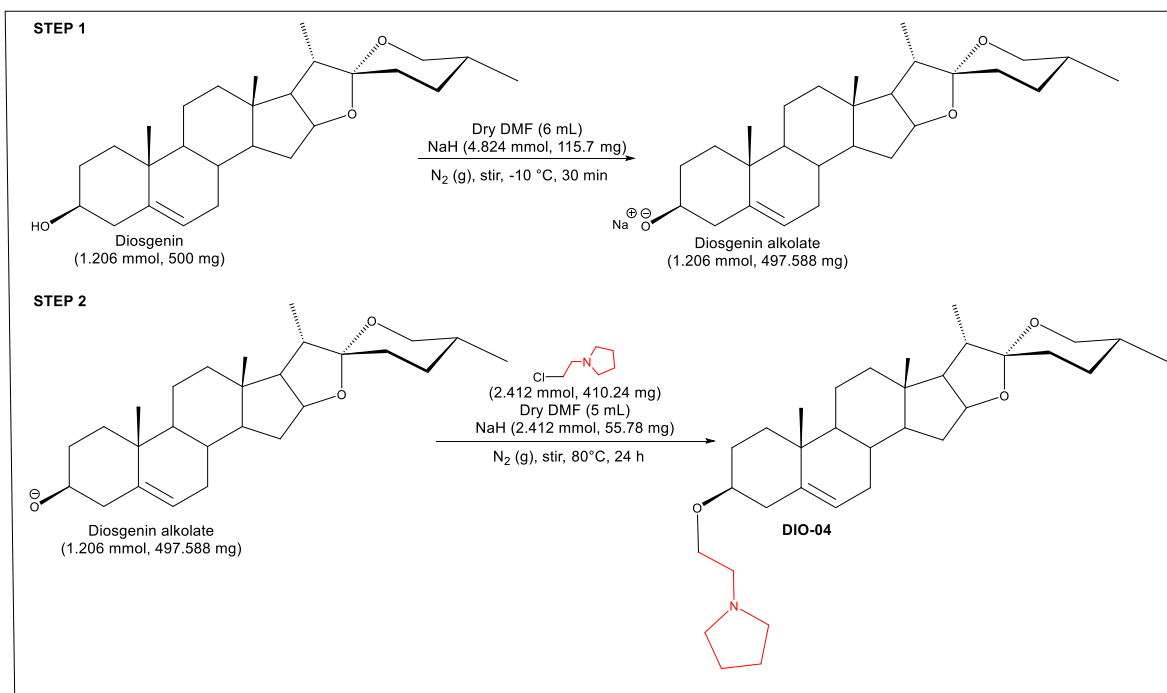


**Scheme 7.** Synthesis of aminoether derivative DIO-03

After the reaction time was completed, the crude of reaction was diluted in 50 mL of EtOAc and LLP was performed consecutively with 50 mL of H<sub>2</sub>O, HCl 1M, K<sub>2</sub>CO<sub>3</sub> 50% and Brine. After the four partitions, the organic phase was dried using sodium sulfate and concentrated to dryness in vacuum. Two consecutive open column chromatography (CC) were performed using silica gel as stationary phase eluting in both CC with a gradient of cyclohexane/EtOAc/CH<sub>3</sub>OH increasing the polarity by 5% until CH<sub>3</sub>OH 100%. The pure product of reaction **DIO-03** was obtained as the fraction (6-15)(125-160) (fraction volume: 3 mL, fraction polarity: CH<sub>3</sub>OH 100%, fraction dry weight: 150 mg).

#### 4.2.5.4. Synthesis of derivative DIO-04

The step one of the reaction consisted in add solid NaH (4.824 mmol, 115.7 mg) at -10 °C under N<sub>2</sub> atmosphere to a solution of dry DMF (6 mL) containing the starting material diosgenin (1.206 mmol, 500 mg), the mixture was stirred for 30 min and afterward, the step two consisted in heat at 80 °C to subsequently add by dropwise a solution of dry DMF (5 mL) containing the aminoalkyl halide modulation 1-(2-chloroethyl)pyrrolidine hydrochloride (2.412 mmol, 410.24 mg) and NaH (2.412 mmol, 55.7 mg). The reaction was stirred for 24 h at 80 °C under N<sub>2</sub> atmosphere (scheme 8). The reaction was monitored every 3 h by thin layer chromatography (TLC) eluting with the gradient CHCl<sub>3</sub>/CH<sub>3</sub>OH 9:1, the product showed considerable higher polarity than the starting material and the minority side products.



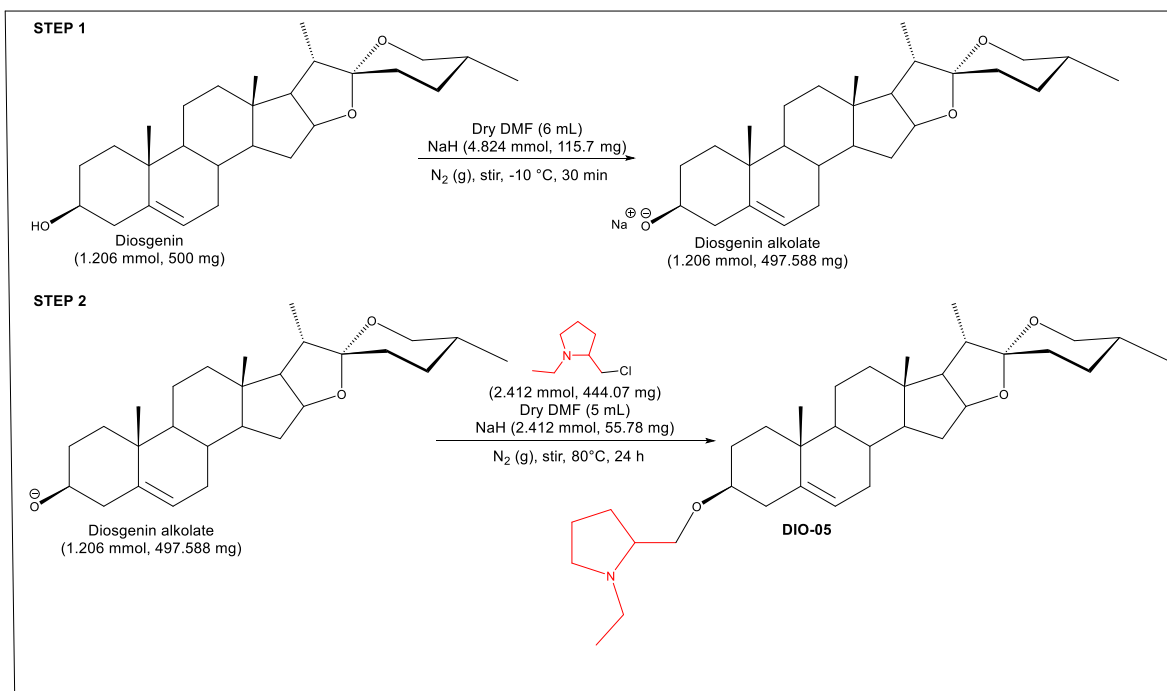
**Scheme 8.** Synthesis of aminoether derivative DIO-04

After the reaction time was completed, the crude of reaction was diluted in 50 mL of EtOAc and LLP was performed consecutively with 50 mL of H<sub>2</sub>O, HCl 1M, K<sub>2</sub>CO<sub>3</sub> 50% and Brine. After the four partitions, the organic phase was dried using sodium sulfate and concentrated to dryness *in vacuo*. Open column chromatography (CC) was performed using silica gel as stationary phase eluting with a gradient of cyclohexane/EtOAc/CH<sub>3</sub>OH increasing the polarity by 5% until CH<sub>3</sub>OH 100%. The pure product of reaction **DIO-04** was obtained as the fraction (69-128) (fraction volume: 10 mL, faction polarity: CH<sub>3</sub>OH 100%, fraction dry weight: 27 mg).

#### 4.2.5.5. Synthesis of derivative DIO-05

The step one of the reaction consisted in add solid NaH (4.824 mmol, 115.7 mg) at -10 °C under N<sub>2</sub> atmosphere to a solution of dry DMF (6 mL) containing the starting material diosgenin (1.206 mmol, 500 mg), the mixture was stirred for 30 min and afterward, the step two consisted in heat at 80 °C to subsequently add by dropwise a solution of dry DMF (5 mL) containing the aminoalkyl halide modulation 2-(chloromethyl)-1-ethylpyrrolidine hydrochloride (2.412 mmol, 444.07 mg) and NaH (2.412 mmol, 55.7 mg). The reaction was stirred for 24 h at 80 °C under N<sub>2</sub> atmosphere (scheme 9). The reaction was monitored every 3 h by thin layer chromatography (TLC) eluting with the gradient CHCl<sub>3</sub>/CH<sub>3</sub>OH 9:1, the product showed considerable higher polarity than the starting material and the minority side products.



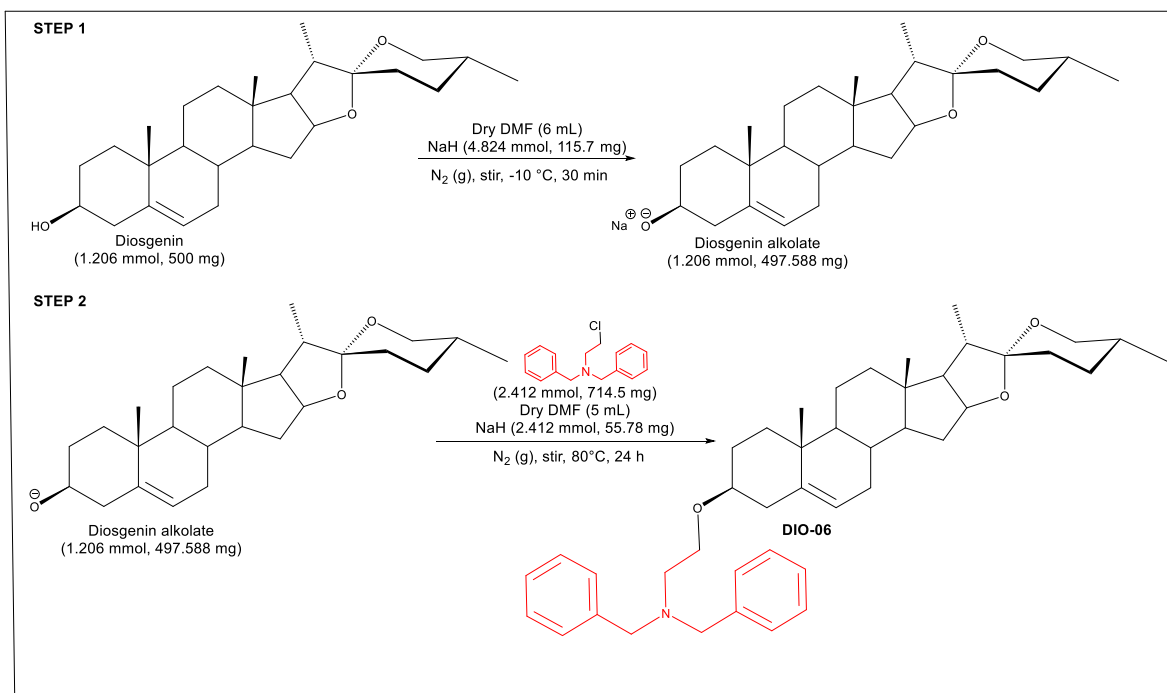


**Scheme 9.** Synthesis of aminoether derivative DIO-05

After the reaction time was completed, the crude of reaction was diluted in 50 mL of EtOAc and LLP was performed consecutively with 50 mL of H<sub>2</sub>O, HCl 1M, K<sub>2</sub>CO<sub>3</sub> 50% and Brine. After the four partitions, the organic phase was dried using sodium sulfate and concentrated to dryness *in vacuo*. Flash column chromatography (FCC) was performed using a silica gel BUCHI flash cartridge (12 g, 15-40 μm particle size, 17 mL column volume) eluting with a gradient of cyclohexane/EtOAc/CH<sub>3</sub>OH increasing the polarity by 5% until cyclohexane/EtOAc 70:30 was reached, then the gradient was changed to CH<sub>3</sub>OH 100% and eluted until product detection by electroevaporative light-scattering detection (ELSD) stopped. The pure product of reaction **DIO-05** was obtained as the fraction 19-37 (fraction volume: 20 mL, fraction polarity: CH<sub>3</sub>OH 100%, fraction dry weight: 91.6 mg).

#### 4.2.5.6. Synthesis of derivative DIO-06

The step one of the reaction consisted in add solid NaH (4.824 mmol, 115.7 mg) at  $-10\text{ }^{\circ}\text{C}$  under  $\text{N}_2$  atmosphere to a solution of dry DMF (6 mL) containing the starting material diosgenin (1.206 mmol, 500 mg), the mixture was stirred for 30 min and afterward, the step two consisted in heat at  $80\text{ }^{\circ}\text{C}$  to subsequently add by dropwise a solution of dry DMF (5 mL) containing the aminoalkyl halide modulation N-(2-chloroethyl)dibenzylamine hydrochloride (2.412 mmol, 714.5 mg) and NaH (2.412 mmol, 55.7 mg). The reaction was stirred for 24 h at  $80\text{ }^{\circ}\text{C}$  under  $\text{N}_2$  atmosphere (scheme 10). The reaction was monitored every 3 h by thin layer chromatography (TLC) eluting with the gradient  $\text{CHCl}_3/\text{acetone}$  98:2, the product showed lower polarity than the starting material.

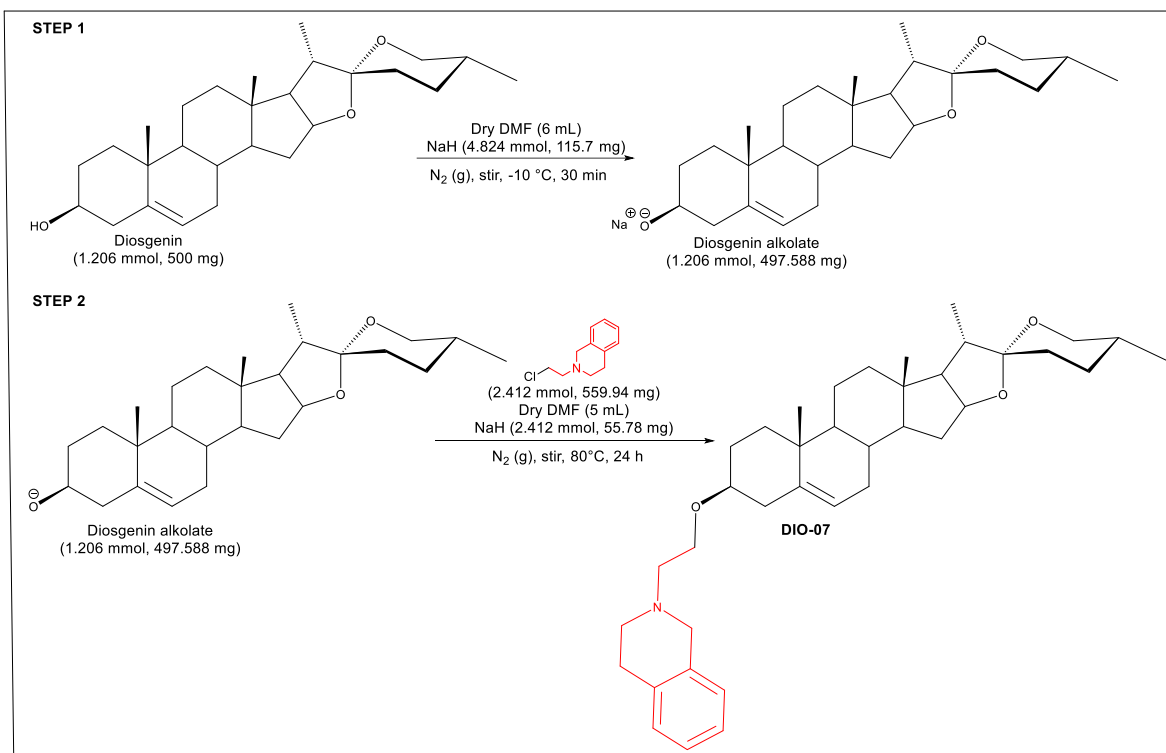


**Scheme 10.** Synthesis of aminoether derivative DIO-06

After the reaction time was completed, the crude of reaction was diluted in 50 mL of EtOAc and LLP was performed consecutively with 50 mL of H<sub>2</sub>O, HCl 1M, K<sub>2</sub>CO<sub>3</sub> 50% and Brine. After the four partitions, the organic phase was dried using sodium sulfate and concentrated to dryness *in vacuum*. Flash column chromatography (FCC) was performed using a silica gel BUCHI flash cartridge (12 g, 15-40 μm particle size, 17 mL column volume) eluting with a gradient of cyclohexane/EtOAc/CH<sub>3</sub>OH increasing the polarity by 5% until cyclohexane/EtOAc 70:30 was reached. It wasn't possible to purify the product of reaction by FCC, however the recovered crude of reaction (544 mg) was subjected to precipitation with CH<sub>3</sub>OH, and after filtration the pure product **DIO-06** was obtained as a white solid (90 mg).

#### 4.2.5.7. Synthesis of derivative DIO-07

The step one of the reaction consisted in add solid NaH (4.824 mmol, 115.7 mg) at -10 °C under N<sub>2</sub> atmosphere to a solution of dry DMF (6 mL) containing the starting material diosgenin (1.206 mmol, 500 mg), the mixture was stirred for 30 min and afterward, the step two consisted in heat at 80 °C to subsequently add by dropwise a solution of dry DMF (5 mL) containing the aminoalkyl halide modulation 2-(2-chloroethyl)-1,2,3,4-tetrahydroisoquinoline hydrochloride (2.412 mmol, 559.94 mg) and NaH (2.412 mmol, 55.7 mg). The reaction was stirred for 24 h at 80 °C under N<sub>2</sub> atmosphere /scheme 11). The reaction was monitored every 3 h by thin layer chromatography (TLC) eluting with the gradient CHCl<sub>3</sub>/CH<sub>3</sub>OH 9:1, the product showed lower polarity than the starting material.

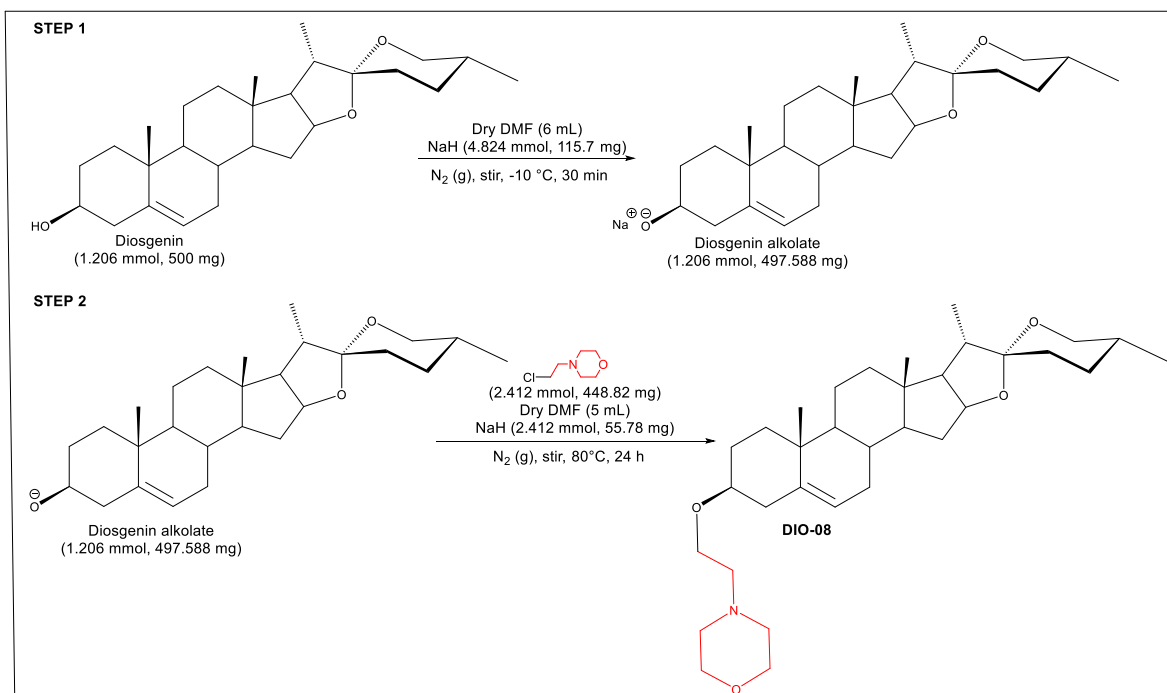


**Scheme 11.** Synthesis of aminoether derivative DIO-07

After the reaction time was completed, the crude of reaction was diluted in 50 mL of EtOAc LLP was performed consecutively with 50 mL of H<sub>2</sub>O, HCl 1M, K<sub>2</sub>CO<sub>3</sub> 50% and Brine. After the four partitions, the organic phase was dried using sodium sulfate and concentrated to dryness *in vacuo*. Flash column chromatography (FCC) was performed using a silica gel BUCHI flash cartridge (12 g, 15-40 μm particle size, 17 mL column volume) eluting with a gradient of cyclohexane/EtOAc/CH<sub>3</sub>OH increasing the polarity by 5% until cyclohexane/EtOAc 70:30 was reached, then the gradient was changed to CH<sub>3</sub>OH 100% and eluted until product detection by electroevaporative light-scattering detection (ELSD) stopped. The pure product of reaction **DIO-07** was obtained as the fraction 19-30 (fraction volume: 20 mL, fraction polarity: CH<sub>3</sub>OH 100%, fraction dry weight: 156.2 mg).

#### 4.2.5.8. Synthesis of derivative DIO-08

The step one of the reaction consisted in add solid NaH (4.824 mmol, 115.7 mg) at  $-10\text{ }^{\circ}\text{C}$  under  $\text{N}_2$  atmosphere to a solution of dry DMF (6 mL) containing the starting material diosgenin (1.206 mmol, 500 mg), the mixture was stirred for 30 min and afterward, the step two consisted in heat at  $80\text{ }^{\circ}\text{C}$  to subsequently add by dropwise a solution of dry DMF (5 mL) containing the aminoalkyl halide modulation 4-(2-chloroethyl)morpholine hydrochloride (2.412 mmol, 448.82 mg) and NaH (2.412 mmol, 55.7 mg). The reaction was stirred for 24 h at  $80\text{ }^{\circ}\text{C}$  under  $\text{N}_2$  atmosphere (scheme 12). The reaction was monitored every 3 h by thin layer chromatography (TLC) eluting with the gradient  $\text{CHCl}_3/\text{CH}_3\text{OH}$  9:1, the product showed lower polarity than the starting material.



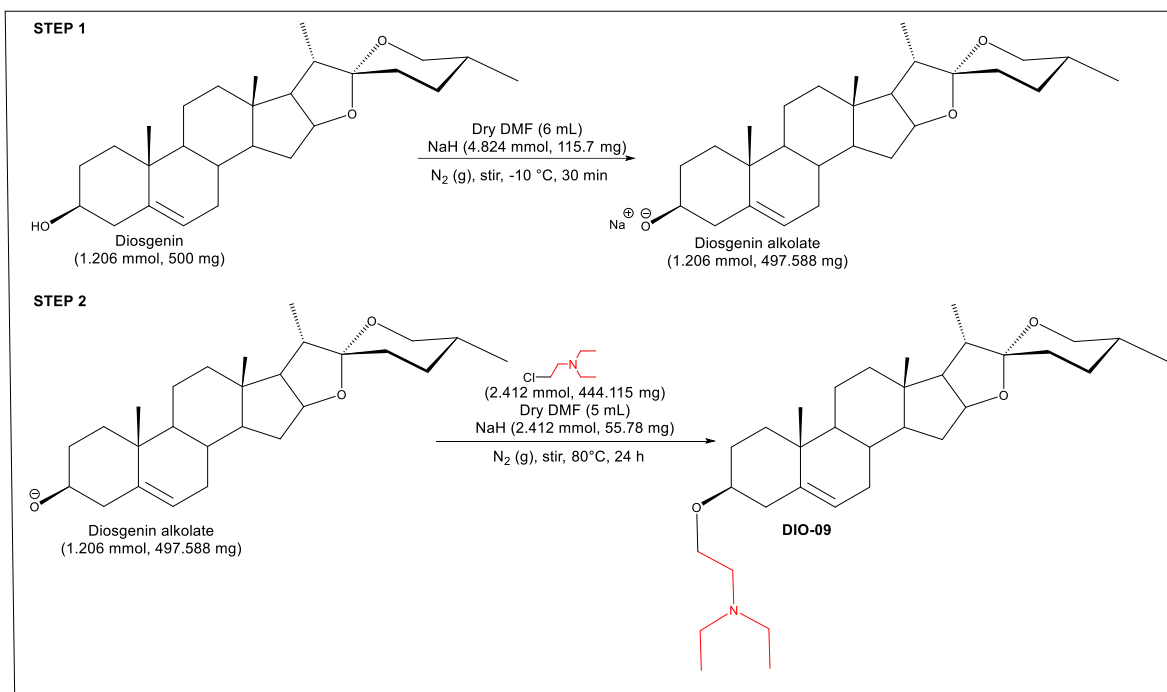
**Scheme 12.** Synthesis of aminoether derivative DIO-08

After the reaction time was completed, the crude of reaction was diluted in 50 mL of EtOAc and LLP was performed consecutively with 50 mL of H<sub>2</sub>O, HCl 1M, K<sub>2</sub>CO<sub>3</sub> 50% and Brine. After the four partitions, the organic phase was dried using sodium sulfate and concentrated to dryness *in vacuo*. Flash column chromatography (FCC) was performed using a silica gel BUCHI flash cartridge (12 g, 15-40 μm particle size, 17 mL column volume) eluting with a gradient of cyclohexane/EtOAc/CH<sub>3</sub>OH increasing the polarity by 5% until cyclohexane/EtOAc 70:30 was reached, then the gradient was changed to CH<sub>3</sub>OH 100% and eluted until product detection by electroevaporative light-scattering detection (ELSD) stopped. The pure product of reaction **DIO-08** was obtained as the fraction 45-55 (fraction volume: 20 mL, faction polarity: CH<sub>3</sub>OH 100%, fraction dry weight: 113.6 mg).

#### 4.2.5.9. Synthesis of derivative DIO-09

The step one of the reaction consisted in add solid NaH (4.824 mmol, 115.7 mg) at -10 °C under N<sub>2</sub> atmosphere to a solution of dry DMF (6 mL) containing the starting material diosgenin (1.206 mmol, 500 mg), the mixture was stirred for 30 min and afterward, the step two consisted in heat at 80 °C to subsequently add by dropwise a solution of dry DMF (5 mL) containing the aminoalkyl halide modulation N,N-diethylethylamine hydrochloride (2.412 mmol, 415.1 mg) and NaH (2.412 mmol, 55.7 mg). The reaction was stirred for 24 h at 80 °C under N<sub>2</sub> atmosphere (scheme 13). The reaction was monitored every 3 h by thin layer chromatography (TLC) eluting

with the gradient  $\text{CHCl}_3/\text{CH}_3\text{OH}$  9:1, the product showed lower polarity than the starting material.



**Scheme 13.** Synthesis of aminoether derivative DIO-09

After the reaction time was completed, the crude of reaction was diluted in 50 mL of EtOAc and LLP was performed consecutively with 50 mL of  $\text{H}_2\text{O}$ , HCl 1M,  $\text{K}_2\text{CO}_3$  50% and Brine. After the four partitions, the organic phase was dried using sodium sulfate and concentrated to dryness *in vacuo*. Open column chromatography (CC) was performed using silica gel as stationary phase eluting with a gradient of Hexane/EtOAc/ $\text{CH}_3\text{OH}$  increasing the polarity by 5% until  $\text{CH}_3\text{OH}$  100%. The pure product of reaction **DIO-09** was obtained as the fraction 86-100 (fraction volume: 6 mL, faction polarity:  $\text{CH}_3\text{OH}$  100%, fraction dry weight: 55.5 mg).

#### **4.2.6. Structural characterization of compounds**

The structural characterization of the compounds was performed by analysis of  $^1\text{H}$  and  $^{13}\text{C}$  NMR spectrums and 2D NMR experiments such as COSY, NOESY, HSQC, and HMBC.

#### **4.2.7. Biological assays**

##### **4.2.7.1. Microdilution method for the determination of antibacterial activity against clinical isolates of drug-resistant bacteria**

The antibacterial activity of extracts was assessed by the microdilution method<sup>26</sup> against six clinical isolates of gram-negative bacteria (carbapenem-resistant (CR) *Acinetobacter baumannii* (12-666), extended spectrum  $\beta$ -lactamase-positive (ESBL) *Escherichia coli* (14-2081), (CR) *Pseudomonas aeruginosa* (13-1391), carbapenem and broad spectrum cephalosporins-resistant (CCR) *Klebsiella pneumoniae* (14-3335), carbapenem and broad spectrum cephalosporins-resistant (CCR) *Klebsiella pneumoniae* NDM-1+ positive (14-3335), ESBL *Klebsiella pneumoniae* (14-2081) and three clinical isolates of gram-positive bacteria (methicillin-resistant (MR) *Staphylococcus aureus* (MRSA, 14-2095), linezolid-resistant (LR) *Staphylococcus epidermidis* (14-583) and vancomycin-resistant (VR) *Enterococcus faecium* (10-984). The bacterial drug-resistant clinical isolates were stored and handled at the Hospital Universitario Dr. José Eleuterio González, Monterrey, Nuevo León, Mexico.



**Bacterial inoculum preparation:** the tested bacterial strains were cultured in blood-agar plates (5% of blood) and incubated for 24 h (48 h for *Pseudomonas aeruginosa*). Once obtained the colonies of each bacterial strain, 1 to 3 colonies were transferred to a tube containing 5 mL of sterile saline solution (0.85 %) equaling the turbidity to the 0.5 Mc Farland standard ( $1.5 \times 10^8$  CFU/mL), then, 10  $\mu$ L of the solution is transferred to a tube containing 11 mL of Muller Hinton broth to obtain the assay inoculum with a concentration of  $5 \times 10^5$  CFU/mL.

**Biological assay:** using a 96-well sterile plate with lid, 100  $\mu$ L of Muller Hinton broth was added to all the wells, then 100  $\mu$ L of the tested compounds were added by duplicate in the line A of the plate (the concentration of compounds solutions are 200  $\mu$ g/mL and were prepared with DMSO and Muller Hinton broth as solvents). Once added the solutions, serial dilution (1:2) were performed by transferring 100  $\mu$ L of each well in line A to the line B, mixing in line B and repeating the procedure from line B to line C and so on to the line G and discarding the last 100  $\mu$ L took from this last line (the line H will be used as control). The last step was the addition of 100  $\mu$ L of the assay inoculum to all the wells of the plate except for the ones of line H, then the plate was sealed with its lid and incubated at 37 °C for 24/48 h depending on the tested bacterial strain. After the addition of the assay inoculum to the wells, the final concentrations of compound in each line were: A: 50  $\mu$ g/mL, B: 25  $\mu$ g/mL, C: 12.5  $\mu$ g/mL, D: 6.25  $\mu$ g/mL, E: 3.125  $\mu$ g/mL, F: 1.56  $\mu$ g/mL, G: 0.78  $\mu$ g/mL. After incubation, the minimal inhibitory concentration (MIC) for each tested compound was evaluated visually, being considered as inhibition of the bacterial growing the absence of turbidity on the wells, while the formation of bacterial pellets on the

bottom of the wells and turbidity were considered a sign of bacteria growing. The MIC for each compound was determined as the lower concentration of the compound in which inhibition for the bacterial growth was observed.

#### **4.2.7.2. Alamar blue method for the determination of antibacterial activity against sensitive and drug-resistant *Mycobacterium tuberculosis***

The antibacterial activity against *M. tuberculosis* (antimycobacterial activity) was determined by the Alamar blue method<sup>27</sup>, applying the modifications described by Favela-Hernández *et al.*, 2012<sup>28</sup>. The tested strains were the sensitive ATTC strain H37Rv (sensitive to rifampicin, isoniazid, ethambutol, and pyrazinamide) and the G122 strain, a drug-resistant clinical isolate (resistant to rifampicin, ethambutol, and streptomycin). The *M. tuberculosis* strains were stored and handled at the Hospital Universitario Dr. José Eleuterio González, Monterrey, Nuevo León, Mexico.

**Bacterial inoculum preparation:** the tested *M. tuberculosis* strains were cultured in Lowenstein-Jensen medium and incubated 14 days at 37 °C. After the incubation time, one colony was transferred from the Lowenstein-Jensen medium to a tube containing 5 mL of Middlebrook 7H9 broth enriched with 10 % of OADC (oleic, albumin, dextrose, catalase), then the tube was incubated for 14 days at 37 °C to obtain the liquid inoculum. After incubation time, the liquid inoculum must be equal in turbidity to the 1.0 Mc Farland standard to further transfer 1 volume of the liquid inoculum to 19 volumes of Middlebrook 7H9 broth enriched with 10 % of OADC, to obtain the assay inoculum.

**Biological assay:** in a 96-well sterile plate with lid the wells in line A and the wells H1, H2, H3, H10, H11, and H12 were filled with 200  $\mu$ L of sterile deionized water, then 100  $\mu$ L of Middlebrook 7H9 broth enriched with 10% of OADC was added to all the wells from line B to line G, and to the wells H4 and H5. The wells H6 and H7 were filled with 180  $\mu$ L of broth and the wells H8 and H9 with 200  $\mu$ L respectively. The next step consisted in the addition of 100  $\mu$ L of the tested compounds by duplicate in line B (the concentration of compounds solutions were 200  $\mu$ g/mL and were prepared with DMSO and Middlebrook 7H9 broth as solvents). Once added the solutions, serial dilution (1:2) were performed by transferring 100  $\mu$ L of each well in line B to the line C, mixing in line C and repeating the procedure reaching line G and discarding the last 100  $\mu$ L of this line. After serial dilution 100  $\mu$ L of assay inoculum was added to the wells in lines B to G and in wells H4 and H5 (100  $\mu$ L) and H6 and H7 (20  $\mu$ L), then the plate was sealed with its lid and further incubated 5 days at 37  $^{\circ}$ C. After incubation time, 12  $\mu$ L of tween 80 (10 %) and 20  $\mu$ L of resazurin were added to the wells H4, H5, H6, H7, H8, and H9 (bacterial growth controls), then the plate was sealed and incubated 24 h at 37  $^{\circ}$ C. After incubation time, the wells H4 and H5 displayed pink color (abundant bacterial growth), wells H6 and H7 displayed violet color (poor bacterial growth), and wells H8 and H9 displayed blue color (absence of bacterial growth) indicating that the bacterial growth was appropriate for the addition of tween 80 and resazurin to all the wells in lines B to G to further seal the plate and incubate 24 h at 37  $^{\circ}$ C. After incubation time, the minimal inhibitory concentration (MIC) for each tested compound was evaluated visually, being observed as inhibition of the bacterial growth the blue colored wells, while the bacterial growth was observed in the pink colored wells. The MIC for each compound

was determined as the lower concentration of the compound in which inhibition of the bacterial growth was observed.

#### **4.2.8. Disposal of waste**

The disposal of the waste generated during the phytochemical work was carried out as established by the regulation of Environment and Safety department of the Facultad de Ciencias Químicas de la Universidad Autónoma de Nuevo León. The disposal of the waste generated during the synthesis of aminoether derivatives work was carried out as established by the regulation of Environment and Safety department of the Université de Nantes. The disposal of the waste generated during the biological assays was carried out according to the internal regulations of the Laboratorio de Diagnóstico Microbiológico Especializado del Hospital Universitario Dr. José Eleuterio González.

## 5. RESULTS AND DISCUSSION

### 5.1. Structural elucidation of some compounds isolated from the methanol extract of *S. chrysotrichum*

From the methanol extract (230 g) of *S. chrysotrichum* were isolated and structurally characterized salicylic acid (SC10), campesterol- $\beta$ -D-glucoside (SC7B), the saponins SC5A, SC5B and SC5C that were characterized by analyzing its acetylated derivatives (SC5AcA, SC5AcB and SC5AcC), and the flavonol isorhamnetin-3-O-glucoside (SC11). The physical and spectroscopic properties as well as the structural characterization of the compounds are discussed in this chapter.

#### 5.1.1. Physical and spectroscopic data of salicylic acid (SC10)

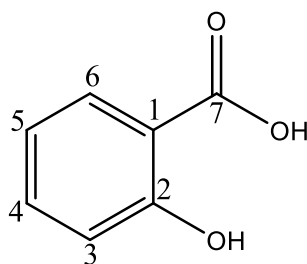


**Figure 4.** Salicylic acid (SC10)

**Compound SC10** (Figure 4): colorless crystals (11 mg, 0.000856 %), soluble in  $\text{CHCl}_3$ , acetone, and  $\text{CH}_3\text{OH}$ . mp. 155-158 °C,  $\text{C}_7\text{H}_6\text{O}_3$ , M.W. 138.032 g/mol. IR  $\nu_{\text{max}}$ : 3231  $\text{cm}^{-1}$ (OH stretch), 2917.9, 2850.12  $\text{cm}^{-1}$  (C-H stretching) 1653  $\text{cm}^{-1}$ (C=O

stretching), 1610  $\text{cm}^{-1}$ (C=C stretching aromatic), 1442  $\text{cm}^{-1}$ (C-C stretching), 1383  $\text{cm}^{-1}$  (C-O stretching), 1252  $\text{cm}^{-1}$ , 1243  $\text{cm}^{-1}$ (Ar-H deformation in the plane), 852  $\text{cm}^{-1}$ , 783  $\text{cm}^{-1}$ (Ar-H, deformation disubstituted *ortho*)  $\text{cm}^{-1}$ .  $^1\text{H}$  NMR (400 MHz,  $\text{CDCl}_3$ )  $\delta$  10.37 (s, 1H, H-COOH), 7.96 (dd,  $J = 7.98$ , 1.58 Hz, 1H, H-6), 7.56 (ddd,  $J = 7.81$ , 7.00, 1.66 Hz, 1H, H-4), 7.04 (d,  $J = 8.4$  Hz, 1H, H-3), 6.97 (ddd,  $J = 7.98$ , 7.16, 0.82 Hz, 1H, H-5).  $^{13}\text{C}$  NMR (100 MHz,  $\text{CDCl}_3$ )  $\delta$  174.71 (C-7), 162.19 (C-2), 136.98 (C-4), 130.95 (C-6), 119.60 (C-5), 117.84 (C-3), 111.31 (C-1).

#### 5.1.1.1. Structural elucidation of salicylic acid (SC10)

The IR spectrum of SC10 (Figure 5) displayed the characteristic band of carboxylic acid group [2500-3200  $\text{cm}^{-1}$ , OH (s) and 1653  $\text{cm}^{-1}$ , C=O (s)]; phenolic group (3231  $\text{cm}^{-1}$  and 1383  $\text{cm}^{-1}$ ); and aromatic bands (1610, 1252, 1243, 852, 783) of aromatic ring *ortho* substituted. The IR spectrum was almost identical to the published by Mikenda *et al.*, 1995<sup>29</sup> and Sigala *et al.*, 2015<sup>30</sup>. Both intra and intermolecular hydrogen bonding between phenolic group and carboxylic group were observed for SC10 in solution, a very likely situation in aprotic solvents such as the one used to record the spectra on the present study ( $\text{CDCl}_3$ ), and the fact is well reinforced by experimental evidence as discussed before and even theoretic studies like the one performed by Chen *et al.* 2001<sup>31</sup>.

The NMR  $^1\text{H}$  spectrum of SC10 (Figure 6) showed a broad signal of carboxylic acid at  $\delta$  10.37 (s, 1H, COOH), an aromatic methine at  $\delta$  7.96 (dd,  $J = 7.98$ ,  $J = 1.58$  Hz, 1H, H-6) coupling in *ortho* with H-5 and in *meta* with H-4; a second aromatic methine

at  $\delta$  7.56 (ddd,  $J=7.81$ ,  $J=7.00$ ,  $J=1.66$  Hz, 1H, H-4) coupling in *ortho* with H-5 and H-3 and in *meta* with H-6; then a third aromatic methine was observed at  $\delta$  7.04 (d,  $J=8.4$  Hz, 1H, H-3) coupling in *ortho* with H-4; and a fourth aromatic methine at  $\delta$  6.97 (ddd,  $J=7.59$ ,  $J=7.16$ ,  $J=0.82$  Hz, 1H, H-5) coupling in *ortho* with H-4 and H-6 and in *meta* with H-3. On this particular  $^1\text{H}$  NMR spectrum, it is noteworthy the absence of the hydroxyl proton signal on the spectrum of salicylic acid, which could be explained because of the formation of intramolecular hydrogen bonding between the carboxylic acid function and the hydroxyl on the molecule, resulting in a dramatic deshielding effect on the hydroxyl proton and displacing its corresponding singlet signal farther downfield ( $\delta$  13-18 ppm), exceeding the range in which the  $^1\text{H}$  NMR spectrum was recorded. The COSY spectrum (Figure 7) displayed the following cross-peaks at three bond distance ( $^3J_{\text{H-H}}$ ): H-6/H-5, H-5/H-4, H-4/H-3, and four bond distance ( $^4J_{\text{H-H}}$ ): H-6/H-4 and H-5/H-3 showing concordance with the substitution pattern proposed for SC10.

The  $^{13}\text{C}$  NMR spectrum (Figure 8) showed the presence of a carboxylic carbon  $\delta$  174.70 (C7), a phenolic quaternary carbon  $\delta$  162.19 (C2), four aromatic methines  $\delta$  136.98 (C4), 130.94 (C6), 119.60 (C5), 117.84 (C3) and one aromatic quaternary carbon  $\delta$  111.308 (C1). The analysis of the  $^{13}\text{C}$  NMR spectrum shows concordance with the observations on the  $^1\text{H}$  NMR spectrum and the carbon types (quaternary and methines) were confirmed by DEPT90 and DEPT135 experiments, however, the planar structure of SC10 was confirmed by analysis of 2D NMR data (HSQC, HMBC, COSY). The HSQC (figure 10) spectrum of SC10 confirmed the assignment of the aromatic methines and quaternary carbons. The HMBC (Figure 10) spectrum



displayed cross-peaks between the carbons and protons of the aromatic rings at two bonds distance ( $^2J_{C-H}$ ): C-2/H-3, three bond distance ( $^3J_{C-H}$ ): C-1/H-3, C-1/H-5, C-2/H-4, C-2/H-6, C-3/H-5, C-4/H-6, C-5/H-3, C-6/H-4, and the key correlation C-7/H-6 that is the main evidence of the substitution pattern in SC10, being the molecule an *ortho*-disubstituted six-member aromatic ring. Based on the analysis of the NMR and IR data, and comparing with the reports in the literature<sup>29,30</sup>, and database<sup>32,33</sup>, the compound SC10 was salicylic acid.

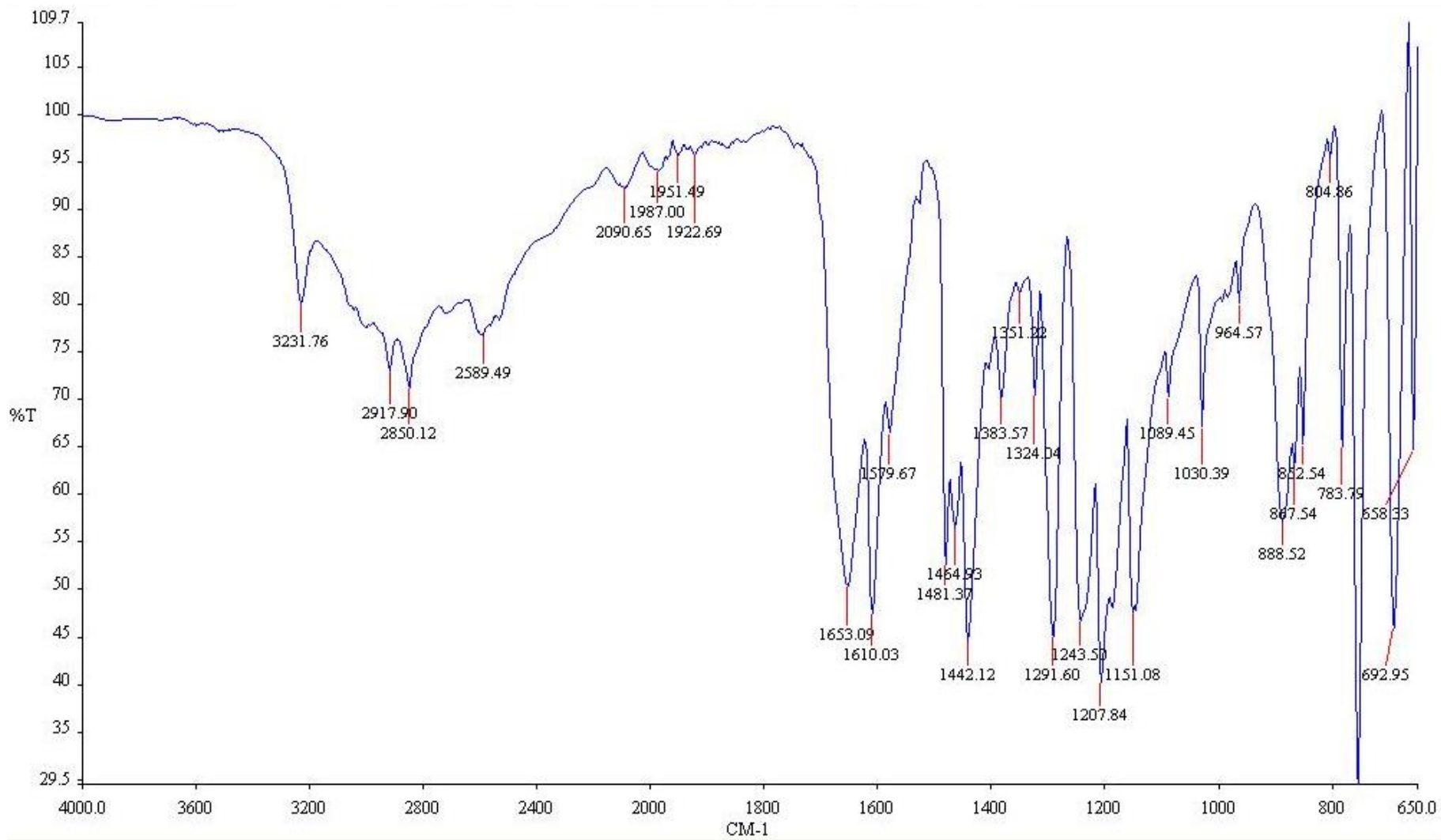


**Figure 5.** FT-IR spectrum of salicylic acid (SC10)

SC10A  
18069-02  
SC10 / CDCl<sub>3</sub>  
1H-RMN

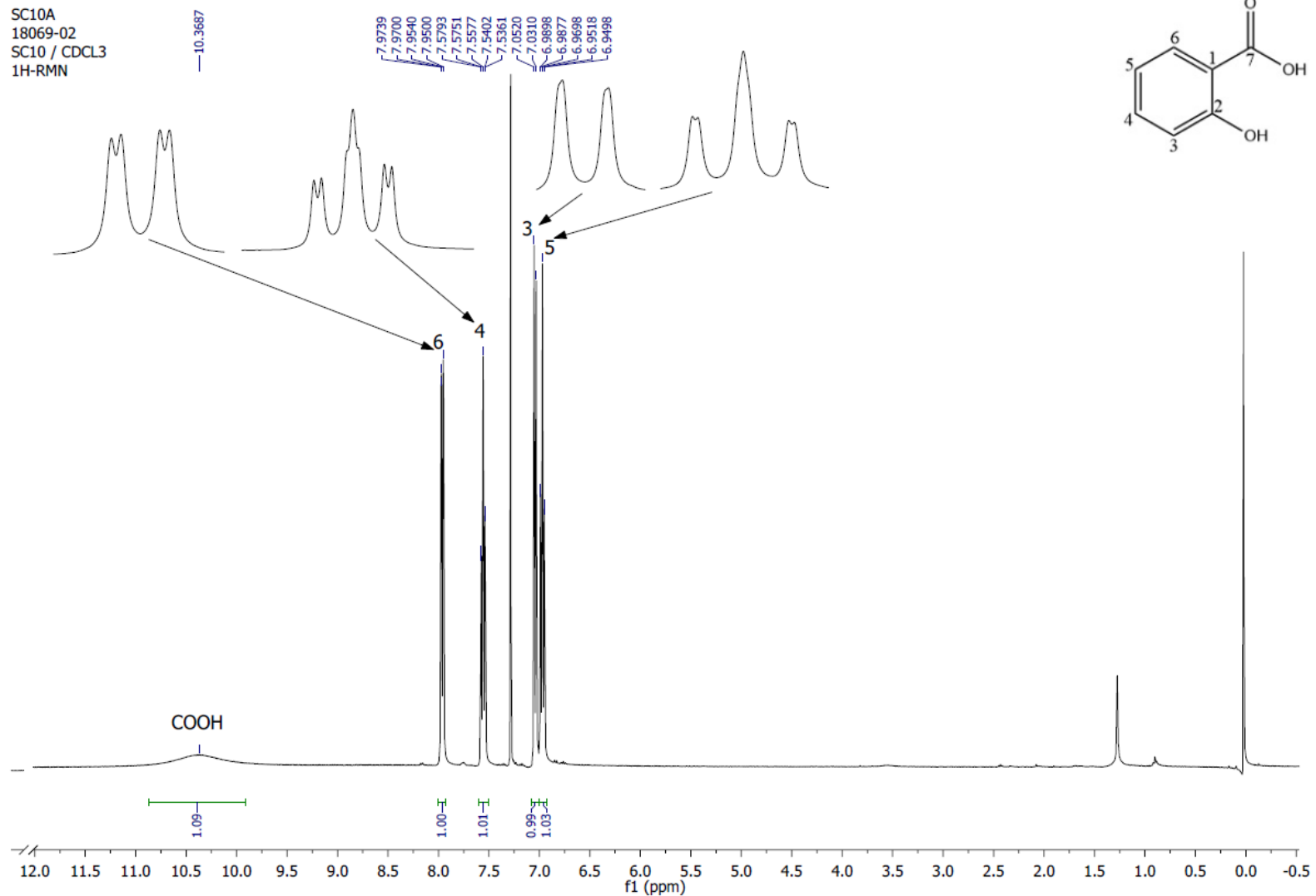
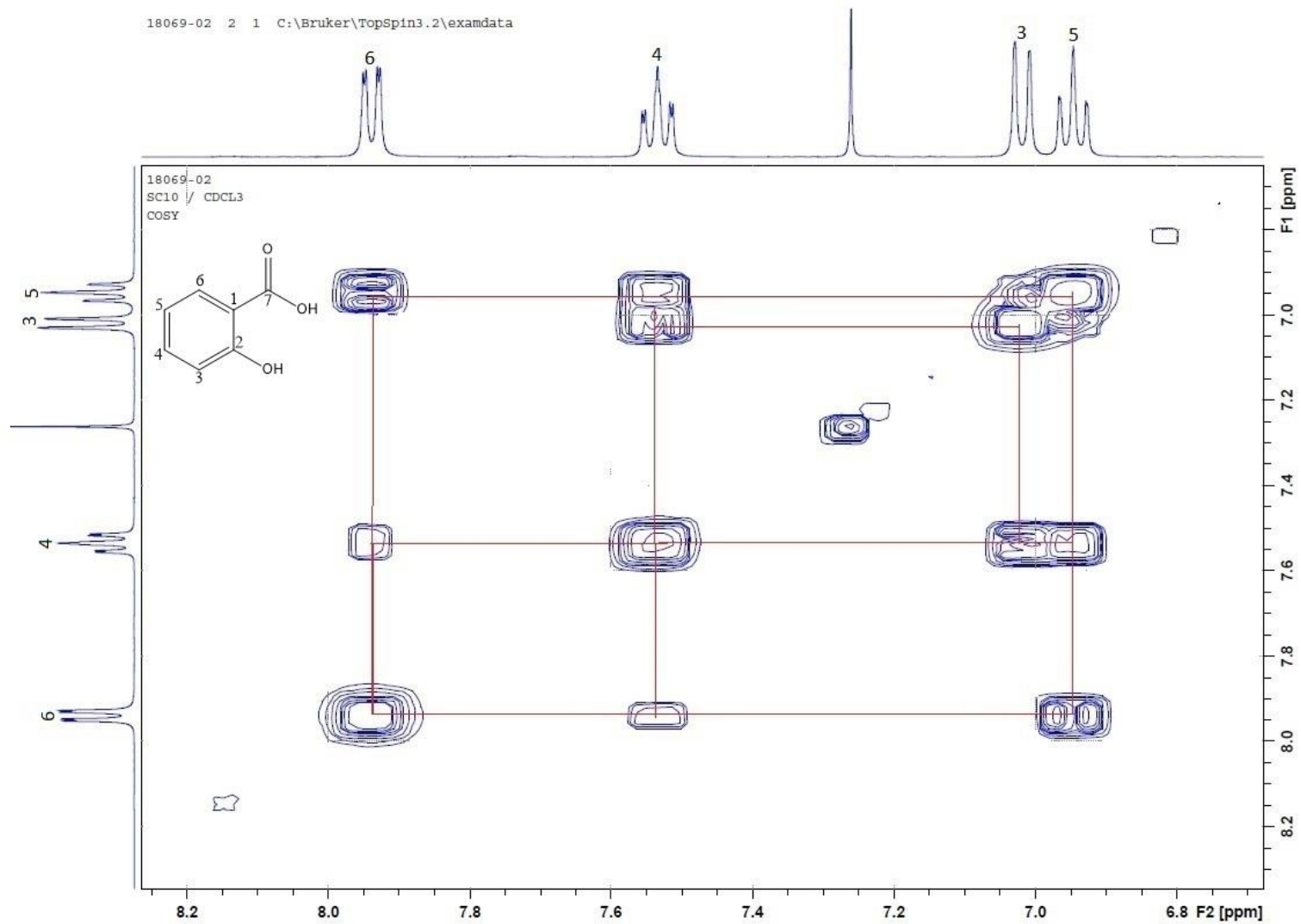
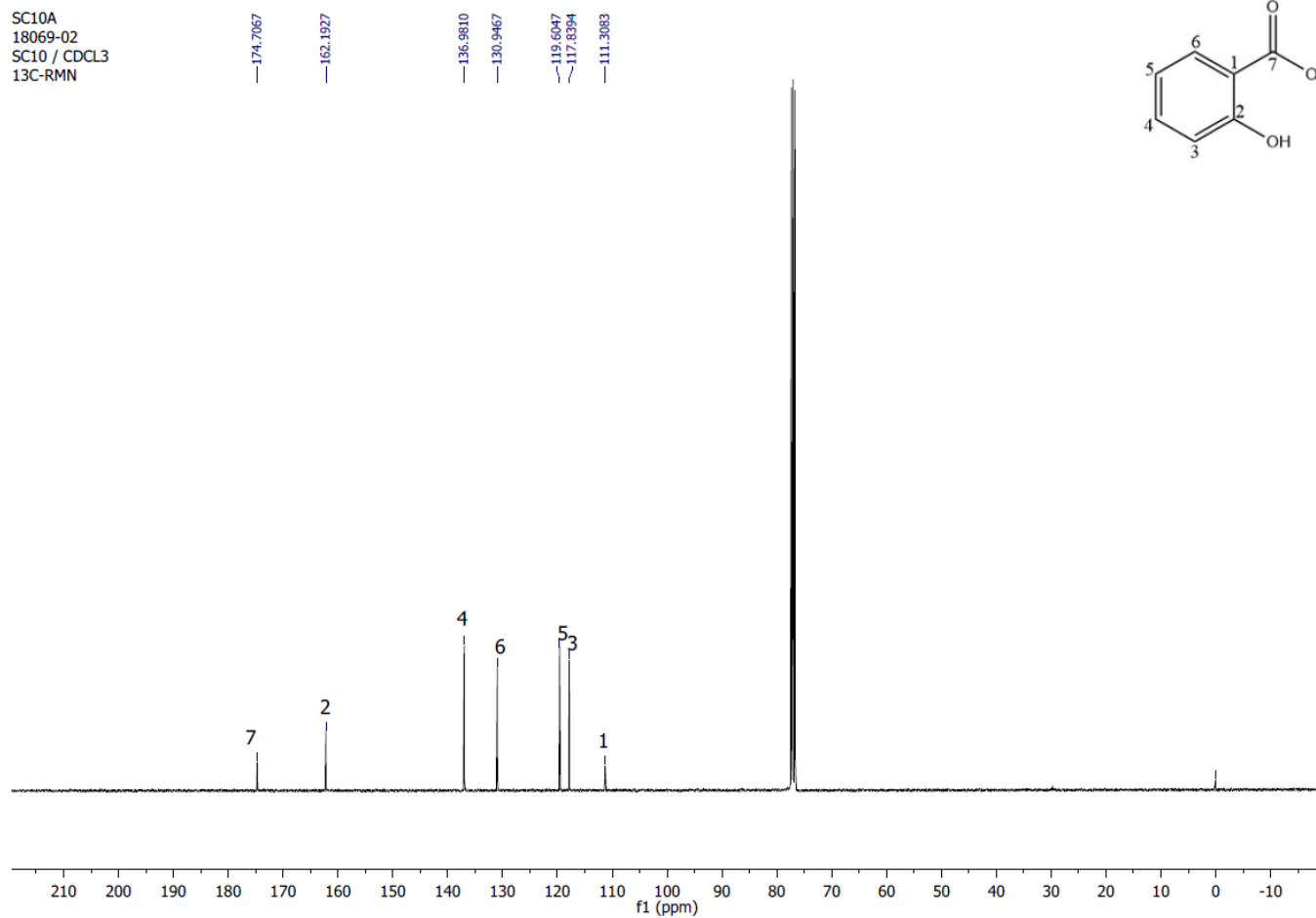


Figure 6. <sup>1</sup>H NMR spectrum (400 MHz, CDCl<sub>3</sub>) of salicylic acid (SC10)



**Figure 7.** COSY NMR spectrum (400 MHz, CDCl<sub>3</sub>) of salicylic acid (SC10)

SC10A  
18069-02  
SC10 / CDCl<sub>3</sub>  
13C-RMN



**Figure 8.** <sup>13</sup>C NMR spectrum (100 MHz, CDCl<sub>3</sub>) of salicylic acid (SC10)

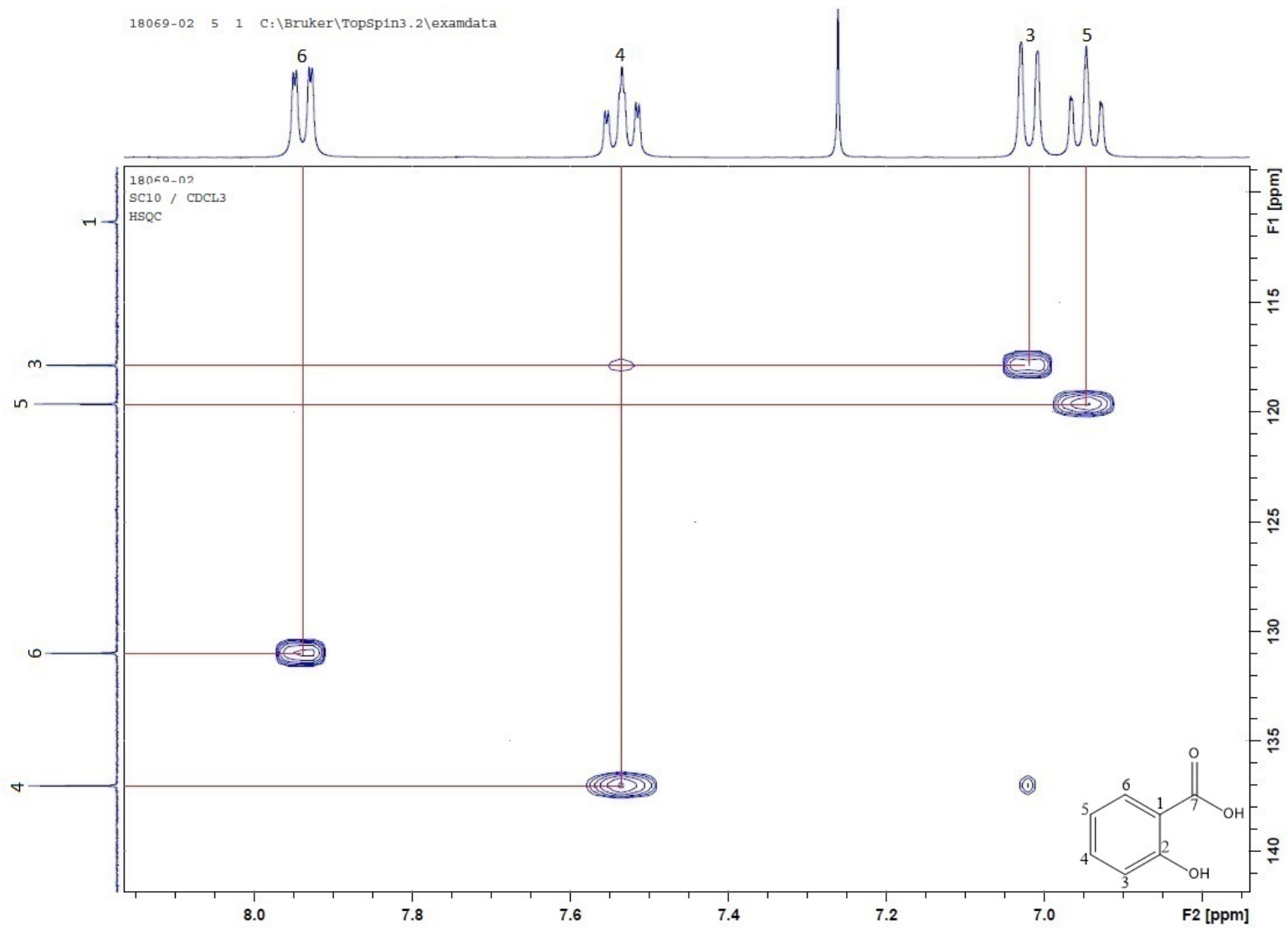


**Figure 9.** HSQC NMR spectrum (400 MHz, CDCl<sub>3</sub>) of salicylic acid (SC10)

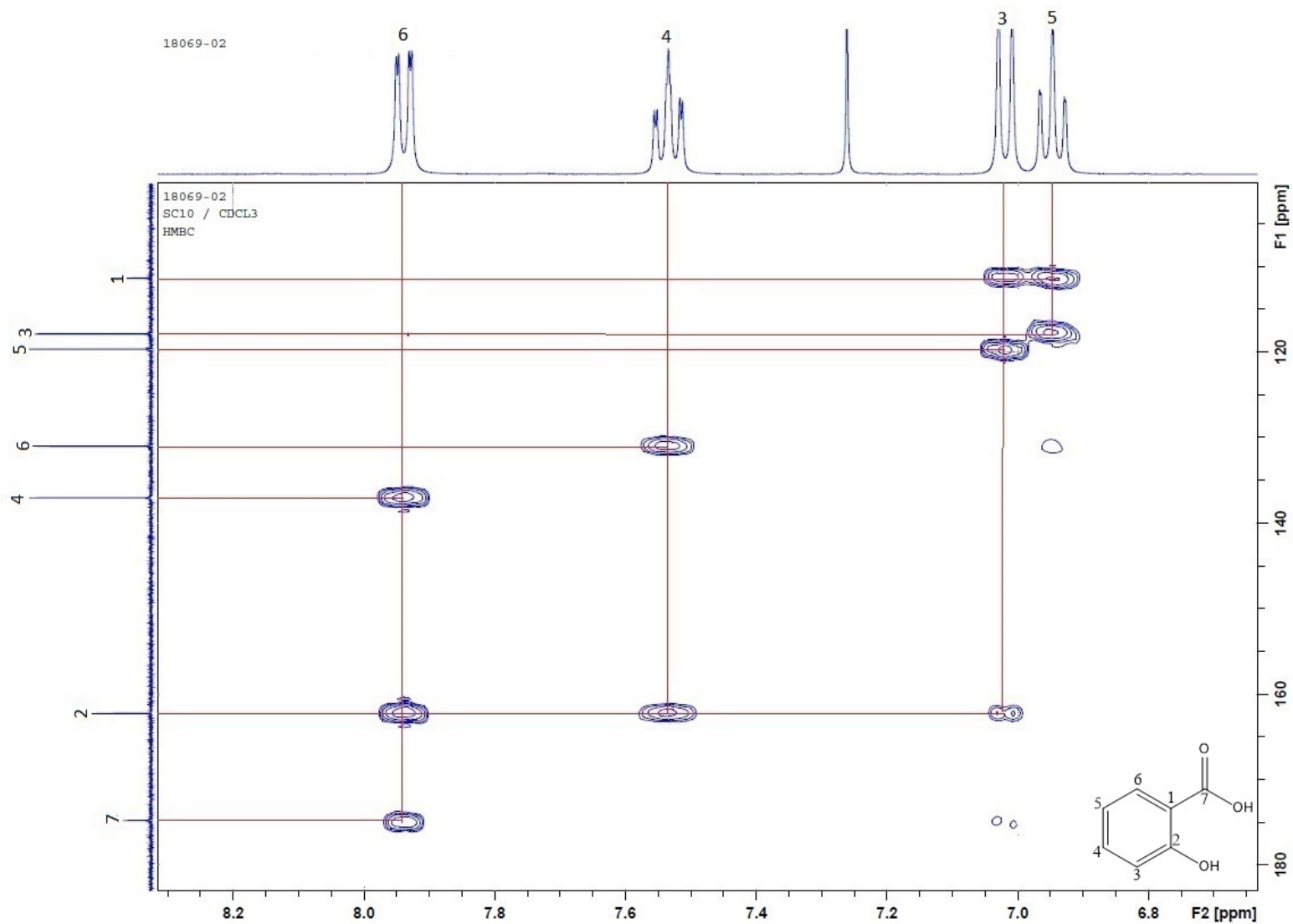


**Figure 10.** HMBC NMR spectrum (400 MHz, CDCl<sub>3</sub>) of salicylic acid (SC10)

### 5.1.2. Physical and spectroscopic data of campesterol- $\beta$ -D-glucoside (SC7B)

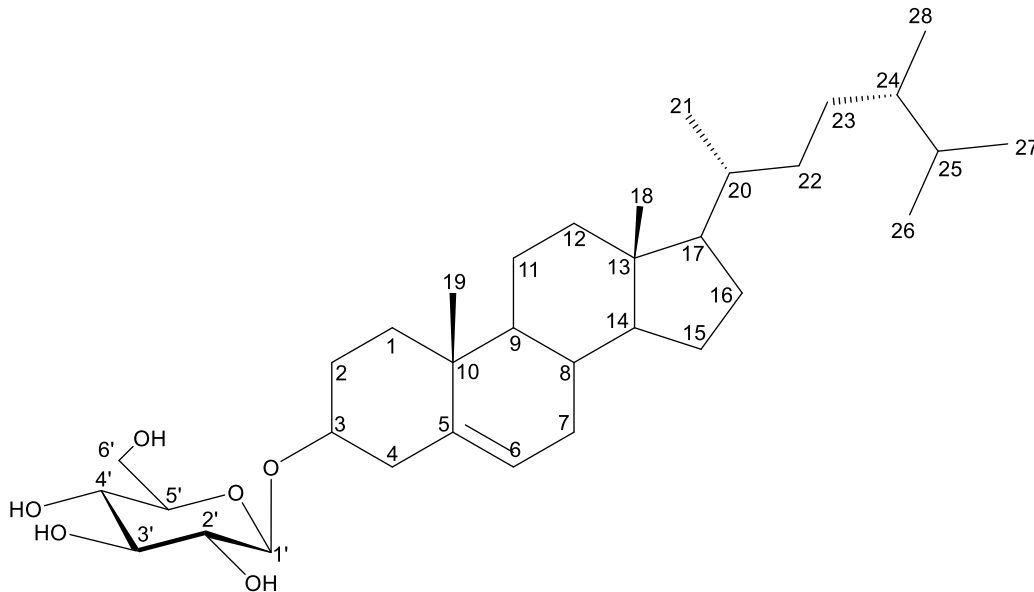


**Figure 11.**  $\beta$ -campesterol-D-glucoside (SC7B)

**Compound SC7B** (Figure 11): white solid (10 mg, yield: 0.000778 %), soluble in  $\text{CHCl}_3/\text{CH}_3\text{OH}$ . mp. Decomposition at 280 °C,  $\text{C}_{34}\text{H}_{58}\text{O}_6$ , M.W. 563.4234 g/mol.

The structural elucidation of the compound was carried out analyzing the NMR data of the acetylated derivative SC7Ac. For  $^1\text{H}$  NMR (400 MHz,  $\text{CDCl}_3$ ) and  $^{13}\text{C}$  NMR (100 MHz,  $\text{CDCl}_3$ ) see table 3.



### 5.1.2.1. Structural elucidation of 2',3',4',5'-tetraacetoxy- campesterol- $\beta$ -D-glucopyranoside (SC7BAc)

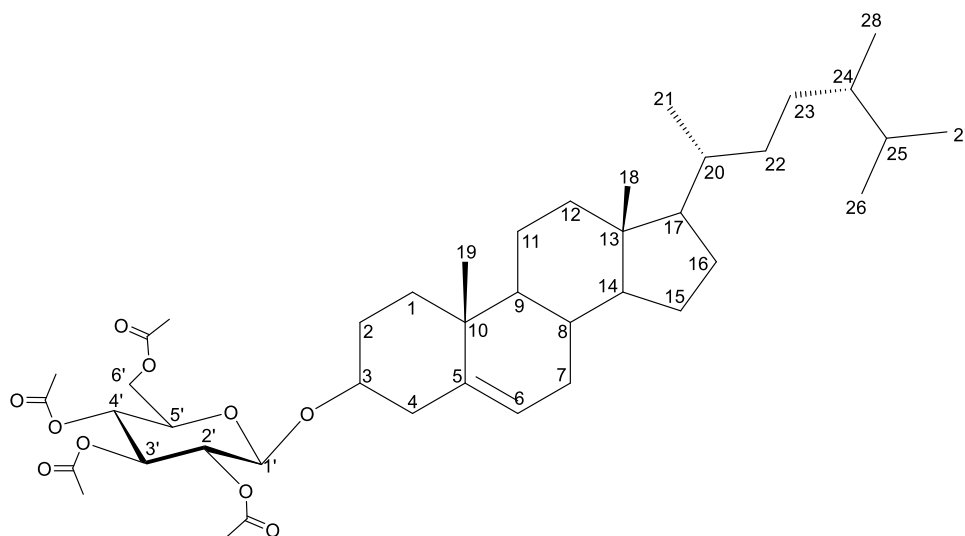


**Figure 12.** 2',3',4',5'-tetraacetoxy- campesterol-  $\beta$ -D-glucopyranoside (SC7BAc)

The NMR  $^1\text{H}$  spectrum of SC7BAc (Figure 13) showed a olefinic proton signal at  $\delta$  5.3795 (d,  $J=4.8$  Hz, 1H, H-6) and from  $\delta$  3.65-5.26 was observed the signals corresponding to a saccharide moiety (D-glucose) with the characteristic anomeric proton signal at  $\delta$  4.6123 (d,  $J=8$  Hz, 1H, H-1') and five signals of protons geminal to hydroxyl functions [  $\delta$  4.9799 (dd,  $J=9.54, 8.1$  Hz, 1H, H-2'), 5.2264 (t,  $J=9.52$  Hz, 1H, H-3'), 5.0977 (t,  $J=9.68$  Hz, 1H, H-4'), 3.6967 (ddd,  $J=9.96, 4.75, 2.42$  Hz, 1H, H-5'), 4.2788 (dd,  $J= 12.24, 4.48$  Hz, 1H, H-6' $\alpha$ ), 4.1301 (dd,  $J= 12.2, 2.32$  Hz, 1H, H-6' $\beta$ )]. The signal corresponding to a proton geminal to the saccharide moiety was observed at  $\delta$  3.5075 (m, 1H, H-3), and the overlapped signals corresponding to the protons of the sterol skeleton of the molecule were observed from  $\delta$  0.8 to 2.3 (see table 3). From  $\delta$  0.7 to 1.3 were observed two exocyclic methyl signals at  $\delta$  1.0074 (s, 3H, H-19) and 0.6955 (s, 3H, H-18) and four methyl signals of the aliphatic chain

of the sterol at  $\delta$  0.9394 (d,  $J$ = 6.44 Hz, 1H, H-21), 0.8552 (d,  $J$ =7.16 Hz, 1H, H-26), 0.8329 (d,  $J$ = 7.08 Hz, 1H, H-27), and 0.8154 (d,  $J$ = 6.92 Hz, 1H, H-28). Four acetyl proton signals were observed as well in the  $^1\text{H}$  spectrum (see table 3) confirming the acetylation of the positions H-2', H-3', H-4' and H-6' of the saccharide moiety of SC7BAc.

The above signals were confirmed with the  $^{13}\text{C}$  NMR spectrum of SC7BAc (Figure 14) which showed two olefinic carbon signals being one a quaternary carbon  $\delta$  140.36 (C-5) and the other a methine carbon  $\delta$  122.1782 (C-6), six signals corresponding to the saccharide moiety being the anomeric carbon at  $\delta$  99.65 (C-1') and the oxymethine carbons at 72.92 (C-3'), 71.69 (C-5'), 71.50 (C-2'), 68.54 (C-4'), and 62.11 (C-6'). Further, one signal corresponding to saccharide base carbon of the aglycone at  $\delta$  80.09 (C-3), two exocyclic methyl base quaternary carbons at  $\delta$  36.72 (C-10) and 42.3325 (C-13), four methine signals of the sterol skeleton at  $\delta$  31.86 (C-8), 50.17 (C-9), 56.05 (C-14) and 56.76 (C-17), three methine signal of the hydrocarbonated side chain of the sterol at  $\delta$  36.13 (C-20), 45.84 (C-24), 29.45 (C-25), eight methylene signals of the steroidal skeleton at  $\delta$  37.20 (C-1), 29.15 (C-2), 38.92 (C-4), 39.65 (C-7), 21.05 (C-11), 39.74 (C-12), 28.24 (C-15), 31.94 (C-16), and two methylenes of the hydrocarbonated lateral chain at  $\delta$  33.94 (C-22), 23.07 (C-23), two exocyclic methyl at  $\delta$  11.86 (C-18), and 19.36 (C-19) and four methyl of the hydrocarbonated side chain of the sterol at  $\delta$  18.81 (C-21), 19.82 (C-26), 19.36 (C-27), and 18.79 (C-28). The structure proposed for SC7BAc was confirmed by analysis of 2D NMR data. The HSQC spectrum (Figure 15) confirmed the correct assignation for the quaternary carbons, methyl, methylene, and methine in

concordance with DEPT90 and DEPT135 experiments. The substitution pattern of SC7Bac was determined with the HMBC spectrum (figure 16) showing the key heteronuclear correlations C-3/H-1' and C-3/H-4 confirming the substitution of C-3 with the saccharide portion. The position of the olefinic carbons (C-5, C-6) was confirmed with the key correlation C-5/H-4, C-5/H-1, C-5/H-19 for the quaternary C-5, and for the methine C-6 the observed correlations were C-1/H-6, C-6/H-4, C-7/H6, C-8-H-6. The position of the exocyclic methyls was confirmed with the key correlations C-12/H-18, C-13/H-18, C-17/H-18 for C-18, and for C-19 the correlations were C-5/H-19, C-9/H19, and C-10/H-19. The analysis of the NMR 1D and 2D data confirmed SC7Bac as the acetylated glucoside 2',3',4',5'-tetraacetoxy- $\beta$ -campesterol-D-glucoside, the data analysis was compared with reports in the literature<sup>34,35</sup>, in order to ensure the correct proposal for the SC7Bac chemical structure.

Table 3. <sup>13</sup>C NMR and <sup>1</sup>H NMR of SC7Bac and reference compound<sup>35</sup>

SC5Bac			Campesterol signals <sup>35</sup>		β-D-Glucose signals		
Position	δ (ppm)		δ (ppm)		Position	δ (ppm)	
	<sup>13</sup> C (100 MHz, CDCl <sub>3</sub> )	<sup>1</sup> H (400 MHz, CDCl <sub>3</sub> )	<sup>13</sup> C (100 MHz, CDCl <sub>3</sub> )	<sup>1</sup> H (400 MHz, CDCl <sub>3</sub> )		<sup>13</sup> C (100 MHz, CDCl <sub>3</sub> )	<sup>1</sup> H (400 MHz, CDCl <sub>3</sub> )
1	37.2034	1.8727 (m overlapped)	-	-	Glu-1'	99.6517	4.6123 (d, J=8 Hz)
2	29.1554	1.6907 (m)	-	-	2'	71.5048	4.9799 (dd, J=9.54, 8.1 Hz)
3	80.0937	3.5075 (m)	71.81	3.51 (m)	3'	72.9275	5.2264 (t, J=9.52 Hz)
4	38.9240	2.2465 (d, J= 7.28 Hz)	-	2.28 (d, J=7.3 Hz)	4'	68.5497	5.0977 (t, J=9.68 Hz)
5	140.3688	-	140.77	-	5'	71.6989	3.6967 (ddd, J=9.96, 4.75, 2.42 Hz)
6	122.1782	5.3795 (d, J=4.8 Hz)	121.72	5.33 (d, J= 5.2 Hz)	6'α	62.1176	4.2788 (dd, J= 12.24, 4.48 Hz)
7	39.6518	1.1786 (m)	-	-	6'β	62.1176	4.1301 (dd, J= 12.2, 2.32 Hz)
8	31.8697	1.5294 (m overlapped)	-	-	<b>Acetyl groups signals</b>		
9	50.1745	0.9215 (dd overlapped)	-	-	Position	δ (ppm)	
10	36.7279	-	-	-		<sup>13</sup> C (100 MHz, CDCl <sub>3</sub> )	<sup>1</sup> H (400 MHz, CDCl <sub>3</sub> )
11	21.0518	1.5068 (m overlapped)	-	-	C=O	169.3208	-
12	39.7443	1.1888 (m overlapped)	-	-	C=O	169.4205	-
13	42.3325	-	-	-	C=O	170.7217	-
14	56.0599	1.1334 (m overlapped)	-	-	C=O	170.3785	-
15	28.2458	1.8731 (m overlapped)	-	-	C=O	170.3785	-
16	31.9495	1.9862 (m overlapped)	-	-	CH <sub>3</sub> C=O	20.6221	2.0266 (s)
17	56.7622	1.0314 (brs)	-	-	CH <sub>3</sub> C=O	20.6538	2.0432 (s)
18	11.8612	0.6955 (s)	11.87	0.67 (s)	CH <sub>3</sub> C=O	20.7326	2.0711 (s)
19	19.3640	1.0074 (s)	19.40	1.00 (s)	CH <sub>3</sub> C=O	20.7785	2.0995 (s)
20	36.1369	1.3812 (m overlapped)	-	-			
21	18.8162	0.9394 (d, J= 6.44 Hz)	18.71	0.90 (d, J= 6.2 Hz)			
22	33.9489	1.3493 (m overlapped)	-	-			
23	23.0722	1.2897 (m overlapped)	-	-			
24	45.8449	0.9553 (m overlapped)	-	-			
25	29.4532	1.0942 (m overlapped)	-	-			
26	19.8280	0.8552 (d, J=7.16 Hz)	20.21	0.84 (d, J=6.8 Hz)			
27	19.3640	0.8329 (d, J= 7.08 Hz)	18.26	0.79 (d, J= 6.8 Hz)			
28	18.7987	0.8154 (d, J= 6.92 Hz)	15.38	0.77 (d, J= 6.6 Hz)			

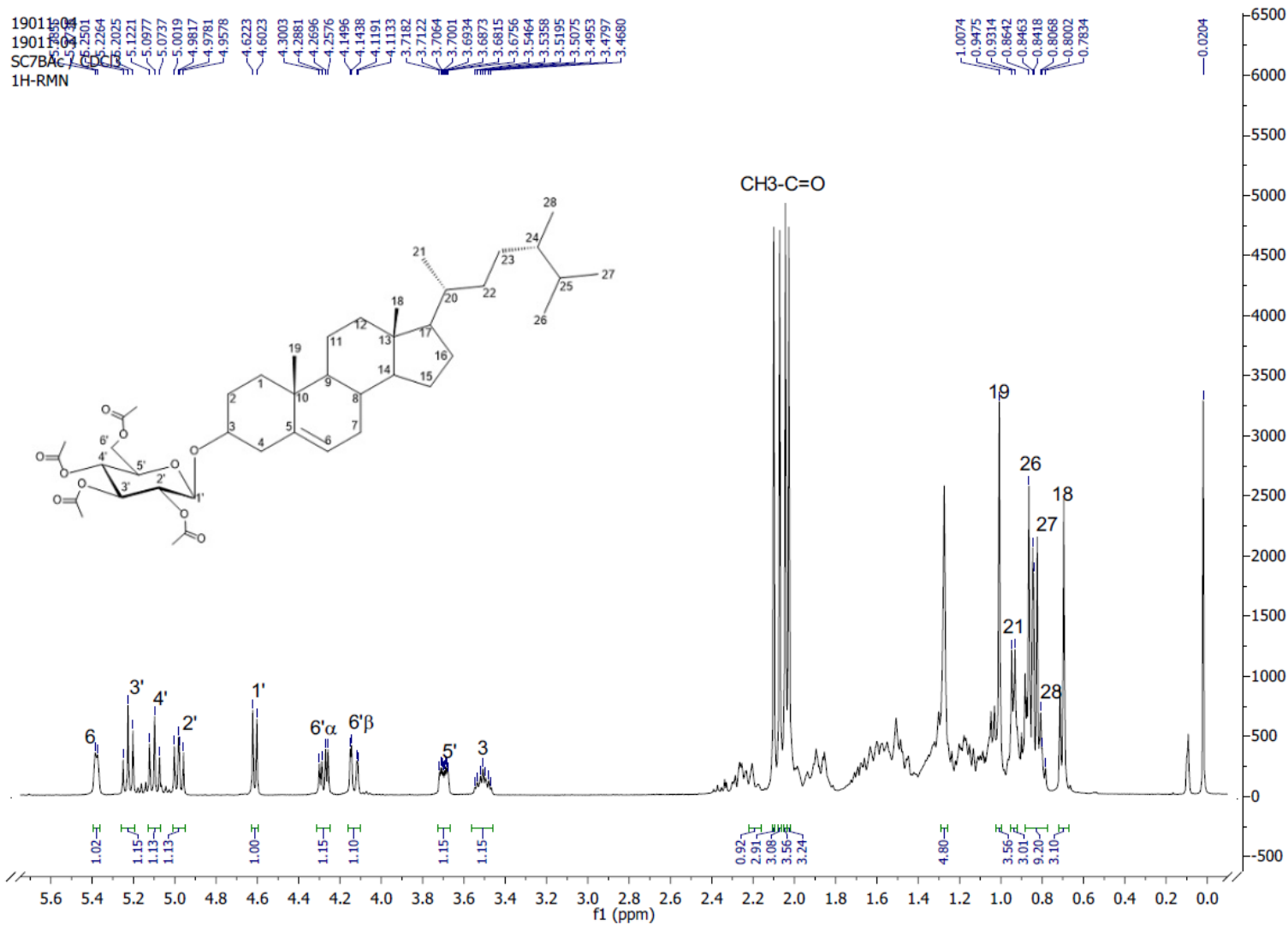


**Figure 13.** <sup>1</sup>H NMR spectrum (400 MHz, CDCl<sub>3</sub>) of 2',3',4',5'-tetraacetoxy-campesterol-β-D-glucoside (SC7BAc)





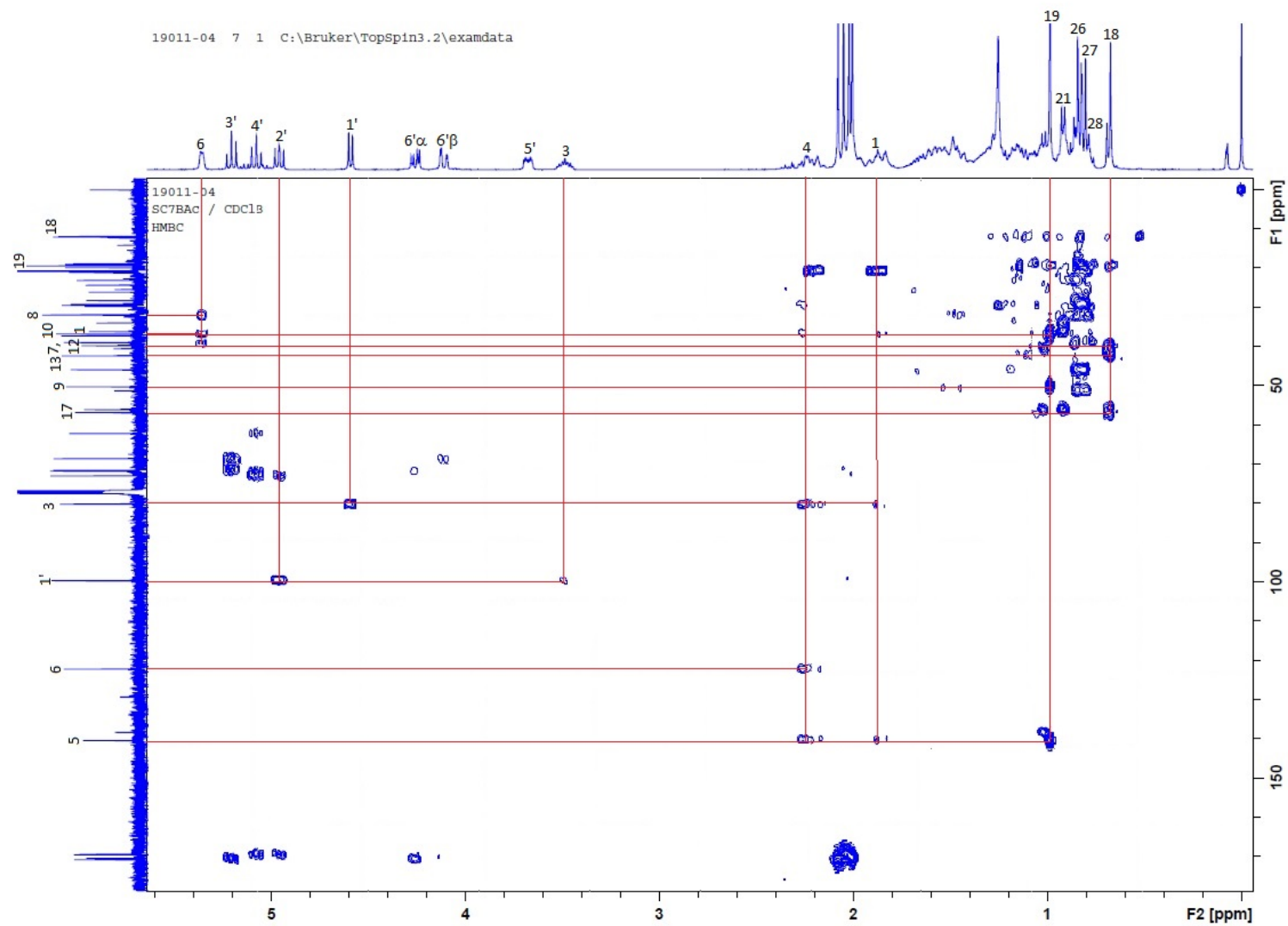


**Figure 16.** HMBC spectrum (400 MHz, CDCl<sub>3</sub>) of 2',3',4',5'-tetraacetoxy- campesterol- β-D-glucoside (SC7BAc)



5.1.3. Physical, spectroscopic and spectrometric data of 2'',3'',5''-triacetoxy-6- $\alpha$ -O- $\alpha$ -L-rhamnopyranosyl-(1 $\rightarrow$ 3)-2',4'-diacetoxy- $\beta$ -D-quinovopyranosyl-(25S)-5 $\alpha$ -spirostan-3 $\beta$ -acetate (SC5AcA)

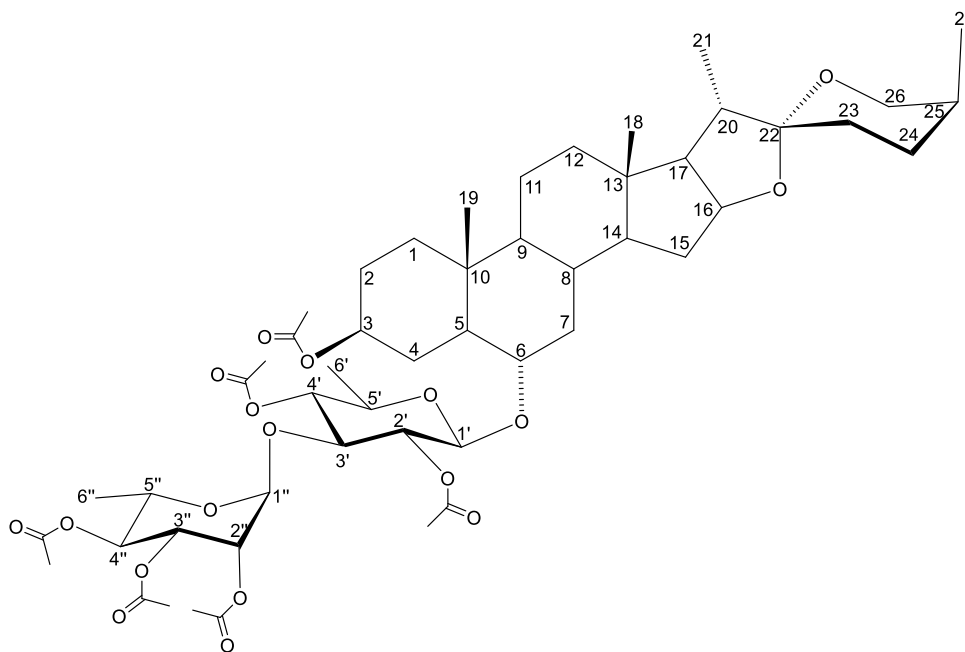


**Figure 17.** 2'',3'',5''-triacetoxy-6- $\alpha$ -O- $\alpha$ -L-rhamnopyranosyl-(1 $\rightarrow$ 3)-2',4'-diacetoxy- $\beta$ -D-quinovopyranosyl-(25S)-5 $\alpha$ -spirostan-3 $\beta$ -acetate (SC5AcA)

**Compound SC5AcA:** colorless solid (10 mg, yield: 0.000778 %), mp 250-253 °C,  $[\alpha]_{25}^D$  -20° (c 0.2, CHCl<sub>3</sub>), soluble in CHCl<sub>3</sub>, M.W. 976.50317 g/mol. The positive ion mode HRESIMS gave a quasimolecular ion peak  $m/z$  999.4660 [M+Na]<sup>+</sup> corresponding to the molecular formula C<sub>51</sub>H<sub>76</sub>O<sub>18</sub>Na. For <sup>1</sup>H NMR (400 MHz, CDCl<sub>3</sub>) and <sup>13</sup>C NMR (100 MHz, CDCl<sub>3</sub>) see table 4.

**5.1.3.1. Structural elucidation of 2'',3'',5''-triacetoxy-6- $\alpha$ -O- $\alpha$ -L-rhamnopyranosyl-(1 $\rightarrow$ 3)-2',4'-diacetoxy- $\beta$ -D-quinovopyranosyl-(25S)-5 $\alpha$ -spirostan-3 $\beta$ -acetate (SC5AcA)**

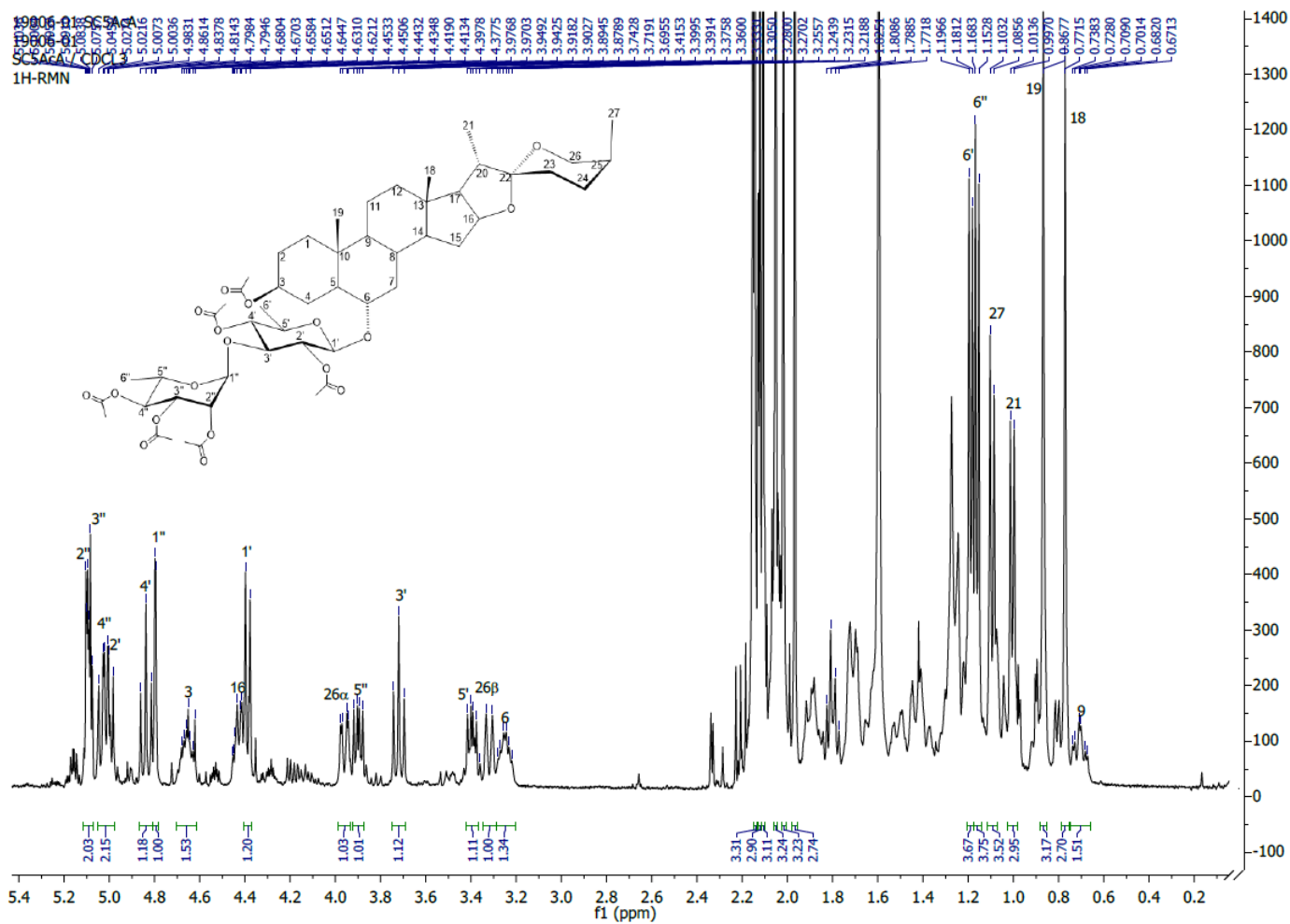
The  $^1\text{H}$  NMR spectrum of SC5AcA (Figure 18) showed from  $\delta$  0.63 to 2.2, the overlapped signals of a steroidal saponin aglycone, and from  $\delta$  3.1 to 5.1 were observed signals of oxymethines and saccharide moieties (table 4). In the spectrum were identified representative signals of a spirostane steroid saponin, with three steroid methyls at  $\delta$  0.77 (s, 3H, Me-18), 0.86 (s, 3H, Me-19), 1.00 (d,  $J=6.64$  Hz, 3H, Me-21), and a methyl of a spirostane ring at  $\delta$  1.09 (d,  $J=7.04$  Hz, 3H, H-27). Two anomeric hydrogens were observed at  $\delta$  4.38 (d,  $J=8.12$  Hz, 1H, H-1') and 4.79 (d,  $J=1.52$  Hz, 1H, H-1''). In addition two methyl signals at  $\delta$  1.18 (d,  $J=6.16$  Hz, 3H, Me-6') and 1.16 (d,  $J=6.20$  Hz, 3H, Me-6''), suggesting the presence of two hexoses as sugar moieties. The value of the coupling constant for the anomeric proton at  $\delta$  4.38 ( $J_{1'_{ax}-2'_{ax}}=8.12$  Hz) indicates  $\alpha$ -orientation, being vicinal axial-axial coupled, while for the anomeric proton at 4.79 ( $J_{1''_{eq}-2'_{ax}}=1.52$  Hz) the orientation is beta due to a vicinal axial-equatorial coupling. The signals corresponding to the spin systems of the anomeric hydrogens were attributed by analysis of COSY and HMBC spectra (figure 22 and 23), the data indicated good agreement with the signals of the acetylated hexoses  $\beta$ -D-quinovopyranose diacetate and  $\alpha$ -L-rhamnopyranose triacetate (Table 4), showing concordance with the reports in the literature<sup>23,36</sup>. The  $^{13}\text{C}$  NMR spectrum of SC5AcA (figure 19) showed 27 signals of the aglycone and 12 signals corresponding to the disaccharide moiety being assigned the methyl,

methylene, and methine signals by analysis of DEPT90, DEPT135, and HSQC spectroscopic data (figure 20). The characteristic signals of the spirostane steroidal saponins were observed: the carbon C-22 ( $\delta$  109.7), the oxygenated carbons of the aglycone [C-3 ( $\delta$  73.21), C-6 ( $\delta$  80.73), C-16 ( $\delta$  80.74), C-26 ( $\delta$  65.1)], the anomeric carbons of the saccharide moiety C-1' ( $\delta$  102.18) and C-1'' ( $\delta$  99.47), and the aglycone methyl carbons [C-18 ( $\delta$  16.45), C-19 ( $\delta$ : 13.38), C-21 ( $\delta$ : 14.31), C-27 ( $\delta$ : 16.05)]. The carbon signals C-22, C-25, and C-26 ( $\delta$  109.7, 27.0, and 65.1) along with the methyl C-27 ( $\delta$  16.0) were identified as the typical signals of a spirostane ring in the aglycone<sup>21,36,37,38</sup>. The (S) relative configuration for C-25 was deduced by analysis of the coupling constants for hydrogens H-26 $\alpha$  ( $\delta$  4.38,  $J_{26ax-26eq}=11.08$  Hz,  $J_{26ax-25eq}=2.64$  Hz) and H-26 $\beta$  ( $\delta$  3.96,  $J_{26ax-26eq}=11.24$  Hz), indicating a  $\beta$ -axial orientation for the methyl C-27 positioned in C-25, a characteristic feature of *neo*-spirostane saponins. The assignment of the oxymethine carbon signals C-3 and C-6 ( $\delta$  73.2, 80.7) was confirmed by comparison with the literature<sup>21,36,37,38</sup>, and the orientation of their respective hydrogens H-3 ( $\delta$  4.66, m, 1H) and H-6 ( $\delta$  3.24, m, 1H) were determined by observing their multiplicity in the <sup>1</sup>H spectrum, being this multiplicities characteristic for an  $\alpha$ -oriented H-3 and  $\beta$ -oriented H-6 in good agreement with the literature<sup>21,23</sup>. The assignment of the hydrogen and carbon signals for positions 3 and 6 along with the analysis of the spectroscopic data of the spirostane ring allowed the attribution of neochlorogenin as the aglycone of SC5AcA, in good agreement with reports in the literature<sup>36,37,38</sup>. The glycosidation position in SC5AcA was determined by the analysis of HMBC spectroscopic data (figure 19). The correlation (<sup>3</sup>J<sub>C-H</sub>): C-6( $\delta$  80.7) /H-3'( $\delta$  3.71) indicates C-6 as the

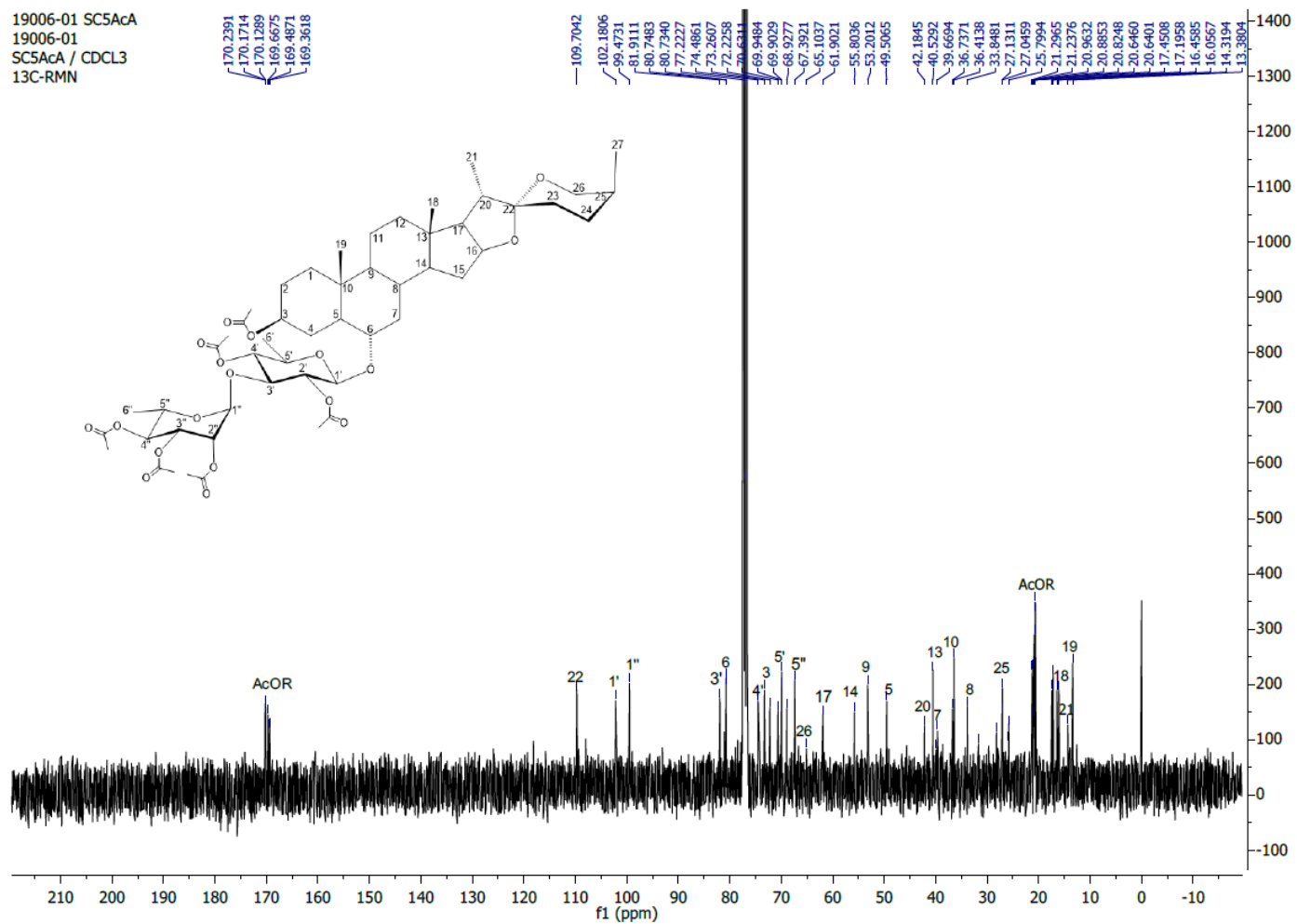
glycosidation site in the aglycone, while the cross-peak ( $^3J_{C-H}$ ): C-3'( $\delta$  81.9)/H-1''( $\delta$  4.79) revealed a 1 $\rightarrow$ 3 bonding between the acetylated hexoses. Based on the previous analysis it could be deduced that  $\beta$ -D-quinovopyranose diacetate is bonded to C-6 in the aglycone and  $\alpha$ -L-rhamnopyranose triacetate is 1 $\rightarrow$ 3 bonded to  $\beta$ -D-quinovopyranose diacetate. All  $^1H$  and  $^{13}C$  assignments for SC5AcA were confirmed with a basis on HSQC, HMBC, COSY, and NOESY spectroscopic data analysis and by comparison with literature<sup>21,23,36,37,38</sup>. The spectroscopic constants of compound SC5AcA were compared with literature finding that the acetylated saponin 5a reported by Zamilpa *et al.*, 2002<sup>23</sup> displays the same planar structure of SC5AcA, being the only difference between the molecules the relative configuration in the carbon C-25, for SC5AcA was observed as 25S while for 5a was observed as 25R. Based on the previous analysis can be deduced that SC5AcA is the acetylated *neo*-spirostanic form of the acetylated *iso*-spirostanic saponin 5a reported by Zamilpa *et al.*, 2002<sup>23</sup>. The compound SC5AcA was elucidated as the acetylated derivative 2'',3'',5''-triacetoxo-6- $\alpha$ -O-  $\alpha$ -L-rhamnopyranosyl-(1 $\rightarrow$ 3)-2',4'-diacetoxo- $\beta$ -D-quinovopyranosyl-(25S)-5 $\alpha$ -spirostan-3 $\beta$ -acetate, an acetylated derivative of a new natural product.

Table 4. <sup>13</sup>C NMR and <sup>1</sup>H NMR constants for SC5AcA and reference compound 5a<sup>23</sup>

Aglycone signals: (25S)-5 $\alpha$ -spirostan-3 $\beta$ -acetate			Aglycone signals: (25R)-5 $\alpha$ -spirostan-3 $\beta$ -acetate <sup>23</sup>			Saccharide signals: $\alpha$ -L-rhamnopyranose triacetate and $\beta$ -D-quinovopyranose diacetate			Saccharide signals: $\alpha$ -L-rhamnopyranose triacetate and $\beta$ -D-quinovopyranose diacetate <sup>23</sup>		
Position	$\delta$ (ppm), J (Hz)		$\delta$ (ppm), J (Hz)		Position	$\delta$ (ppm), J (Hz)		$\delta$ (ppm), J (Hz)			
	<sup>13</sup> C (100 MHz, CDCl <sub>3</sub> )	<sup>1</sup> H (400 MHz, CDCl <sub>3</sub> )	<sup>13</sup> C (100 MHz, CDCl <sub>3</sub> )	<sup>1</sup> H (500 MHz, CDCl <sub>3</sub> )		<sup>13</sup> C (100 MHz, CDCl <sub>3</sub> )	<sup>1</sup> H (400 MHz, CDCl <sub>3</sub> )	<sup>13</sup> C (100 MHz, CDCl <sub>3</sub> )	<sup>1</sup> H (500 MHz, CDCl <sub>3</sub> )		
1	36.7371	1.6919 (m overlapped)	36.67	1.62, 0.99	Qui-1'	102.1806	4.3876 (d, J=8.12 Hz)	102.1	4.36 (d, J=8 Hz)		
2	25.9542	2.07 (m overlapped)	27.07	1.65, 1.21	2'	72.2258	5.0052 (dd overlapped, J= 9.6, 8.12 Hz)	72.12	5.05 (dd, J=9.6, 8 Hz)		
3	73.2182	4.6636 (m)	73.25	4.62 (dddd, J= 11, 10.5, 6, 5 Hz)	3'	81.9111	3.7191 (t, J=9.46 Hz)	81.93	3.6 (t, J= 9.6 Hz)		
4	28.1901	2.03	28.14	2.05, 1.2	4'	74.4861	4.8378 (t, J= 9.42 Hz)	74.41	4.81 (t, J= 9.6 Hz)		
5	49.5065	1.26 (m)	49.43	1.25	5'	69.9029	3.3954 (dd, J= 9.52, 6.28 Hz)	69.8	3.41 (m)		
6	80.7340	3.2497 (m)	80.78	3.22 (ddd, J= 11, 10, 4.5 Hz)	6'	17.4508	1.1890 (d, 6.16 Hz)	17.49	1.17 (d, J= 6.4 Hz)		
7	39.6694	1.7119 (m overlapped)	39.62	2.51, 1.27	Rha-1''	99.4731	4.7965 (d, J= 1.52 Hz)	99.45	4.77 (d, J= 1,2 Hz)		
8	33.8238	1.6159 (m)	33.8	1.60	2''	69.9484	5.0959 (m overlapped)	69.8	5.08 (m)		
9	53.2012	0.7053 (td, J=11.3, 3.81Hz)	53.12	0.68	3''	68.9277	5.0838 (m overlapped)	68.89	5.1 (m)		
10	36.4138	-	36.39	-	4''	70.6311	5.0245 (dd overlapped, J= 9.62, 7.3 Hz)	70.54	5.13 (dd, J= 10, 9.6 Hz)		
11	20.8853	1.4561, 1.2271 (m)	21.2	1.45, 1.2	5''	67.3921	3.8986 (dd, J= 9.48, 6.22 Hz)	67.36	3.87 (dd, J= 10, 6.4 Hz)		
12	39.9452	2.14, 1.7172 (m overlapped)	39.91	2.01, 1.68	6''	17.1958	1.1605 (d, 6.2 Hz)	17.17	1.13 (d, 6.4 Hz)		
13	40.5292	-	41.51	-	<b>Acetyl signals</b>			<b>Acetyl signals<sup>36</sup></b>			
14	55.8036	1.1326 (m)	55.76	1.2, 1.14	Position	$\delta$ (ppm), J (Hz)		$\delta$ (ppm), J (Hz)			
15	31.6640	2.04, 1.2739	31.66	2.01, 1.2		<sup>13</sup> C (100 MHz, CDCl <sub>3</sub> )	<sup>1</sup> H (400 MHz, CDCl <sub>3</sub> )	<sup>13</sup> C (100 MHz, CDCl <sub>3</sub> )	<sup>1</sup> H (500 MHz, CDCl <sub>3</sub> )		
16	80.7483	4.4272 (m)	81.74	4.39 (ddd, J= 7.5, 7.4, 7 Hz)	C=O	169.36	-	-	-		
17	61.9021	1.7942 (dd, J=14.68, 6.64 Hz)	61.98	1.68 (dd, J= 8.4, 6.8 Hz)	C=O	169.48	-	-	-		
18	16.4585	0.7715 (s)	17.12	0.75	C=O	169.66	-	-	-		
19	13.3804	0.8677 (s)	13.36	0.84	C=O	170.12	-	-	-		
20	42.1845	1.7916 (m)	41.6	1.80	C=O	170.17	-	-	-		
21	14.3194	1.0051 (d, J=6.64 Hz)	14.49	0.95 (d, J= 6.4 Hz)	C=O	170.23	-	-	-		
22	109.7042	-	109.24	-	CH <sub>3</sub> C=O	20.64	1.96 (s)	-	-		
23	27.1297	1.8958 (m)	31.3	1.7, 1.2	CH <sub>3</sub> C=O	20.65	2.01 (s)	-	-		
24	25.7994	1.4167 (m)	28.76	1.2, 0.5	CH <sub>3</sub> C=O	20.83	2.05 (s)	-	-		
25	27.044	1.7212 (m)	30.24	1.77	CH <sub>3</sub> C=O	20.97	2.10 (s)	-	-		
26 $\alpha$	65.1037	3.9611 (dd, J= 11.08, 2.64 Hz)	66.82	3.36 (dd, , J= 11, 10 Hz)	CH <sub>3</sub> C=O	21.24	2.14 (s)	-	-		
26 $\beta$	65.1037	3.3202 (d, J= 11.24 Hz)	66.82	3.45 (dd, , J= 11, 2.4 Hz)	CH <sub>3</sub> C=O	21.30	2.15 (s)	-	-		
27	16.0567	1.0944 (d, 7.04 Hz)	16.44	0.79 (d, J= 6.4 Hz)							



**Figure 18.**  $^1\text{H}$  NMR spectrum (400 MHz,  $\text{CDCl}_3$ ) of 2'',3'',5''-triacetoxy-6- $\alpha$ -O- $\alpha$ -L-rhamnopyranosyl-(1 $\rightarrow$ 3)-2',4'-diacetoxy- $\beta$ -D-quinovopyranosyl-(25S)-5 $\alpha$ -spirostan-3 $\beta$ -acetate (SC5AcA)



**Figure 19.**  $^{13}\text{C}$  NMR spectrum (100 MHz,  $\text{CDCl}_3$ ) of 2'',3'',5''-triacetoxy-6- $\alpha$ -O- $\alpha$ -L-rhamnopyranosyl-(1 $\rightarrow$ 3)-2',4',4'-diacetoxy- $\beta$ -D-quinovopyranosyl-(25S)-5 $\alpha$ -spirostan-3 $\beta$ -acetate (SC5AcA)





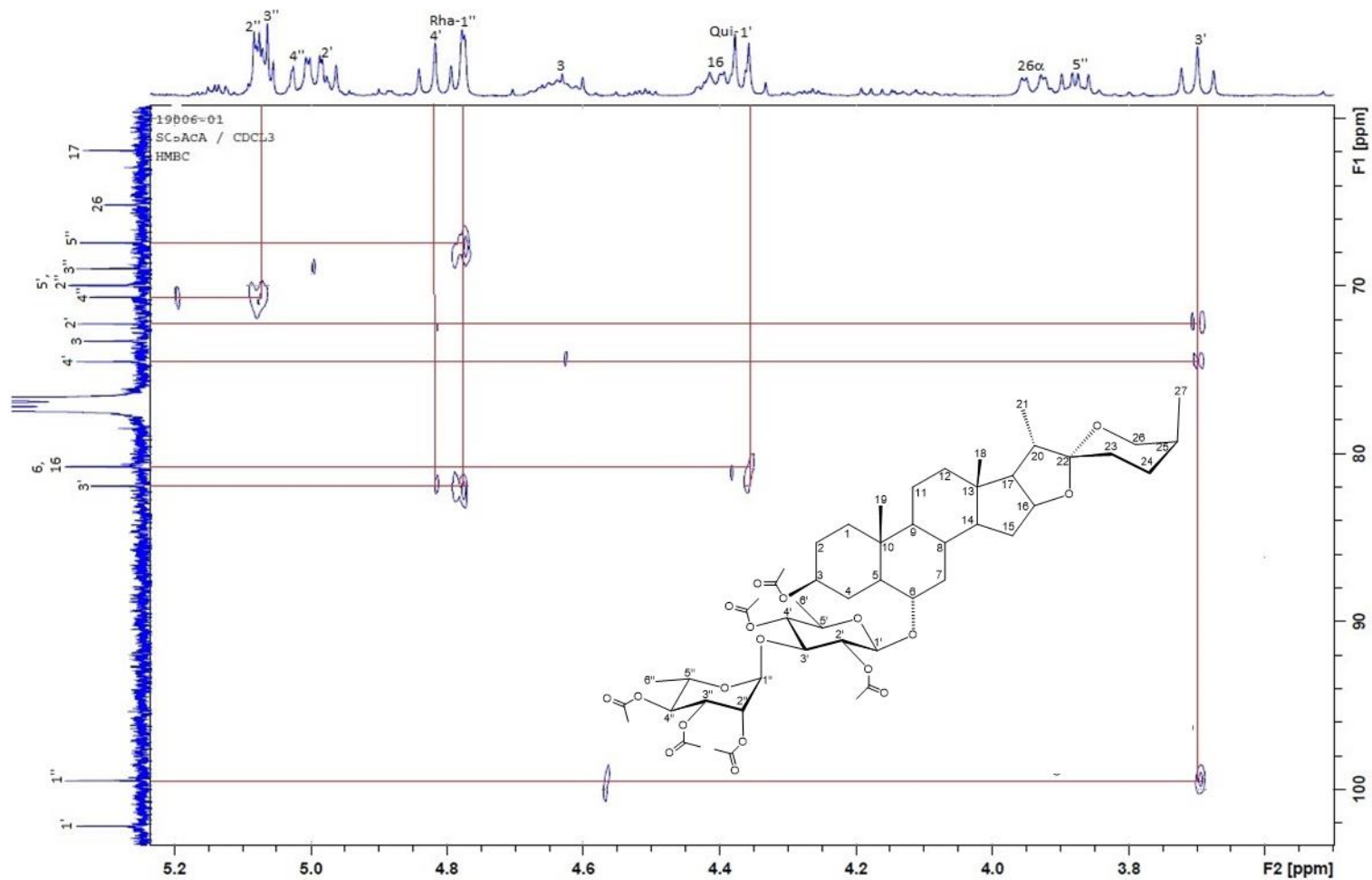


**Figure 21.** HMBC partial spectrum (400 MHz, CDCl<sub>3</sub>) of 2'',3'',5''-triacetoxy-6- $\alpha$ -O- $\alpha$ -L-rhamnopyranosyl-(1 $\rightarrow$ 3)-2',4'-diacetoxy- $\beta$ -D-quinovopyranosyl-(25S)-5 $\alpha$ -spirostan-3 $\beta$ -acetate (SC5AcA)

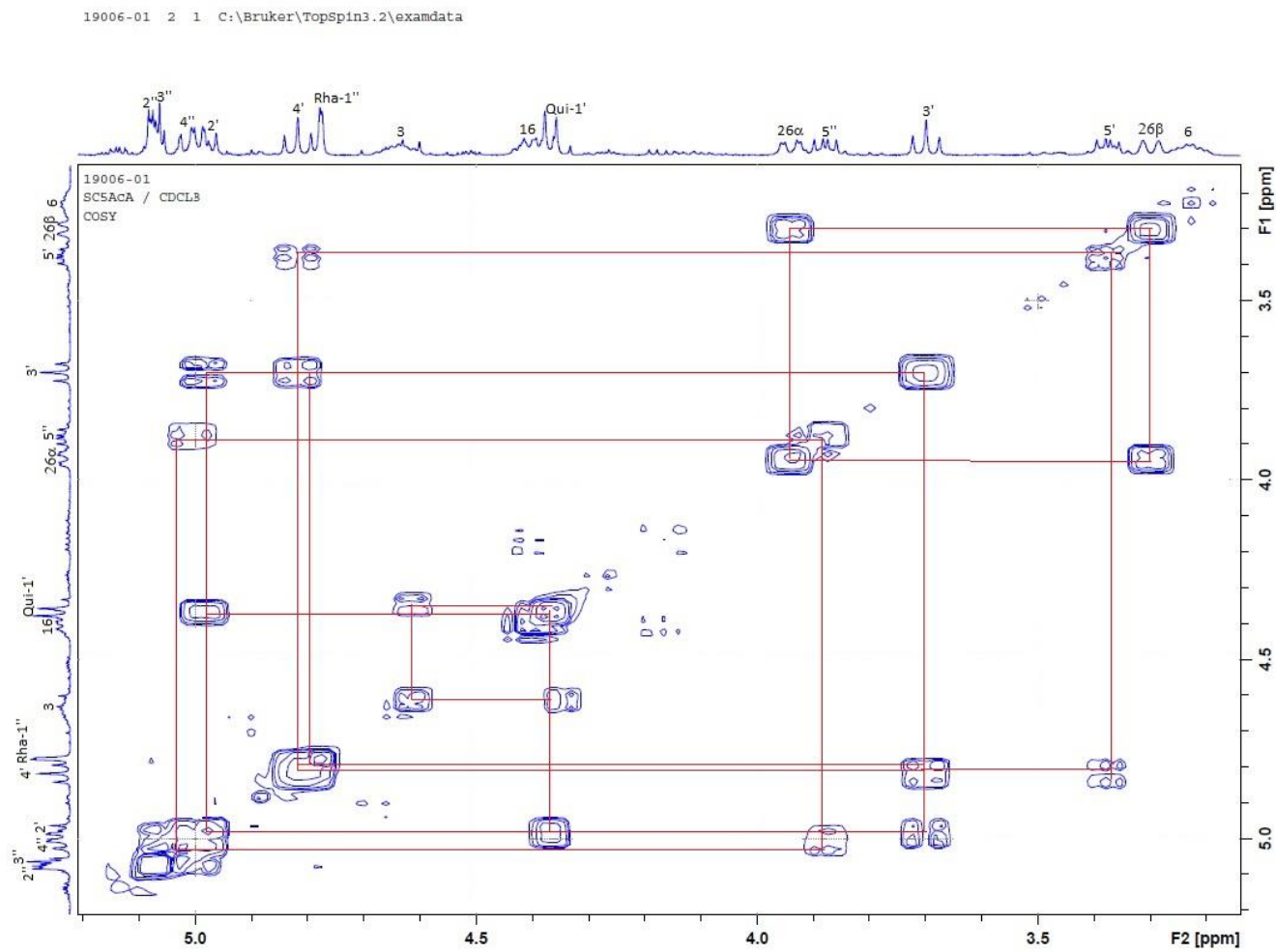


**Figure 22.** COSY partial spectrum (400 MHz, CDCl<sub>3</sub>) of 2'',3'',5''-triacetoxy-6- $\alpha$ -O- $\alpha$ -L-rhamnopyranosyl-(1 $\rightarrow$ 3)-2',4'-diacetoxy- $\beta$ -D-quinovopyranosyl-(25S)-5 $\alpha$ -spirostan-3 $\beta$ -acetate (SC5AcA)

5.1.4. Physical and spectrometric data of 6- $\alpha$ -O- $\alpha$ -L-rhamnopyranosyl-(1 $\rightarrow$ 3)- $\beta$ -D-quinovopyranosyl-(25S)-5 $\alpha$ -spirostan-3 $\beta$ -ol (SC5A)

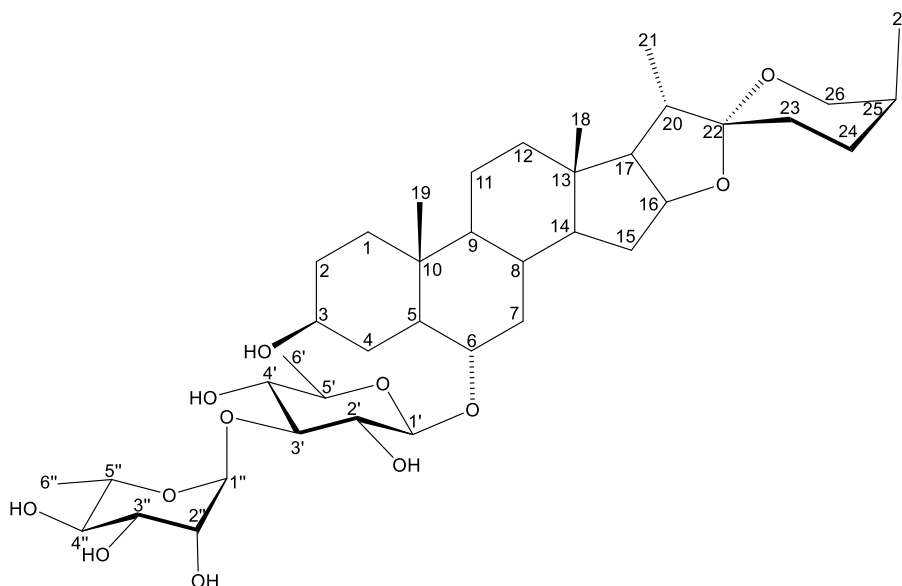


**Figure 23.** 6- $\alpha$ -O- $\alpha$ -L-rhamnopyranosyl-(1 $\rightarrow$ 3)- $\beta$ -D-quinovopyranosyl-(25S)-5 $\alpha$ -spirostan-3 $\beta$ -ol (SC5A)

**Compound SC5A:** the compound 6- $\alpha$ -O- $\alpha$ -L-rhamnopyranosyl-(1 $\rightarrow$ 3)- $\beta$ -D-quinovopyranosyl-(25S)-5 $\alpha$ -spirostan-3 $\beta$ -ol (SC5A) was obtained as white powder, mp 183-186 °C,  $[\alpha]_{25}^D$  -20°(c 0.2, CH<sub>3</sub>OH). The negative ion mode HRESIMS showed the molecular ion peak  $m/z$  723.4295 [M-H]<sup>-</sup>, and quasimolecular ion peak  $m/z$  769.4382 [M+COOH]<sup>-</sup>, in agreement with the molecular formulas C<sub>39</sub>H<sub>63</sub>O<sub>12</sub> and C<sub>40</sub>H<sub>65</sub>O<sub>14</sub>. The structural elucidation of compound SC5A was performed by spectroscopic analysis of its acetylated derivative SC5AcA.

5.1.5. Physical and spectrometric data of 2'',3'',5''-triacetoxy-6- $\alpha$ -O- $\alpha$ -L-rhamnopyranosyl-(1 $\rightarrow$ 3)-2',4'-diacetoxy- $\beta$ -D-quinovopyranosyl-(23R,25S)-5 $\alpha$ -spirostan-3 $\beta$ ,23 $\beta$ -acetate (SC5AcB)

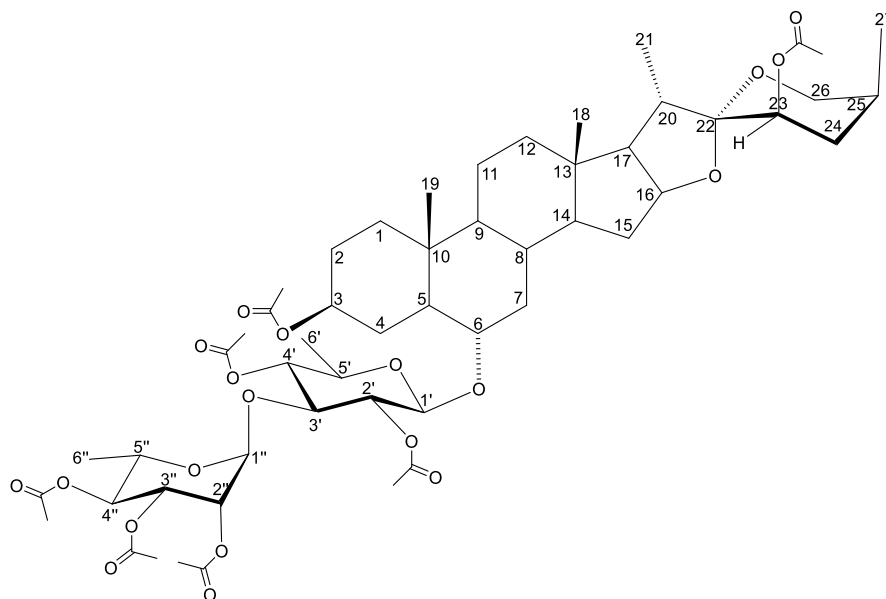


**Figure 24.** 2'',3'',5''-triacetoxy-6- $\alpha$ -O- $\alpha$ -L-rhamnopyranosyl-(1 $\rightarrow$ 3)-2',4'-diacetoxy- $\beta$ -D-quinovopyranosyl-(23R,25S)-5 $\alpha$ -spirostan-3 $\beta$ ,23 $\beta$ -acetate (SC5AcB)

**Compound SC5AcB:** white crystals, mp 170-173 °C, (10 mg, yield: 0.000778 %),  $[\alpha]_{25}^D$  -40° (c 0.2, CHCl<sub>3</sub>), soluble in CHCl<sub>3</sub>, M.W. 1034.50864 g/mol. The positive ion mode HRESIMS showed concordance of the quasimolecular ion peak  $m/z$  1057.4996 [M+Na]<sup>+</sup> with the molecular formula C<sub>53</sub>H<sub>78</sub>O<sub>20</sub>Na. For <sup>1</sup>H NMR (400 MHz, CDCl<sub>3</sub>) and <sup>13</sup>C NMR (100 MHz, CDCl<sub>3</sub>) see table 5.

**5.1.5.1. Structural elucidation of 2'',3'',5''-triacetoxy-6- $\alpha$ -O- $\alpha$ -L-rhamnopyranosyl-(1 $\rightarrow$ 3)-2',4'-diacetoxy- $\beta$ -D-quinovopyranosyl-(23R,25S)-5 $\alpha$ -spirostan-3 $\beta$ ,23 $\beta$ -acetate (SC5AcB)**

The  $^1\text{H}$  NMR spectrum of SC5AcB (figure 25) showed the same representative signals for SC5AcA (Table 4 and 5), with three steroid methyls at  $\delta$  0.76 (s, 3H, H-18), 0.86 (s, 3H, H-19), 0.99 (d,  $J=6.9$  Hz, 3H, H-21), and the methyl in the spirostane ring at 1.09 (d,  $J=6.9$  Hz, 3H, H-27). The same two anomeric protons identified for SC5AcA were observed for SC5AcB at  $\delta$  4.38 (d,  $J=8.0$  Hz, 1H, H-1') and 4.79 (d,  $J=1.2$  Hz, 1H, H-1'') along with two hexose sugar unit methyl signals at  $\delta$  1.19 (d,  $J=6.1$  Hz, 3H, H-6') and 1.15 (d,  $J=6.2$  Hz, 3H, H-6''). The  $^{13}\text{C}$  NMR spectrum of SC5AcB (figure 26) showed 27 signals of the aglycone and 12 of the disaccharide moiety being assigned the methyl, methylene, and methine signals by analysis of DEPT90, DEPT135, and HSQC spectroscopic data (figure 27). The characteristic carbon signals for the aglycone of SC5AcB were almost the same for SC5AcA, with the aglycone oxymethine carbon signals C-3 and C-6 ( $\delta$  73.2, 80.5) along with the spirostane ring signals C-22, C-25, C-26 and C-27 ( $\delta$  109.2, 25.7, 64.6, and 16.6), however, C-23 ( $\delta$  71.8) was observed in SC5AcB as an oxymethine in contrast with the methylene C-23 ( $\delta$  27.1) in SC5AcA. The carbon C-23 in SC5AcB possess an additional acetoxy, and the orientation of this function was determined by analyzing the spin-spin coupling for the hydrogen H-23 ( $\delta$  4.78, t,  $J=2.8$  Hz, 1H), with H-24 $\alpha$  ( $J_{23\text{eq}-24\text{eq}}=2.8$  Hz) and H-24 $\beta$  ( $J_{23\text{eq}-24\text{ax}}=2.8$  Hz), indicating  $\beta$ -axial orientation for the acetoxy function, and relative configuration (R) for C-23, a fact in good agreement

with the reports in the literature<sup>21,23</sup>. Additionally, when comparing the chemical shift of C-20 carbon signal for SC5AcA ( $\delta$  42.1) and SC5AcB ( $\delta$  40.4), it was observed an upfield displacement for the C-20 signal in SC5AcB. This phenomenon can only be explained by the presence of a  $\beta$ -axial function in C-23, which causes a shielding effect in C-20 due to *skew-pentane* interactions between the C-23  $\beta$ -axial acetoxy group and the C-21 methyl group in SC5AcB<sup>36,37,38</sup>. In the same fashion an upfield displacement was observed when comparing the C-25 signals for SC5AcA ( $\delta$  27.0) and SC5AcB ( $\delta$  25.7), being this shielding effect explained by the 1,3-diaxial interactions between the C-23  $\beta$ -axial acetoxy and the C-27  $\beta$ -axial methyl in the spirostane ring of SC5AcB<sup>36,37,38</sup>. The 25S relative configuration for SC5AcB was deduced with the same coupling constants analysis performed for SC5AcA. This indicated that SC5AcB is a *neo*-spirostane steroidal saponin as well, and altogether with the previous analysis of the spectroscopic data, the aglycone moiety was elucidated as neosolaspigenin in good agreement with the literature<sup>21,36,37,38</sup>. The acetylated disaccharide moiety for SC5AcB showed the same hexopyranoses and connectivity pattern as SC5AcA, with the same C-6- $\alpha$ -O bonding with the aglycone and (1 $\rightarrow$ 3) connectivity between the  $\beta$ -D-quinovopyranose diacetate and  $\alpha$ -L-rhamnopyranose triacetate units, such deductions were clarified by analysis of HMBC and COSY spectroscopic data (figure 28 and 29) and by comparison with reports in the literature<sup>21,23</sup>. The spectroscopic coupling constants of the compound SC5AcB were compared with reports in the literature finding that the acetylated saponin 6a reported by Zamilpa et al., 2002<sup>23</sup> displays the same planar structure as SC5AcB, being the only differences between the molecules the relative configuration

of C-23 and C-25, for SC5AcB was observed as 23R,25S while for 6a was observed as 23S,25R. Based on the previous analysis can be concluded that SC5AcB is the acetylated *neo*-spirostanic diastereomer of the acetylated *iso*-spirostanic saponin 6a reported by Zamilpa et al., 2002<sup>23</sup>. The compound SC5AcB was elucidated as 2'',3'',5''-triacetoxo-6- $\alpha$ -O- $\alpha$ -L-rhamnopyranosyl-(1 $\rightarrow$ 3)-2',4'-diacetoxo- $\beta$ -D-quinovopyranosyl-(23R,25S)-5 $\alpha$ -spirostan-3 $\beta$ ,23 $\beta$ -acetate, an acetylated derivative of a new steroidal saponin.

Table 5. <sup>13</sup>C NMR and <sup>1</sup>H NMR data for SC5AcB and reference compound 6a<sup>23</sup>

Aglycone signals: (23R,25S)-5 $\alpha$ -spirostan-3 $\beta$ ,6 $\alpha$ ,23 $\alpha$ diacetate			Aglycone signals: (23S,25R)-5 $\alpha$ -spirostan-3 $\beta$ ,6 $\alpha$ ,23 $\alpha$ - diacetate <sup>23</sup>		Saccharide signals: $\alpha$ -L-rhamnopyranose triacetate and $\beta$ -D- quinovopyranose diacetate			Saccharide signals: $\alpha$ -L-rhamnopyranose triacetate and $\beta$ -D- quinovopyranose diacetate <sup>23</sup>	
Position	$\delta$ (ppm), J (Hz)		$\delta$ (ppm), J (Hz)		Position	$\delta$ (ppm), J (Hz)		$\delta$ (ppm), J (Hz)	
	<sup>13</sup> C (100 MHz, CDCl <sub>3</sub> )	<sup>1</sup> H (400 MHz, CDCl <sub>3</sub> )	<sup>13</sup> C (100 MHz, CDCl <sub>3</sub> )	<sup>1</sup> H (500 MHz, CDCl <sub>3</sub> )		<sup>13</sup> C (100 MHz, CDCl <sub>3</sub> )	<sup>1</sup> H (400 MHz, CDCl <sub>3</sub> )	<sup>13</sup> C (100 MHz, CDCl <sub>3</sub> )	<sup>1</sup> H (500 MHz, CDCl <sub>3</sub> )
1	36.7450	1.7023, 1.0624	36.71	1.77, 1.05	Qui-1'	102.1905	4.3805 (d, J=8.08 Hz)	102.17	4.37 (d, J=8 Hz)
2	27.1235	1.8873, 1.4463	27.09	1.93, 1.46	2'	72.2190	5.0025 (dd overlapped, J= 9.6, 8.14 Hz)	72.16	5.06 (dd, J=9.6, 8 Hz)
3	73.2324	4.6471 (m)	73.19	4.63 (dddd, J= 10.5, 10, 6, 5 Hz)	3'	81.8661	3.7182 (t, J=9.36 Hz)	81.88	3.7 (t, J= 9.6 Hz)
4	28.1858	2.0567, 1.2427	28.15	2.09, 1.25	4'	74.4845	4.8347 (t, J= 9.32 Hz)	74.43	5.0 (t, J= 9.6 Hz)
5	49.5329	1.2362	49.5	1.22	5'	69.9401	3.3979 (dd, J= 9.56, 6.16 Hz)	69.87	3.44 (m)
6	80.5715	3.2542 (m)	80.52	3.22 (ddd, J= 10, 10, 5 Hz)	6'	17.4427	1.1952 (d, 6.16 Hz)	17.44	1.18 (d, J= 6.4 Hz)
7	39.2448	1.7109, 1.0683	39.55	2.01 1.72	Rha-1''	99.4627	4.7950 (d, J= 1.28 Hz)	99.46	4.79 (d, J= 1.6 Hz)
8	33.9667	1.6074	33.8	1.61	2''	69.9059	5.0910 (t, J= 3.9 Hz overlapped)	69.87	5.07 (m)
9	53.2001	0.6801 (td, J=11.44, 3.68)	53.1	0.69	3''	68.9174	5.0955 (t, J=4.8 Hz overlapped)	68.89	5.08 (m)
10	36.3911	-	36.39	-	4''	70.6271	5.0195 (dd overlapped, J= 10.76, 9.7)	70.56	5.02 (dd, J= 10, 9.6 Hz)
11	20.7445	1.4691, 1.2024	20.78	1.6, 1.2	5''	67.3934	3.8933 (dd, J= 9.54, 6.26 Hz)	67.38	3.88 (dd, J= 10, 6.4 Hz)
12	39.9032	2.1351, 1.0745	39.91	2.08, 1.68	6''	17.1910	1.1574 (d, J= 6.2)	17.18	1.14 (d, 6.4 Hz)
13	40.9123	-	41.02	-	Acetyl signals			Acetyl signals <sup>13</sup>	
14	55.8109	1.26, 1.1441	55.78	1.23, 1.14	Position	$\delta$ (ppm), J (Hz)		$\delta$ (ppm), J (Hz)	
15	31.7263	2.04, 1.2739	31.65	2.05		<sup>13</sup> C (100 MHz, CDCl <sub>3</sub> )	<sup>1</sup> H (400 MHz, CDCl <sub>3</sub> )	<sup>13</sup> C (100 MHz, CDCl <sub>3</sub> )	<sup>1</sup> H (500 MHz, CDCl <sub>3</sub> )
16	81.5021	4.5021 (m)	81.1	4.46 (ddd, J= 7.5, 7.4, 7 Hz)	C=O	169.3831	-	-	-
17	63.7210	1.7262 (dd, J= 7.96, 5.42 Hz)	61.42	0.69 (dd, J= 8.4, 6.4 Hz)	C=O	169.4926	-	-	-
18	16.0828	0.7655 (s)	16.09	0.79	C=O	169.6871	-	-	-
19	13.3695	0.8615 (s)	13.35	0.84	C=O	170.1131	-	-	-
20	40.4399	2.0069	36.03	2.09	C=O	170.1785	-	-	-
21	13.9458	0.9949 (d, J= 6.92 Hz)	14.09	0.94 (d, J= 6.4 Hz)	C=O	170.2342	-	-	-
22	109.2227	-	108.58	-	C=O	170.2868	-	-	-
23	71.8426	4.8149 (t, J=13.6 Hz)	68.6	4.81 (m)	CH <sub>3</sub> C=O	-	1.96 (s)	-	-
24	30.6427	2.1468, 1.6303	34.0	1.70, 1.61	CH <sub>3</sub> C=O	-	2.01 (s)	-	-
25	25.7910	1.7198	30.65	1.88	CH <sub>3</sub> C=O	-	2.05 (s)	-	-
26 $\alpha$	64.6925	4.0416 (dd, J= 11.24, 3.12 Hz)	65.68	3.36 (dd, J= 11, 10 Hz)	CH <sub>3</sub> C=O	-	2.10 (s)	-	-
26 $\beta$	64.6925	3.4212 (d, J= 9.88 Hz)	65.68	3.46 (dd, J= 11, 3 Hz)	CH <sub>3</sub> C=O	-	2.14 (s)	-	-
27	16.6604	1.0954 (d, 6.92Hz)	16.4	0.83 (d, J= 6.4 Hz)	CH <sub>3</sub> C=O	-	2.15 (s)	-	-
					CH <sub>3</sub> C=O	-	2.15 (s)	-	-



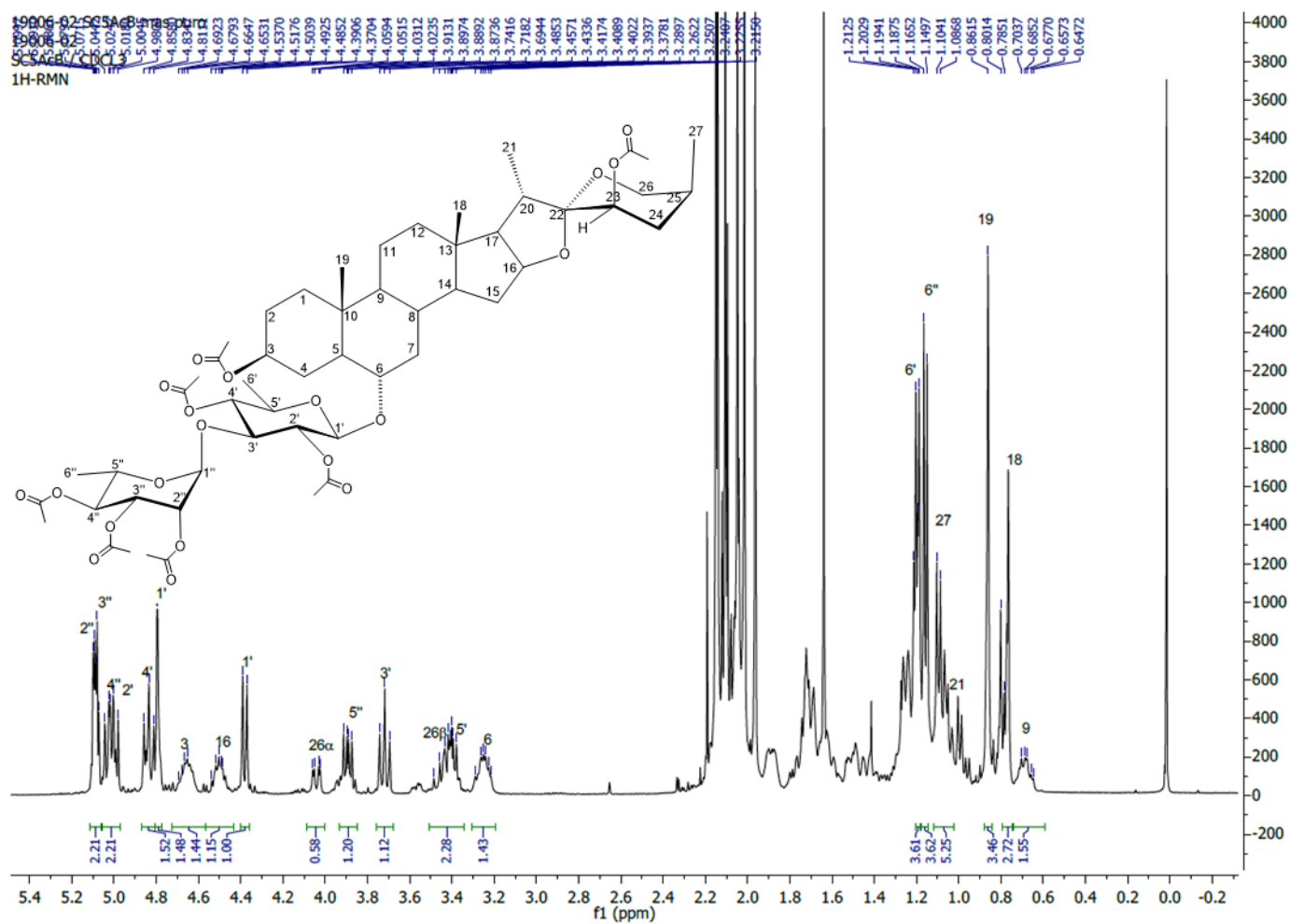


**Figure 25.**  $^1\text{H}$  NMR spectrum (400 MHz,  $\text{CDCl}_3$ ) of 2'',3'',5''-triacetoxy-6- $\alpha$ -O- $\alpha$ -L-rhamnopyranosyl-(1 $\rightarrow$ 3)-2',4'-diacetoxy- $\beta$ -D-quinovopyranosyl-(23R,25S)-5 $\alpha$ -spirostan-3 $\beta$ ,23 $\beta$ -acetate (SC5AcB)

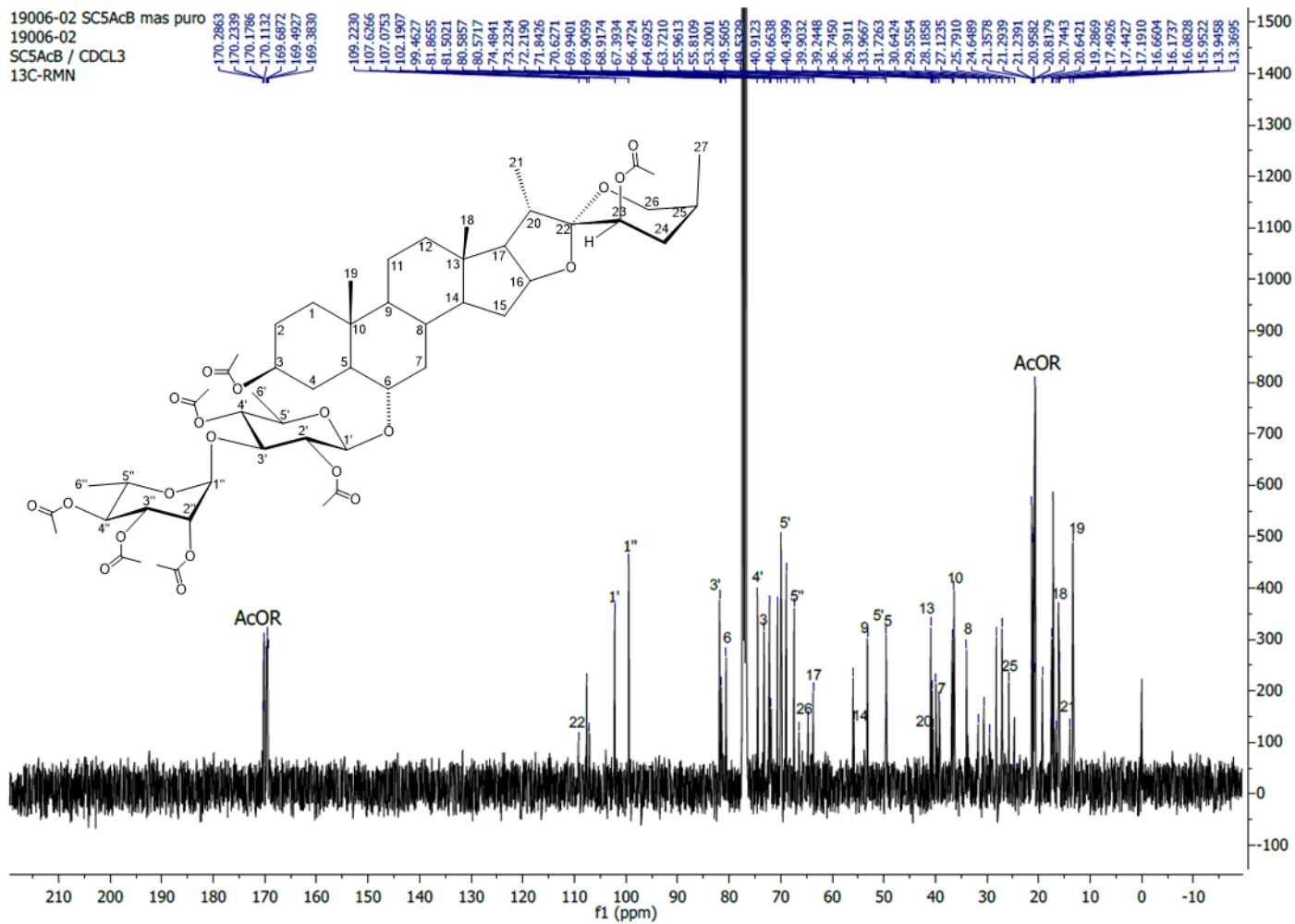


**Figure 26.**  $^{13}\text{C}$  NMR spectrum (400 MHz,  $\text{CDCl}_3$ ) of 2'',3'',5''-triacetoxy-6- $\alpha$ -O- $\alpha$ -L-rhamnopyranosyl-(1 $\rightarrow$ 3)-2',4'-diacetoxy- $\beta$ -D-quinovopyranosyl-(23R,25S)-5 $\alpha$ -spirostan-3 $\beta$ ,23 $\beta$ -acetate (SC5AcB)

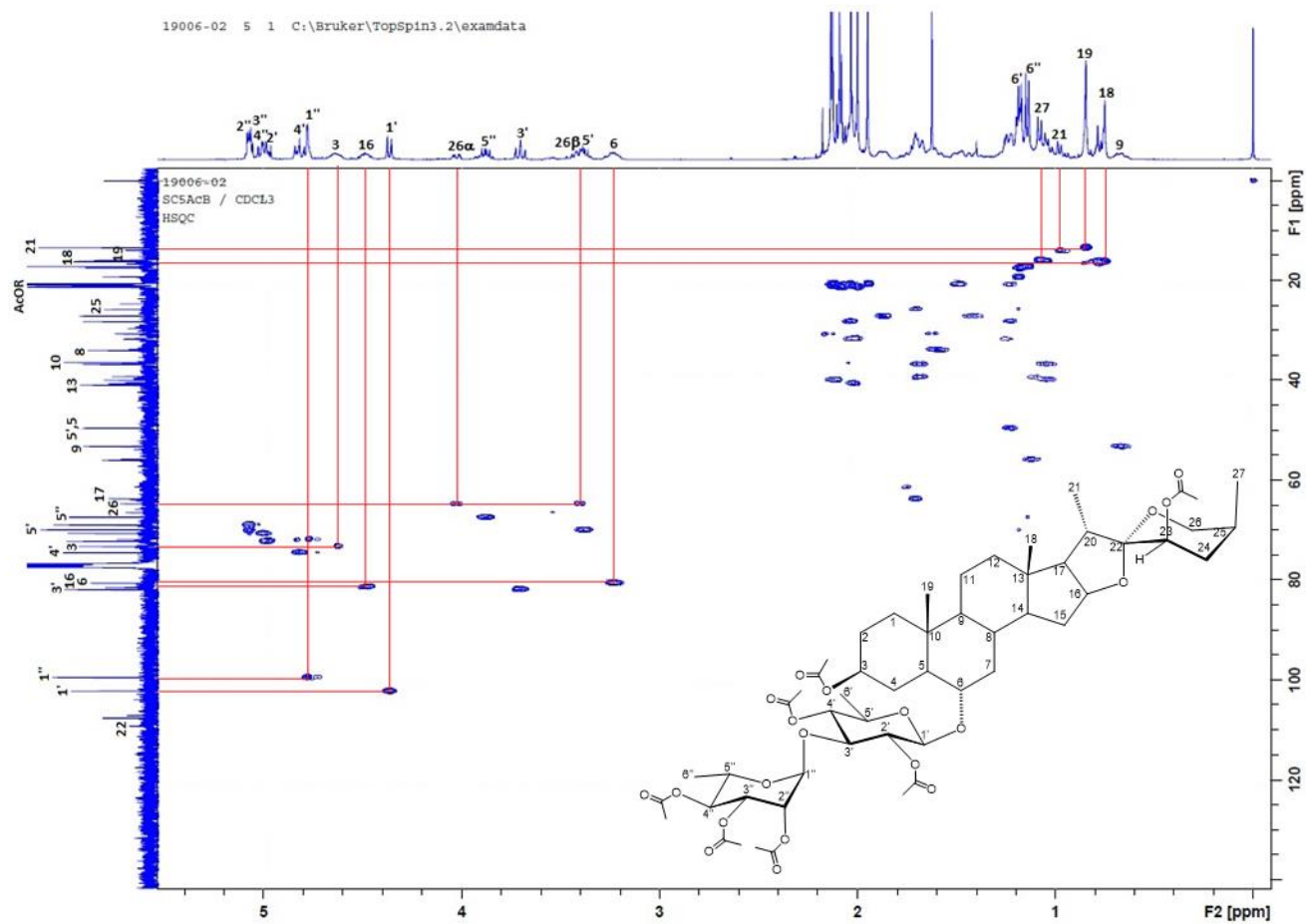


**Figure 27.** HSQC spectrum (400 MHz, CDCl<sub>3</sub>) of 2'',3'',5''-triacetoxy-6- $\alpha$ -O- $\alpha$ -L-rhamnopyranosyl-(1 $\rightarrow$ 3)-2',4'-diacetoxy- $\beta$ -D-quinovopyranosyl-(23R,25S)-5 $\alpha$ -spirostan-3 $\beta$ ,23 $\beta$ -acetate (SC5AcB)

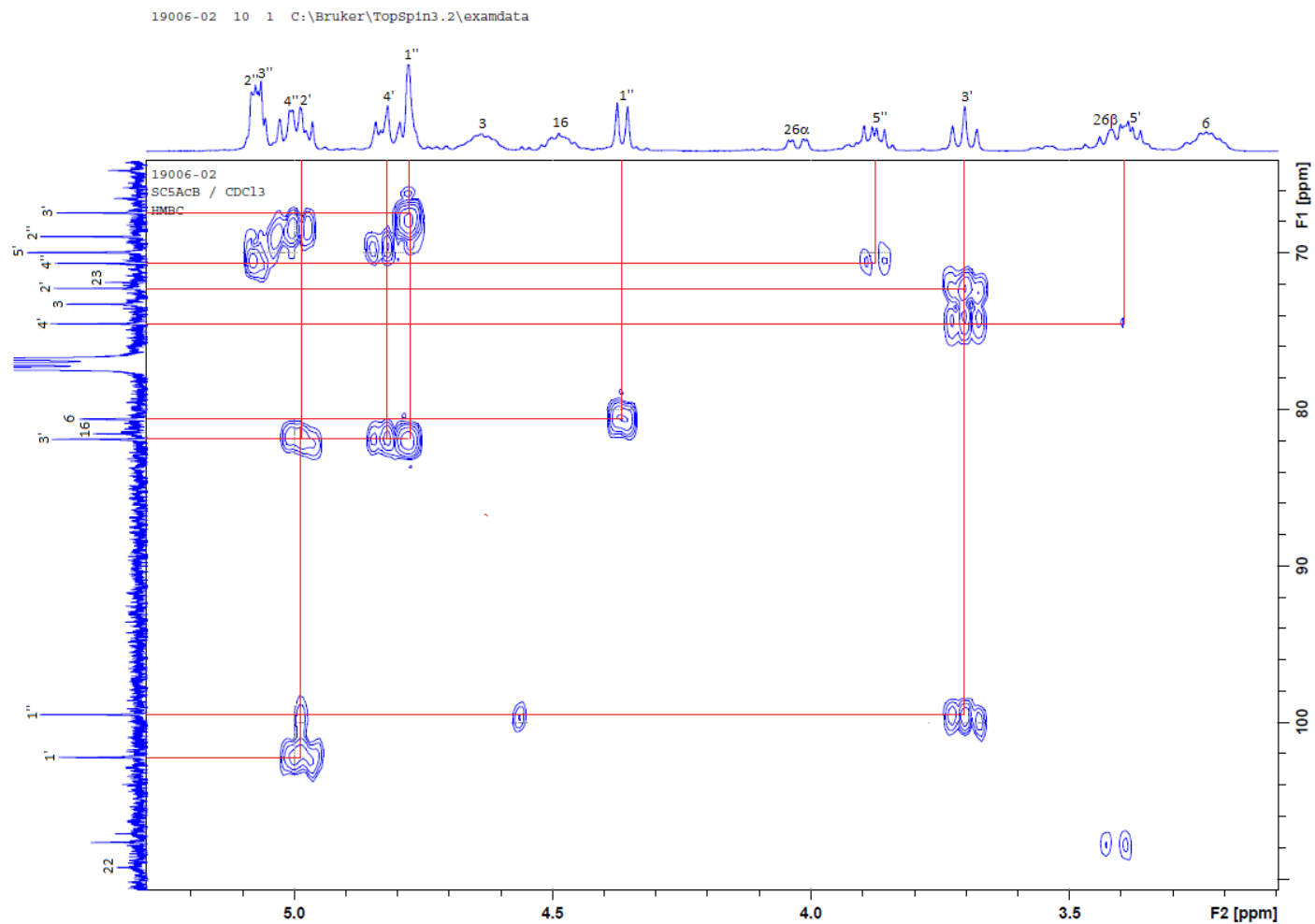


**Figure 28.** HMBC partial spectrum (400 MHz, CDCl<sub>3</sub>) of 2'',3'',5''-triacetoxy-6- $\alpha$ -O- $\alpha$ -L-rhamnopyranosyl-(1 $\rightarrow$ 3)-2',4'-diacetoxy- $\beta$ -D-quinovopyranosyl-(23R,25S)-5 $\alpha$ -spirostan-3 $\beta$ ,23 $\beta$ -acetate (SC5AcB)

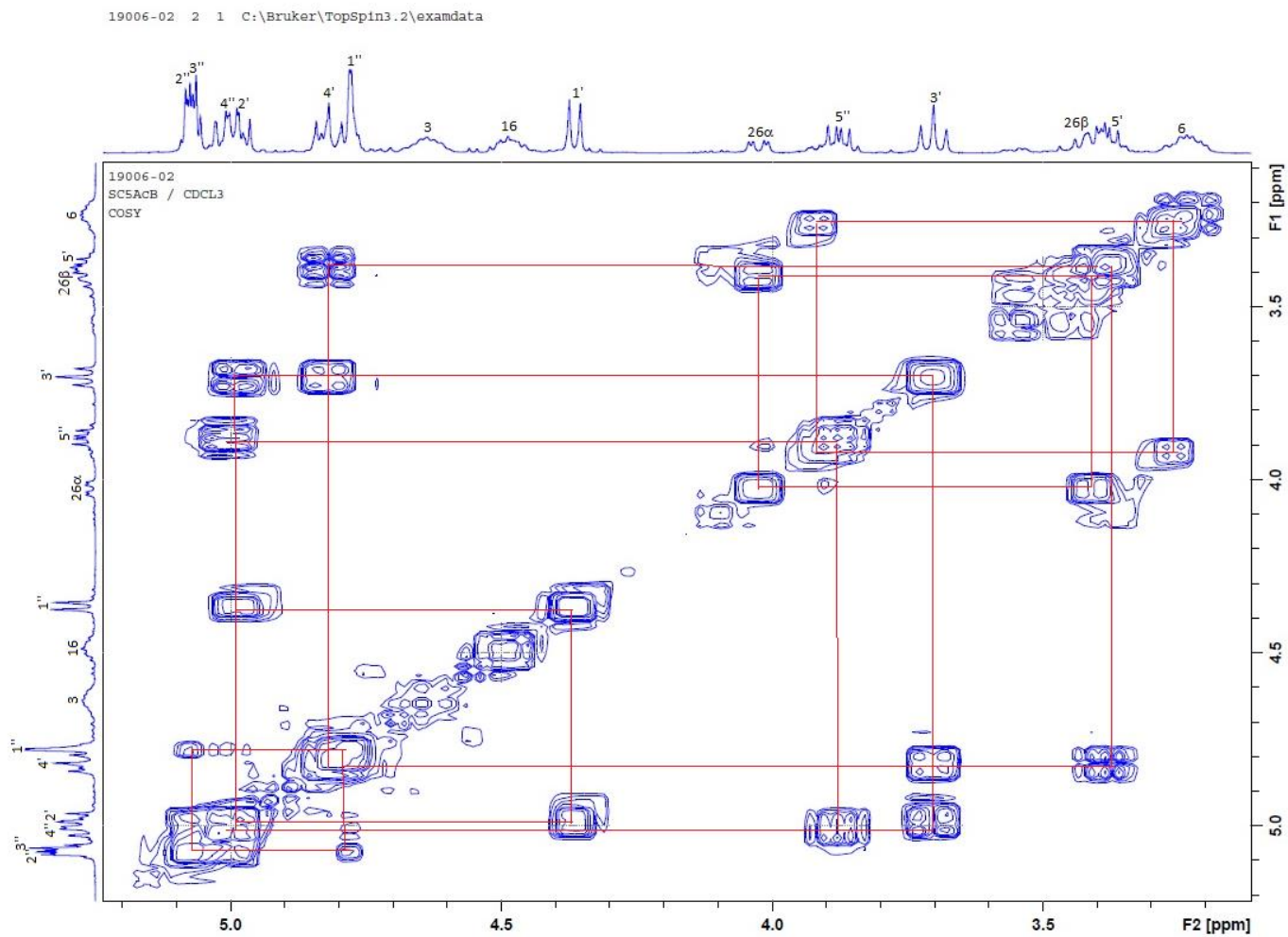


**Figure 29.** COSY partial spectrum (400 MHz, CDCl<sub>3</sub>) of 2'',3'',5''-triacetoxy-6- $\alpha$ -O- $\alpha$ -L-rhamnopyranosyl-(1 $\rightarrow$ 3)-2',4'-diacetoxy- $\beta$ -D-quinovopyranosyl-(23R,25S)-5 $\alpha$ -spirostan-3 $\beta$ ,23 $\beta$ -acetate (SC5AcB)

5.1.6. Physical and spectrometric data of 6- $\alpha$ -O- $\alpha$ -L-rhamnopyranosyl-(1 $\rightarrow$ 3)- $\beta$ -D-quinovopyranosyl-(23R,25S)-5 $\alpha$ -spirostan-3 $\beta$ ,23 $\beta$ -ol (SC5B)

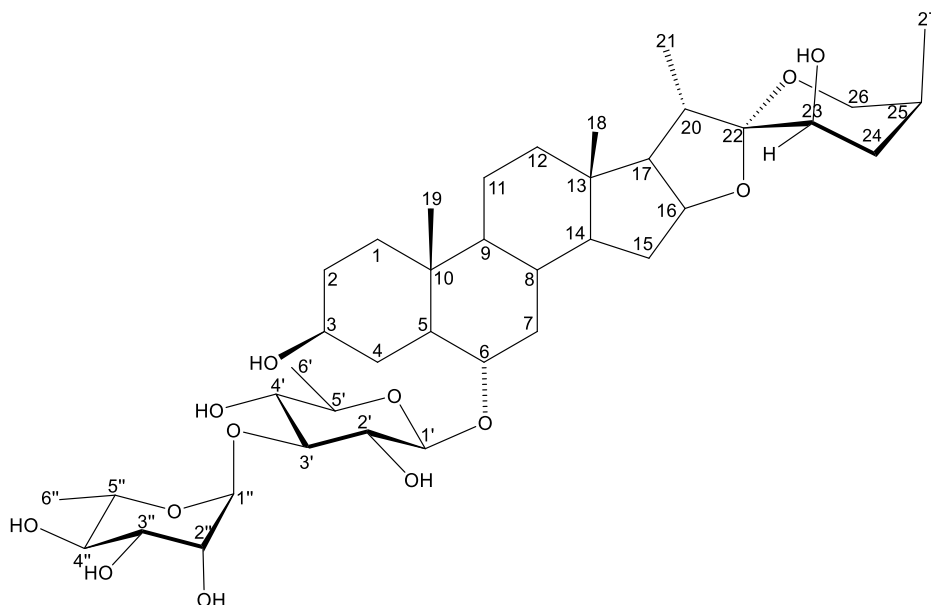


**Figure 30.** 6- $\alpha$ -O- $\alpha$ -L-rhamnopyranosyl-(1 $\rightarrow$ 3)- $\beta$ -D-quinovopyranosyl-(23R,25S)-5 $\alpha$ -spirostan-3 $\beta$ ,23 $\beta$ -ol (SC5B)

**Compound SC5B:** the compound 6- $\alpha$ -O- $\alpha$ -L-rhamnopyranosyl-(1 $\rightarrow$ 3)- $\beta$ -D-quinovopyranosyl-(23R,25S)-5 $\alpha$ -spirostan-3 $\beta$ ,23 $\beta$ -ol (SC5B) was obtained as white powder, mp 207-210 °C,  $[\alpha]_{25}^D$  -40°(c 0.2, CH<sub>3</sub>OH). The negative ion mode HRESIMS showed the quasimolecular ion peak  $m/z$  785.4337 [M+COOH]<sup>-</sup> in agreement with the molecular formula C<sub>40</sub>H<sub>65</sub>O<sub>15</sub>. The structural elucidation of compound SC5B was performed by spectroscopic analysis of its acetylated derivative SC5AcB.

5.1.7. Physical, spectroscopic and spectrometric data of 2'',3'',5''-triacetoxy-6- $\alpha$ -O- $\beta$ -D-xylopyranosyl-(1 $\rightarrow$ 3)-2',4'-diacetoxy- $\beta$ -D-quinovopyranosyl-(23R,25S)-5 $\alpha$ -spirostan-3 $\beta$ ,23 $\beta$ -acetate (SC5AcC)

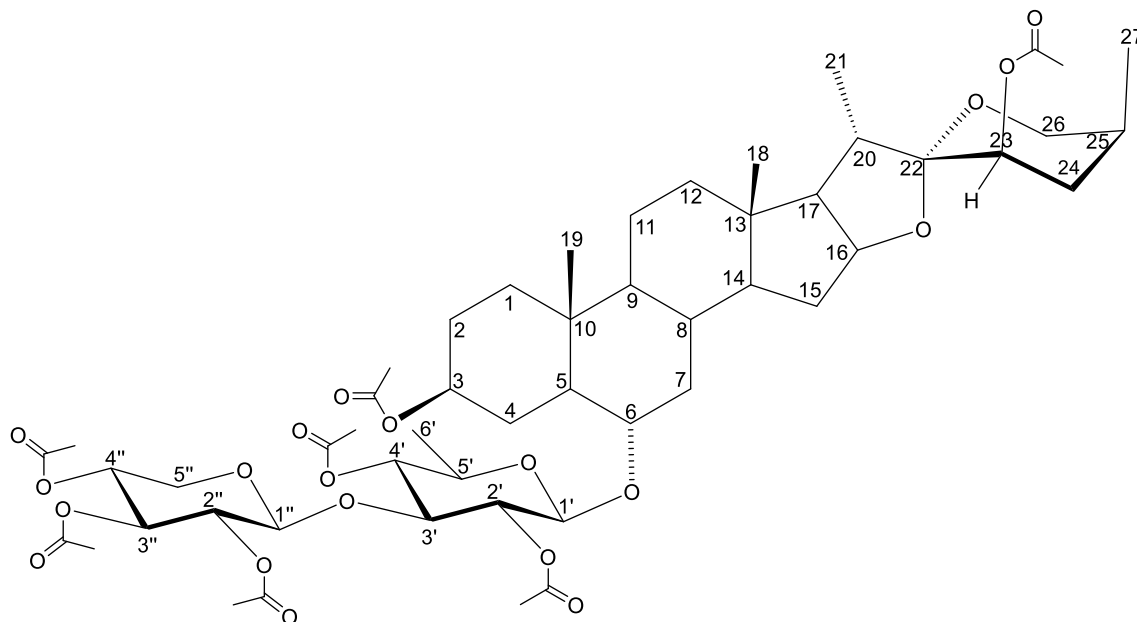


**Figure 31.** 2'',3'',5''-triacetoxy-6- $\alpha$ -O- $\beta$ -D-xylopyranosyl-(1 $\rightarrow$ 3)-2',4'-diacetoxy- $\beta$ -D-quinovopyranosyl-(23R,25S)-5 $\alpha$ -spirostan-3 $\beta$ ,23 $\beta$ -acetate (SC5AcC)

**Compound SC5AcC:** white powder, mp 144-147 °C, (10 mg, yield: 0.000778 %),  $[\alpha]_{25}^D$  -40° (c 0.2, CHCl<sub>3</sub>), soluble in CHCl<sub>3</sub>, M.W. 1020.49299 g/mol. The positive ion mode HRESIMS showed concordance of the quasimolecular ion peak  $m/z$  1043.4844 [M+Na]<sup>+</sup> with the molecular formula C<sub>52</sub>H<sub>76</sub>O<sub>20</sub>Na. For <sup>1</sup>H NMR (400 MHz, CDCl<sub>3</sub>) and <sup>13</sup>C NMR (100 MHz, CDCl<sub>3</sub>) see table 6.

**5.1.7.1. Structural elucidation of 2'',3'',5''-triacetoxy-6- $\alpha$ -O- $\beta$ -D-xylopyranosyl-(1 $\rightarrow$ 3)-2',4'-diacetoxy- $\beta$ -D-quinovopyranosyl-(23R,25S)-5 $\alpha$ -spirostan-3 $\beta$ ,23 $\beta$ -acetate (SC5AcC)**

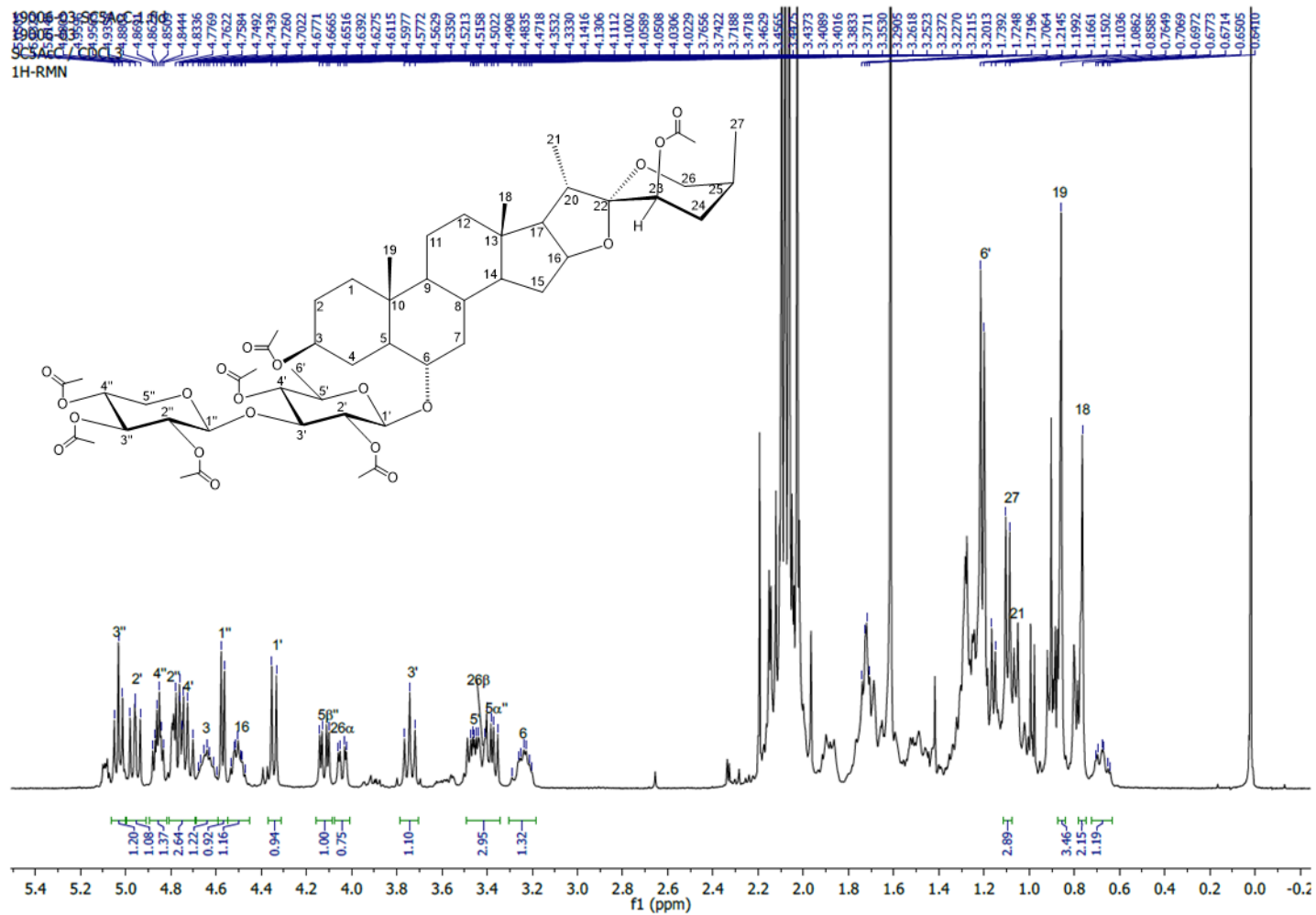
The  $^1\text{H}$  NMR spectrum of SC5AcC (figure 32) showed the same aglycone signals for SC5AcB (Table 5 and 6), showing the same steroid methyls at  $\delta$  0.76 (s, 3H, H-18), 0.85 (s, 3H, H-19), 1.05 (d,  $J=6.9$  Hz, 3H, H-21), and the methyl in the spirostane ring at 1.09 (d,  $J=6.92$  Hz, 3H, H-27), However, one of the two anomeric protons identified for SC5AcC was different when compared with SC5AcB, being the one at  $\delta$  4.34 (d,  $J=8.08$  Hz, 1H, H-1') present in both compounds and the one at 4.57 (d,  $J=5.72$  Hz, 1H, H-1'') only observed in SC5AcC, and additionally only one hexose sugar unit methyl was observed in SC5AcC at  $\delta$  1.2 (d,  $J=6.12$  Hz, 3H, H-6'), which means that the disaccharide moiety in SC5AcC is composed by an hexose and a pentose. The  $^{13}\text{C}$  NMR spectrum of SC5AcC (figure 33) displayed the same 27 aglycone signals observed in SC5AcB, and regarding the disaccharide moiety, only six hexose signals were in common with SC5AcB, being the remaining five signals corresponding to a pentose. The methyl, methylene, and methine signals attributions were confirmed by analysis of DEPT90, DEPT135, and HSQC (figure 34) spectroscopic data. All the hydrogen and carbon spectroscopic constants for SC5AcC aglycone were the same than SC5AcB, which means that neosolaspigenin is the aglycone in SC5AcC<sup>23,36,37,38</sup>. When compared the acetylated disaccharide moiety for SC5AcC with SC5AcB it was identified the  $\beta$ -D-quinovopyranose diacetate spin system in both compounds, being this acetylated hexose connected



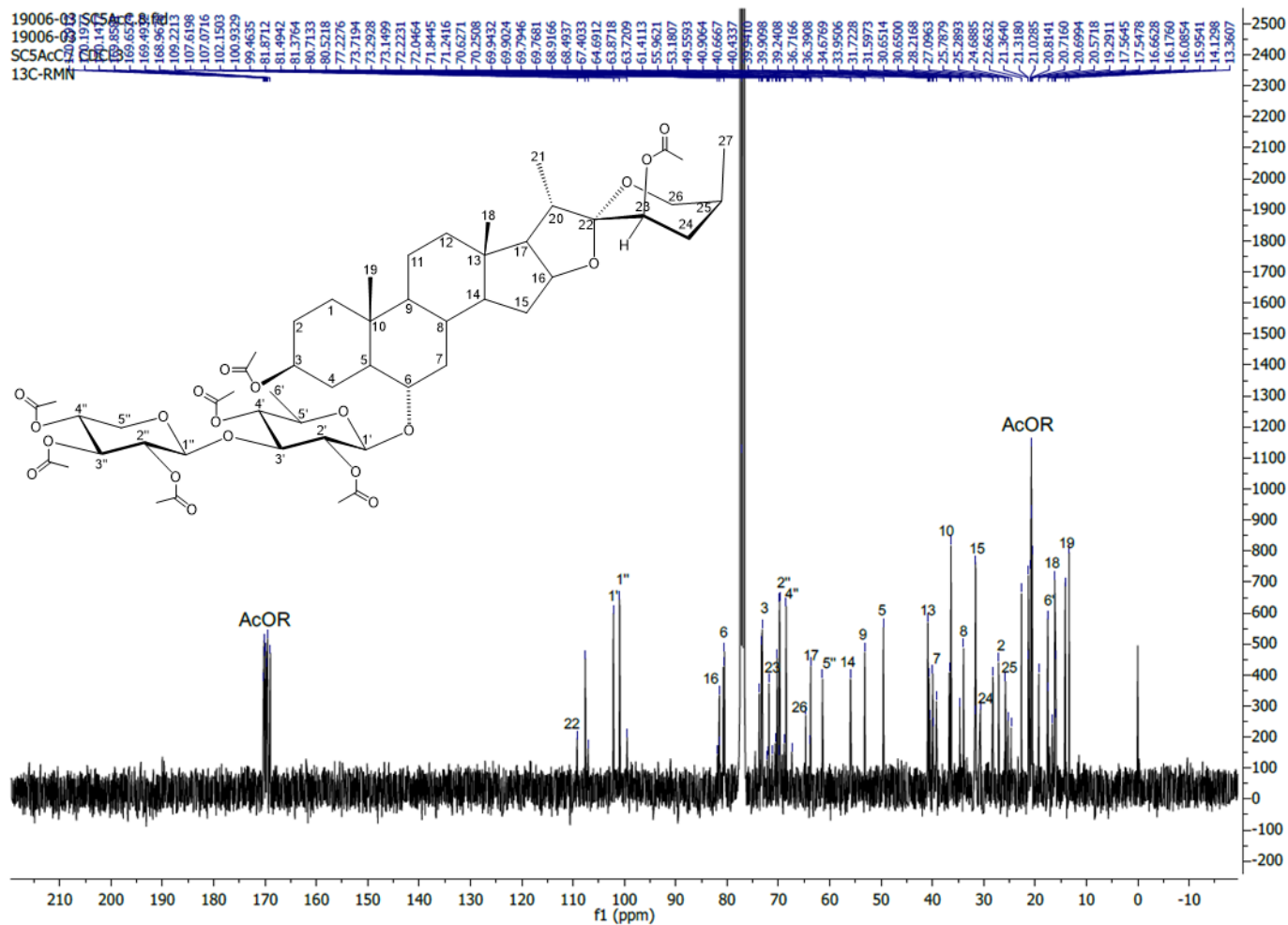
directly to the aglycone moiety in C-6 in both compounds, such deductions were determined by analysis of HMBC (figure 35) and COSY (figure 36) spectroscopic data. The spin system corresponding to the terminal pentose unit in SC5AcC corresponded to  $\beta$ -D-xylopyranose triacetate, and all the hydrogen and carbon spectroscopic constants for this sugar moiety were in good agreement with the reports in the literature<sup>21,23</sup>. The connectivity between the sugar units was deduced by analysis of HMBC spectroscopic data, by identification of the correlation ( $^3J_{C-H}$ ):C-3'( $\delta$  80.71)/H-1''( $\delta$  4.57), indicating 1 $\rightarrow$ 3 bonding for the terminal pentose with the hexose bonded with the aglycone. With a basis on the complete 1D and 2D NMR spectroscopic data analysis of SC5AcC, and comparing with the literature, it was found that the acetylated derivative SC5AcC was previously reported as the compound 3a by González *et al.* 2004<sup>21</sup>, being the compound elucidated as 2'',3'',5''-triaceoxy-6- $\alpha$ -O- $\beta$ -D-xylopyranosyl-(1 $\rightarrow$ 3)-2',4'-diaceoxy- $\beta$ -D-quinovopyranosyl-(23R,25S)-5 $\alpha$ -spirostan-3 $\beta$ ,23 $\beta$ -acetate (SC5AcC), a previously reported acetylated steroidal saponin from the plant *Solanum hispidum*.

Table 6. <sup>13</sup>C NMR and <sup>1</sup>H NMR data for SC5AcC and reference compound 3a<sup>21</sup>

Aglycone signals: (25S)-5 $\alpha$ -spirostan-3 $\beta$ -acetate			Aglycone signals: (25R)-5 $\alpha$ -spirostan-3 $\beta$ -acetate <sup>21</sup>		Saccharide signals: $\beta$ -D-xylopyranose and $\beta$ -D-quinovopyranose			Saccharide signals: $\beta$ -D-xylopyranose and $\beta$ -D-quinovopyranose <sup>21</sup>	
Position	$\delta$ (ppm), J (Hz)		$\delta$ (ppm), J (Hz)		Position	$\delta$ (ppm), J (Hz)		$\delta$ (ppm), J (Hz)	
	<sup>13</sup> C (100 MHz, CDCl <sub>3</sub> )	<sup>1</sup> H (400 MHz, CDCl <sub>3</sub> )	<sup>13</sup> C (125 MHz, CDCl <sub>3</sub> )	<sup>1</sup> H (500 MHz, CDCl <sub>3</sub> )		<sup>13</sup> C (100 MHz, CDCl <sub>3</sub> )	<sup>1</sup> H (400 MHz, CDCl <sub>3</sub> )	<sup>13</sup> C (125 MHz, CDCl <sub>3</sub> )	<sup>1</sup> H (500 MHz, CDCl <sub>3</sub> )
1	36.7166	1.7079, 1.0279	36.69	-	Qui-1'	102.1503	4.3431 (d, J= 8.08 Hz)	102.13	4.32 (d, J= 8.5 Hz)
2	27.0963	1.8731, 1.4736	27.08	-	2'	73.2928	4.9579 (dd, J= 9.56, 8.24 Hz)	73.16	4.93 (dd, J= 9.5, 8.5 Hz)
3	73.1499	4.6392 (m)	73.28	4.62 (m)	3'	80.7133	3.7422 (t, J= 9.36 Hz)	80.67	3.72 (t, J= 9.6 Hz)
4	28.2169	2.0042, 1.2077	28.20	-	4'	73.7194	4.7260 (t, J= 9.4 Hz)	73.73	4.72 (t, J= 9.5 Hz)
5	49.5593	1.2316	49.54	-	5'	69.9432	3.4594 (m)	69.70	3.45 (m)
6	80.5218	3.2320 (m)	80.48	3.22 (m)	6'	17.5645	1.2070 (d, J= 6.12 Hz)	17.50	1.18 (d, J= 6.0 Hz)
7	39.9410	2.1206, 1.0509	39.20	-	Xyl-1''	100.9329	4.57 (d, J= 5.72 Hz)	100.93	4.55 (d, 6.0 Hz)
8	33.9506	1.6119	33.94	-	2''	69.7946	4.76 (dd, J= 7.36, 5.84 Hz)	69.81	4.74 (dd, J= 7.0, 6.0 Hz)
9	53.1807	0.6743 (td, J= 11.08, 3.84 Hz)	53.17	-	3''	70.2508	5.0322 (t, J= 7.32 Hz)	70.26	5.01 (t, J= 7.0 Hz)
10	36.3908	-	36.36	-	4''	68.4937	4.8509 (m)	68.50	4.83 (ddd, J= 7.0, 7.0, 4.5 Hz)
11	20.8141	1.4734, 1.2234	20.67	-	5 $\alpha$ ''	61.4113	3.3771 (dd, J= 12.16, 7.28 Hz)	61.41	3.35 (dd, J= 12.0, 7.0 Hz)
12	39.9098	2.1358, 0.9887	39.91	-	5 $\beta$ ''	61.4113	4.1215 (dd, J= 12.16, 4.4 Hz)	61.41	4.09 (dd, J= 12.0, 4.5 Hz)
13	40.9064	-	40.89	-	<b>Acetyl signals</b>			<b>Acetyl signals<sup>36</sup></b>	
14	55.9621	1.1166	55.96	-	Position	$\delta$ (ppm), J (Hz)		$\delta$ (ppm), J (Hz)	
15	31.7228	2.0298, 1.2739	29.67	-		<sup>13</sup> C (100 MHz, CDCl <sub>3</sub> )	<sup>1</sup> H (400 MHz, CDCl <sub>3</sub> )	<sup>13</sup> C (125 MHz, CDCl <sub>3</sub> )	<sup>1</sup> H (500 MHz, CDCl <sub>3</sub> )
16	81.4942	4.5022 (m)	81.48	-	C=O	168.9678	-	-	-
17	63.7209	1.7227 (dd, J= 7.6, 5.52 Hz)	63.72	-	C=O	169.4932	-	-	-
18	16.1760	0.7649 (s)	16.13	0.78 (s)	C=O	169.6524	-	-	-
19	13.3606	0.8585 (s)	13.32	0.84 (s)	C=O	169.8581	-	-	-
20	40.4337	2.0436 (m)	40.50	-	C=O	170.1477	-	-	-
21	15.9541	1.0599 (d, J= 6.92 Hz)	15.90	0.97 (d, J= 7.0 Hz)	C=O	170.1977	-	-	-
22	109.2213	-	107.62	-	C=O	170.2912	-	-	-
23	71.8444	4.7921 (t, J= 3.56 Hz)	71.84	4.77 (t, J=3.0 Hz)	CH <sub>3</sub> C=O	20.5775	overlapped	-	-
24	30.6500	2.1693, 1.5933	30.03	-	CH <sub>3</sub> C=O	20.6994	2.0269	-	-
25	25.7828	1.7222 (m)	25.77	-	CH <sub>3</sub> C=O	20.7160	2.0609	-	-
26 $\alpha$	64.6912	4.04 (dd, J= 11.24, 3.16 Hz)	64.50	3.91 (dd, J= 11.0, 2.5 Hz)	CH <sub>3</sub> C=O	20.8141	2.0646	-	-
26 $\beta$	64.6912	3.4228 (d, J= 11.36 Hz)	64.50	3.25 (dd, J= 11.0 Hz)	CH <sub>3</sub> C=O	21.0285	2.0955	-	-
27	16.0854	1.0954 (d, J= 6.96 Hz)	19.30	1.11 (d, J= 6.8 Hz)	CH <sub>3</sub> C=O	21.3180	2.0799 overlapped	-	-
					CH <sub>3</sub> C=O	21.3640	2.0799 overlapped	-	-



**Figure 32.** <sup>1</sup>H NMR spectrum (400 MHz, CDCl<sub>3</sub>) of 2'',3'',5''-triacetoxy-6- $\alpha$ -O- $\beta$ -D-xylopyranosyl-(1 $\rightarrow$ 3)-2',4'-diacetoxy- $\beta$ -D-quinovopyranosyl-(23R,25S)-5 $\alpha$ -spirostan-3 $\beta$ ,23 $\beta$ -acetate (SC5AcC)



**Figure 33.**  $^{13}\text{C}$  NMR spectrum (100 MHz,  $\text{CDCl}_3$ ) of 2'',3'',5''-triacetoxy-6- $\alpha$ -O- $\beta$ -D-xylopyranosyl-(1 $\rightarrow$ 3)-2',4'-diacetoxy- $\beta$ -D-quinovopyranosyl-(23R,25S)-5 $\alpha$ -spirostan-3 $\beta$ ,23 $\beta$ -acetate (SC5AcC)

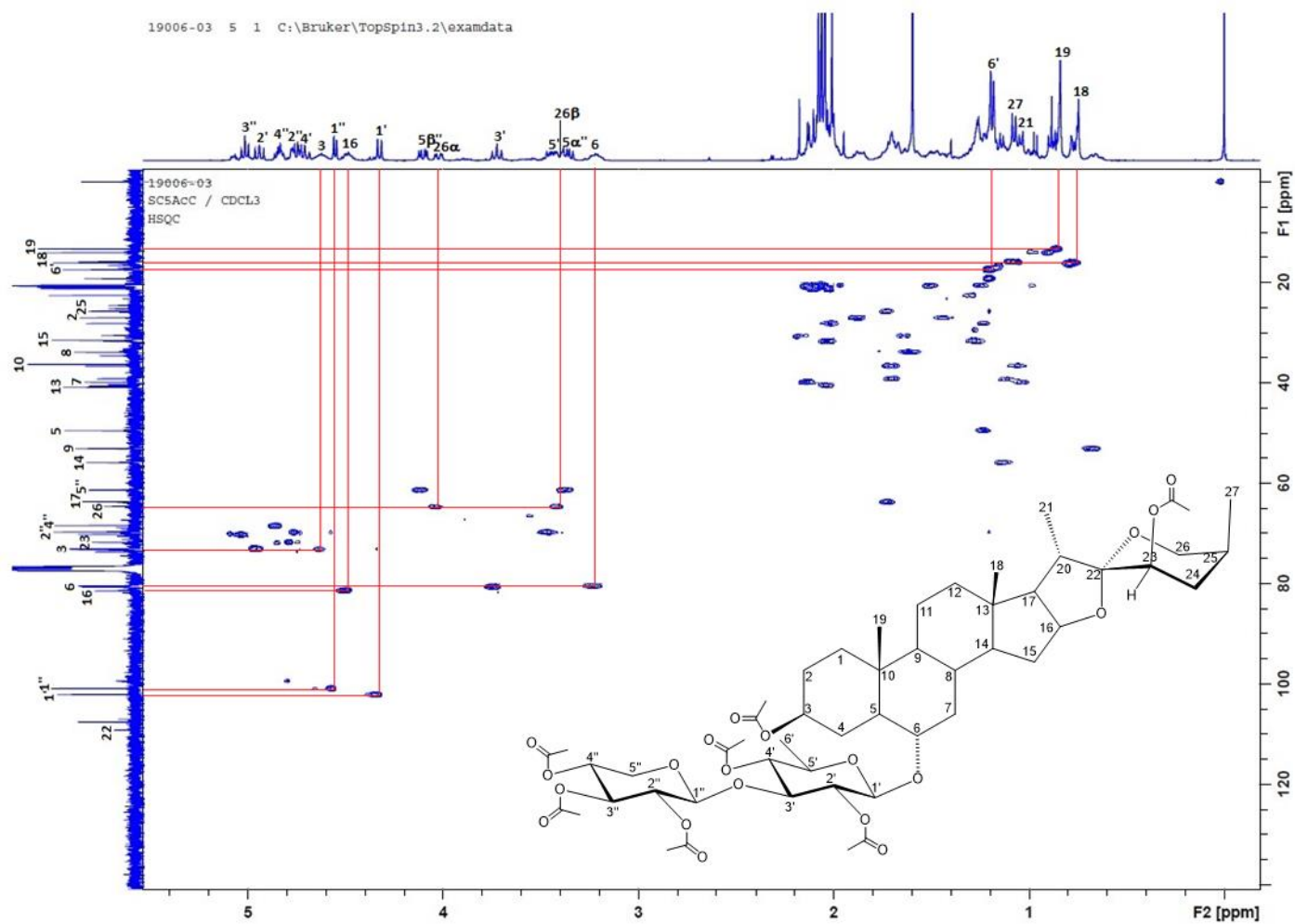


**Figure 34.** HSQC spectrum (400 MHz, CDCl<sub>3</sub>) of 2'',3'',5''-triacetoxy-6- $\alpha$ -O- $\beta$ -D-xylopyranosyl-(1 $\rightarrow$ 3)-2',4'-diacetoxy- $\beta$ -D-quinovopyranosyl-(23R,25S)-5 $\alpha$ -spirostan-3 $\beta$ ,23 $\beta$ -acetate (SC5AcC)

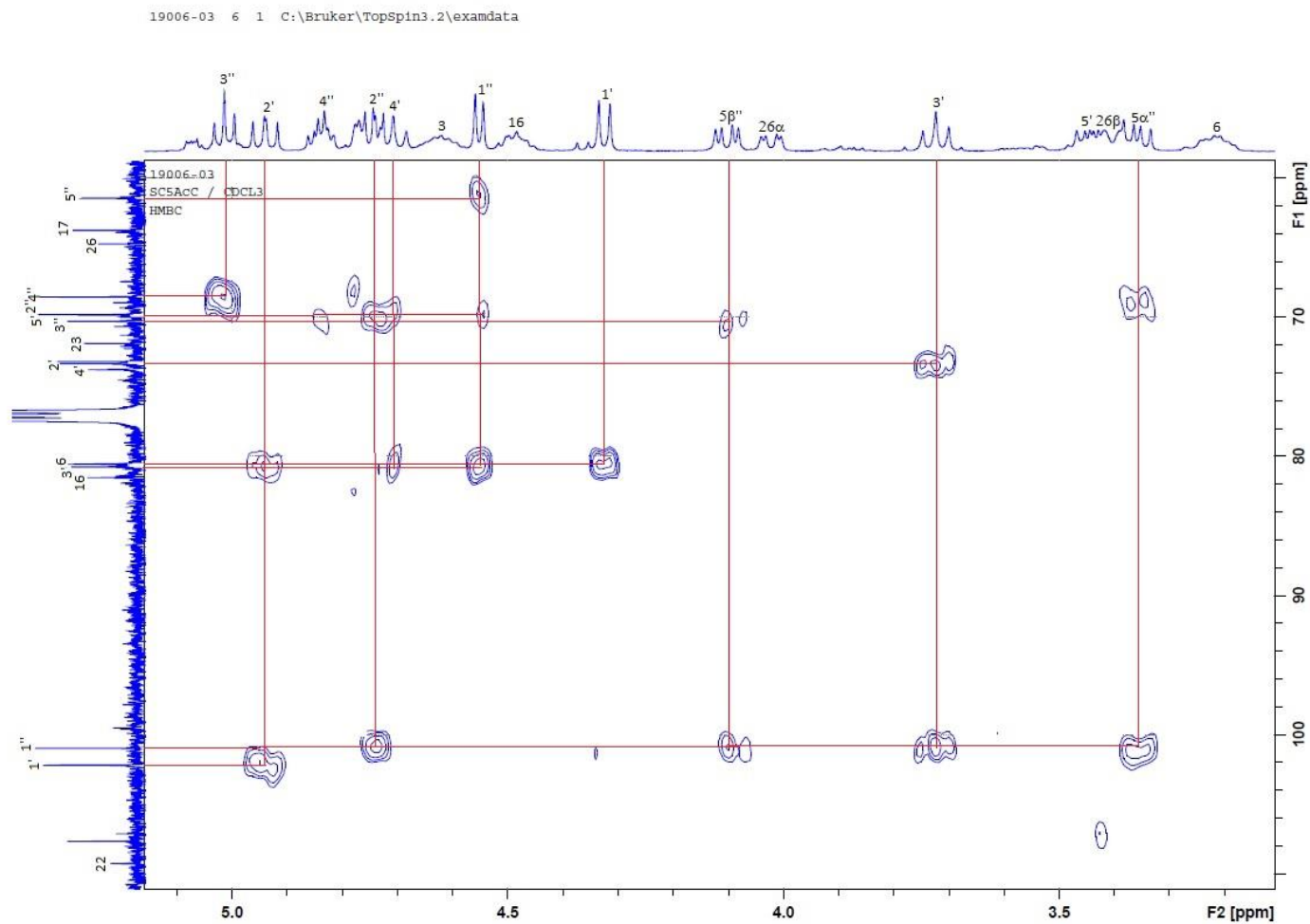


**Figure 35.** HMBC spectrum (400 MHz, CDCl<sub>3</sub>) of 2'',3'',5''-triacetoxy-6- $\alpha$ -O- $\beta$ -D-xylopyranosyl-(1 $\rightarrow$ 3)-2',4'-diacetoxy- $\beta$ -D-quinovopyranosyl-(23R,25S)-5 $\alpha$ -spirostan-3 $\beta$ ,23 $\beta$ -acetate (SC5AcC)

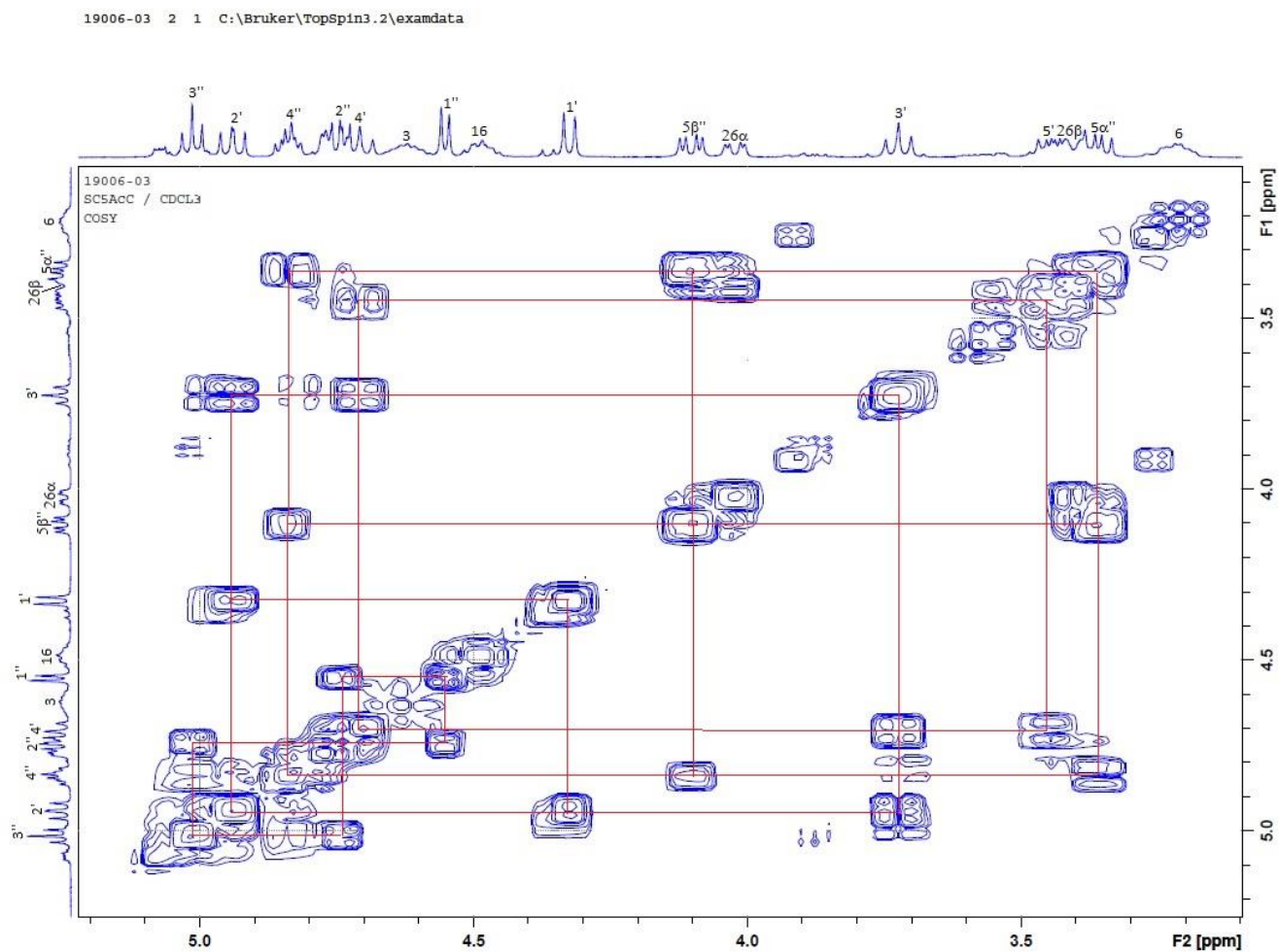


**Figure 36.** COSY spectrum (400 MHz, CDCl<sub>3</sub>) of 2'',3'',5''-triacetoxy-6- $\alpha$ -O- $\beta$ -D-xylopyranosyl-(1 $\rightarrow$ 3)-2',4'-diacetoxy- $\beta$ -D-quinovopyranosyl-(23R,25S)-5 $\alpha$ -spirostan-3 $\beta$ ,23 $\beta$ -acetate (SC5AcC)

5.1.8. Physical and spectrometric data of 6- $\alpha$ -O- $\beta$ -D-xylopyranosyl-(1 $\rightarrow$ 3)- $\beta$ -D-quinovopyranosyl-(23R,25S)-5 $\alpha$ -spirostan-3 $\beta$ ,23 $\beta$ -ol (SC5C)

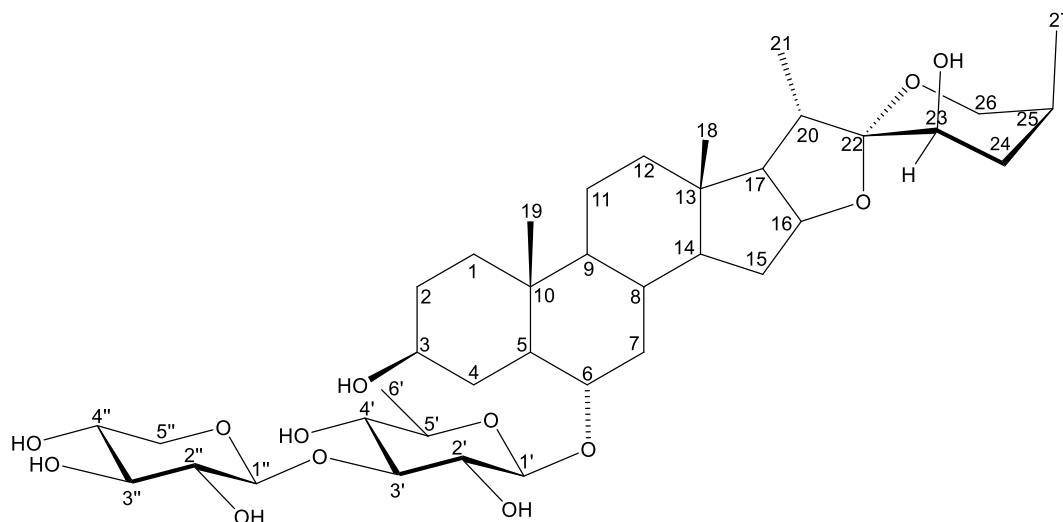


**Figure 37.** 6- $\alpha$ -O- $\beta$ -D-xylopyranosyl-(1 $\rightarrow$ 3)- $\beta$ -D-quinovopyranosyl-(23R,25S)-5 $\alpha$ -spirostan-3 $\beta$ ,23 $\beta$ -ol (SC5C)

**Compound SC5C:** the compound 6- $\alpha$ -O- $\beta$ -D-xylopyranosyl-(1 $\rightarrow$ 3)- $\beta$ -D-quinovopyranosyl-(23R,25S)-5 $\alpha$ -spirostan-3 $\beta$ ,23 $\beta$ -ol (SC5C) was obtained as white powder, mp 209-214 °C,  $[\alpha]_{25}^D$  -40°(c 0.2, CH<sub>3</sub>OH). The negative ion mode HRESIMS showed the quasimolecular ion peak  $m/z$  771.4175  $[M+COOH]^-$  in agreement with the molecular formula C<sub>39</sub>H<sub>63</sub>O<sub>15</sub>. The structural elucidation of compound SC5C was performed by spectroscopic analysis of its acetylated derivative SC5AcC. This compound has been previously reported as compound 3 by González *et al.*, 2004<sup>21</sup>



**5.1.9. Physical and spectroscopic data of 3'-O-methyl-quercetin-3-O-β-D-glucopyranoside (SC11)**

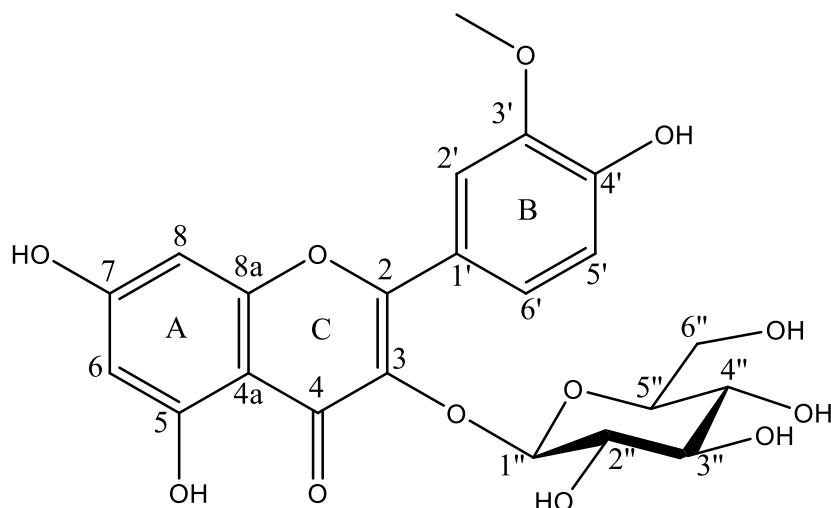


**Figure 38.** 3'-O-methyl-quercetin-3-O-β-D-glucopyranoside (SC11)

**Compound SC11:** yellow resin (5 mg, yield: 0.000389 %), soluble in CH<sub>3</sub>OH. C<sub>22</sub>H<sub>22</sub>O<sub>12</sub>, M.W. 478.1111 g/mol. <sup>1</sup>H NMR (400 MHz, CD<sub>3</sub>OD) δ 7.90 (d, *J*=1.96 Hz, 1H, H-2'), 7.60 (dd, *J*= 8.48, 2.00 Hz, 1H, H-6'), 6.88 (d, *J*=8.48 Hz, 1H, H-5'), 6.17 (d, *J*= 1.88 Hz, 1H, H-8), 6.03 (d, *J*= 1.92 Hz, 1H, H-6), 5.21 (d, *J*= 7.32 Hz, 1H, H-1'') 3.95 (s, 3H, OCH<sub>3</sub>), 3.73 (dd, *J*= 10.66, 2.26 Hz, 1H, H-6''<sub>α</sub>), 3.58 (dd, *J*= 11.9, 5.3 Hz, 1H, H-6''<sub>β</sub>), 3.49 (t overlapped, *J*= 9.08 Hz, 1H, H-2''), 3.45 (t overlapped, *J*= 9.12 Hz, 1H, H-3''), 3.33 (t overlapped, *J*= 11.24 Hz, 1H, H-4''), 3.24 (ddd, *J*=9.66, 5.57, 2.36 Hz, 1H, H-5''). <sup>13</sup>C NMR (100 MHz, CD<sub>3</sub>OD) δ 174.36 (C4), 161.09 (C7), 157.77 (C5), 156.05 (C8a), 150.26 (C3'), 147.27 (C4'), 133.58 (C3), 122.43 (C6'), 121.41 (C1'), 114.79 (C5'), 112.69 (C2'), 103.23 (C1''), 101.7 (C6), 95.6 (C8), 77.04 (C5''), 76.8 (C3''), 74.48 (C2''), 70.00 (C4''), 61.13 (C6''), 55.26 (OCH<sub>3</sub>).

### 5.1.9.1. Structural elucidation of 3'-O-methyl-quercetin-3-O-β-D-glucopyranoside (SC11)

The  $^1\text{H}$  NMR spectrum of SC11 (Figure 39) showed the typical signals of the aromatic spin system of quercetin ( $\delta$  6.02-7.90)<sup>39</sup>, the signals corresponding to a  $\beta$ -D-glucopyranose ( $\delta$  3.20-3.95). The aromatic ABX spin system of ring B of the flavonol displayed the following signals: a doublet signal at  $\delta$  7.90 (d,  $J=1.96$  Hz, 1H, H-2') coupling in *meta* with H-6', a doublet of doublets signals at  $\delta$  7.60 (dd,  $J= 8.48$ ,  $J= 2.00$  Hz, 1H, H-6') coupling in *ortho* with H-5' and in *meta* with H-2', at  $\delta$  6.88 (d,  $J= 8.48$  Hz, 1H, H-5') was observed a doublet coupling in *ortho* with H-6'. The spins system of ring A of the flavonol showed the following signals. A doublet at  $\delta$  6.17 (d,  $J= 1.88$  Hz, 1H, H-8) coupling in *meta* with H-6, a doublet at 6.03 (d,  $J= 1.92$  Hz, 1H, H-6) coupling in *meta* with H-8. A singlet methoxyl signal was observed at  $\delta$  3.95 (s, 3H, OCH<sub>3</sub>), however, the hydroxyl signals were not observed due to the exchange with deuterium. The spin system corresponding to the saccharide moiety were observed, being the anomeric proton at  $\delta$  5.21 (d,  $J= 7.32$  Hz, 1H, H-1''), and the signals corresponding to the oxymethines of  $\beta$ -D-glucopyranose were observed from at  $\delta$  3.73 (dd,  $J= 10.66$ , 2.26 Hz, 1H, H-6'' $\alpha$ ), 3.58 (dd,  $J= 11.9$ , 5.3 Hz, 1H, H-6'' $\beta$ ), 3.49 (t overlapped,  $J= 9.08$  Hz, 1H, H-2''), 3.45 (t overlapped,  $J= 9.12$  Hz, 1H, H-3''), 3.33 (t overlapped,  $J= 11.24$  Hz, 1H, H-4''), and 3.24 (ddd,  $J=9.66$ , 5.57, 2.36 Hz, 1H, H-5''). In order to define the glycosidation position in SC11,  $^1\text{H}$  NMR spectra were recorded using DMSO as solvent (figure 40), and as result a Related-hydroxyl signal was observed far downfield at  $\delta$  12.37 (s), and this signal represent conclusive

evidence of an hydrogen-bond between the hydroxyl in C-5 and the carbonyl function in C-4, indicating that SC11 could not be glycosidated in the hydroxyl of C5 position.

The  $^{13}\text{C}$  NMR spectrum of SC11 (Figure 41) showed one carbonyl carbon signal at  $\delta$  174.36 (C-4), 14 aromatic carbon signals [ $\delta$  161.09 (C-7), 157.77 (C-5), 156.05 (C-8a), 150.26 (C-3'), 147.27 (C-4'), 133.58 (C-3), 122.43 (C-6'), 121.41 (C-1'), 114.79 (C-5'), 112.69 (C-2'), 101.7 (C-6), 95.6 (C-8)] being overlapped the signals corresponding to C-4a and C-2, 1 methoxyl carbon signal at  $\delta$  55.26 ( $\text{OCH}_3$ ) and the 6 signals corresponding to the carbons of the  $\beta$ -D-glucose with the anomeric carbon at  $\delta$  103.23 (C-1''), and the oxymethines carbons at  $\delta$  77.04 (C-5''), 76.8 (C-3''), 74.48 (C-2''), 70.00 (C-4''), 61.13 (C-6''). To confirm the structure proposal for SC11 2D NMR spectroscopic data were analyzed in order to define the substitution pattern of SC11. The HSQC spectrum of SC11 (figure 42) confirms the assignation of protons and carbons for the spin systems of the flavonol and the saccharide moiety, the carbon types of the molecule were confirmed by DEPT90 and DEPT135 experiments showing concordance with the HSQC spectrum. The HMBC spectrum (Figure 43) showed the key correlation ( $^3\text{J}_{\text{C-H}}$ ): C-3/H-1'', indicating C-3 as the glycosidation site in the flavonol glucoside, while the correlation ( $^3\text{J}_{\text{C-H}}$ ): C-4'/H- $\text{CH}_3\text{O}$  positions the methoxyl group on C-3'. The COSY spectrum (figure 44) confirms the observations of the HMBC spectrum with the key correlation ( $^4\text{J}_{\text{H-H}}$ ): H-2'/H- $\text{CH}_3\text{O}$ , and displayed cross-peaks in concordance with the proton systems proposed for SC11. The NOESY spectrum of SC11 (figure 45) displayed spatial correlations

according to the proposed structure for SC11, standing out the cross-peak H-2'/H-CH<sub>3</sub>O, confirming the position of the methoxyl group of the molecule.

The 1D and 2D spectroscopic data and reports in the literature<sup>39</sup> confirms SC11 as the previously reported glucosidated flavonol 3'-O-methyl-queracetin-3-O-β-D-glucopyranoside known as Isorhamnetin-3-O-glucoside.

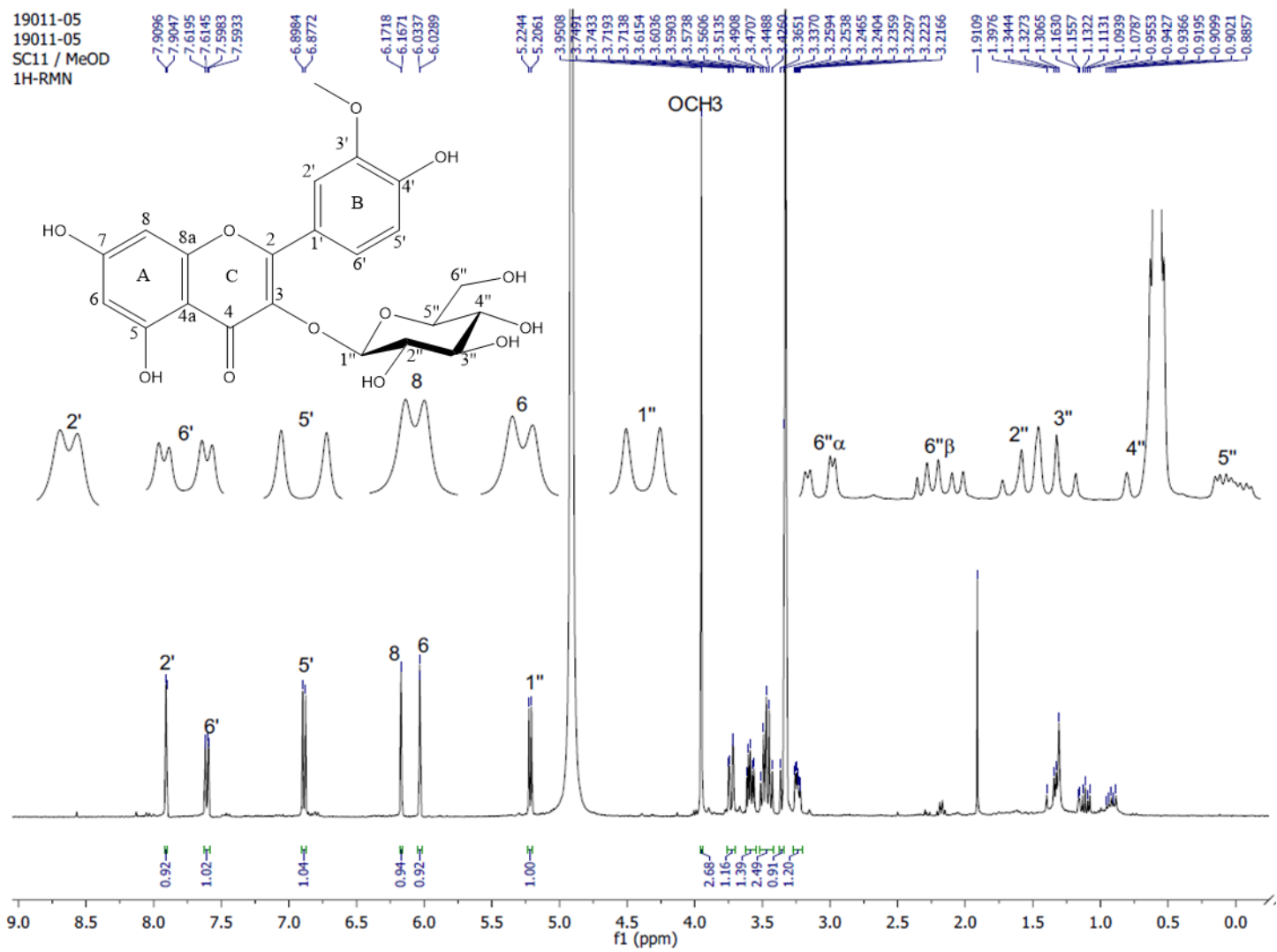
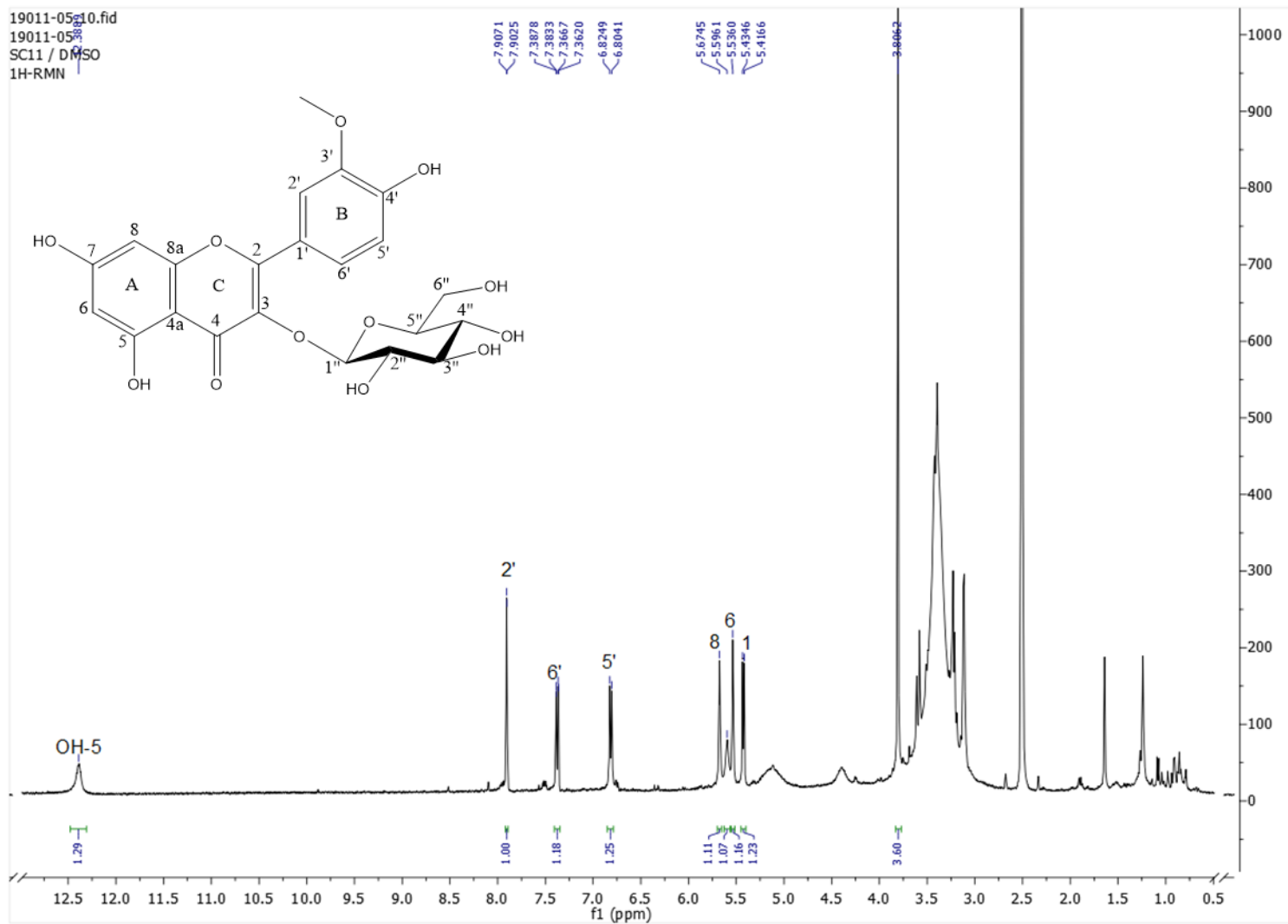
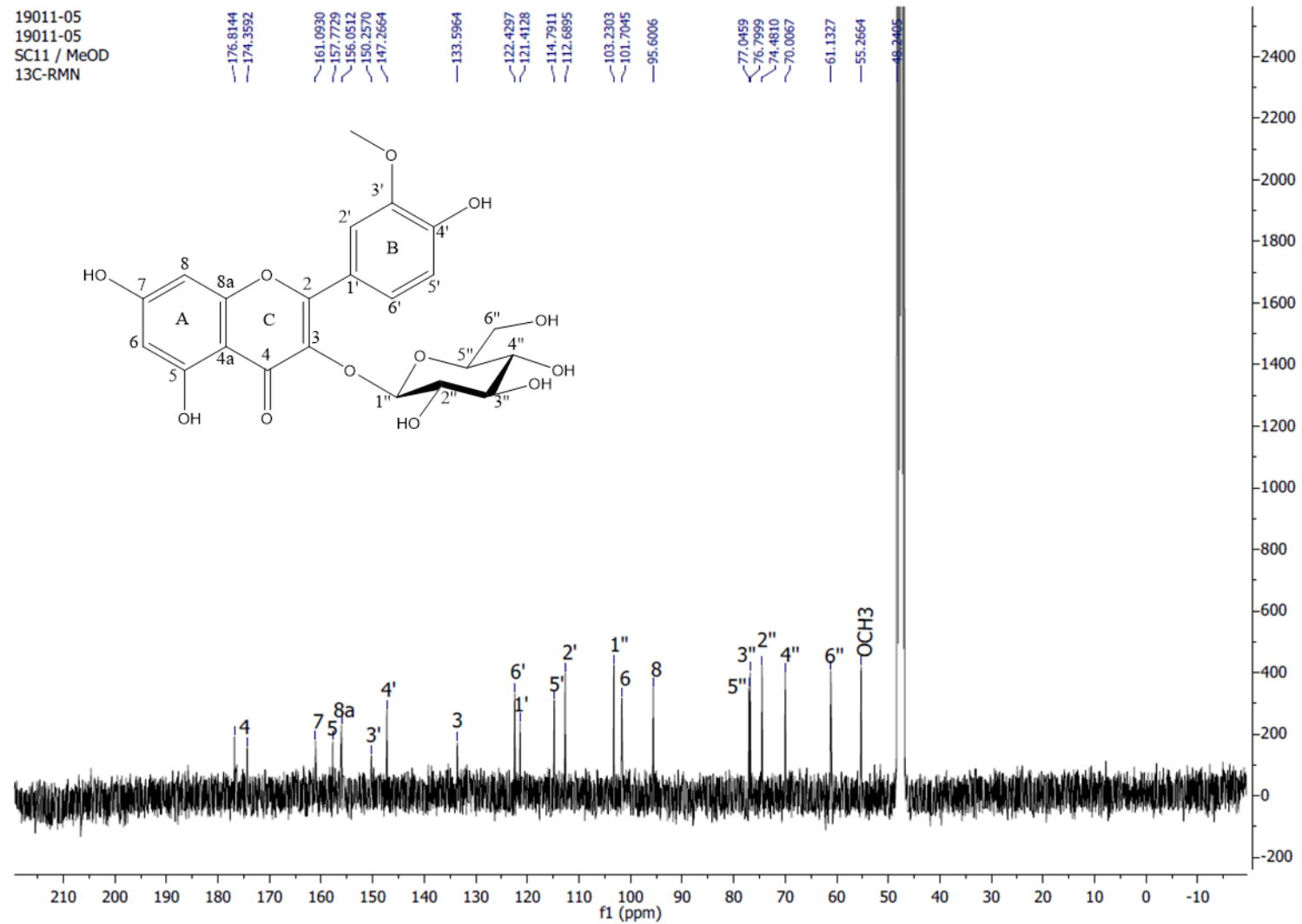


Figure 39.  $^1\text{H}$  NMR (400 MHz,  $\text{CD}_3\text{OD}$ ) spectrum of 3'-O-methyl-quercetin-3-O- $\beta$ -D-glucopyranoside (SC11)



**Figure 40.**  $^1\text{H}$  NMR (400 MHz, DMSO) spectrum of 3'-O-methyl-quercetin-3-O- $\beta$ -D-glucopyranoside (SC11)



**Figure 41.**  $^{13}\text{C}$  NMR (100 MHz,  $\text{CD}_3\text{OD}$ ) spectrum of 3'-O-methyl-quercetin-3-O- $\beta$ -D-glucopyranoside (SC11)

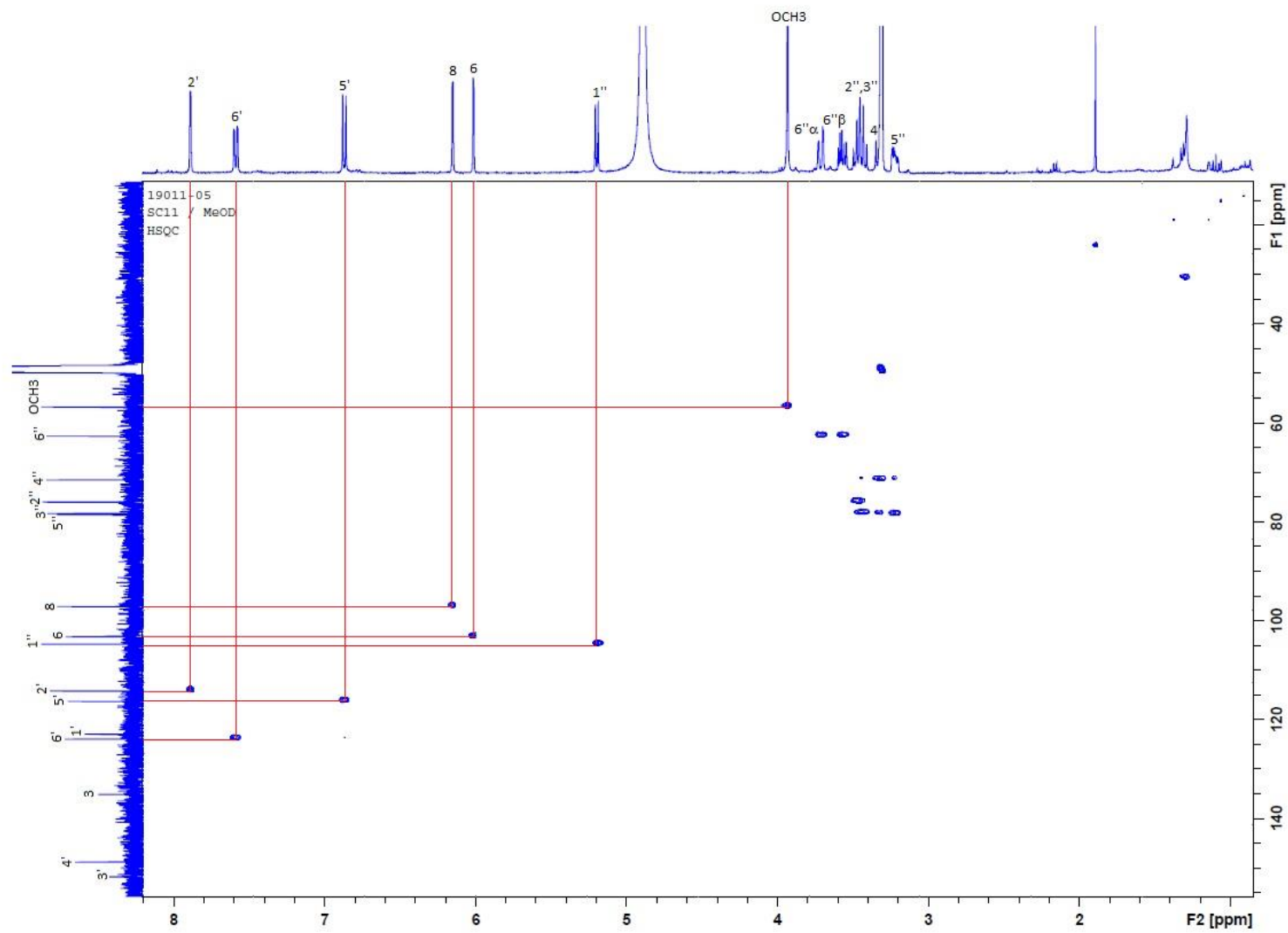


**Figure 42.** HSQC NMR (400 MHz, CD<sub>3</sub>OD) spectrum of 3'-O-methyl-quercetin-3-O- $\beta$ -D-glucopyranoside (SC11)



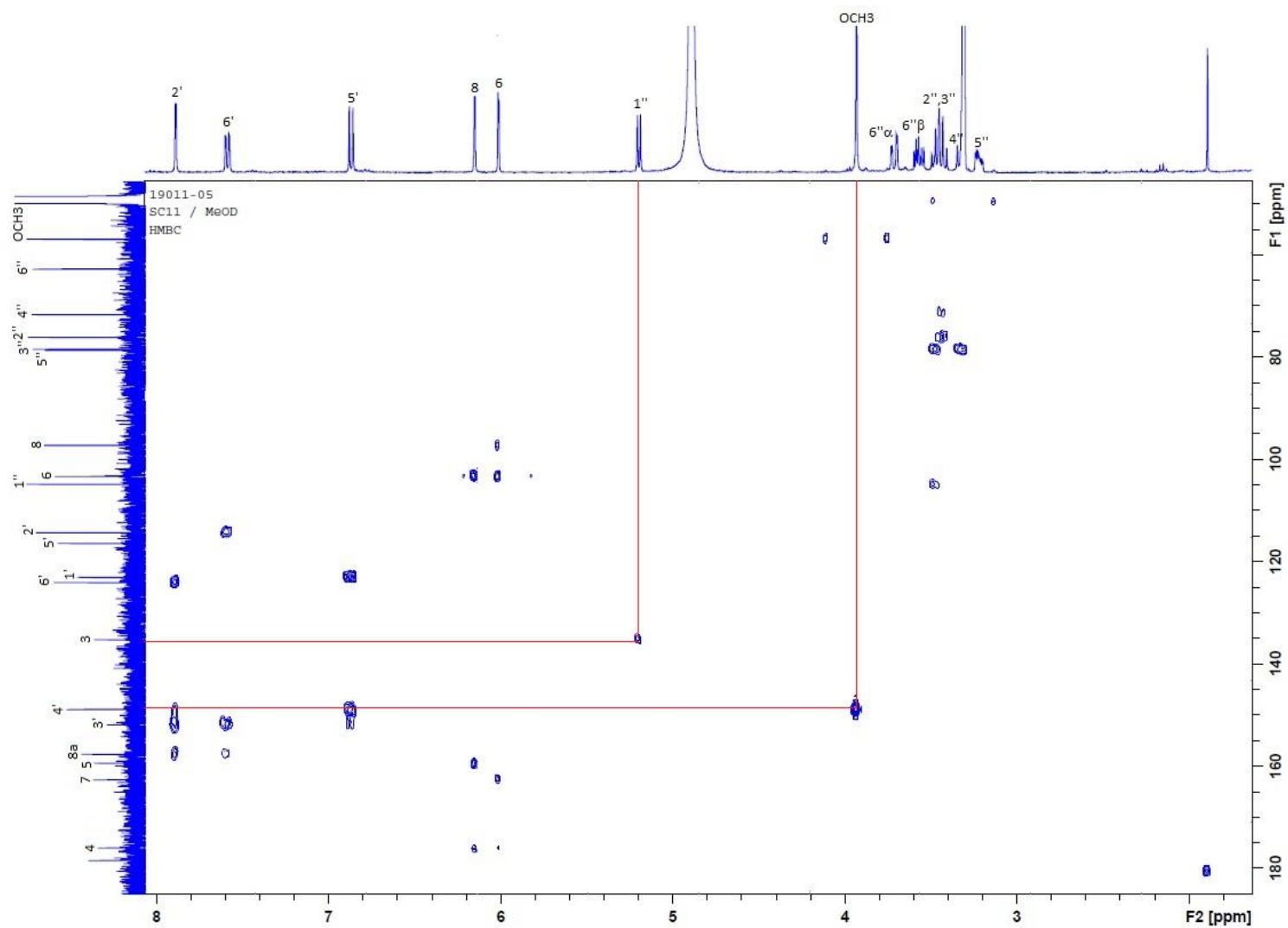


**Figure 43.** HMBC NMR (400 MHz, CD<sub>3</sub>OD) spectrum of 3'-O-methyl-quercetin-3-O-β-D-glucopyranoside (SC11)

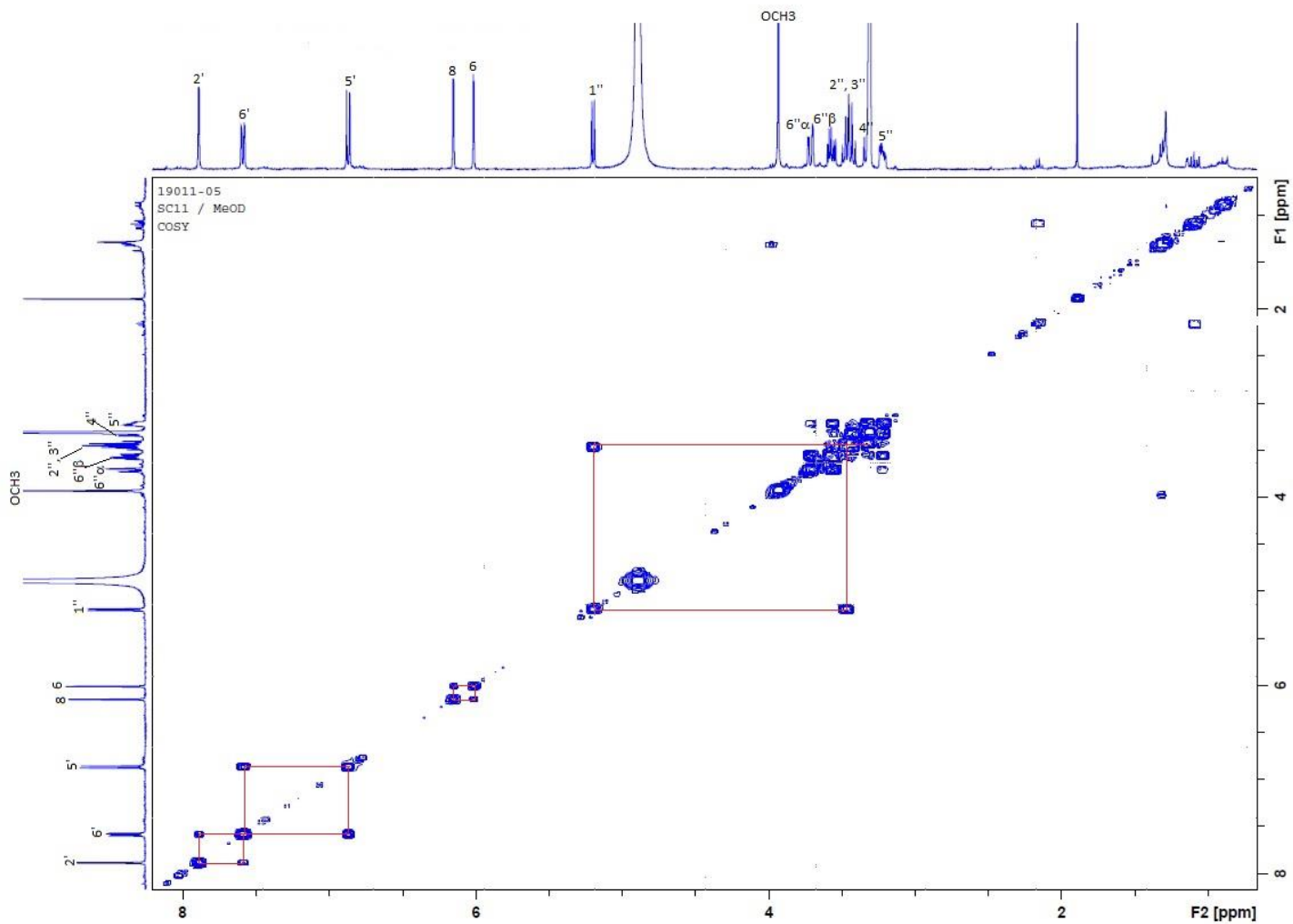


**Figure 44.** COSY NMR (400 MHz, CD<sub>3</sub>OD) spectrum of 3'-O-methyl-quercetin-3-O- $\beta$ -D-glucopyranoside (SC11)

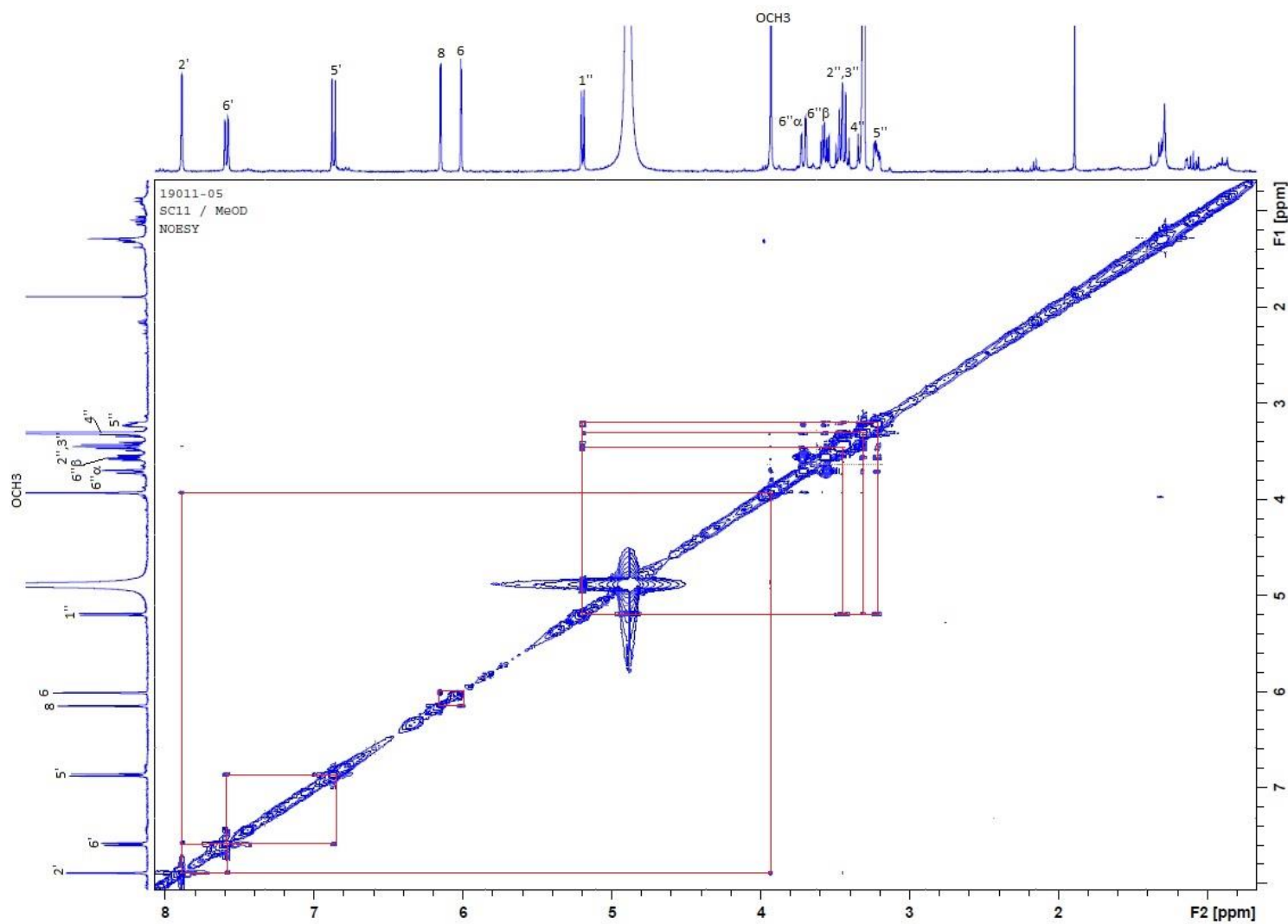


**Figure 45.** NOESY NMR (400 MHz, CD<sub>3</sub>OD) spectrum of 3'-O-methyl-quercetin-3-O-β-D-glucopyranoside (SC11)

## 5.2. Analysis of the hexane and dichloromethane extracts of *S.*

### *chrysotrichum*

The hexane and dichloromethane extracts of *S. chrysotrichum* were analyzed by gas chromatography coupled with mass spectrometry (GC/MS) identifying 13 phytocomponents (Table 7) in the hexane extract, being the major compounds the superior alkanes tritriacontane (44.505 %) and dotriacontane (32.811 %), and for the dichloromethanol extract were identified 10 phytocomponents (table 8) being the major compounds the superior alkanes tritriacontane (38.177 %) and hexatriacontane (27.195 %), and the diterpenic alcohol phytol (20.992 %). The compounds were identified by comparison of the spectrometric data with the database NIST versión 1.7.

Table 7. GC-MS analysis of *S. chrysotrichum* hexane extract

Compound name	RT (min)	%Area
Hexadecanoic acid methyl ester	62.347	0.489
9,12-Octadecadienoic acid (Z,Z),methyl ester	70.000	0.372
9,12,15- Octadecatrienoic acid (Z,Z,Z),methyl ester	70.282	0.296
Phytol	70.887	1.618
Octadecanoic acid methyl ester	71.596	0.336
Heptacosane	94.199	3.441
Squalene	98.449	0.650
Nonacosane	101.063	4.337
Hexatriacontane	106.331	3.942
Dotriacontane	107.678	32.811
$\alpha$ -tacopherol	108.203	5.490
Stigmasta-5,22-dien-3-ol	111.369	1.712
Tritriacontane	113.773	44.505

**Table 8. GC-MS analysis of *S. chrysotrichum* dichloromethane extract**

<b>Compound name</b>	<b>RT (min)</b>	<b>%Area</b>
3,7,11,15-Tetramethyl-2-hexadecen-1-ol	59.221	0.741
Hexadecanoic acid methyl ester	62.334	0.592
Methyl-(Z)-5,11,14,17-eicosatetraenoato	70.263	0.325
Phytol	70.926	20.992
Heptacosane	94.166	2.478
Nonacosane	101.043	3.125
Stigmasta-3,5-dien	106.121	1.878
Hexatriacontane	107.540	27.125
$\alpha$ -tacopherol	108.177	4.496
Tritriacontane	113.609	38.177

Some of the phytoconstituents identified in the hexane and dichloromethanol extracts of *S. chrysotrichum* were previously identified by GC/MS in other plant extracts of the genera *Solanum*, standing out the phytol as one of the more interesting compounds because of its biological activities. The hexane leaf extract of *S. pseudocapsicum* showed the phytol (35.8 %) as its major constituents<sup>40</sup>, and the ethanolic leaf extract of *S. villosum* with the phytol (8.54 %) as one of their major constituents<sup>41</sup>. The ethanolic leaf extract of *S. torvum* Sw with the phytol (14.09 %)<sup>42</sup> as one of their major constituents, being the previous examples a good reference of the main constituents identified by GC/MS in *Solanum* extracts. The presence of phytol in the hexane and dichloromethanol extracts of *S. chrysotrichum* is a key fact regarding the antibacterial activity of the studied plant, because of the reports of bactericidal activity such as the study provided by Lee *et al.*, 2016<sup>43</sup> in which the minimal inhibitory concentration (MIC) of phytol was determined as 20  $\mu\text{g/mL}$  against an *P. aeruginosa*. Additionally, phytol displays interesting activities regarding lipid metabolism acting as an activator of the peroxisome proliferator activated receptor

(PPAR $\alpha$ ) and a regulator of gene expression involved in lipid metabolism in PPAR $\alpha$ -expressing HepG2 hepatocytes<sup>44</sup>. However, the compound showed toxicity *in vivo* when administered in doses of 2-5% per kilogram in the diet of mice, rabbits, rats and chinchillas, presenting accumulation until lethal doses at the fourth week of administration<sup>45</sup>.

### **5.3. Antibacterial activity of organic and aqueous extracts of *S. chrysotrichum***

The organic and aqueous extracts of *S. chrysotrichum* displayed antibacterial activity against the tested clinical isolates of gram-negative, gram-positive, and *M. tuberculosis* strains (Table 9). The concentrations tested for the extracts were 500, 250, 125, 62.5, 32.25, 15.62  $\mu\text{g/mL}$ , and the controls levofloxacin and rifampicin were tested at 50, 25, 12.5, 6.25, 3.15, 1.57, 0.78, 0.39, 0.19, 0.098, 0.049, 0.024  $\mu\text{g/mL}$ . Against the gram-negative clinical isolates (ESBL) *E. coli*, (CCR) *K. pneumonia*, (CCR) *K. pneumoniae* NDM-1+, and (ESBL) *K. pneumonia*, all the three organic extracts and the aqueous extract were active at 500  $\mu\text{g/mL}$ , except in the case of the dichloromethane extract being inactive at the concentrations tested (>500  $\mu\text{g/mL}$ ) against (CCR) *K. pneumonia* and (ESBL) *K. pneumonia*. The best antibacterial activity against gram-negative bacteria was displayed by the three organic extracts with the same MIC value of 125  $\mu\text{g/mL}$  against (CR) *A. baumannii* and 250  $\mu\text{g/mL}$  against (CR) *P. aeruginosa*, in the other hand, the aqueous extract showed the lowest activity against *A. baumannii* (>500  $\mu\text{g/mL}$ ) and *P. aeruginosa*

(500 µg/mL). Against the gram-positive clinical isolates. The three organic extracts and the aqueous extract were active against (MR) *S. aureus* and (VR) *E. faecium* at 500 µg/mL, however, against (LR) *S. epidermidis* all the extracts were inactive at the concentrations tested (>500 µg/mL), except for the hexane extract with a MIC value of 500 µg/mL. Against the two clinical isolates of *M. tuberculosis* all the extracts were not active at the concentrations tested (>500 µg/mL) except the hexane extract that displayed a MIC value of 250 µg/mL against the sensitive (H37Rv) and drug-resistant (G122) strains.

Results showed that *S. chrysotrichum* possessed relevant antibacterial activity mainly against gram-negative bacteria such as *A. baumannii* and *P. aeruginosa*, and for the hexane and dichloromethanol extracts. The antibacterial activity could be attributed to the presence of phytol<sup>43</sup>, even if the superior alkanes like tritriacontane were the major compounds in both extracts, because of the deficient antibacterial activity of the alkanes when compared with other phytochemicals<sup>46</sup> like terpenes, sterols and esters. As mentioned before, there are reports of good antibacterial activity of phytol against gram-negative bacteria like *P. aeruginosa* as reported by Lee *et al.*, 2016, exhibiting the phytochemical a MIC value of 20 µg/mL with a possible mechanism of action of induction of oxidative stress response in the bacteria. However, the toxicity of phytol<sup>45</sup> could reduce the therapeutic applications for the hexane and dichloromethanol extracts when compared with alcoholic and hydroalcoholic extracts of *S. chrysotrichum*<sup>16</sup>. It is noteworthy the antimycobacterial activity of the hexane extract against the *M. tuberculosis* strains (MIC: 200 µg/mL)

considering that previous reports in the literature determined antimycobacterial activity with MIC values of 1250-1600 µg/mL for alcoholic and hydroalcoholic extracts<sup>12,13</sup>, being the hexane extract of *S. chrysotrichum* a possibly better option to obtain antitubercular natural products.

The antibacterial activity observed for the methanol extract against gram-negative drug-resistant bacteria was the same as the observed with the hexane and dichloromethanol extract. However, the composition of the methanol extract is different and its biological activity cannot be attributed to the same factors as for the hexane and dichloromethanol extracts. Previous studies such as the one reported by Velasco-Lezama *et al.*, 2018<sup>47</sup> illustrate the differences between the antibacterial activities of extracts of *S. chrysotrichum*, being the extracts assayed by the microdilution method against gram-positive and gram-negative ATTC bacteria (*Bacillus subtilis*, *E. coli* SOS, *E. coli* ATTC8739, *Salmonella typhi* ATTC 6539, *S. aureus* ATTC 6538, *Proteus mirabilis* NCTC 2896). These authors reported that the hexane and chloroform extracts were inactive against all the bacteria at the tested concentrations (10000-25000 mg/mL) and activity of the methanol extract was observed against *E. coli* SOS at all the concentrations tested. Comparing the results of the present work with the results reported by Velasco-Lezama *et al.*, 2018<sup>47</sup> its notable the difference in activities of the methanol extract against ATTC strains and drug-resistant clinical isolates, being the extract much more active against the drug-resistant clinical isolates used for the present work. About the toxicity of the methanol extract, it has been reported low toxic effects when compared with other organic extracts of *S. chrysotrichum*<sup>16</sup>, and despite of the presence of molecules with



hemolytic activity<sup>48</sup> such as the steroidal saponins reported in the present work (saponin mixture SC5), the study performed by Velasco-Lezama *et al.*, 2018<sup>47</sup> reported no cytotoxic effect on erythroid cell precursors in spleen cultures by the methanol extract of *S. chrysotrichum*, sustaining the low clinical relevance of the adverse effects of the methanol extract.

The aqueous extract of *S. chrysotrichum* showed the lowest antibacterial activity among all the tested extracts, however, its toxicity is lower than the methanol extract<sup>16</sup>. Its ethnomedical applications in traditional medicine as an antifungal remedy<sup>14</sup>, makes the aqueous extract an interesting prospect for analysis with the aim of identify the phytochemicals that displays only antifungal activity, in order to differentiate them from the components that possess antibacterial activity as well, and the information obtained could be a lead for the future biodirected studies with *S. chrysotrichum*.

**Table 9. Antibacterial and antimycobacterial activities of extracts of *S. chrysoviridum***

Extract	Gram-negative clinical isolates MIC (µg/mL)						Gram-positive clinical isolates MIC (µg/mL)			<i>M. tuberculosis</i> clinical Isolates MIC (µg/mL)	
	CR A. <i>baumanni</i>	CR P. <i>aeruginosa</i>	ESBL E. <i>coli</i>	CCR K. <i>pneumoniae</i> NDM-1+	CCR K. <i>pneumoniae</i>	ESBL K. <i>pneumoniae</i>	VR <i>E. faecium</i>	MR S. <i>aureus</i>	LR S. <i>epidermidis</i>	H37Rv	G122
Hexane	125	250	500	500	500	500	500	500	500	250	250
CH <sub>2</sub> Cl <sub>2</sub>	125	250	500	500	>500	>500	500	500	>500	>500	>500
CH <sub>3</sub> OH	125	250	500	500	500	500	500	500	>500	>500	>500
H <sub>2</sub> O	>500	500	500	500	500	500	500	500	>500	>500	>500
LEV	12.5	3.125	25	50	50	1.15	6.25	6.25	12.5	N.D.	N.D.
Rif	N.D.	N.D.	N.D.	N.D.	N.D.	N.D.	N.D.	N.D.	N.D.	0.195	1.560

**CR:** carbapenem resistant. **ESBL:** extended spectrum β-lactamase positive. **CCR:** carbapenem resistant and broad spectrum cephalosporins. **VR:** vancomycin resistant. **MR:** methicilin resistant. **LR:** linezolid resistant. **LEV:** levofloxacin. **H37Rv:** sensitive to first line drugs (rifampicin, isoniazid, ethambutol, streptomycin), **G122:** resistant to rifampicin, ethambutol, and streptomycin. **N.D.:** not determined.

#### **5.4. Antibacterial and antimycobacterial activity of isolated compounds from the methanol extract of *S. chrysostrictum* and acetylated derivatives**

The isolated compounds from the methanol extract and the steroidal saponins acetylated derivatives were tested against clinical isolates of gram-negative, gram-positive, and *M. tuberculosis* strains (Table 10). The concentrations tested for the compounds were 50, 25, 12.5, 6.25, 3.15, 1.57  $\mu\text{g/mL}$ , and the controls levofloxacin and rifampicin were tested at 50, 25, 12.5, 6.25, 3.15, 1.57, 0.78, 0.39, 0.19, 0.098, 0.049, 0.024  $\mu\text{g/mL}$ .

Antibacterial activity was observed only against the gram-positive clinical isolates, being the steroidal saponin SC5C the only compound active against (VR) *E. faecium* and (MR) *S. aureus*, with a MIC value of 12.5  $\mu\text{g/mL}$  (Table 8), being two-fold less active than the control drug levofloxacin (MIC 6.25  $\mu\text{g/mL}$ ). However, SC5C showed the same antibacterial activity than levofloxacin against (LR) *S. epidermidis* with a MIC value of 12.5  $\mu\text{g/mL}$ . All the tested compounds and acetylated derivatives were inactive against all the clinical isolates of gram-negative bacteria and against the two strains of *M. tuberculosis* (table 10). The chemical structure-biological activity analysis for the steroidal saponins indicates the possible factors responsible for the antibacterial activity of compound SC5C, noticing that the compounds SC5A and SC5B were inactive against bacteria in contrast with the compound SC5C which show good antibacterial activity against all gram-positive bacteria tested. This could be explained by the differences in the spirostane ring, disaccharide moiety, and the

acetylation of hydroxyl groups (figure 46). When comparing the compounds SC5A and SC5C (figure 46), it is noteworthy that the molecules possess different terminal sugars, in the case of SC5A is  $\alpha$ -L-rhamnopyranose and for SC5C is the pentose  $\beta$ -D-xylopyranose; the second difference is the C-23 hydroxyl function present only in SC5C. The previously mentioned factors could be the possible reasons for the antibacterial activity of compound SC5C. However, when comparing with the compound SC5B (figure 46), it is noteworthy that the compounds possess the same aglycone moiety (neosolaspigenin), being the only difference the terminal sugar  $\beta$ -D-xylopyranose in SC5C, leading to the conclusion that the hydroxyl group in C-23 do not attribute antibacterial activity to compound SC5C. Based on the previous analysis, it can be deduced that the key factor for the biological activity of compound SC5C is the presence of the terminal sugar  $\beta$ -D-xylopyranose, and this is confirmed by comparing SC5C with the acetylated derivative SC5AcC that was inactive against all the bacteria, indicating that modification on the terminal sugar moiety leads to the loss of the antibacterial activity. As preliminary conclusion, variations in the spirostane ring in the aglycone moiety do not affect the antibacterial activity for this type of *neo*-spirostane steroidal saponins and the type of disaccharide moiety can lead to an enhancement of the antibacterial activity for these compounds.

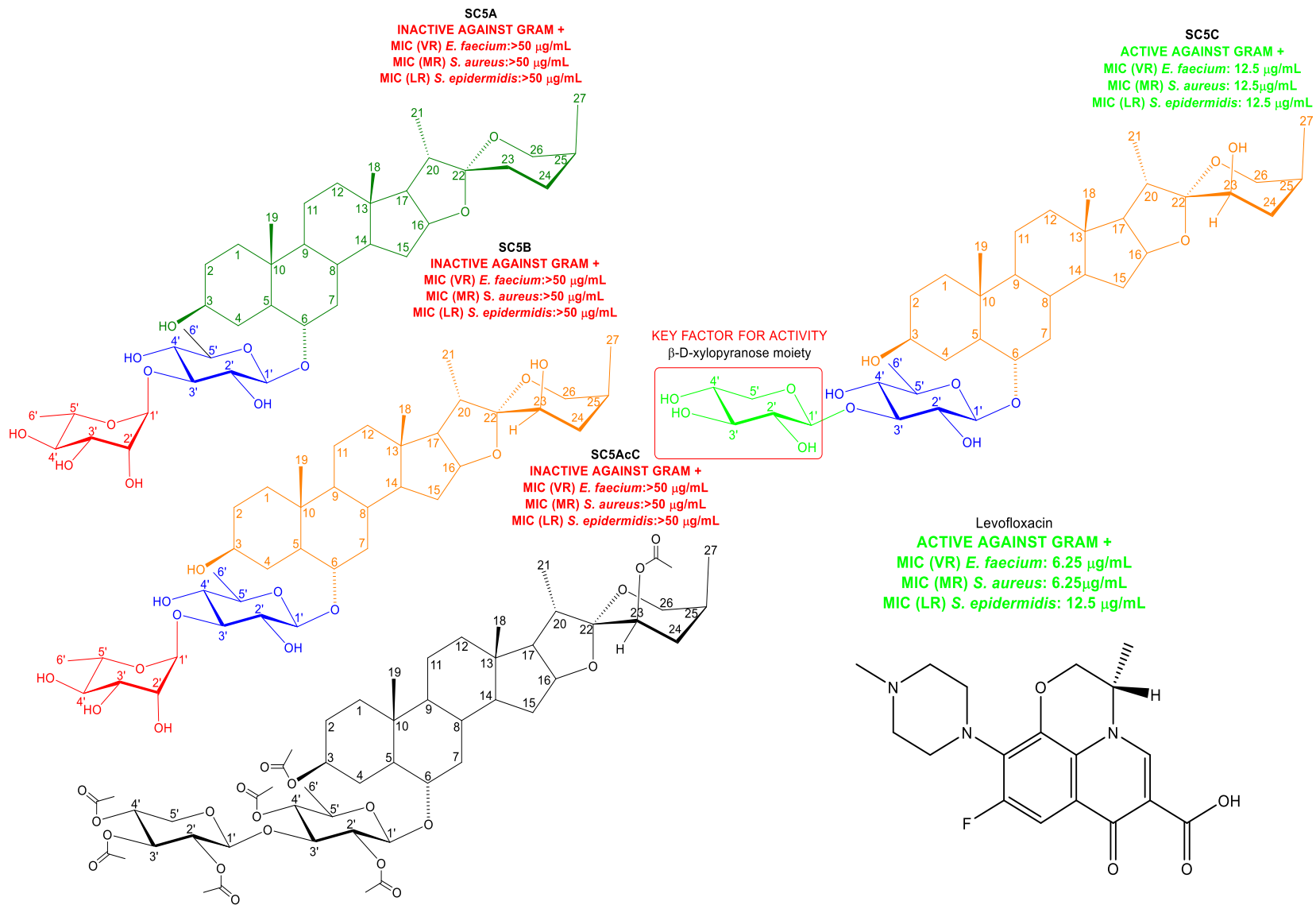


**Figure 46.** Chemical structure and antibacterial activities comparison of some steroidal saponins from *S. chrysotrichum* and acetylated derivative SC5AcC

Table 10. Antibacterial and antimycobacterial activities of compounds from *S. chrysoviridum* and acetylated derivatives

Compound	Gram-negative clinical isolates MIC (µg/mL)						Gram-positive clinical isolates MIC (µg/mL)			<i>M. tuberculosis</i> clinical Isolates MIC (µg/mL)	
	CR A. <i>baumannii</i>	CR P. <i>aeruginosa</i>	ESBL E. <i>coli</i>	CCR K. <i>pneumoniae</i> NDM-1+	CCR K. <i>pneumoniae</i>	ESBL K. <i>pneumoniae</i>	VR E. <i>faecium</i>	MR S. <i>aureus</i>	LR S. <i>epidermidis</i>	H37Rv	G122
SC5A	>50	>50	>50	>50	>50	>50	>50	>50	>50	>50	>50
SC5B	>50	>50	>50	>50	>50	>50	>50	>50	>50	>50	>50
SC5C	>50	>50	>50	>50	>50	>50	12.5	12.5	12.5	>50	>50
SC5AcA	>50	>50	>50	>50	>50	>50	>50	>50	>50	>50	>50
SC5AcB	>50	>50	>50	>50	>50	>50	>50	>50	>50	>50	>50
SC5AcC	>50	>50	>50	>50	>50	>50	>50	>50	>50	>50	>50
SC10	>50	>50	>50	>50	>50	>50	>50	>50	>50	>50	>50
SC11	>50	>50	>50	>50	>50	>50	>50	>50	>50	>50	>50
LEV	12.5	3.125	25	50	50	1.15	6.25	6.25	12.5	N.D.	N.D.
Rif	N.D.	N.D.	N.D.	N.D.	N.D.	N.D.	N.D.	N.D.	N.D.	0.195	1.560

CR: carbapenem-resistant. ESBL: extended spectrum β-lactamase positive. CCR: carbapenem-resistant and broad spectrum cephalosporin. VR: vancomycin-resistant. MR: methicillin-resistant. LR: linezolid-resistant. LEV: levofloxacin. H37Rv: sensitive to first line drugs (rifampicin, isoniazid, ethambutol, streptomycin). G122: resistant to rifampicin, ethambutol, and streptomycin. N.D.: not determined.

Regarding the  $\beta$ -D-xylopyranose moiety, it could be inferred that this sugar attribute antibacterial activity, because, it has such activity by itself, and thus makes the saponin SC5C active by being the terminal sugar in the compound. Reports in the literature indicates that the sugar xylose slightly affects the bacterial growth as proposed by Bhoj Raj Singh; 2014<sup>49</sup>. These authors determined the susceptibility of different strains of gram-positive and gram-negative bacteria by the agar diffusion method observing inhibition in cultures of *Citrobacter diversus*, *Enterococcus asacchrolyticus* and *Enterococcus raffinosus*, and subsequently was determined the activity of xylose as bacteriostatic against this strains<sup>49</sup>. Additionally, the study performed by Villagra *et al.*, 2012<sup>50</sup> determined that using xylose as sole carbon source, decreases efflux-mediated resistance of *A. baumannii* and *K. pneumoniae* to tetracycline and chloramphenicol *in vitro*, increasing 32 times the activity of the antibiotics against the previous mentioned bacteria. However, in this study the sugar xylose did not displayed antibacterial activity against bacteria, indicating that its activity will be effected only as synergistic with other antibiotics, and not as bactericidal or bacteriostatic by itself<sup>50</sup>. The previous study was confirmed by Hidalgo *et al.*, 2018<sup>51</sup> observing good synergistic activity of xylose with tetracycline and chloramphenicol *in vivo* using a model of topic infection in mice, and observing an increase of the activity for the antibiotics<sup>51</sup>. At this point is clear that the pentose xylose does not possess good antibacterial activity, but in combination with other antibiotics, or as substituent in other molecules, could improve the antibacterial activity against drug-resistant bacteria as the ones used for the present work, and as result steroidal saponins like SC5C has almost the same activity as levofloxacin

against gram-positive bacteria. It is noteworthy that there are no reports of good antibacterial activity of steroidal sapogenins, so it can be concluded that for a saponin, the aglycone moiety and the sugar residues independently do not possess antibacterial activity, however bonded as a saponin could display good activity against bacteria.

### **5.5. Acid hydrolysis of steroidal saponin SC5B**

The attempts of purification for the aglycone of SC5B were unrewarded regardless of the acetylation reaction applied to the compound, neither none of the chromatographic methods used were efficient. Therefore, the sapogenin from the major steroid saponin obtained cannot be used as starting material for synthesizing aminoether derivatives. At this point it is clear that the work with steroidal saponins and sapogenins requires a high investment in time and resources. Thus, in order to evaluate the cost-benefit of using sapogenins as starting material for synthesis of antibacterial agents, an easily obtainable sapogenin was used for the synthesis of aminoether derivatives in the present work. The steroidal sapogenin diosgenin (figure 47) was obtained from a commercial source (Alfa Aesar, Thermo Fisher Scientific), and was used as starting material for the synthesis of sapogenin aminoether derivatives. If the resulting aminoether derivatives display *in vitro* antibacterial activity, it could be considered as a future perspective to attempt the hydrolysis of steroid saponins from *S. chrysotrichum* by enzymatic methods in order



to obtain sapogenins for derivatization, otherwise the cost-benefit of using sapogenins as starting material will be unsatisfactory for research purposes.

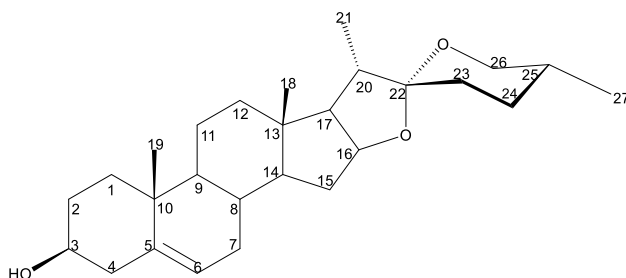


**Figure 47.** Chemical structure of diosgenin

### 5.6. Physical constants and yields of diosgenin aminoether derivatives

Parting from diosgenin as starting material nine aminoether derivatives were synthesized by the Williamson etherification reaction. The product yields varied from 4.37 to 43.31%. Melting points were determined only for the solid derivatives and all the compounds were soluble in  $\text{CHCl}_3$  (table 11). Precipitation with  $\text{CH}_3\text{OH}$  was attempted with all the compounds, however only derivative DIO-06 and DIO-07 were recovered as a solid. All the derivatives showed higher polarity than the starting material diosgenin, except for compound DIO-06.

**Table 11. Physical constants and yields of diosgenin aminoether derivatives**

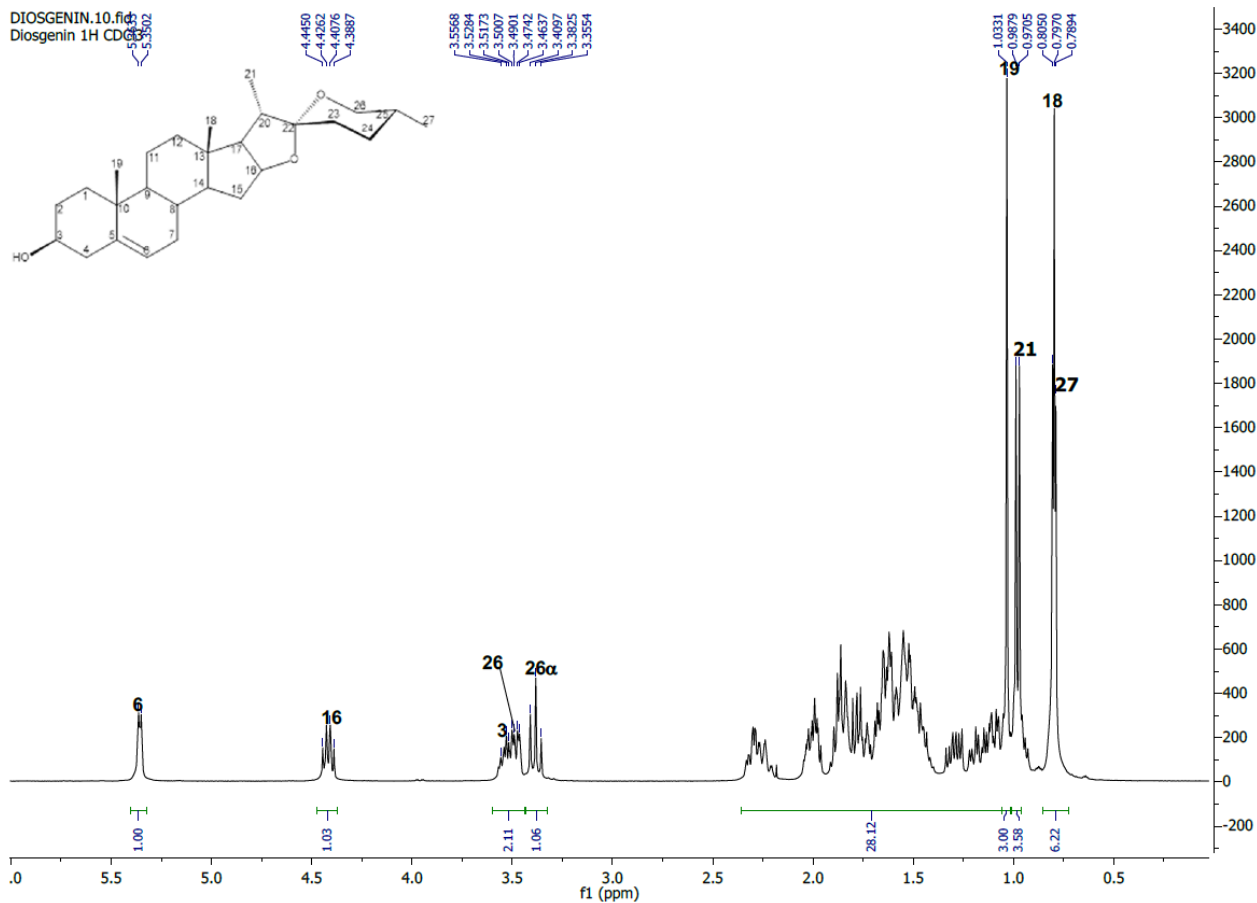
Derivative	Yield (% mmol)	Yield (mg)	Appearance	Melting Point (°C)	Solubility
DIO-01	43.31	275	Beige resin	-	$\text{CHCl}_3$
DIO-02	22.00	128	Colorless resin	-	$\text{CHCl}_3$
DIO-03	23.05	150	Beige resin	-	$\text{CHCl}_3$
DIO-04	4.37	27	Orange resin	-	$\text{CHCl}_3$
DIO-05	14.45	91.6	Yellow resin	-	$\text{CHCl}_3$
DIO-06	11.70	90	White solid	205	$\text{CHCl}_3$
DIO-07	22.58	156.2	Yellowish solid	175	$\text{CHCl}_3$
DIO-08	17.86	113.6	Orange resin	-	$\text{CHCl}_3$
DIO-09	4.48	40	Beige resin	-	$\text{CHCl}_3$

## 5.7. Structural elucidation of diosgenin aminoether derivatives

In order to structural elucidate the diosgenin aminoether derivatives, comparison with the  $^1\text{H}$  and  $^{13}\text{C}$  spectroscopic data of the starting material diosgenin was performed (table 12)<sup>52,53,54,55</sup>, being the key for the identification of the spin systems of the aminoether moieties in the derivatives, the comparison between the  $^1\text{H}$  spectrum of the starting material (figure 48) with the  $^1\text{H}$  spectrum of the derivatives.

**Table 12.  $^1\text{H}$  and  $^{13}\text{C}$  NMR spectroscopic constants of diosgenin**

Diosgenin reference <sup>52,53,54,55</sup>		
Position	$\delta$ (ppm), J (Hz)	
	$^{13}\text{C}$	$^1\text{H}$
1	37.24	-
2	31.60	-
3	71.75	3.51 (m) overlapped
4	42.27	-
5	140.83	-
6	121.38	5.30 (m)
7	32.05	-
8	31.44	-
9	50.06	-
10	36.64	-
11	20.87	-
12	39.79	-
13	40.25	-
14	56.53	-
15	31.84	-
16	80.82	4.38 (m)
17	62.09	-
18	16.29	0.76 (s)
19	19.42	1.04 (s)
20	41.60	-
21	14.53	0.92 (d, $J= 7$ Hz)
22	109.28	-
23	31.38	-
24	28.79	-
25	30.29	-
26 $\alpha$	66.83	3.40 (t, $J= 11$ Hz)
26 $\beta$	66.83	3.49 (ddd, $J= 10.9, 4.1, 2.1$ Hz ) overlapped
27	17.15	0.76 (d, 6.92Hz)



### 5.7.1. Structural elucidation of DIO-01

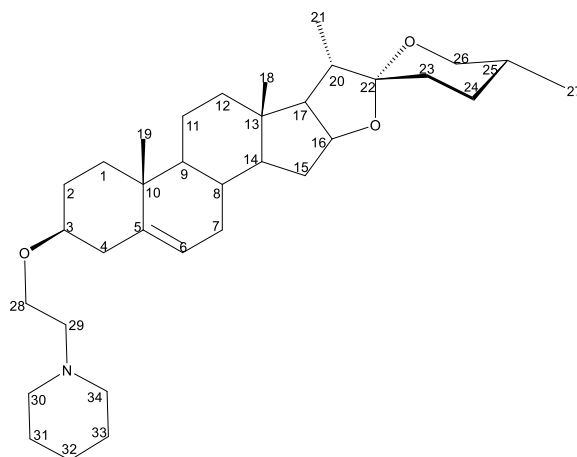


Figure 49. Aminoether derivative DIO-01

$^1\text{H}$  NMR DIO-01 characteristic signals ( $\text{CDCl}_3$ , 400 MHz):  $\delta$  5.3494 (d,  $J= 4.88$  Hz, 1H, H-6), 4.4212 (q,  $J= 7.4, 7.4, 7.6$  Hz, 1H, H-16), 3.6442 (t,  $J= 6.38$  Hz, 2H, H-28), 3.4833 (dd,  $J= 10.72, 3.52$  Hz, 1H, H-26 $\beta$ -equatorial), 3.3876 (t,  $J= 10.88$  Hz, 1H, H-26 $\alpha$ -axial), 3.1569 (m, 1H, H-3), 2.5969 (t,  $J= 6.36$  Hz, 2H, H-29), 2.4969 (brs, 4H, H-30; H-34), 1.6209 (m, 4H, H-31; H-33), 1.449 (m, 2H, H-32), 1.0230 (s, 3H, H-19), 0.9837 (d,  $J= 6.92$  Hz, 3H, H-21), 0.8051 (d,  $J= 5.24$  Hz, 3H, H-27), 0.7970 (s, 3H, H-18).  $^{13}\text{C}$  NMR DIO-01 signals ( $\text{CDCl}_3$ , 100 MHz):  $\delta$  37.0286 (C-1), 28.3814 (C-2), 79.2892 (C-3), 39.0911 (C-4), 141.0069 (C-5), 121.2727 (C-6), 32.0955 (C-7), 31.4398 (C-8), 50.1016 (C-9), 37.2133 (C-10), 20.8574 (C-11), 39.7942 (C-12), 40.2727 (C-13), 56.5297 (C-14), 31.8546 (C-15), 80.8342 (C-16), 62.0959 (C-17), 16.2989 (C-18), 19.4162 (C-19), 41.6065 (C-20), 14.5392 (C-21), 109.2963 (C-22), 24.1261 (C-23), 28.8050 (C-24), 30.3084 (C-25), 66.8512 (C-26), 17.1520 (C-27), 65.6139 (C-28), 58.7355 (C-29), 54.9339 (C-30), 25.6919 (C-31), 24.1261 (C-32), 25.6919 (C-33), 54.9339 (C-34).

In the  $^1\text{H}$  NMR spectrum of DIO-01 (figure 50) are clearly displayed the signals corresponding to the spin system of the ethylpiperidine moiety, corresponding the triplets  $\delta$  3.6442 (t,  $J= 6.38$  Hz, 2H, H-28) and 2.5969 (t,  $J= 6.36$  Hz, 2H, H-29) to the ethyl portion of the substituent, the singlet  $\delta$  2.4969 (brs, 4H, H-30; H-34) corresponding to two methylene alfa to N, the multiplet  $\delta$  1.6209 (m, 4H, H-3; H-33) corresponding to the methylenes beta to N, and the multiplet 1.449 (m, 2H, H-32) corresponding to the methylene gama to N in the piperidine ring. The  $^{13}\text{C}$  NMR spectrum of DIO-01 (figure 51) clearly displayed the signals of the ethylpiperidine

moiety as well, with the characteristic carbon signals of the ethyl portion at  $\delta$  65.6139 (C-28) and  $\delta$  58.7355 (C-29), the overlapped signals of the carbons alpha to N on the piperidine ring at 54.9339 ( $\delta$  C-30, C-34), the overlapped signals corresponding to the carbons beta to N of piperidine ring at 25.6919 ( $\delta$  C-31, C-33), and the carbon gamma to nitrogen at 24.1261 ( $\delta$  C-32) in the piperidine ring. When comparing the spectroscopic data of DIO-01 with the starting material diosgenin (table 12) it is noteworthy that almost all the  $^1\text{H}$  and  $^{13}\text{C}$  chemical shifts corresponding to the diosgenin scaffold remain virtually the same in DIO-01. However, an interesting difference between the C-3 position chemical shifts for diosgenin and DIO-01 was a key factor to clarify the proper substitution in the derivative. An upfield displacement was observed for hydrogen H-3 ( $\delta$  3.1569, m, 1H) in the  $^1\text{H}$  spectrum of DIO-01 ( $\delta$  3.51 for diosgenin) (figure 50) because of the shielding effect induced by the ethylpiperidine moiety of the derivative, confirming the proper substitution in the OH function of C-3 in DIO-01. Additionally, in the  $^{13}\text{C}$  spectrum of DIO-01 (figure 51) was observed a shielding effect for the carbons C-2 ( $\delta$  28.3814) and C-4 ( $\delta$  39.0911) adjacent to C-3 (for diosgenin C-2 ( $\delta$  31.60) and C-4 ( $\delta$  42.27)), indicating close proximity to the aminoether moiety and thus confirming the substitution in C-3. It could be expected that C-3 ( $\delta$  79.2892) in DIO-01 experienced the same shielding effect of C-2 and C-4, however, the opposite situation was observed, being C-3 deshielded, this could possibly be explained because of the effect of the partially positive carbons C-28 ( $\delta$  65.6139) and C-29 ( $\delta$  58.7355), of ethyl moiety positioned between an oxygen and a nitrogen electronegative atoms, and as result the deshielding effect of the aminoether moiety bonded directly to C-3 is far superior

than the shielding effect caused by the electronic density of the bulky piperidine ring  
in DIO-01

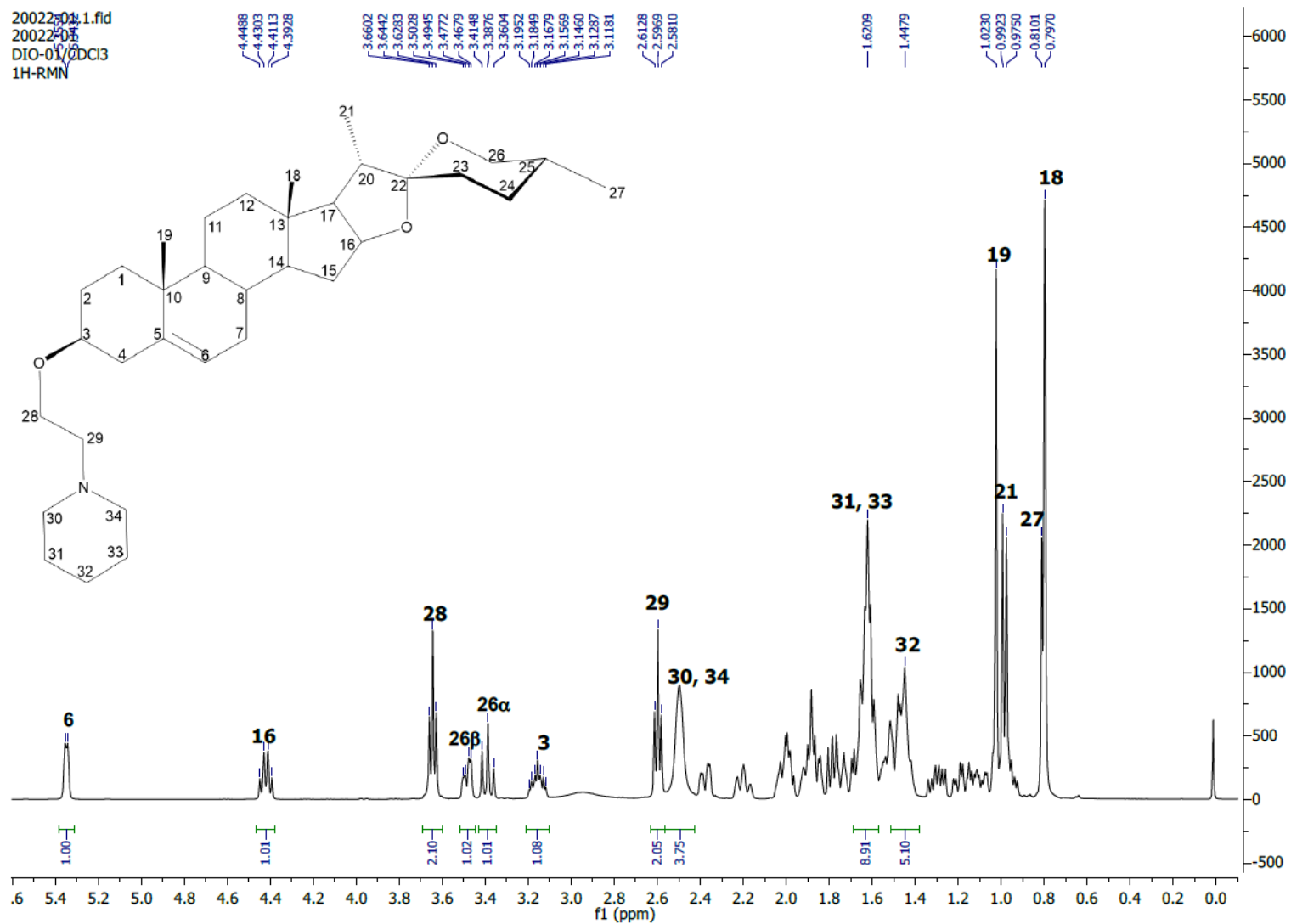


Figure 50. <sup>1</sup>H NMR (400 MHz, CDCl<sub>3</sub>) spectrum of DIO-01

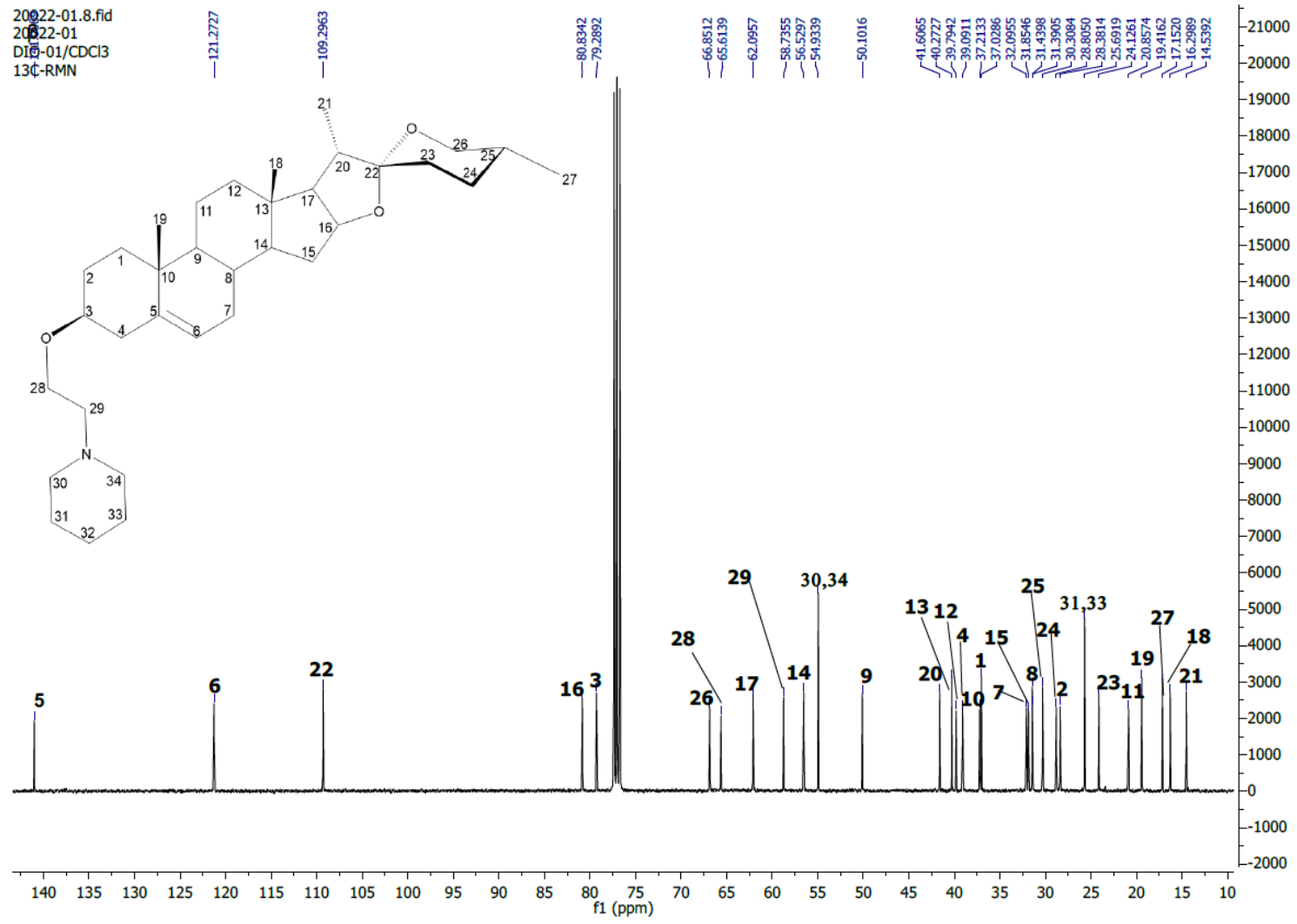
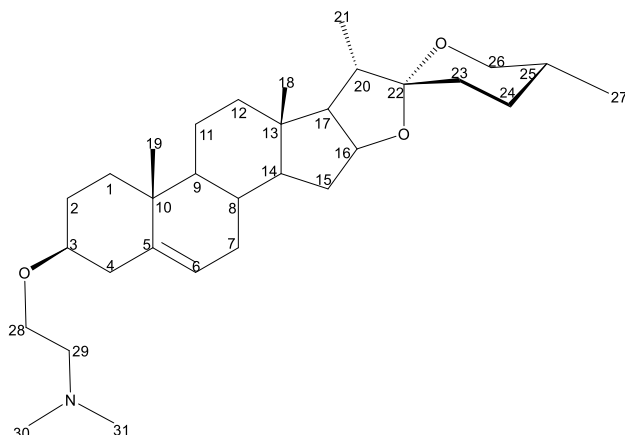


Figure 51. <sup>13</sup>C NMR (100 MHz, CDCl<sub>3</sub>) spectrum of DIO-01



### 5.7.2. Structural elucidation of DIO-02



**Figure 52.** Aminoether derivative DIO-02

$^1\text{H}$  NMR DIO-02 characteristic signals ( $\text{CDCl}_3$ , 400 MHz):  $\delta$  5.3515 (d,  $J$ = 4.76 Hz, 1H, H-6), 4.4155 (q,  $J$ = 7.4, 7.4, 7.56 Hz, 1H, H-16), 3.8712 (t,  $J$ = 4.85 Hz, 2H, H-28), 3.4833 (dd,  $J$ = 10.84, 3.06 Hz, 1H, H-26 $\beta$ ), 3.3801 (t,  $J$ = 10.88 Hz, 1H, H-26 $\alpha$ ), 3.2072 (m, 1H, H-3), 3.0472 (t,  $J$ = 4.84 Hz, 2H, H-29), 2.7276 (s, 6H, H-30; H-31), 1.0141 (s, 3H, H-19), 0.9780 (d,  $J$ = 6.92 Hz, 3H, H-21), 0.7984 (d,  $J$ = 5.52 Hz, 3H, H-27), 0.7902 (s, 3H, H-18).  $^{13}\text{C}$  NMR DIO-02 signals ( $\text{CDCl}_3$ , 100 MHz):  $\delta$  36.9450 (C-1), 28.1912 (C-2), 79.6862 (C-3), 39.7392 (C-4), 140.2627 (C-5), 121.8323 (C-6), 32.0493 (C-7), 31.3895 (C-8), 50.0105 (C-9), 38.8699 (C-10), 20.8429 (C-11), 39.7392 (C-12), 40.2560 (C-13), 56.4618 (C-14), 32.0493 (C-15), 80.8088 (C-16), 62.0699 (C-17), 16.2854 (C-18), 19.3868 (C-19), 41.6031 (C-20), 14.5303 (C-21), 109.2960 (C-22), 31.3796 (C-23), 28.7971 (C-24), 30.2940 (C-25), 66.8470 (C-26), 17.1447 (C-27), 63.5140 (C-28), 57.8619 (C-29), 44.2859 (C-30), 44.2859 (C-31)

In the  $^1\text{H}$  NMR spectrum of DIO-02 (figure 53) are shown the signals corresponding to the spin system of the N,N-dimethylethylamine moiety, corresponding the triplets  $\delta$  3.8712 (t,  $J= 4.85$  Hz, 2H, H-28) and 3.0472 (t,  $J= 4.84$  Hz, 2H, H-29) to the ethyl portion, the singlet 2.7276 (s, 6H, H-30; H-31) corresponds to the two methyl groups of the dimethyl amine portion of the substituent. The  $^{13}\text{C}$  NMR spectrum of DIO-02 (figure 54) displayed the signals of the N,N-dimethylethylamine moiety as well, with the characteristic carbon signals of the ethyl portion at  $\delta$  63.5140 (C-28), 57.8619 (C-29), and the overlapped signals of the methyl carbons in the amine at  $\delta$  44.2859 (C-30, C-31). When comparing the spectroscopic data of DIO-02 with the starting material diosgenin (table 12), it was observed the same shielding effects displayed in DIO-01 for hydrogen H-3 ( $\delta$  3.2072, m, 1H) and for the carbon C-2 ( $\delta$  28.1912) adjacent to C-3 (for diosgenin H-3 ( $\delta$  3.51), C-2 ( $\delta$  31.60)), indicating close proximity to the aminoether moiety and thus confirming the substitution in C-3.

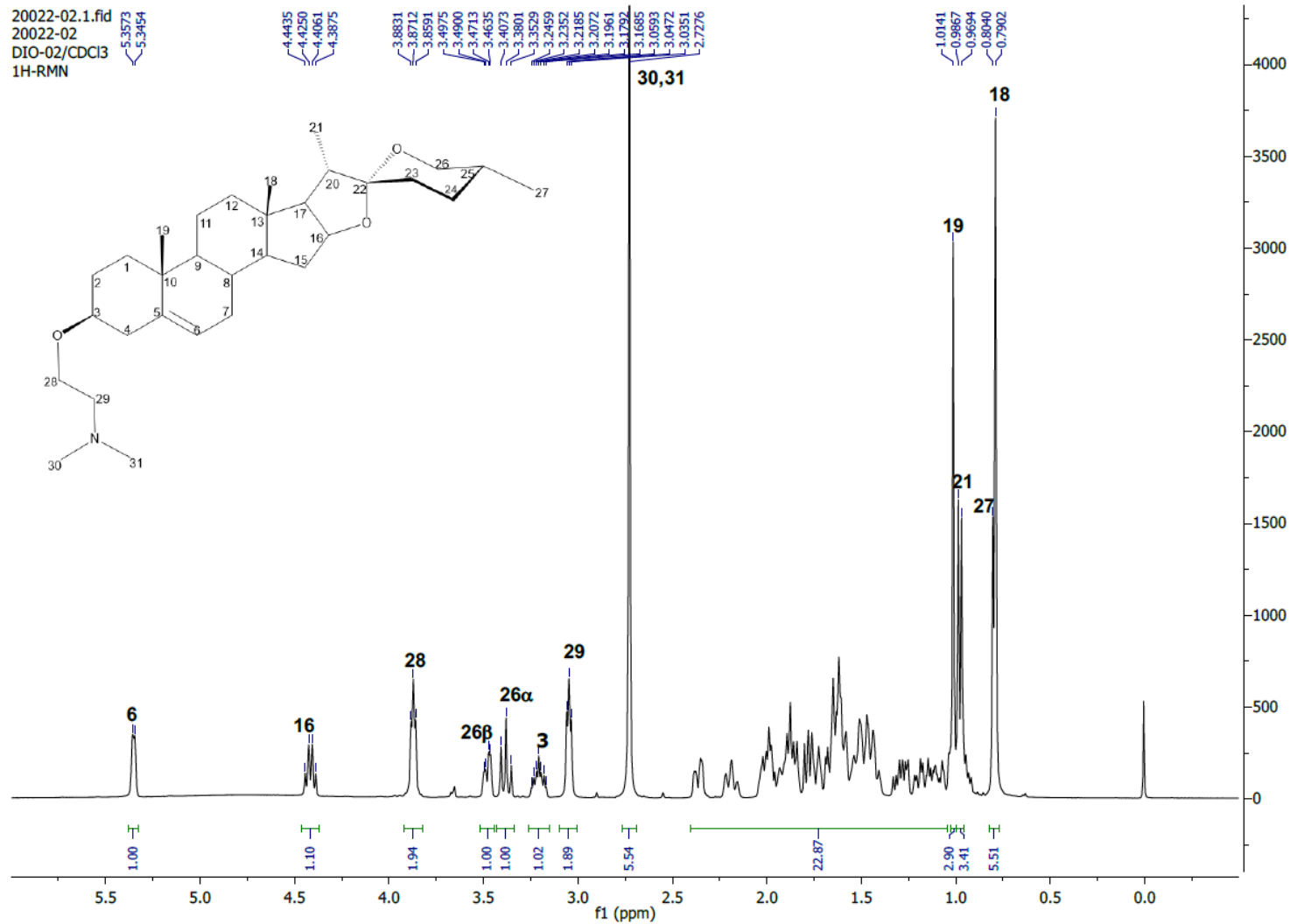


Figure 53. <sup>1</sup>H NMR (400 MHz, CDCl<sub>3</sub>) spectrum of DIO-02

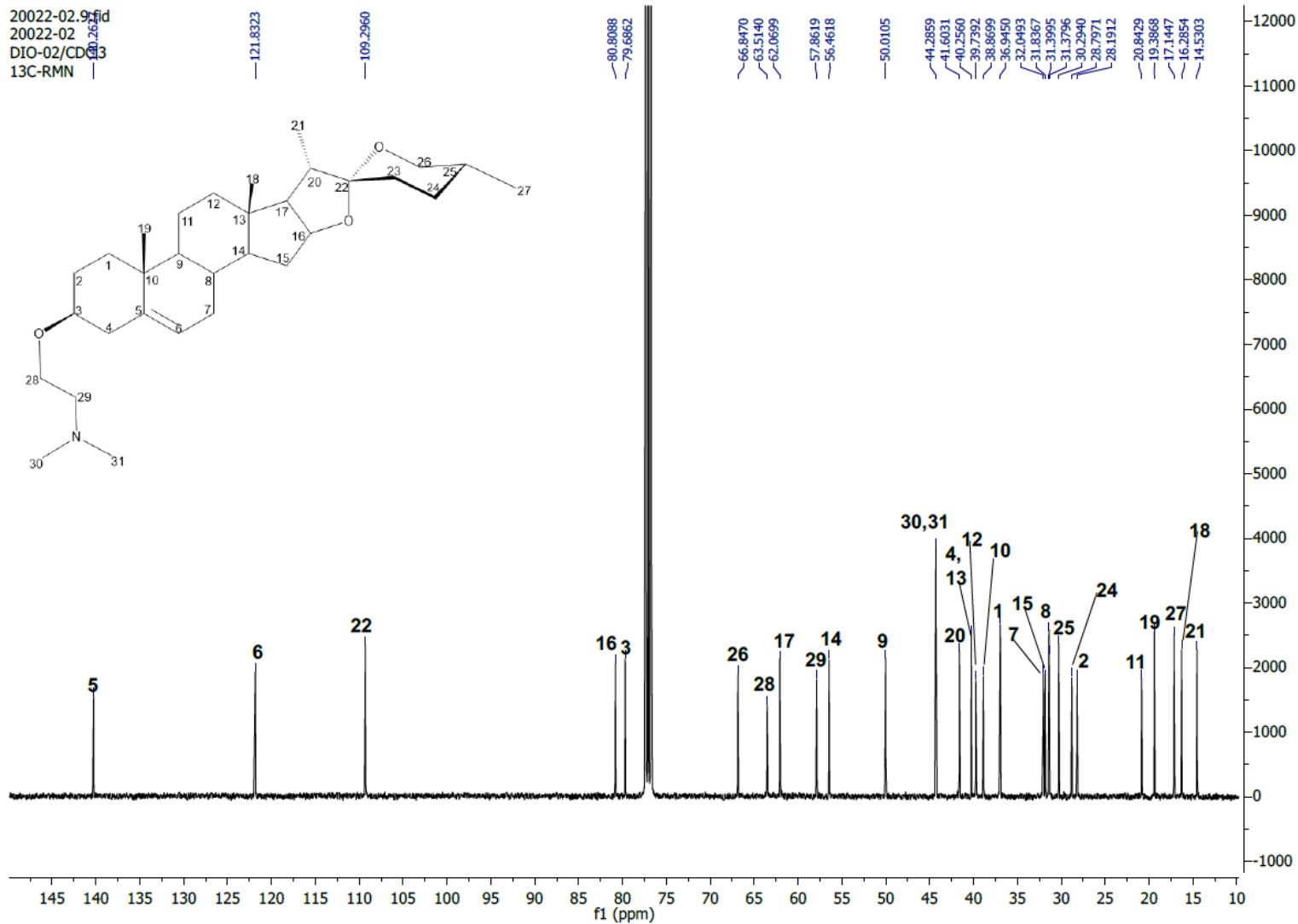
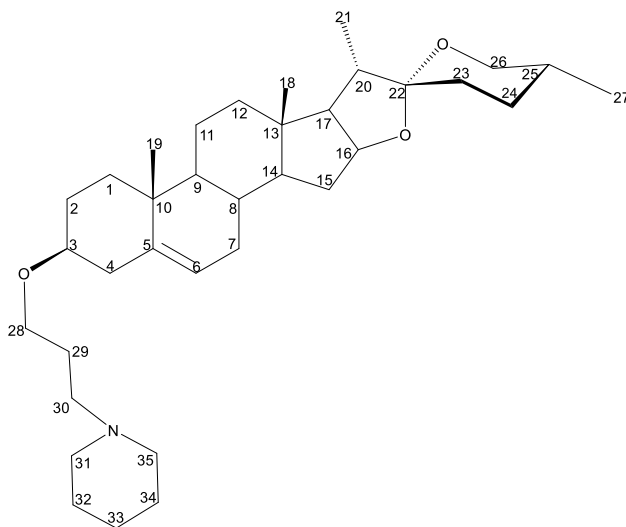


Figure 54. <sup>13</sup>C NMR (100 MHz, CDCl<sub>3</sub>) spectrum of DIO-02

### 5.7.3. Structural elucidation of DIO-03



**Figure 55.** Aminoether derivative DIO-03

$^1\text{H}$  NMR DIO-03 characteristic signals ( $\text{CDCl}_3$ , 400 MHz):  $\delta$  5.3497 (d,  $J$ = 4.80 Hz, 1H, H-6), 4.4227 (q,  $J$ = 7.36, 7.36, 7.6 Hz, 1H, H-16), 3.5053 (t,  $J$ = 6.48 Hz, 2H, H-28), 3.4864 (dd,  $J$ = 10.72, 3.52 Hz, 1H, H-26 $\beta$ -equatorial), 3.3895 (t,  $J$ = 10.88 Hz, 1H, H-26 $\alpha$ -axial), 3.1331 (m, 1H, H-3), 2.4251 (t,  $J$ = 56 Hz, 4H, H-29; H-30), 2.4251 (brs, 4H, H-31; H-35), 1.7862 (m, 4H, H-32; H-34), 1.4549 (m, 2H, H-33), 1.0262 (s, 3H, H-19), 0.9854 (d,  $J$ = 6.88 Hz, 3H, H-21), 0.8069 (d,  $J$ = 4.96 Hz, 3H, H-27), 0.7991 (s, 3H, H-18).  $^{13}\text{C}$  NMR DIO-03 signals ( $\text{CDCl}_3$ , 100 MHz):  $\delta$  37.0406 (C-1), 28.4545 (C-2), 78.9301 (C-3), 39.1487 (C-4), 141.1154 (C-5), 121.1807 (C-6), 32.1004 (C-7), 31.8567 (C-8), 50.1883 (C-9), 37.2490 (C-10), 20.8595 (C-11), 39.8002 (C-12), 40.2754 (C-13), 56.5597 (C-14), 31.8546 (C-15), 80.8408 (C-16), 62.0984 (C-17), 16.2983 (C-18), 19.4224 (C-19), 41.6083 (C-20), 14.5375 (C-21), 109.3013 (C-22), 27.3558 (C-23), 28.8054 (C-24), 30.3090 (C-25), 66.8539 (C-26),

17.1499 (C-27), 66.5572 (C-28), 56.5340 (C-29), 56.2518 (C-30), 54.4235 (C-31), 25.7229 (C-32), 24.3107 (C-33), 25.7229 (C-34), 54.4235 (C-35).

In the  $^1\text{H}$  NMR spectrum of DIO-03 (figure 56) are shown the signals corresponding to the spin system of the propilpiperidine moiety, corresponding the triplets  $\delta$  3.5053 (t,  $J= 6.48$  Hz, 2H, H-28) and 2.4251 (t,  $J= 56$  Hz, 2H, H-30) to the ether and amine methylenes of the propil moiety, and being the methylene H-29 ( $\delta$  1.7729, m, 2H) overlapped in this portion of the substituent. The singlet  $\delta$  2.4251 (s, 4H, H-31; H-35) correspond to the methylenes alfa to piperidine ring N, the multiplet 1.7862 (m, 4H, H-32; H-34) correspond to the methylenes beta to N, and the multiplet 1.4549 (m, 2H, H-33) correspond to the methylene gamma to N in the piperidine ring. The  $^{13}\text{C}$  NMR spectrum of DIO-03 (figure 57) displayed the signals of the propilpiperidine moiety as well, with the characteristic carbon signals of the propil portion at  $\delta$  66.5572 (C-28), 56.5340 (C-29), 56.2518 (C-30), and the signals of the piperidine ring at  $\delta$  54.4235 (C-31), 25.7229 (C-32), 24.3107 (C-33), 25.7229 (C-34), 54.4235 (C-35). When comparing the spectroscopic data of DIO-03 whit the starting material diosgenin (table 12), it was observed the same shielding effects displayed in the other DIO derivatives for hydrogen H-3 ( $\delta$  3.1331, m, 1H) and for the carbons C-2 ( $\delta$  28.4545) and C-4 ( $\delta$  39.1487) adjacent to C-3, indicating close proximity to the aminoether moiety and thus confirming the substitution in C-3.

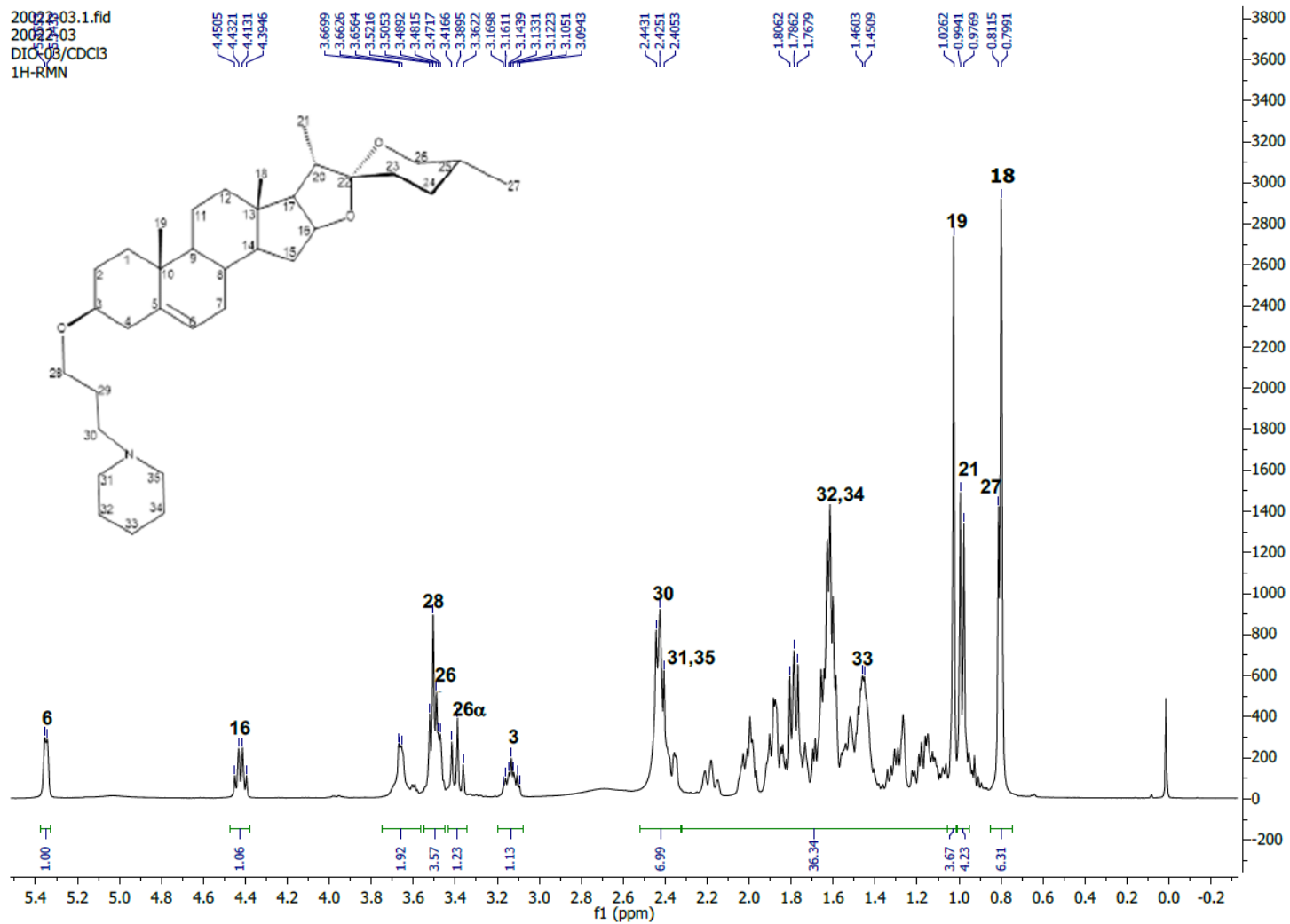


Figure 56. <sup>1</sup>H NMR (400 MHz, CDCl<sub>3</sub>) spectrum of DIO-03

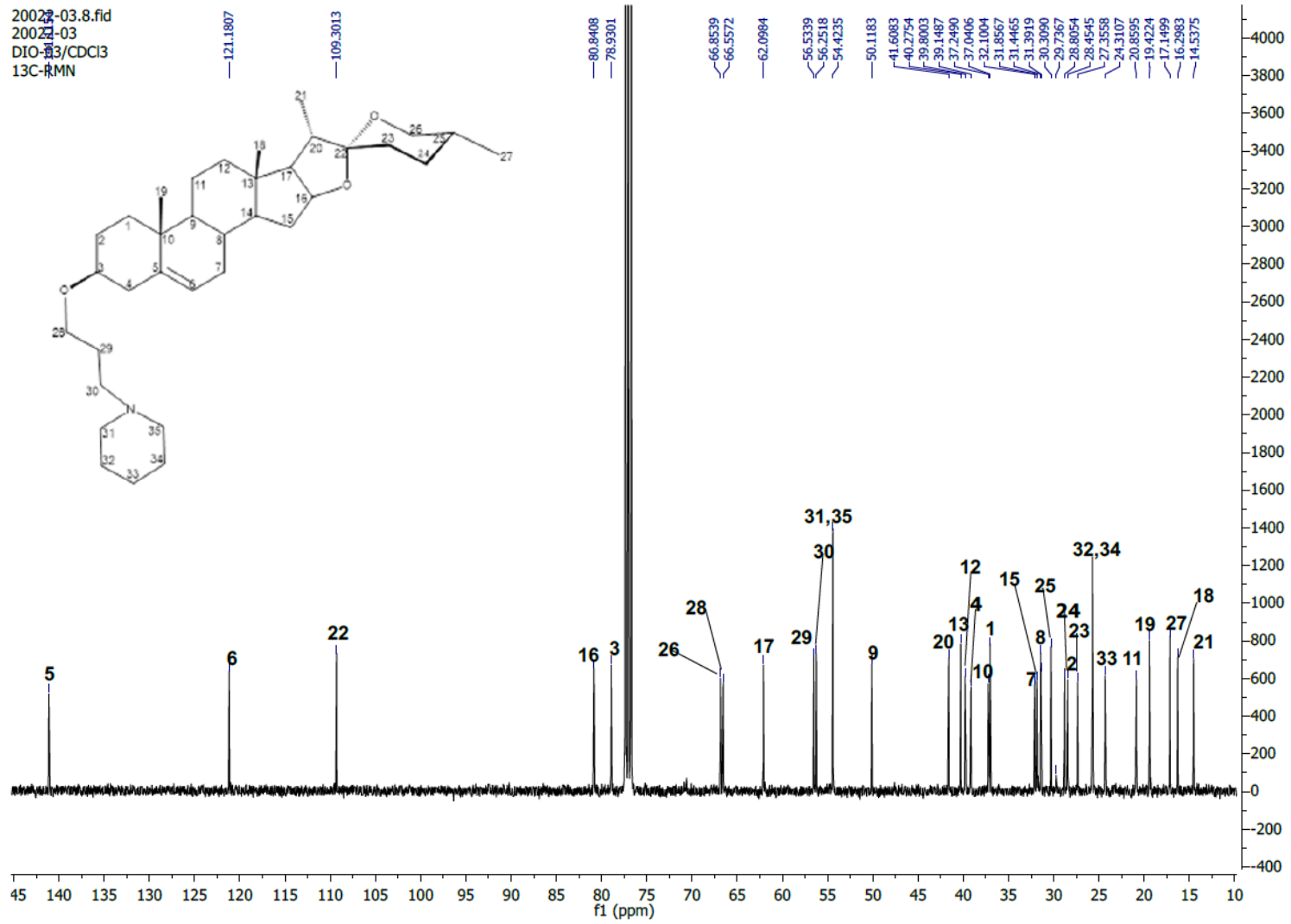
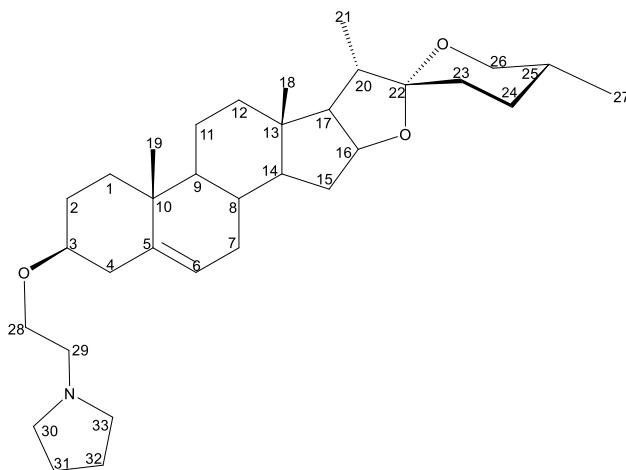


Figure 57.  $^{13}\text{C}$  NMR (100 MHz,  $\text{CDCl}_3$ ) spectrum of DIO-03



### 5.7.4. Structural elucidation of DIO-04



**Figure 58.** Aminoether derivative DIO-04

$^1\text{H}$  NMR DIO-04 characteristic signals ( $\text{CDCl}_3$ , 400 MHz):  $\delta$  5.3475 (d,  $J = 5.16$  Hz, 1H, H-6), 4.4184 (q,  $J = 7.4, 7.4, 7.52$  Hz, 1H, H-16), 3.6642 (t,  $J = 6.12$  Hz, 2H, H-28), 3.4808 (dd,  $J = 9.36, 3.88$  Hz, 1H, H-26 $\beta$ -equatorial), 3.3847 (t,  $J = 10.68$  Hz, 1H, H-26 $\alpha$ -axial), 3.1694 (m, 1H, H-3), 2.7892 (t,  $J = 6.06$  Hz, 2H, H-29), 2.7127 (brs, 4H, H-30; H-33), 1.8348 (m, 4H, H-31; H-32), 1.0222 (s, 3H, H-19), 0.9817 (d,  $J = 6.92$  Hz, 3H, H-21), 0.8015 (d,  $J = 4.96$  Hz, 3H, H-27), 0.7949 (s, 3H, H-18).  $^{13}\text{C}$  NMR DIO-01 signals ( $\text{CDCl}_3$ , 100 MHz):  $\delta$  37.0129 (C-1), 28.3158 (C-2), 79.3195 (C-3), 39.0368 (C-4), 140.9205 (C-5), 121.3155 (C-6), 32.0835 (C-7), 31.4345 (C-8), 50.0914 (C-9), 37.1745 (C-10), 20.8501 (C-11), 39.7834 (C-12), 40.2658 (C-13), 55.6981 (C-14), 31.8464 (C-15), 80.8257 (C-16), 62.0976 (C-17), 16.1829 (C-18), 19.4026 (C-19), 41.6034 (C-20), 14.5208 (C-21), 109.2839 (C-22), 26.9114 (C-23), 28.8004 (C-24), 30.2996 (C-25), 66.8426 (C-26), 17.1339 (C-27), 66.3196 (C-28), 56.5170 (C-29), 54.3566 (C-30), 23.3733 (C-31), 23.3733 (C-32), 54.3566 (C-33).

In the  $^1\text{H}$  NMR spectrum of DIO-04 (figure 59) are shown the signals corresponding to the spin system of the ethylpyrrolidine moiety, corresponding the triplets  $\delta$  3.6642 (t,  $J= 6.12$  Hz, 2H, H-28) and 2.7892 (t,  $J= 6.06$  Hz, 2H, H-29), to ethyl portion. The broad singlet  $\delta$  2.7127 (brs, 4H, H-30; H-33) correspond to the methylenes alfa to N, and the multiplet 1.8348 (m, 4H, H-31; H-32) correspond to the methylenes beta to N, in the pyrrolidine ring. The  $^{13}\text{C}$  NMR spectrum of DIO-04 (figure 60) displayed the signals of the ethylpyrrolidine moiety, being the characteristic carbon signals of the ethyl portion at  $\delta$  66.3196 (C-28), 56.5170 (C-29), and the signals of the pyrrolidine ring at  $\delta$  54.3566 (C-30), 23.3733 (C-31), 23.3733 (C-32), 54.3566 (C-33). When comparing the spectroscopic data of DIO-04 whit the starting material diosgenin (table 12), it was observed the same shielding effects displayed in the other DIO derivatives for hydrogen H-3 ( $\delta$  3.1694, m, 1H) and for the carbons C-2 ( $\delta$  28.3158) and C-4 ( $\delta$  39.0368) adjacent to C-3, indicating close proximity to the aminoether moiety and thus confirming the substitution in C-3.

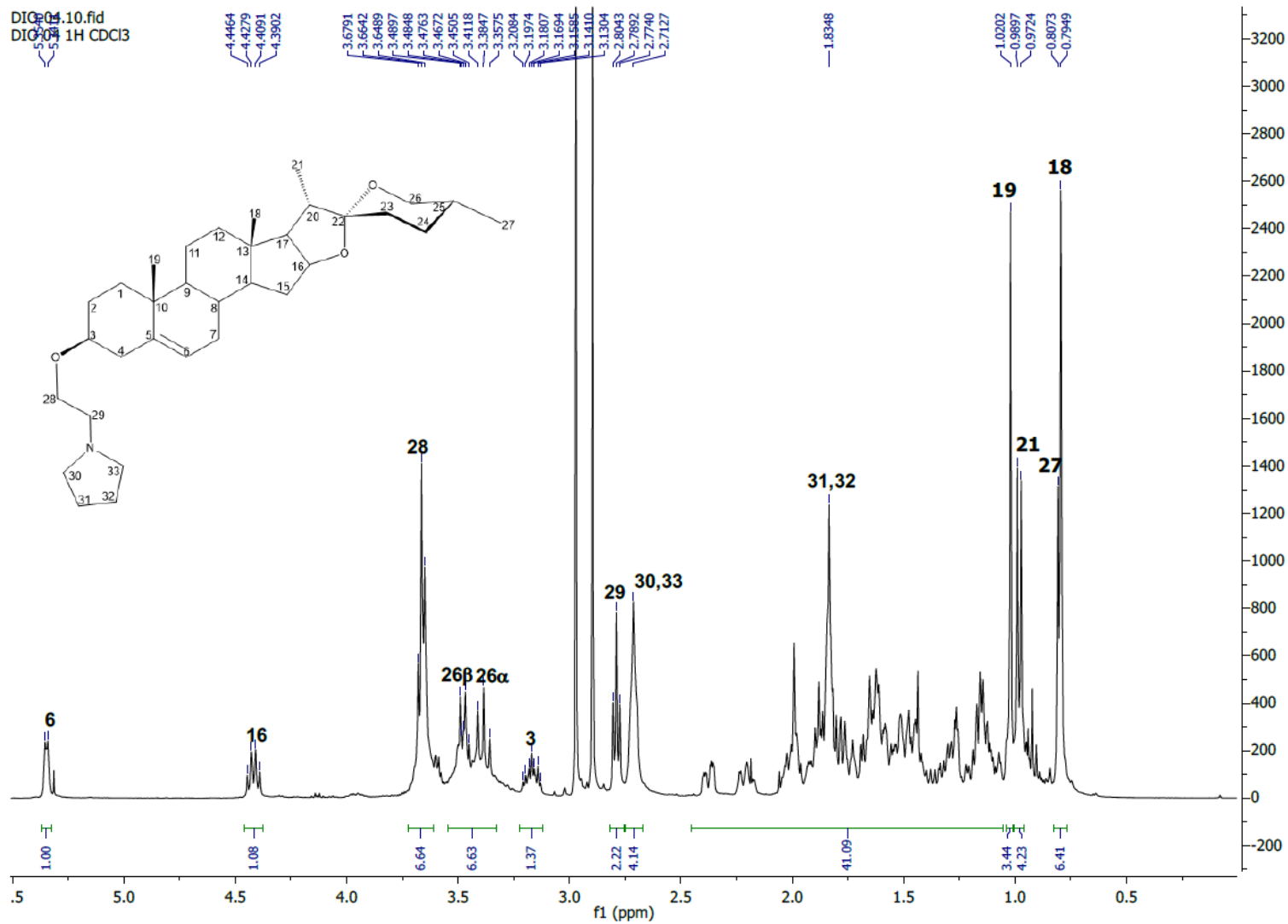


Figure 59. <sup>1</sup>H NMR (400 MHz, CDCl<sub>3</sub>) spectrum of DIO-04

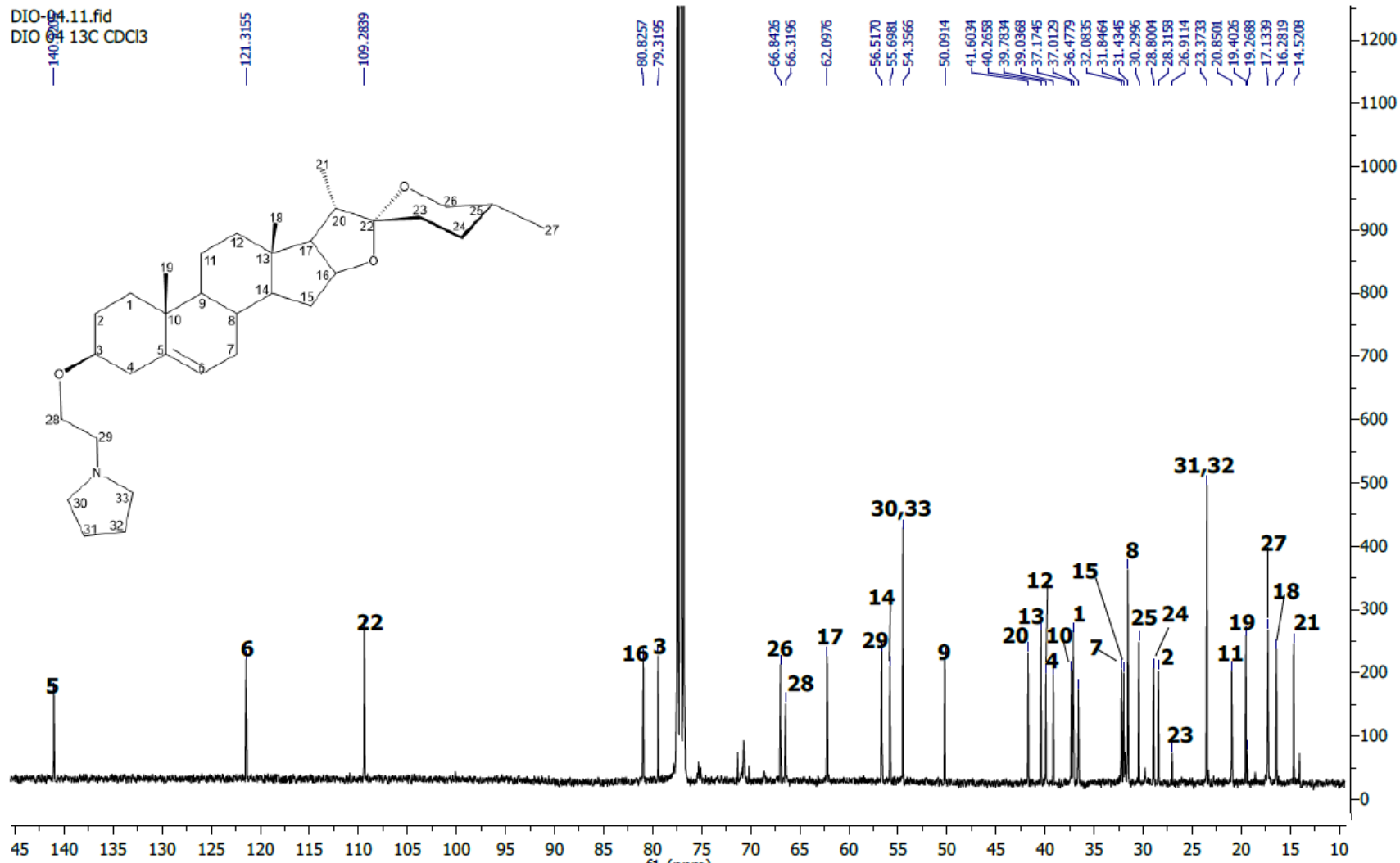
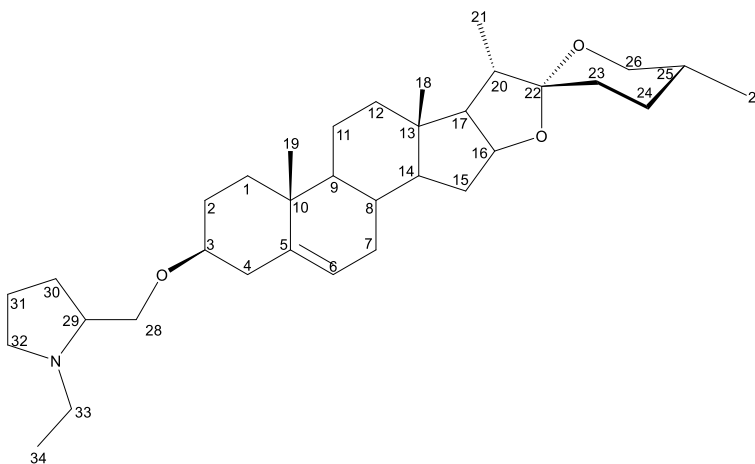


Figure 60. <sup>13</sup>C NMR (100 MHz, CDCl<sub>3</sub>) spectrum of DIO-04

### 5.7.5. Structural elucidation of DIO-05



**Figure 61.** Aminoether derivative DIO-05

$^1\text{H}$  NMR DIO-05 characteristic signals ( $\text{CDCl}_3$ , 400 MHz):  $\delta$  5.3487 (d,  $J$ = 4.8 Hz, 1H, H-6), 4.4224 (q,  $J$ = 7.4, 7.4, 7.6 Hz, 1H, H-16), 3.6031 (dd,  $J$ = 9.6, 5.18 Hz, 1H, H-28 $\beta$ -equatorial), 3.4872 (dd,  $J$ = 10.32, 3.44 Hz, 1H, H-26 $\beta$ -equatorial), 3.4247 (d,  $J$ = 6.44 Hz, 1H, H-28 $\alpha$ -axial), 3.3895 (t,  $J$ = 10.78 Hz, 1H, H-26 $\alpha$ -axial), 3.2417 (m, 1H, H-32 $\beta$ ) 3.1611 (m, 1H, H-3), 3.0292 (m, 1H, H-33 $\beta$ ) 2.6993 (p,  $J$ = 6.44, 6.56, 6.32, 6.12 Hz, 1H, H-29), 2.4511 (m, 1H, H-33 $\alpha$ ), 2.2922 (dd,  $J$ = 17.28, 8.68 Hz, 1H, H-32 $\alpha$ ), 1.1534 (t,  $J$ = 7.2 Hz, 3H, H-34), 1.0252 (s, 3H, H-19), 0.9852 (d,  $J$ = 6.92 Hz, 3H, H-21), 0.8047 (d,  $J$ = 5.36 Hz, 3H, H-27), 0.7980 (s, 3H, H-18).  $^{13}\text{C}$  NMR DIO-05 signals ( $\text{CDCl}_3$ , 100 MHz):  $\delta$  37.0332 (C-1), 28.4090 (C-2), 79.4783 (C-3), 39.0054 (C-4), 141.0071 (C-5), 121.2677 (C-6), 32.0961 (C-7), 31.3890 (C-8), 50.0979 (C-9), 37.2126 (C-10), 20.8582 (C-11), 39.7912 (C-12), 40.2733 (C-13), 56.5246 (C-14), 31.8532 (C-15), 80.8394 (C-16), 62.0903 (C-17), 16.2962 (C-18), 19.4281 (C-19), 41.6085 (C-20), 14.5360 (C-21), 109.3030 (C-22), 22.6692 (C-23),

28.6807 (C-24), 30.3063 (C-25), 66.8516 (C-26), 17.1493 (C-27), 71.1104 (C-28), 63.8718 (C-29), 28.6807 (C-30), 31.4429 (C-31), 53.7808 (C-32), 49.2920 (C-33), 13.2889 (C-34).

In the  $^1\text{H}$  NMR spectrum of DIO-05 (figure 62) are shown the signals corresponding to the spin system of the 1-(methyl)-N-ethylpyrrolidine moiety, corresponding the doublet of doublets  $\delta$  3.6031 (dd,  $J= 9.6, 5.18$  Hz, 1H, H-28 $\beta$ ), and the overlapped doublet 3.4247 (d,  $J= 6.44$  Hz, 1H, H-28 $\alpha$ ) to the oxymethylene portion. The N-ethyl portion was attributed to the methylene hydrogen signals  $\delta$  3.0292 (m, 1H, H-33 $\beta$ ), 2.4511 (m, 1H, H-33 $\alpha$ ) and the terminal methyl at 1.1534 (t,  $J= 7.2$  Hz, 3H, H-34). For the pyrrolidine ring portion two signals alpha to N were observed, a methine at  $\delta$  2.6993 (p,  $J= 6.44, 6.56, 6.32, 6.12$  Hz, 1H, H-29), and two methylene hydrogens at 2.2922 (dd,  $J= 17.28, 8.68$  Hz, 1H, H-32 $\alpha$ ) and 3.2417 (m, 1H, H-32 $\beta$ ). The signals corresponding to the methylenes beta to N (H-30 and H-31) were overlapped at the region between  $\delta$  1.44 and 1.90 and their proper multiplicity cannot be observed. The  $^{13}\text{C}$  NMR spectrum of DIO-05 (figure 63) displayed the signals of the 1-(methyl)-N-ethylpyrrolidine moiety, being the carbon signal of the oxymethylene portion at  $\delta$  71.1104 (C-28), the signals of the N-ethyl portion at  $\delta$  49.2920 (C-33) and 13.2889 (C-34), and the pyrrolidine ring signals at  $\delta$  63.8718 (C-29), 28.6807 (C-30), 31.4429 (C-31), 53.7808 (C-32). When comparing the spectroscopic data of DIO-05 with the starting material diosgenin (table 12), it was observed the same shielding effects displayed in the other DIO derivatives for hydrogen H-3 ( $\delta$  3.1611, m, 1H) and for

the carbons C-2 (28.4090) and C-4 (39.0054) adjacent to C-3, indicating close proximity to the aminoether moiety and thus confirming the substitution in C-3.

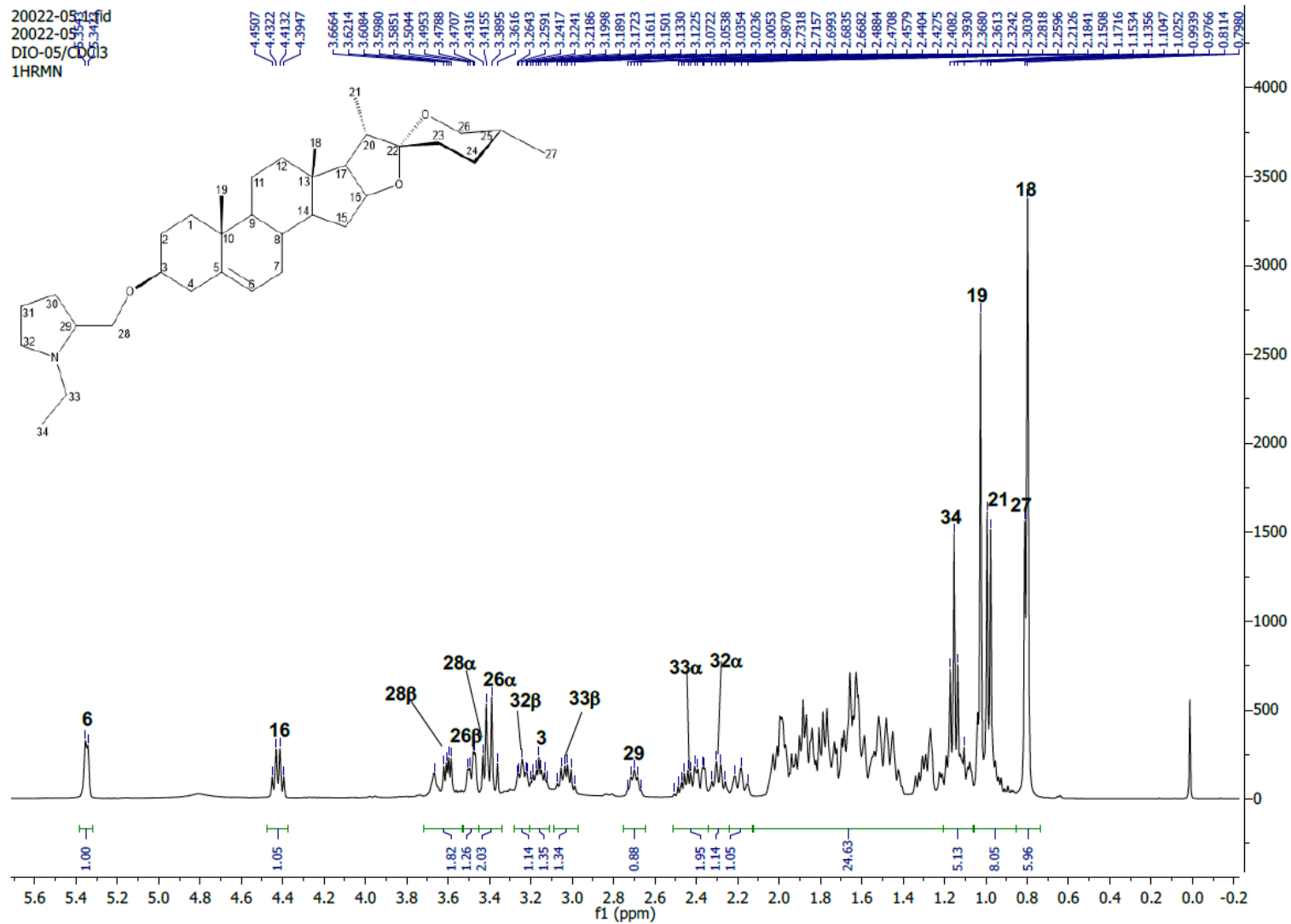


Figure 62. <sup>1</sup>H NMR (400 MHz, CDCl<sub>3</sub>) spectrum of DIO-05



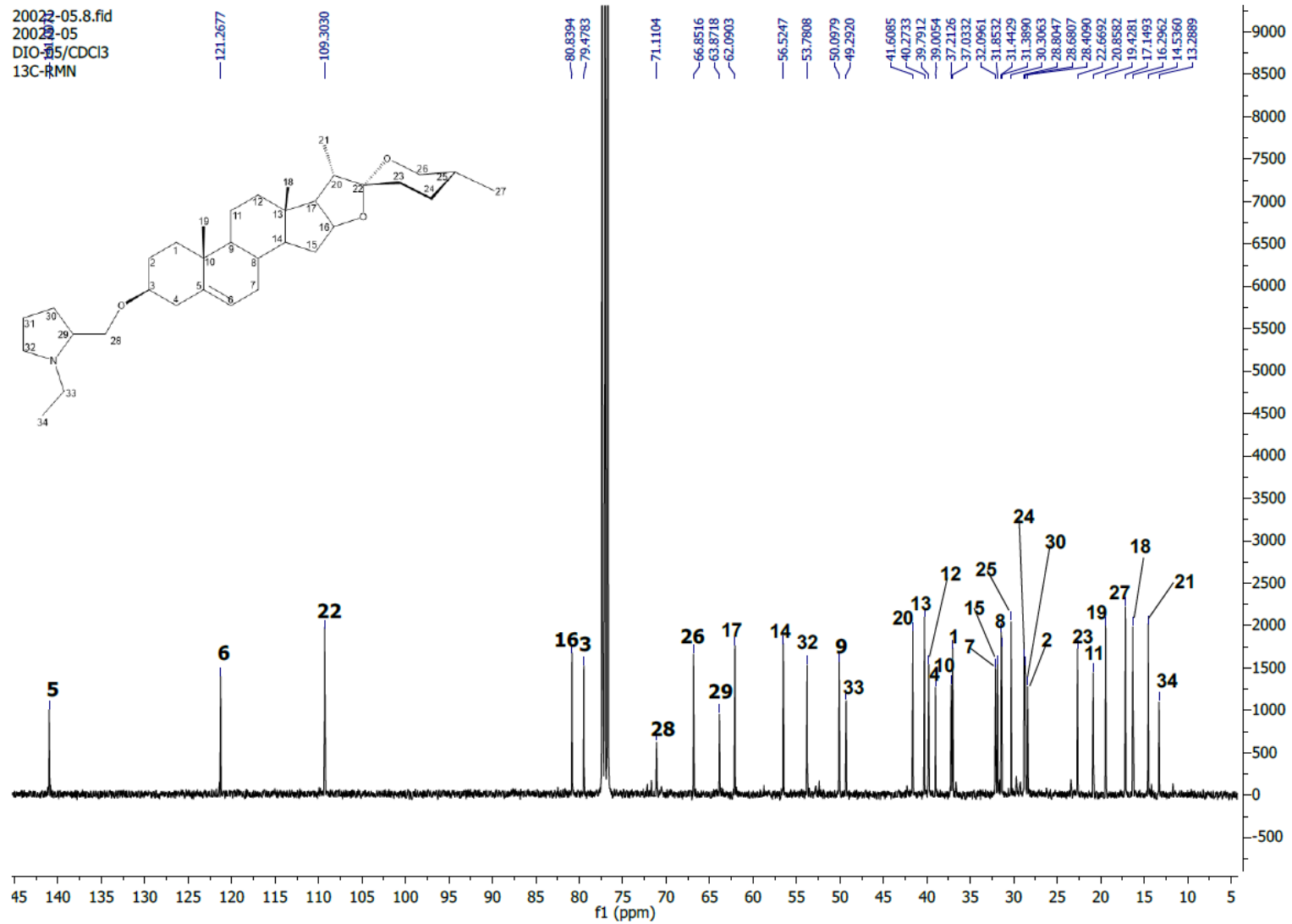
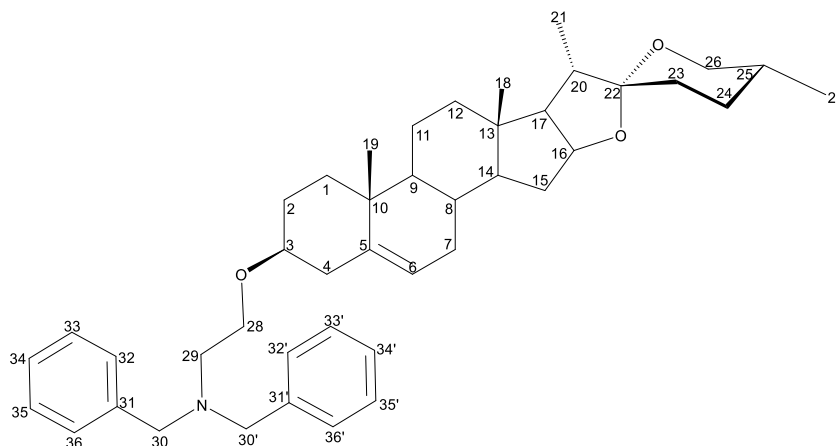


Figure 63. <sup>13</sup>C NMR (100 MHz, CDCl<sub>3</sub>) spectrum of DIO-05

### 5.7.6. Structural elucidation of DIO-06



**Figure 64.** Aminoether derivative DIO-06

$^1\text{H}$  NMR DIO-06 characteristic signals ( $\text{CDCl}_3$ , 400 MHz):  $\delta$  7.3974 (d,  $J = 7.44$  Hz, 4H, H-33; H-33'; H-35; H-35'), 7.3256 (t,  $J = 7.44$  Hz, 4H, H-32; H-32'; H-36; H-36'), 7.2462 (t,  $J = 7.18$  Hz, 4H, H-34; H-34'), 5.3429 (d,  $J = 4.84$  Hz, 1H, H-6), 4.4362 (q,  $J = 7.36, 7.36, 7.6$  Hz, 1H, H-16), 3.6707 (brs, 4H, H-30; H-30'), 3.5920 (t,  $J = 6.26$  Hz, 2H, H-28), 3.5013 (dd,  $J = 10.64, 3.56$  Hz, 1H, H-26 $\beta$ -equatorial), 3.4036 (t,  $J = 10.88$  Hz, 1H, H-26 $\alpha$ -axial), 3.1253 (m, 1H, H-3), 2.6934 (t,  $J = 6.24$  Hz, 2H, H-29), 1.0214 (s, 3H, H-19), 0.9992 (d,  $J = 6.92$  Hz, 3H, H-21), 0.8181 (d,  $J = 6.08$  Hz, 3H, H-27), 0.8093 (s, 3H, H-18).  $^{13}\text{C}$  NMR DIO-06 signals ( $\text{CDCl}_3$ , 100 MHz):  $\delta$  37.0371 (C-1), 28.4147 (C-2), 79.1232 (C-3), 39.0991 (C-4), 141.0542 (C-5), 121.2190 (C-6), 32.1160 (C-7), 31.4495 (C-8), 50.1260 (C-9), 37.2094 (C-10), 20.8677 (C-11), 39.8105 (C-12), 40.2855 (C-13), 56.5471 (C-14), 31.8703 (C-15), 80.8530 (C-16), 62.1092 (C-17), 16.3122 (C-18), 19.4245 (C-19), 41.6203 (C-20), 14.5560 (C-21), 109.3156 (C-22), 31.4042 (C-23), 28.8186 (C-24), 30.3233 (C-25), 66.8690 (C-26), 17.1670 (C-27), 66.6837 (C-28), 53.3119 (C-29), 59.0082 (C-30, C-30'), 139.8672

(C-31, C-31'), 128.1713 (C-32, C-32'), 128.7984 (C-33, C-33'), 126.8125 (C-34, C-34'), 128.7984 (C-35, C-35'), 128.1713 (C-36, C-36').

In the  $^1\text{H}$  NMR spectrum of DIO-06 (figure 65) are clearly displayed the signals corresponding to the spin system of the N-(ethyl)-N,N-dibenzylamine moiety, corresponding the triplets  $\delta$  3.5920 (t,  $J= 6.26$  Hz, 2H, H-28) and 2.6934 (t,  $J= 6.24$  Hz, 2H, H-29) to the ethyl portion of the substituent, the singlet 3.6707 (brs, 4H, H-30; H-30') corresponding to two benzylic methylene alpha to N, and the signals  $\delta$  7.3974 (d,  $J= 7.44$  Hz, 4H, H-33; H-33'; H-35; H-35'), 7.3256 (t,  $J= 7.44$  Hz, 4H, H-32; H-32'; H-36; H-36') and 7.2462 (t,  $J= 7.18$  Hz, 4H, H-34; H-34') corresponding to the aromatic hydrogens of the aromatic rings in the dibenzyl moiety. The  $^{13}\text{C}$  NMR spectrum of DIO-06 (figure 66) displayed the carbon signals of the ethyl portion in the aminoether substituent at  $\delta$  66.6837 (C-28), 53.3119 (C-29), the benzylic methylene carbons were shown at 59.0082 (C-30, C-30'), and the aromatic carbons signals at 139.8672 (C-31, C-31'), 128.1713 (C-32, C-32'), 128.7984 (C-33, C-33'), 126.8125 (C-34, C-34'), 128.7984 (C-35, C-35'), 128.1713 (C-36, C-36'). When comparing the spectroscopic data of DIO-06 with the starting material diosgenin (table 12). It was observed the same shielding effects displayed in the other DIO derivatives for hydrogen H-3 ( $\delta$  3.1253, m, 1H) and for the carbons C-2 ( $\delta$  28.4147) and C-4 ( $\delta$  39.0991) adjacent to C-3, indicating close proximity to the aminoether moiety and thus confirming the substitution in C-3.

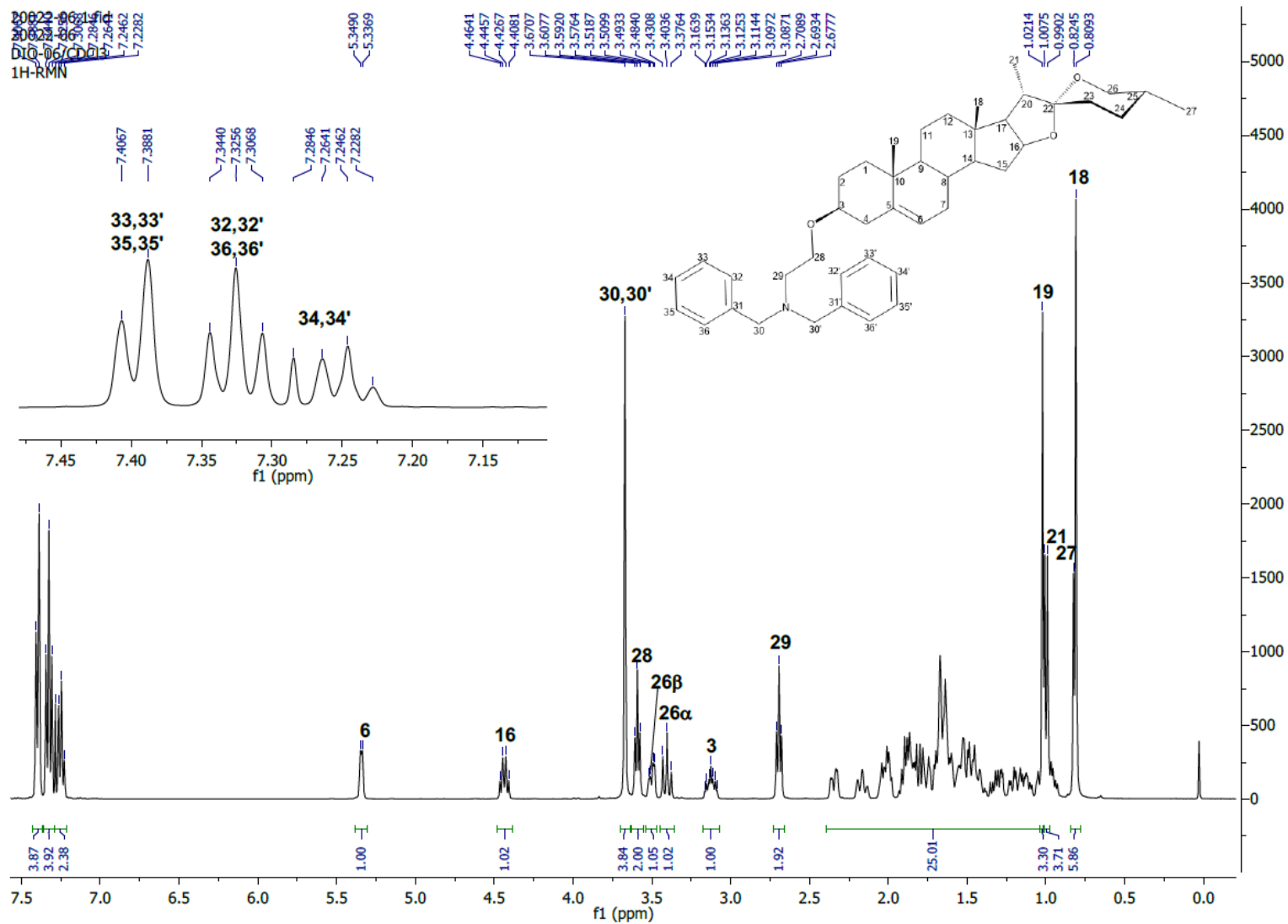


Figure 65. <sup>1</sup>H NMR (400 MHz, CDCl<sub>3</sub>) spectrum of DIO-06

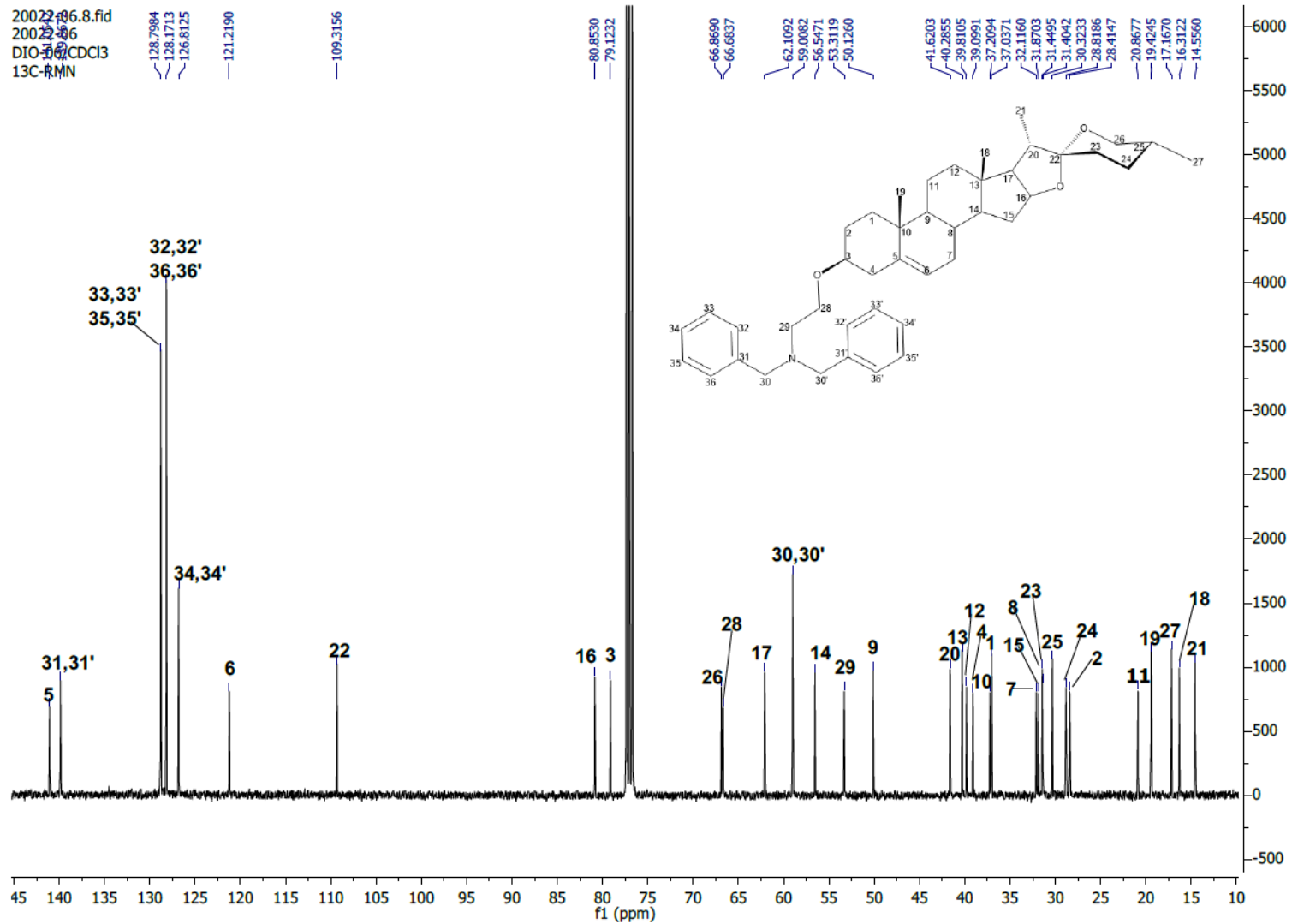
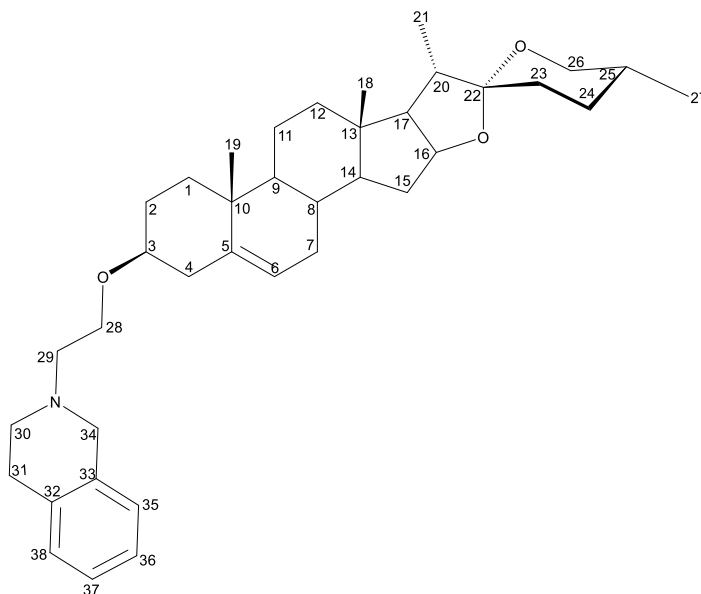


Figure 66. <sup>13</sup>C NMR (100 MHz, CDCl<sub>3</sub>) spectrum of DIO-06

### 5.7.7. Structural elucidation of DIO-07



**Figure 67.** Aminoether derivative DIO-07

$^1\text{H}$  NMR DIO-07 characteristic signals ( $\text{CDCl}_3$ , 400 MHz):  $\delta$  7.1250 (m, 3H, H-36; H-37; H-38), 7.0308 (m, 1H, H-35), 5.3674 (d,  $J$ = 4.84 Hz, 1H, H-6), 4.4273 (q,  $J$ = 7.44, 7.44, 7.6 Hz, 1H, H-16), 3.7339 (t,  $J$ = 6.1 Hz, 2H, H-28), 3.7339 (s, 2H, H-34), 3.4963 (dd,  $J$ = 10.64, 3.56 Hz, 1H, H-26 $\beta$ -equatorial), 3.3979 (t,  $J$ = 10.88 Hz, 1H, H-26 $\alpha$ -axial), 3.2062 (m, 1H, H-3), 2.9296 (t,  $J$ = 5.72 Hz, 2H, H-31), 2.8408 (t,  $J$ = 5.76 Hz, 2H, H-29), 2.7843 (t,  $J$ = 6.18 Hz, 2H, H-30), 1.0424 (s, 3H, H-19), 0.9942 (d,  $J$ = 6.92 Hz, 3H, H-21), 0.8145 (d,  $J$ = 3.84 Hz, 3H, H-27), 0.8097 (s, 3H, H-18).  $^{13}\text{C}$  NMR DIO-07 signals ( $\text{CDCl}_3$ , 100 MHz):  $\delta$  37.0529 (C-1), 28.4216 (C-2), 79.3939 (C-3), 39.1238 (C-4), 141.0250 (C-5), 121.3042 (C-6), 32.1100 (C-7), 31.4534 (C-8), 50.1193 (C-9), 37.2395 (C-10), 20.8725 (C-11), 39.8059 (C-12), 40.2849 (C-13), 56.4932 (C-14), 31.8664 (C-15), 80.8444 (C-16), 62.1072 (C-17), 16.3103 (C-18), 19.4354 (C-19), 41.6172 (C-20), 14.5997 (C-21), 109.3084 (C-22), 31.4010 (C-23),

28.8150 (C-24), 30.3183 (C-25), 66.8634 (C-26), 17.1607 (C-27), 66.1756 (C-28), 51.4036 (C-29), 57.8690 (C-30), 28.9624 (C-31), 134.7432 (C-32), 134.1808 (C-33), 57.8690 (C-34), 126.5852 (C-35), 126.1027 (C-36), 125.2759 (C-37), 128.6581 (C-38).

In the  $^1\text{H}$  NMR spectrum of DIO-07 (figure 68) are shown the signals corresponding to the spin system of the N-(ethyl)-1,2,3,4-tetrahydroisoquinoline spin system, corresponding the triplets  $\delta$  3.7339 (t,  $J$ = 6.1 Hz, 2H, H-28) and 2.8408 (t,  $J$ = 5.76 Hz, 2H, H-29), to the ethyl portion of the substituent, the singlet  $\delta$  3.7339 (brs, 2H-H-34) and the triplet 2.7843 (t,  $J$ = 6.18 Hz, 2H, H-30) corresponding to the methylenes alfa to N, the triplet  $\delta$  2.9296 (t,  $J$ = 5.72 Hz, 2H, H-31) corresponding to a methylene beta to N and the overlapped multiplets at  $\delta$  7.1250 (m, 3H, H-36, H-37, H-38) and 7.0308 (m, 1H, H-35) being attributed to the aromatic hydrogens in the 1,2,3,4-tetrahydroisoquinoline portion of the substituent. The  $^{13}\text{C}$  NMR spectrum of DIO-07 (figure 69) displayed the carbon signals of the substituent, with the ethyl portion signals at  $\delta$  66.1756 (C-28), 51.4036 (C-29), the 1,2,3,4-tetrahydroisoquinoline carbons were shown at  $\delta$  57.8690 (C-30), 28.9624 (C-31), 134.7432 (C-32), 134.1808 (C-33), 57.8690 (C-34), 126.5852 (C-35), 126.1027 (C-36), 125.2759 (C-37), 128.6581 (C-38). When comparing the spectroscopic data of DIO-07 with the starting material diosgenin (table 12), it was observed the same shielding effects displayed in the other DIO derivatives for hydrogen H-3 ( $\delta$  3.2062, m, 1H) and for the carbons C-2 ( $\delta$  28.4216) and C-4 ( $\delta$  39.1238) adjacent to C-3, confirming substitution in C-3.

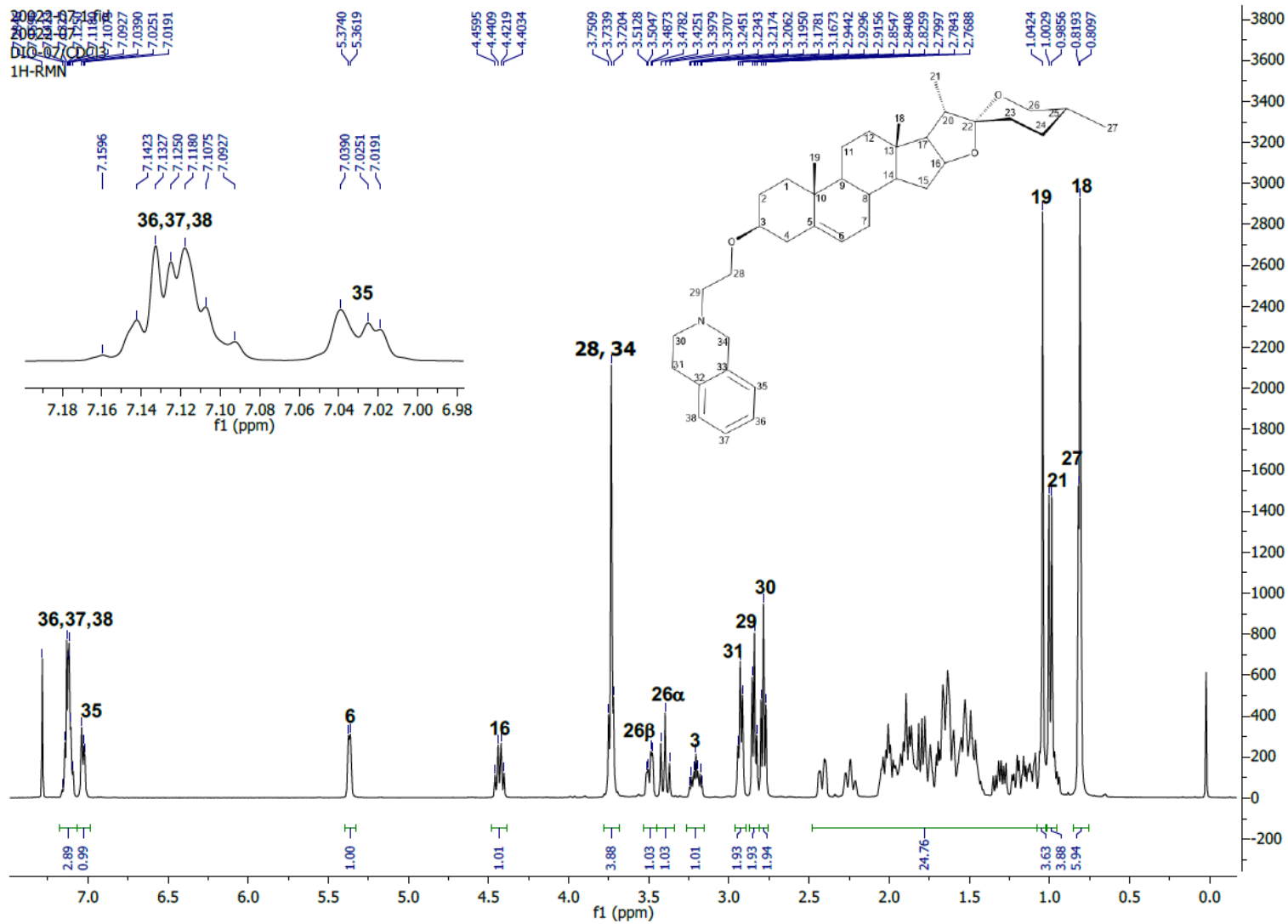


Figure 68. <sup>1</sup>H NMR (400 MHz, CDCl<sub>3</sub>) spectrum of DIO-07



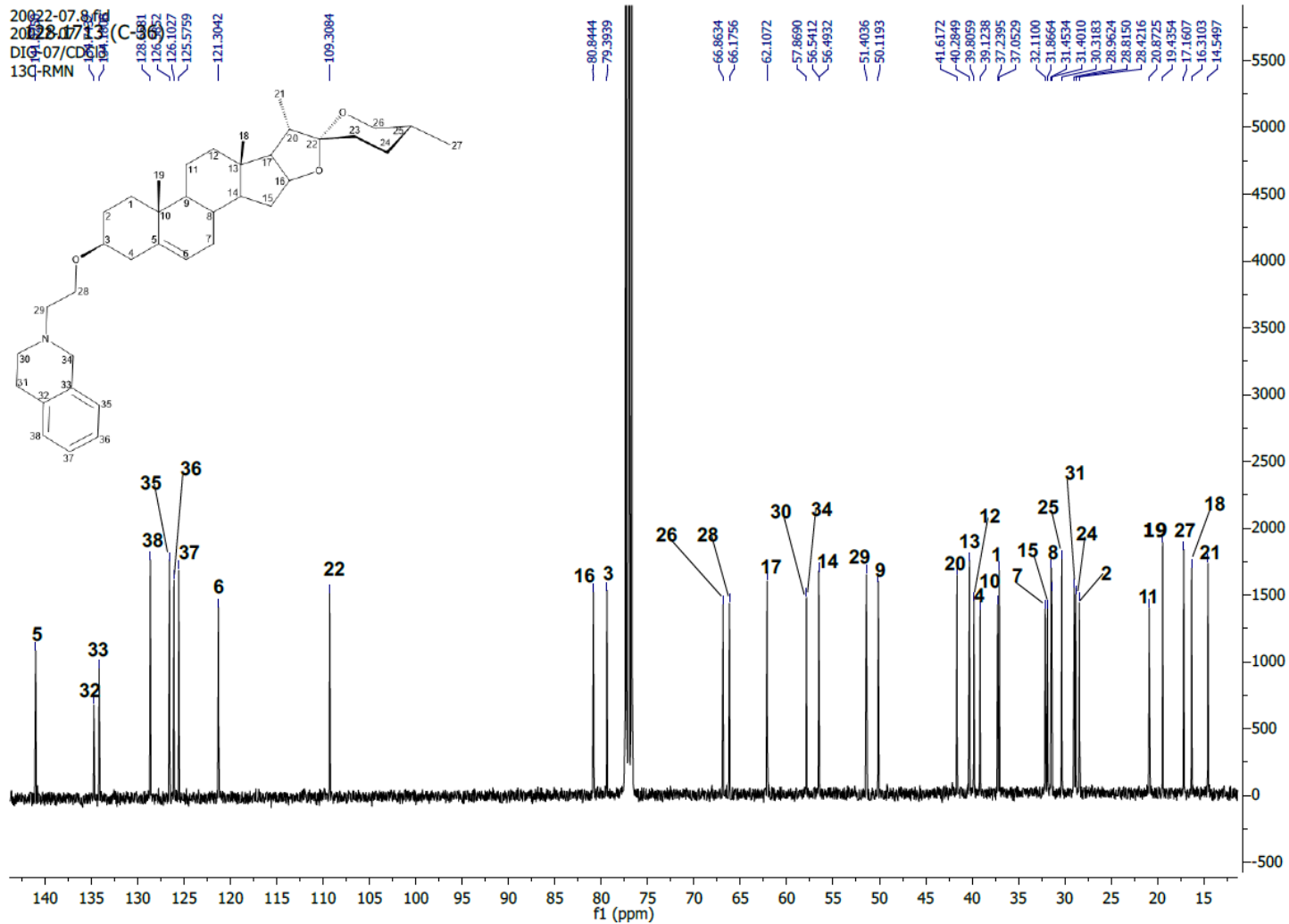


Figure 69. <sup>13</sup>C NMR (100 MHz, CDCl<sub>3</sub>) spectrum of DIO-07



66.2549 (C-26), 17.1488 (C-27), 64.8479 (C-28), 58.3694 (C-29), 53.7773 (C-30), 66.2549 (C-31), 66.2549 (C-32), 53.7773 (C-33).

In the  $^1\text{H}$  NMR spectrum of DIO-08 (figure 71) are displayed the signals corresponding to the spin system of the N-ethylmorpholine moiety, corresponding the triplet signals  $\delta$  3.7028 (t,  $J$ = 5.68 Hz, 2H, H-28) , and 2.7228 (t overlapped,  $J$ = 5.56 Hz, 2H, H-29) to the ethyl portion of the substituent, the overlapped broad signal  $\delta$  2.6901 (m, 4H, H-30; H-33) to the methylenes alfa to N, and the triplet signal  $\delta$  3.8117 (t,  $J$ = 4.64 Hz, 4H, H-31; H-32) corresponding to the methylenes alfa to oxygen in the morpholine ring. The  $^{13}\text{C}$  NMR spectrum of DIO-08 (figure 72) showed the signals of the substituent with the signals of the ethyl portion at  $\delta$  64.8479 (C-28), 58.3694 (C-29) and the morpholine ring signals at  $\delta$  53.7773 (C-30), 66.2549 (C-31), 66.2549 (C-32), 53.7773 (C-33). When comparing the spectroscopic data of DIO-08 whit the starting material diosgenin (table 12), it was observed the same shielding effects displayed in the other DIO derivatives for hydrogen H-3 ( $\delta$  3.1503, m, 1H) and for the carbons C-2 ( $\delta$  28.3284) and C-4 ( $\delta$  39.0165) adjacent to C-3, confirming substitution in C-3.

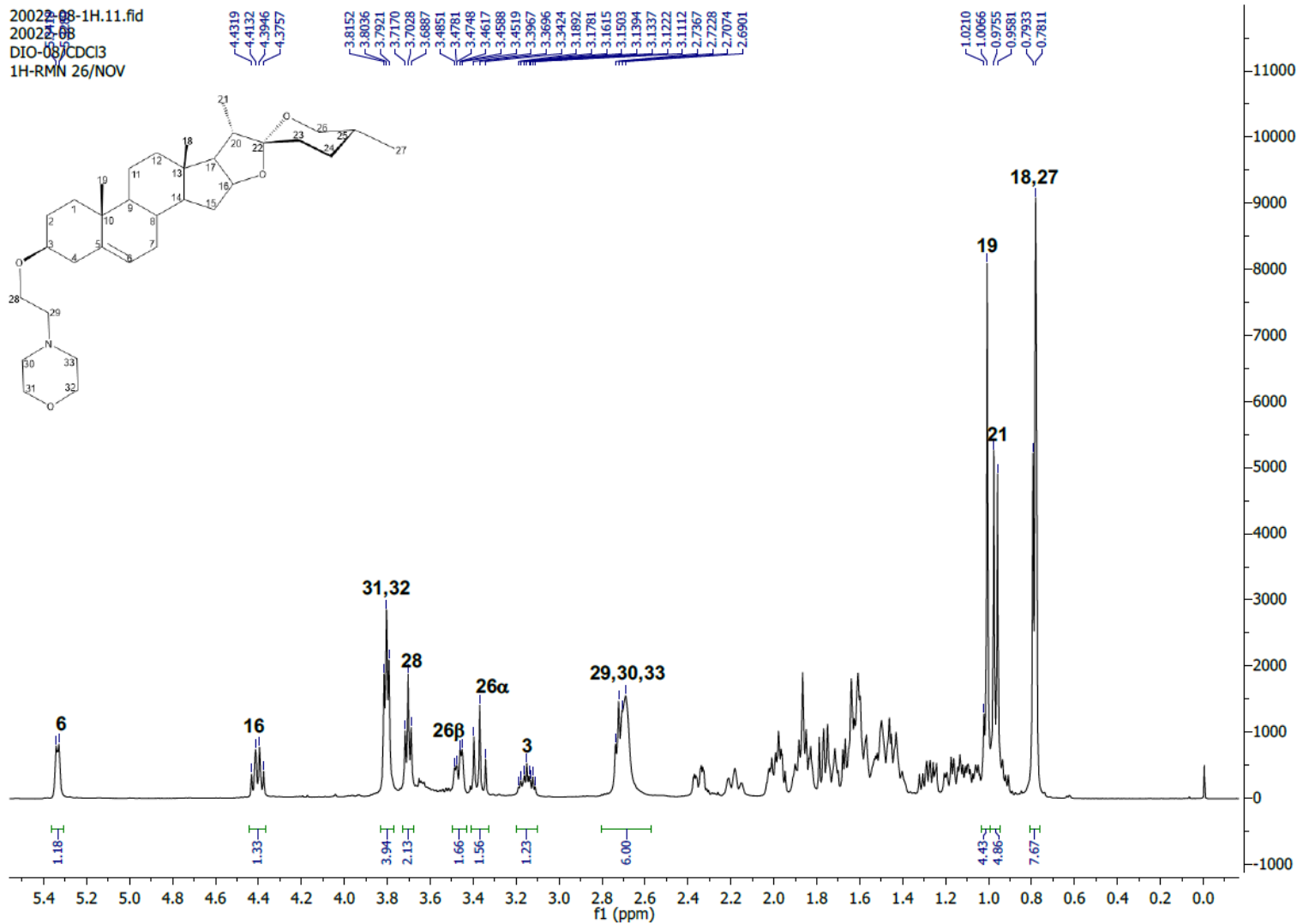


Figure 71. <sup>1</sup>H NMR (400 MHz, CDCl<sub>3</sub>) spectrum of DIO-08

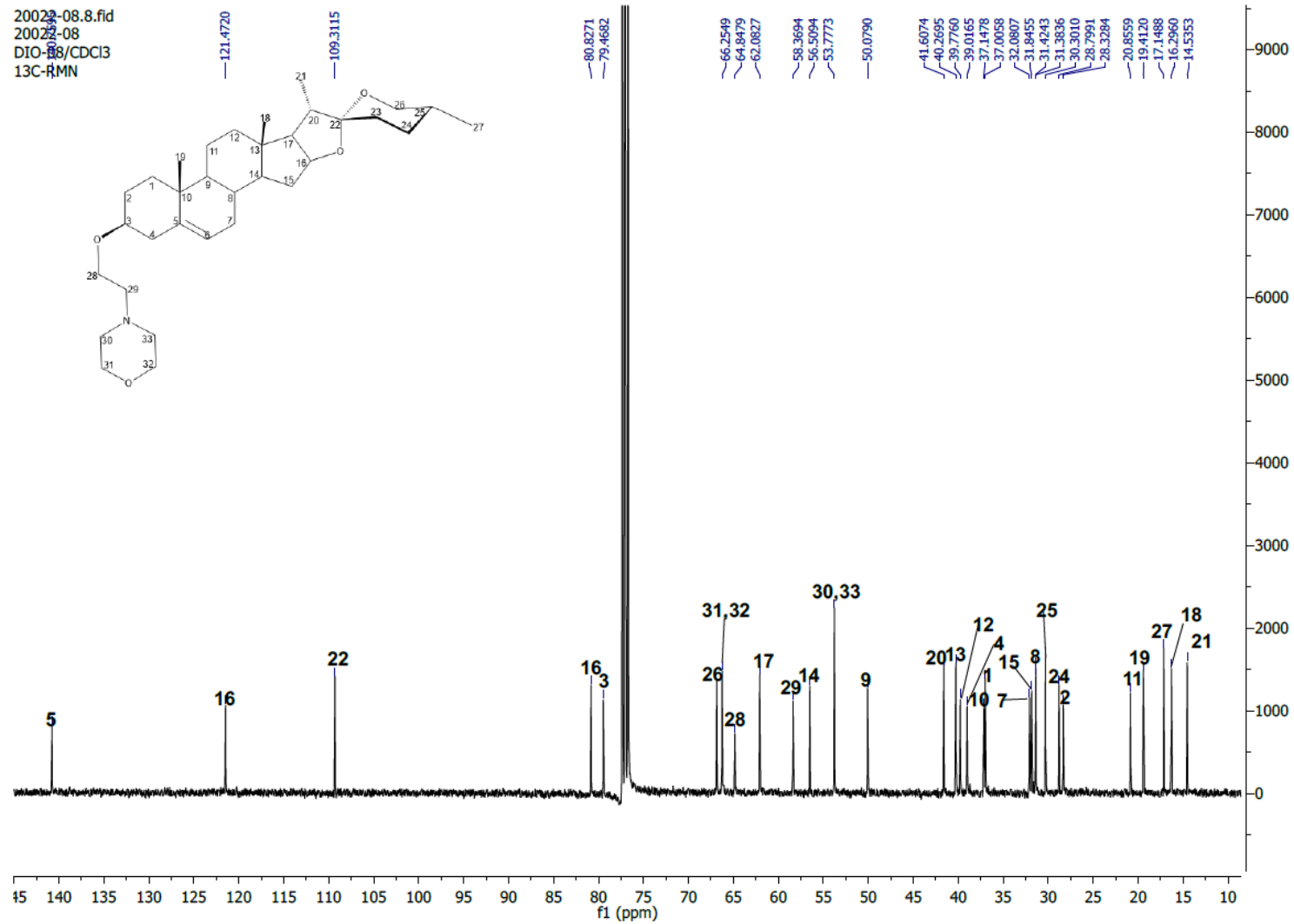
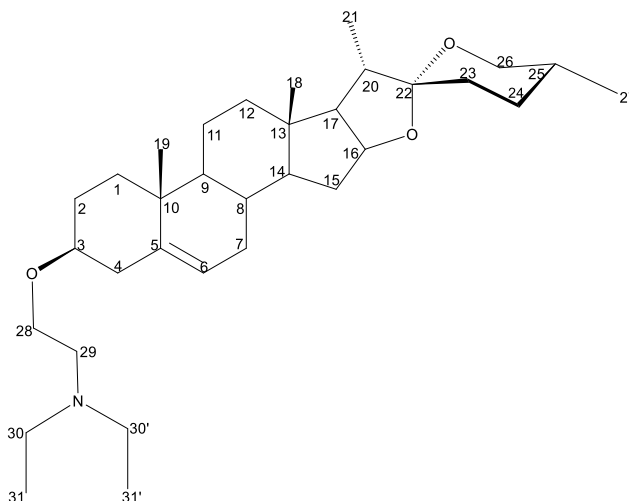


Figure 72. <sup>13</sup>C NMR (100 MHz, CDCl<sub>3</sub>) spectrum of DIO-08

### 5.7.9. Structural elucidation of DIO-09



**Figure 73.** Aminoether derivative DIO-09

$^1\text{H}$  NMR DIO-09 characteristic signals ( $\text{CDCl}_3$ , 400 MHz):  $\delta$  5.3647 (brs, 1H, H-6), 4.4230 (q,  $J = 6.68, 6.68, 7.04$  Hz, 1H, H-16), 4.0234 (brs, 2H, H-28), 3.4906 (d,  $J = 8.68$  Hz, 1H, H-26 $\beta$ -equatorial), 3.3865 (t,  $J = 10.84$  Hz, 1H, H-26 $\alpha$ -axial), 3.25 (brs overlapped, 1H, H-3), 3.2500 (brs overlapped, 2H, H-29), 1.6242 (brs, 4H, H-30, H-30'), 1.4507 (brs, 6H, H-31; H-31'), 1.0198 (s, 3H, H-19), 0.9850 (d,  $J = 6.48$  Hz, 3H, H-21), 0.7965 (brs overlapped, 3H, H-27), 0.7965 (s overlapped, 3H, H-18).  $^{13}\text{C}$  NMR DIO-09 signals ( $\text{CDCl}_3$ , 100 MHz):  $\delta$  36.9418 (C-1), 28.2844 (C-2), 79.8292 (C-3), 38.9292 (C-4), 140.0256 (C-5), 122.0642 (C-6), 32.0479 (C-7), 31.3932 (C-8), 49.9901 (C-9), 36.9418 (C-10), 20.8551 (C-11), 39.7340 (C-12), 40.2584 (C-13), 56.4479 (C-14), 31.8415 (C-15), 80.8100 (C-16), 62.0693 (C-17), 16.2943 (C-18), 19.4381 (C-19), 41.6132 (C-20), 14.5358 (C-21), 109.3015 (C-22), 30.3015 (C-23), 28.8067 (C-24), 30.3015 (C-25), 66.8552 (C-26), 17.1508 (C-27), 62.8984 (C-28), 47.9164 (C-29), 31.3932 (C-30), 31.3932 (C-30'), 9.2222 (C-31), 9.222 (C-31')

In the  $^1\text{H}$  NMR spectrum of DIO-09 (figure 74) are shown the signals corresponding to the N,N,N-triethylamine moiety, corresponding the broad singlets  $\delta$  4.0234 (brs, 2H, H-28) and 3.25 (brs overlapped, 2H, H-29), to the ethyl portion directly bonded to oxygen in the aminoether moiety, the multiplet at  $\delta$  1.6242 (m, 4H, H-30; H-30') correspond to two overlapped methylene signals alfa to N, and the multiplet at  $\delta$  1.4507 (m, 6H, H-31; H-31') correspond to two overlapped signal of the terminal methyl in the N,N,N-triethylamine substituent. The  $^{13}\text{C}$  NMR spectrum of DIO-09 (figure 75) displayed the signals of the N,N,N-triethylethylamine moiety as well, with the characteristic carbon signals of the aminoether ethyl portion at  $\delta$  62.8984 (C-28), 47.9164 (C-29), the overlapped signals of the ethyl carbons alfa to N at  $\delta$  31.3932 (C-30), 31.3932 (C-30'), and the terminal methyls in the substituent at  $\delta$  9.2222 (C-31), 9.222 (C-31'). When comparing the spectroscopic data of DIO-09 whit the starting material diosgenin (table 12), it was observed the same shielding effects displayed the other aminoether derivatives for hydrogen H-3 ( $\delta$  3.25, m, 1H) and for the carbons C-2 ( $\delta$  28.2844) and C-4 ( $\delta$  38.9292) adjacent to C-3, indicating close proximity to the aminoether moiety and thus confirming the substitution in C-3.

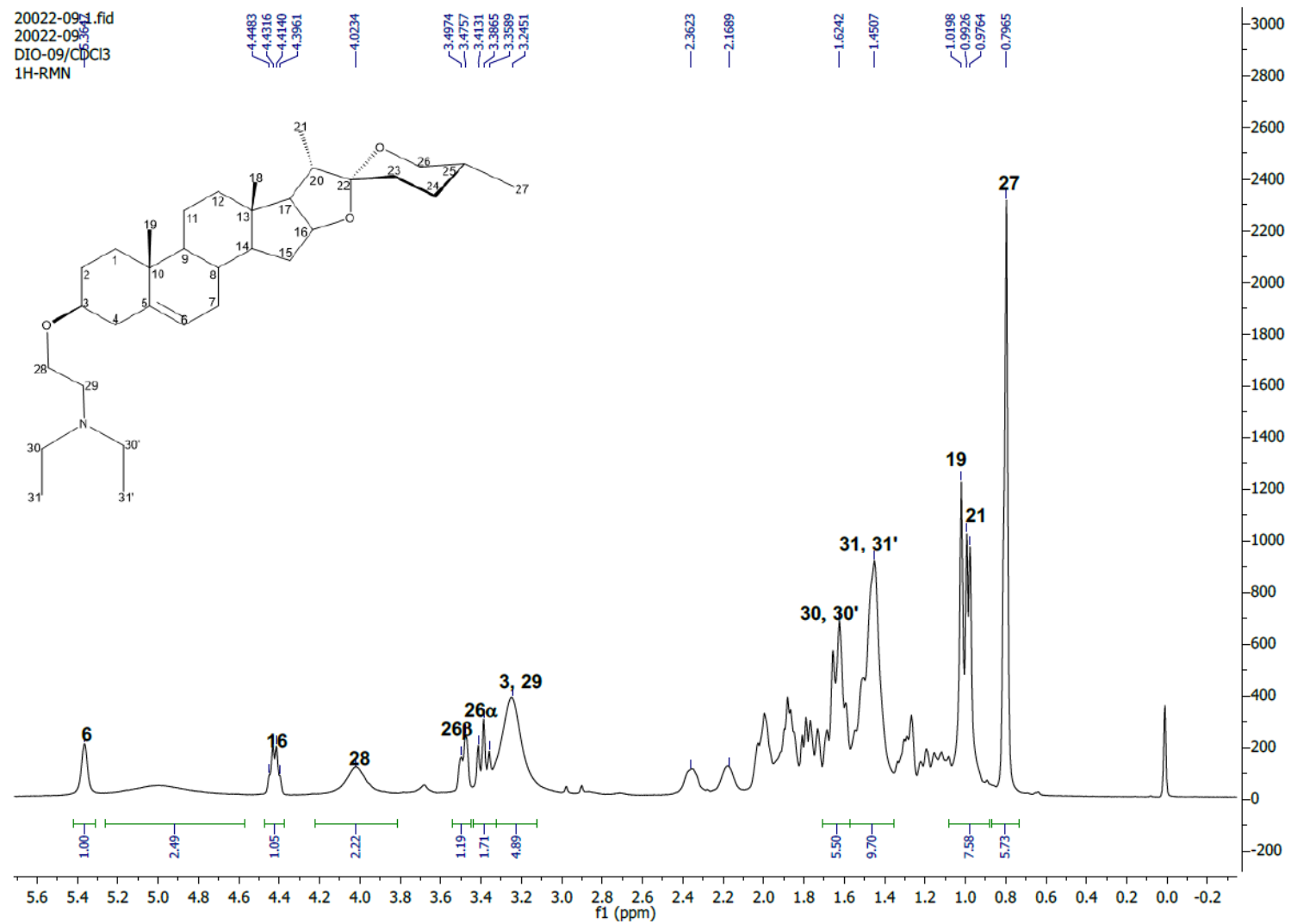


**Figure 74.**  $^1\text{H-NMR}$  (400 MHz,  $\text{CDCl}_3$ ) spectrum of DIO-09



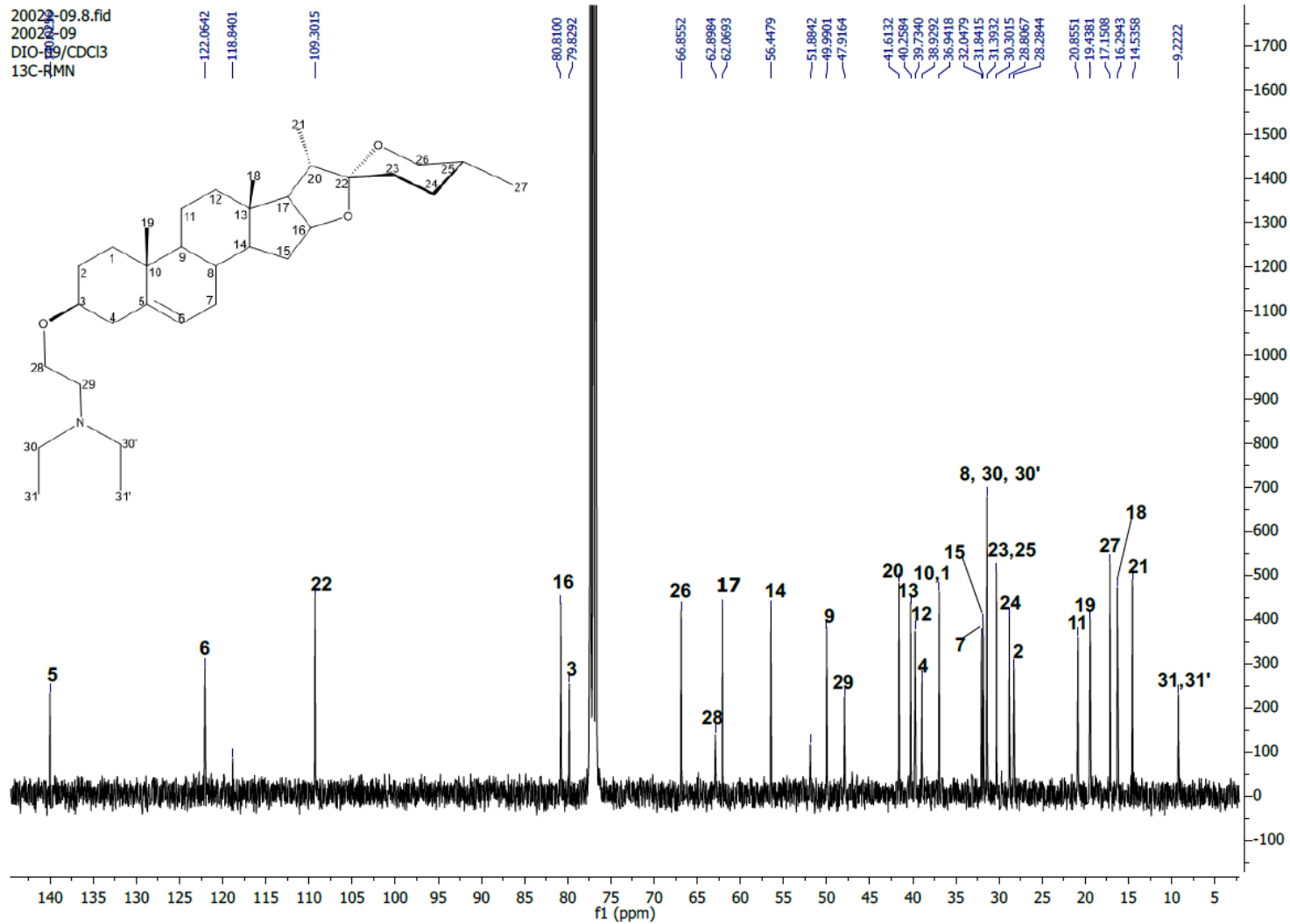


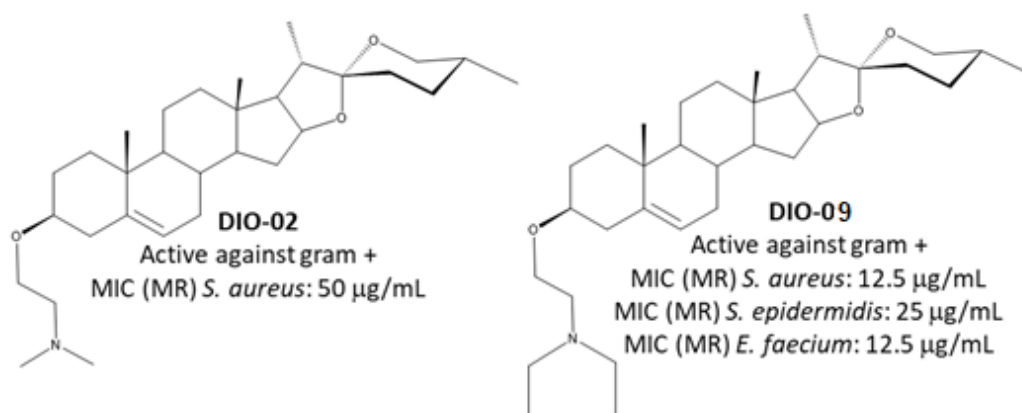
Figure 75. <sup>13</sup>C NMR (100 MHz, CDCl<sub>3</sub>) spectrum of DIO-09

## 5.5. Antibacterial activity of diosgenin aminoether derivatives

The nine synthesized aminoether derivatives and the starting material diosgenin were tested against clinical isolates of gram-negative and gram-positive bacteria (Table 13). The concentrations tested for the compounds were 50, 25, 12.5, 6.25, 3.15, 1.57  $\mu\text{g/mL}$ , and the controls levofloxacin and rifampicin were tested at 50, 25, 12.5, 6.25, 3.15, 1.57, 0.78, 0.39, 0.19, 0.098, 0.049, 0.024  $\mu\text{g/mL}$ .

The aminoether derivatives that showed antibacterial activity were DIO-02 and DIO-09, and such activity was displayed only against gram-positive bacteria. The compound DIO-02 (figure 76) was active against (MR) *S. aureus* having a MIC value of 50  $\mu\text{g/mL}$ , being eight-fold less active than the control drug levofloxacin (MIC 6.25  $\mu\text{g/mL}$ ). The compound DIO-09 (figure 76) was active against (MR) *S. aureus* (MIC 12.5  $\mu\text{g/mL}$ ), (VR) *E. faecium* (MIC 12.5  $\mu\text{g/mL}$ ) and (LR) *S. epidermidis* (MIC 25  $\mu\text{g/mL}$ ), being this derivative two-fold less active against all the gram-positive bacteria than the control drug levofloxacin (table 13). It is noteworthy that the starting material diosgenin was not active against any of the bacteria tested, indicating that the derivatization can indeed enhance the biological activity of virtually inactive sapogenins. The chemical structure-biological activity analysis for the aminoether derivatives suggest that the bulky cyclic modulations like pyrrolidine, piperidine, morpholine, isoquinoline and benzylic rings limits the activity of the amine nitrogen in the substituent, due to steric effect, such argument is supported by the fact that the aminoether derivatives DIO-02 and DIO-09 were the only active compounds

having as common feature non-cyclic portions in the aminoether moieties. With a basis on the previous analysis it can be deduced that steric impediment in the nitrogen free electron pair results in poor interaction with the unknown pharmacological target. Thus such interaction could possibly be mediated by hydrogen bonding, being the nitrogen in the aminoether the hydrogen bond acceptor. The steric impediment hypothesis could be a good approach to explain the lack of activity, however when comparing DIO-02 and DIO-09 (figure 76) its noteworthy that the two terminal N-ethyl substituents of DIO-09 cause a more significant steric effect than the two terminal N-methyl substituents of DIO-02, and despite that fact, DIO-09 was significantly more active than DIO-02 leading to the conclusion that not only the interactions with the electronic pair of the nitrogen is key for the activity and must be considered as well the hydrophobic interactions with non-cyclic aliphatic substituents like the terminal ethyl groups of DIO-09.



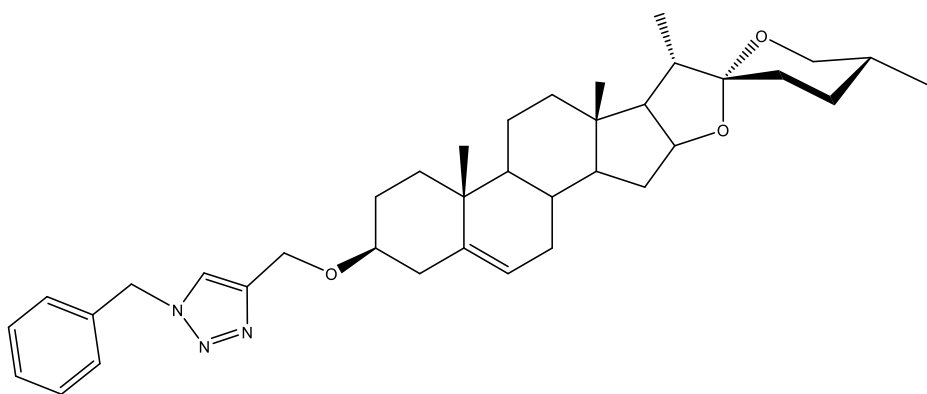
**Figure 76.** Active derivatives DIO-02 and DIO-09

Table 13. Antibacterial and antimycobacterial activities of diosgenin aminoether derivatives

Compound	Gram-negative clinical isolates MIC (µg/mL)						Gram-positive clinical isolates MIC (µg/mL)		
	CR A. <i>baumannii</i>	CR P. <i>aeruginosa</i>	ESBL E. <i>coli</i>	CCR K. <i>pneumoniae</i> NDM-1+	CCR K. <i>pneumoniae</i>	ESBL K. <i>pneumoniae</i>	VR E. <i>faecium</i>	MR S. <i>aureus</i>	LR S. <i>epidermidis</i>
DIO-01	>50	>50	>50	>50	>50	>50	>50	>50	>50
DIO-02	>50	>50	>50	>50	>50	>50	>50	<b>50</b>	>50
DIO-03	>50	>50	>50	>50	>50	>50	>50	>50	>50
DIO-04	>50	>50	>50	>50	>50	>50	>50	>50	>50
DIO-05	>50	>50	>50	>50	>50	>50	>50	>50	>50
DIO-06	>50	>50	>50	>50	>50	>50	>50	>50	>50
DIO-07	>50	>50	>50	>50	>50	>50	>50	>50	>50
DIO-08	>50	>50	>50	>50	>50	>50	>50	>50	>50
DIO-09	>50	>50	>50	>50	>50	>50	<b>12.5</b>	<b>12.5</b>	<b>25</b>
Diosgenin	>50	>50	>50	>50	>50	>50	>50	>50	>50
LEV	<b>12.5</b>	<b>3.125</b>	<b>25</b>	<b>50</b>	<b>50</b>	<b>1.15</b>	<b>6.25</b>	<b>6.25</b>	<b>12.5</b>

**CR:** carbapenem-resistant. **ESBL:** extended spectrum β-lactamase positive. **CCR:** carbapenem-resistant and broad spectrum cephalosporin. **VR:** vancomycin-resistant. **MR:** methicillin-resistant. **LR:** linezolid-resistant. **LEV:** levofloxacin. H37Rv: sensitive to first line drugs (rifampicin, isoniazid, ethambutol, streptomycin). **G122:** resistant to rifampicin, ethambutol, and streptomycin. **N.D.:** not determined

There are reports in the literature regarding the synthesis of antibacterial sapogenin derivatives, as the study conducted by Massod-ur-Ramman *et al.*, 2017<sup>56</sup> in which diverse N-benzyl substituted triazol derivatives (figure 77) were tested against ATCC gram-positive and gram negative bacteria, observing as result total inactivity against all the bacteria. None of the derivatives showed antibacterial activity must probably because of the steric effect caused by the aromatic ring present in the moiety, confirming the hypothesis that the free electron pair in the nitrogen must be free of steric impediments in order to collaborate in some degree to the antibacterial activity.



**Figure 77.** Triazolyl diosgenin derivative

Previously as part of the studies of the research group in which the present work was developed, lignan aminoether derivatives were synthesized using as starting material *meso*-dihydroguaiaretic acid, such derivatives were tested against the same drug-resistant clinical isolates<sup>57</sup>. The derivatives that possessed the same aminoether substituents as DIO-02 and DIO-09 (figure 78) were inactive against gram-positive and gram-negative bacteria, leading to the deduction that the aminoether moiety will effect efficiently its antibacterial activity depending of the scaffold from which is part. The diosgenin in the derivatives could possibly contribute

to the antibacterial activity wen is forming part of the aminoether, despite the fact that diosgenin is inactive by itself.

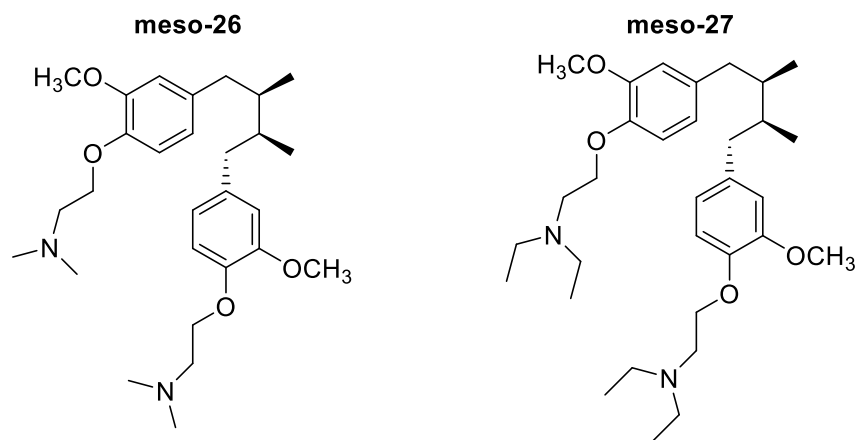


**Figure 78.** Lignan aminoether derivatives meso-26 and meso-27

## 6. CONCLUSIONS

1. The hexane extract of *S. chrysotrichum* is composed mainly of alkanes tritriacontane: 44.505 % and dotriacontane: 32.811 %.
2. The hexane extract of *S. chrysotrichum* possess good antibacterial activity against the gram-negative clinical isolates (CR) *A. baumannii* (MIC: 125 µg/mL), (CR) *P. aeruginosa* (MIC: 250 µg/mL), and the *M. tuberculosis* strains H37Rv and G122 (MIC: 250 µg/mL).
3. The dichloromethane extract of *S. chrysotrichum* is composed mainly of the alkanes tritriacontane (38.177 %), hexatriacontane (27.195 %), and the diterpenic alcohol phytol (20.992 %).
4. Dichloromethane extract of *S. chrysotrichum* possess good antibacterial activity against the gram-negative clinical isolates (CR) *A. baumannii* (MIC: 125 µg/mL) and (CR) *P. aeruginosa* (MIC: 250 µg/mL). The observed results lead to the conclusion that its constituent phytol confers antibacterial activity to this extract.
5. The methanol extract of *S. chrysotrichum* possess good antibacterial activity against the gram-negative clinical isolates (CR) *A. baumannii* (MIC: 125 µg/mL) and (CR) *P. aeruginosa* (MIC: 250 µg/mL).

6. The aqueous extract showed the lower antibacterial activity among all the tested extracts displaying MIC values of 500  $\mu\text{g/mL}$  against almost all the clinical isolates and was inactive against (CR) *A. baumannii* and (LR) *S. epidermidis*.

**7. This work represents the first report of good antibacterial activity of organic extracts of *S. chrysotrichum***, a relevant fact taking on count that all the bacterial clinical isolates tested, presented drug-resistance against the most used antibiotics in clinic. **This work represents the first report of good antitubercular activity of an organic extract of *S. chrysotrichum***, being the antitubercular extract the hexane extract. The newly reported antibacterial activities of the organic extracts is evidence that the studied plant could be a source of new antibacterial agents, and **further phytochemical studies with *S. chrysotrichum* must be performed for the sake of drug discovery.**

8. From the methanol extract of *S. chrysotrichum* has been isolated and structurally characterized the sterol campesterol- $\beta$ -D-glucoside, the phenolic compounds salicylic acid and 3'-O-methyl-quercetin-3-O- $\beta$ -D-glucopyranoside, the new steroidal saponins SC5A and SC5B, and the previously reported steroidal saponin SC5C. **This work represents the first report of the new *neo*-spirostanic steroidal saponins** 6- $\alpha$ -O- $\alpha$ -L-rhamnopyranosyl-(1 $\rightarrow$ 3)- $\beta$ -D-quinovopyranosyl-(23R,25S)-5 $\alpha$ -spirostan-3 $\beta$ ,23 $\beta$ -ol (SC5B) and 6- $\alpha$ -O- $\alpha$ -L-rhamnopyranosyl-(1 $\rightarrow$ 3)- $\beta$ -D-quinovopyranosyl-(25S)-5 $\alpha$ -spirostan-3 $\beta$ -ol (SC5A). The afore mentioned



compounds **represents the first report of the presence of neo-spirostanic saponins in *S. chrysotrichum*.**

9. **This work represents the first report of antibacterial activity for the known saponin 6- $\alpha$ -O- $\beta$ -D-xylopyranosyl-(1 $\rightarrow$ 3)- $\beta$ -D-quinovopyranosyl-(23R,25S)-5 $\alpha$ -spirostan-3 $\beta$ ,23 $\beta$ -ol (SC5C), possessing the same activity than the control drug levofloxacin (MIC 12.5 mg/mL) against linezolid-resistant *S. epidermidis*.** After the chemical structure-biological activity analysis described in the present work, it can be concluded that the substitution pattern and relative configuration in the spirostanic ring of a saponin it's not a critical factor that affect the antibacterial activity, however the composition of the sugar moiety it is critical for the attribution of antibacterial activity of a saponin.

10. It is concluded that the presence of the sugar moiety 6- $\alpha$ -O- $\beta$ -D-xylopyranose in the saponin SC5C is the responsible factor of the attribution of antibacterial activity in the compound.

11. **The project hypothesis is partially accepted**, because of compound SC5C being a constituent of *S. chrysotrichum* as active as the positive control drug levofloxacin, however it wasn't possible to confirm if the derivatization of the hydrolysis product of this type of saponins improves its antibacterial activity, due to the difficulties in the isolation and purification of the aglycones.

12. The acid hydrolysis of the steroidal saponins of *S. chrysotrichum* is not suitable for the isolation of sapogenins. It is concluded that only by enzymatic methods can be possibly be obtained the desired sapogenins with a good quality to be used as starting materials for synthesis of aminoether derivatives.

13. The Williamson ether synthesis resulted suitable for the synthesis of aminoether derivatives, and the recovery of the products and starting material as pure compounds was possible as well. It can be concluded that the steroidal sapogenins can be considered as acceptable starting material for semi-synthesis of new compounds.

14. The antibacterial activity of the only active diosgenin aminoether derivatives, DIO-02 and DIO-09 was two-fold less effective against gram-positive bacteria than the control drug levofloxacin, however, taking on count that the starting material diosgenin was inactive, it can be concluded that the antibacterial activity of sapogenins could be enhanced by derivatization, thus making worthy the attempt of isolation of steroidal sapogenins of *S. chrysotrichum*, as perspective for the project.

15. It can be concluded that the small modulations like N,N-dimethylethylamine and N,N-diethylethylamine enhance the antibacterial activity of sapogenin derivatives due to their hypothetical availability for interaction with the unknown pharmacological target in the bacteria. Bulky aminoethers are not suitable to enhance the antibacterial activity of sapogenins.

## 7. PERSPECTIVES

1. To isolate and characterize the compounds from the dichloromethane extract of *S. chrysotrichum* in order to determine its major antibacterial compound, and to explore the possibility of the isolation of precursor sapogenins of the steroidal saponins SC5A, SC5B and SC5C.
2. To determine by molecular docking if it's possible that saponins possessing xylose like SC5C could interact with efflux pumps like the AedC, CraA, AdeB, AdeG, and AdeJ efflux pumps, which are present in gram-negative drug resistant bacteria like *A. baumannii* and *P. aeruginosa*, in order to explore the possibility of using SC5C as a synergistic agent with others antibiotics against gram-negative bacteria.
3. To determine by molecular docking if it's possible that saponins possessing xylose like SC5C could interact with efflux pumps like the members of the MFS family, like the efflux pump NorA of *S. aureus*, in order to define the grade of affinity for this type of bacterial proteins and explore if this is the possible pharmacological target of SC5.
4. To determine the cytotoxicity of the steroidal saponins of *S. chrysotrichum* against cancer cell lines and the Vero cell line
5. To implement an enzymatic hydrolysis procedure to obtain steroidal sapogenins from *S. chrysotrichum* steroidal saponins.

## 8. REFERENCES

- (1). World Health Organization (WHO). Antimicrobial Resistance Global Report on Surveillance. ISBN 978 92 4 156474 8. **(2014)**.
- (2). Organización Mundial de la Salud (OMS). Plan de acción mundial sobre la resistencia a los antimicrobianos. ISBN 978 92 4 350976 1. **(2016)**.
- (3). World Health Organization (WHO). Global antimicrobial resistance surveillance system (GLASS) report: early implementation 2016-2017. CC BY-NC-SA 3.0 IGO. **(2017)**.
- (4). World Health Organization (WHO). Global priority list of antibiotic-resistant bacteria to guide research, Discovery, and development of new antibiotics. **(2017)**.
- (5). World Health Organization (WHO). Global Tuberculosis Report 2020. **(2020)**.
- (6). Newman, D.J., Cragg, G.M., Snader, K.M. The influence of natural products upon drug Discovery. *Nat Prod Rep.* 17(3):215-34. 17; 215-234. DOI: 10.1039/a902202c. **(2020)**.
- (7). Ahendra, J. Ethnomedical herbs and various approaches in development of new drugs. *World J. Pharm. Res.* 5: 869-876. **(2015)**.

- (8). Fridlender, M., Kapulnik, Y., Koltai, H. Plant derived substances with anti-cancer activity: from folklore to practice. *Front. Plant Sci.* 6: 799. DOI: doi.org/10.3389/fpls.2015.00799. **(2015)**.
- (9). Cowan, M.M. Plant Products as Antimicrobial Agents. *Clin Microbiol Rev.* 12 (4): 564-82. **(1999)**.
- (10). Rzedowski, G.C., Rzedowski, J. Flora fanerogámica del Valle de México. 2a ed. Instituto de Ecología y Comisión Nacional para el Conocimiento y Uso de la Biodiversidad. **(2001)**.
- (11). Mwanzia, N.J., Appiah-Opong, R., Nyarko, A.K., Yeboah-Manu, D., Addo, P.G.A. Medicinal plants used to treat TB in Ghana. *Int J Mycobacteriol.* DOI: 10.1016/j.ijmyco.2015.02.003. 4:116 –123. **(2015)**.
- (12). Mwanzia, N.J., Appiah-Opong, R., Nyarko, A.K., Yeboah-Manu, D., Addo, P., Otchere, I., Twuma, A. *In vitro* antimycobacterial and cytotoxic data on medicinal plants used to treat tuberculosis. *Data in Brief.* 7:1124–1130. **(2016)**.
- (13). Mohamad, S., Zin, N.M., Wahab, H.A., Ibrahim, P., Sulaiman, S.F., Zahariluddin, A.S.M. Antituberculosis potential of some ethnobotanically selected Malaysian plants, J. *Ethnopharmacol.* 133: 1021–1026. DOI: 10.1016/j.jep.2010.11.037 **(2011)**.

(14). Lozoya, X., Navarro, V., García, M., Zurita M. *Solanum Chrysotrichum* (Schldl) a plant used in Mexico for the treatment of skin micosis. *J. Ethnopharmacol.* 36: 127-132. DOI: 10.1016/0378-8741(92)90011-f. **(1992)**.

(15). Herrera-Arellano, A., Jiménez-Ferre., E., Zamilpa, A., Martínez-Rivera, M.A., Rodríguez-Tovar, A.V., Herrera-Alvarez, S., Salas-Andonaegui, M.L., Nava-Xalpa, M.Y., Méndez-Salas, A., Tortoriello, J. Exploratory Study on the Clinical and Mycological Effectiveness of a Herbal Medicinal Product from *Solanum chrysotrichum* in Patients with Candida Yeast-Associated Vaginal Infection. *Planta Med.* 75: 466–471. **(2009)**.

(16). Aguilar-Santamaría, L., Herrera-Arellano, A., Zamilpa, A., Alonso-Cortés, D., Jiménez-Ferrer, E., Tortoriello, J., Zúñiga-González, G. Toxicology, genotoxicity, and cytotoxicity of three extracts of *Solanum chrysotrichum*. *J. Ethnopharmacol.* 150: 275–279. **(2013)**.

(17). Niño, J., Correa, Y.M., Mosquera, O.M. Biological activities of steroidal alkaloids isolated from *Solanum leucocarpum*. *Pharmaceutical Biology.* 47:3, 255-259. **(2009)**.

(18). Chagnon, F., Guay, I., Bonin, M.A., Mitchell, G., Bouarab, K., Malouin, F., Marsault, É. Unraveling the structure-activity relationship of tomatidine, a steroid

alkaloid with unique antibiotic properties against persistent forms of *Staphylococcus aureus*. **Eur J Med Chem.**10:80: 605-20. **(2014)**.

(19). Moreira, R.R., Martins, G.Z., Magalhães, N.O., Almeida, A.E., Pietro, R.C., Silva, F.A., Cicarelli, R.M. *In vitro* trypanocidal activity of solamargine and extracts from *Solanum palinacanthum* and *Solanum lycocarpum* of Brazilian cerrado. *An Acad Bras Cienc.* 85(3): 903-7. **(2013)**.

(20). Milner, S.E., Brunton, N.P., Jones, P.W., O' Brien, N.M., Collins, S.G., Maguire, A.R. Bioactivities of Glycoalkaloids and their Aglycones from *Solanum Species*. *J. Agric. Food Chem.* 59, 3454–3484. **(2011)**.

(21). González, M., Zamilpa, A., Marquina, S., Navarro, V., Alvarez. L., Antimycotic Spirostanol Saponins from *Solanum hispidum* Leaves and Their Structure-Activity Relationships. *J. Nat. Prod.* (67): 938-941. DOI: 10.1021/np0305019. **(2004)**.

(22). Salimon, J., Mudhaffar, B., Salih, A., Salih, N.. Hydrolysis optimization and characterization study of preparing fatty acids from *Jatropha curcas* seed oil. *Chem Cent J.* (5): 67. DOI: 10.1186/1752-153X-5-67. **(2011)**.

(23). Zamilpa, A., Tortoriello, J., Navarro, V., Delgado, G., Alvarez, L. Five New Steroidal Saponins from *Solanum chrysotrichum* Leaves and Their Antimycotic Activity. *J. Nat. Prod.* 65, 1815-1819. **(2002)**.

(24). Tava, A., Biazzi, E., Mella, M., Quadrelli, P., Avato, P. Artefact formation during acid hydrolysis of saponins from *Medicago spp.* *Phytochem.* 138: 116-127. **(2017)**.

(25). Laszlo, K., Czako, B. Strategic Applications of Named Reactions in Organic Synthesis: Background and Detailed Mechanisms. *Elsevier Academic Press*. ISBN: 0-12-429785-4. First edition, pp 484. **(2005)**.

(26). Zgoda, J.R., Porter, J.R. A convenient microdilution method for screening natural products against bacteria and fungi. *Pharm Biol.* 2939:221-225. **(2001)**.

(27). Franzblau, S.G., Witzig, R.S., McLaughlin, J.C., Torres, P., Madico, G., Hernandez, A., Degnan, M.T., Cook, M.B., Quenzer, V.K., Ferguson, R.M., Gilman, R.H. Rapid, low-technology MIC determination with clinical *Mycobacterium tuberculosis* isolates by using microplate Alamar Blue assay. *J.Clin. Microbiol.* 36 (2): 362-366. **(1998)**.

(28). Favela-Hernández, J.M.J., García, A., Garza-González, E., Rivas-Galindo, V.M., Camacho-Corona, M.R. Antibacterial and antimycobacterial Lignans and Flavonoids from *Larrea tridentata*. *Phytother. Res.* 26: 1957-1960. **(2012)**.

(29). Mikenda, W., Steinwender, E., Mereiter, K. Hydrogen Bonding in 2-Hydroxybenzoic, 2-Hydroxythiobenzoic, and 2-Hydroxydithiobenzoic Acid. A Structural and Spectroscopic Study. *Monatshefte ffor Chemie.* 126: 495-504. **(1995)**.



(30). Sigala, P.A., Ruben, E.A., Liu, C.W., Piccoli, P.M.B., Hohenstein, E.G., Martínez, T.J., Schultz, A.J., Herschlag, D. Determination of Hydrogen Bond Structure in Water versus Aprotic Environments to Test the Relationship Between Length and Stability. *J. Am. Chem. Soc.* 137 (17): 5730–5740. **(2015)**.

(31). Chen, C., Shyu, S.F. Conformers and intramolecular hydrogen bonding of the salicylic acid monomer and its anions. *Theochem.* 536: 25-39. **(2001)**.

(32). Human metabolome database.

([http://www.hmdb.ca/spectra/nmr\\_one\\_d/1788](http://www.hmdb.ca/spectra/nmr_one_d/1788)). Consulted 28/05/2019.

(33). Drugbank. ([https://www.drugbank.ca/spectra/nmr\\_one\\_d/2407](https://www.drugbank.ca/spectra/nmr_one_d/2407)). Consulted 28/05/2019.

(34). Jung-Min, C., Eun-Ok, L., Hyo-Jung, L., Kwan-Hyun, K., Kyoo-Seok, A., Bum-Sang S., Nam-II, K., Myoung-Chong, S., Nam-In, B., Sung-Hoon, K. Identification of Campesterol from *Chrysanthemum coronarium* L. and its antiangiogenic activities. *Phytother. Res.* 21, 954–959. **(2007)**.

(35). Panawan, S., Watcharapong, C., Sugunya, M., Suwaporn, L., Somsuda, T., Vijittra, L. Structures of Phytosterols and Triterpenoids with Potential Anti-Cancer Activity in Bran of Black Non-Glutinous Rice. *Nutrients.* 7, 1672-1687. **(2015)**.

(36). Agrawal, P.K., Jain, D.C., Gufta, R.K., Takur, R.S. Carbon-13 NMR spectroscopy of steroidal sapogenins and steroidal saponins. *Phymchemisfry*, (24):11, 2479-2496. **(1985)**.

37. Chakravarty, A.K., Pakrashi, S.C., Uzawa, J. 13C nuclear magnetic resonance spectra of 23-hydroxy spirostane sapogenins of *Solanum hispidum*. *J. Can. J. Chem.* (59): 1328-1330. DOI: 10.1139/v81-195. **(1981)**.

(38). Chakravarty, A.K., Saha, C.R., Pakrash, S.C. New spirostanic saponins and sapogenins from *Solanum hispidum* seeds. *Phytochemistry*. (8). 902-903. **(1979)**.

(39). Hilbert, G., Temsamani, H., Bordenave, L., Pedrot, E., Chaher, N., Cluzet, Jean, S., Delaunay, C., Ollat, N., Delrot, S., Mérillon, J.M., Gomès, E., Richard, T. Flavonol profiles in berries of wild *Vitis* accessions using liquid chromatography coupled to mass spectrometry and nuclear magnetic resonance spectrometry. *Food Chem.* 169 49–58. **(2015)**.

(40). Aliero, A.A., Asekun, O.T., Grierson, D.S., Afolayan, A.J. Chemical composition of the hexane extract from the leaves of *Solanum pseudocapsicum*. *A.J. Afolayan*. 5 (6): 1054-1056. **(2006)**.

(41). Venkatesh, R., Vidya, R., Kalaivani, K. Gas chromatography and mass spectrometry analysis of *Solanum villosum* (Mill) (Solanaceae). *IJPSR*. 5 (12).

**(2014).**

(42). Naimon, N., Pongchairerk, U., Suebkhampet, A. Phytochemical Analysis and antibacterial activity of ethanolic leaf extract of *Solanum torvum* Sw. Against pathogenic bacteria. *Kasetsart J. (Nat. Sci.)*. 49: 516 – 523. **(2015)**.

(43). Lee, W., Woo, E.R., Lee, D.G. Phytol has antibacterial property by inducing oxidative stress response in *Pseudomonas aeruginosa*. *Journal Free Radic. Resear.* 50 (12). DOI: 10.1080/10715762.2016. **(2016)**.

(44). Goto, T., Takahashi, N., Kato, S., Egawa, K., Ebisu, S., Moriyama, T., Fushiki, T., Kawada, T. Phytol directly activates peroxisome proliferator-activated receptor  $\alpha$  (PPAR $\alpha$ ) and regulates gene expression involved in lipid metabolism in PPAR $\alpha$ -expressing HepG2 hepatocytes. *Biochem Biophys Res Commun.* 18;337(2):440-5. DOI: 10.1016/j.bbrc.2005.09.077. **(2005)**.

(45). Steinberg, D., Avigan, J., Mize, C.E., Baxter, J.H., Cammermeyer, J., Fales, H.M., Highet, P.F. Effects of dietary phytol and phytanic acid in animals. *J. Lipid Res.* 7. **(1966)**.

(46). Sharma, R.K. Phytosterols: wide-spectrum antibacterial agents. *Bioorg. Chem.* 21 (1): 49-60. **(1993)**.

(47). Velasco-Lezama, R., Tapia-Aguilar, R., Ortiz Monroy, M.V., Hernández-Pérez, E., Vega-Avila, E., Espejo-Serna, A. Effect of *Solanum chrysotrichum* Schldl on cell proliferation *in vitro*. *IJPSR*. 9 (6). **(2018)**.

(48). Vieyra, J.G.M., Quintino, R.C., Souza, R.T., Hiruma, L.C.A., Vilegas, W. New steroidal saponins and antiulcer activity from *Solanum paniculatum* L. *Food Chem*. 186: 160-167. **(2015)**.

(49). Bhoj Raj Singh. Antibacterial Activity of Glycerol, Lactose, Maltose, Mannitol, Raffinose and Xylose. Noto-are 17223318: *Medicine*. (7): 19. **(2014)**.

(50). Villagra, N.A., Fuentes, J.A., Jofré, M.R., Hidalgo, A.A., Garcia, P., Mora, G.C. The carbon source influences the efflux pump-mediated antimicrobial resistance in clinically important Gram-negative bacteria. *J Antimicrob Chemother*. (67): 921–927. **(2012)**.

(51). Hidalgo, A.A., Arias, A.J., Fuentes, J.A., García-Guido, P., Mora, C., Villagra, N.A. Xylose Improves Antibiotic Activity of Chloramphenicol and Tetracycline against *K. pneumoniae* and *A. baumannii* in a Murine Model of Skin Infection. *J Infect Dis Medical Microbiol*. (2018): 6. DOI: 10.1155/2018/3467219. **(2018)**.

(52). Puri, R., Wong, T.C., Puri, R.K. Solasodine and Diosgenin:  $^1\text{H}$  and  $^{13}\text{C}$  Assignments by Two-Dimensional NMR Spectroscopy. *Magn. Reson. Chem.* (31): 278. **(1993)**.

(53). Han, X.W., Yu, H., Liu, X.M., Bao, X., Yu, B., Li, C., Hui, Y.Z. Complete  $^1\text{H}$  and  $^{13}\text{C}$  NMR assignments of diosgenyl saponins. *Magn. Reson. Chem.* (37): 140. **(1999)**.

(54). Piresa, V.S., Taketab, A.T.C., Gosmanna, G., Schenkel, E.P. Saponins and Sapogenins from *Brachiaria decumbens* Stapf. *J. Braz. Chem. Soc.* (13) 2: 135-139. **(2002)**.

(55). Spectral database for organic compounds (SDBS). [https://sdb.sdb.aist.go.jp/sdb/cgi-bin/direct\\_frame\\_top.cgi](https://sdb.sdb.aist.go.jp/sdb/cgi-bin/direct_frame_top.cgi). Accessed in October 2020.

(56). Masood-ur-Ramman, U.R., Bhat, K.A., Ara, T. Synthesis and antimicrobial activity of triazolyl analogs of diosgenin. *J. Phytopharmacol.* 6(4):227-233. **(2017)**.

(57). Reyes-Melo, M.K., García, A., Romo-Mancillas, A., Garza-González, E., Rivas-Galindo, V.M., Miranda, L.D., Vargas-Villarreal, J., Favela-Hernández, J.M.J

Camacho-Corona, M.R. *meso*-Dihydroguaiaretic acid derivatives with antibacterial and antimycobacterial activity. *Bioorg. Med Chem.* 25: 5247–5259. **(2017)**.

## APPENDIX A

Mass spectrums of steroidal saponins SC5A, SC5B and SC5C and its corresponding acetylated derivatives SC5AcA, SC5AcB and SC5AcC

Formula Predictor Report - 34-SC5A\_2019-10-23.lcd

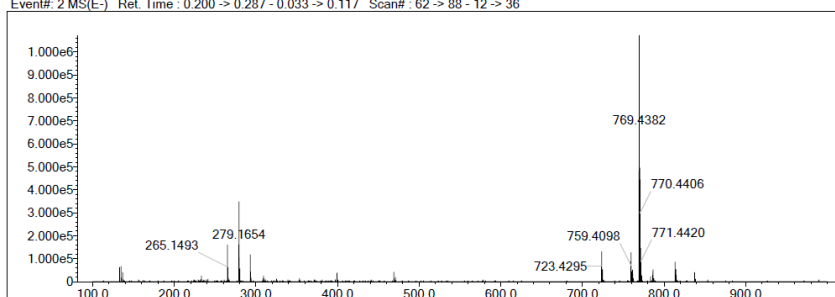
Page 1 of 1

Data File: D:\Recherche\ThalassOMICS\IICIMED\34-SC5A\_2019-10-23.lcd

Elmt	Val.	Min	Max	Elmt	Val.	Min	Max	Elmt	Val.	Min	Max	Use Adduct
H	1	0	300	O	2	0	15	Cl	1	0	3	H
C	4	0	150	F	1	0	3					HCOO
N	3	0	10	S	2	0	3					

Error Margin (mDa): 5.0      DBE Range: -2.0 - 1000.0      Electron Ions: both  
 HC Ratio: unlimited      Apply N Rule: yes      Use MSn Info: yes  
 Max Isotopes: all      Isotope RI (%): 1.00      Isotope Res: 8000  
 MSn Iso RI (%): 75.00      MSn Logic Mode: AND      Max Results: 50

Event#: 2 MS(E-) Ret. Time : 0.200 -> 0.287 - 0.033 -> 0.117 Scan#: 62 -> 88 - 12 -> 36



Rank	Score	Formula (M)	Ion	Meas. m/z	Pred. m/z	Df. (mDa)	Df. (ppm)	Iso	DBE
20	62.96	C39 H64 O12	[M-H]-	723.4295	723.4325	-3.0	-4.15	68.34	8.0

Formula Predictor Report - 34-SC5A\_2019-10-23.lcd

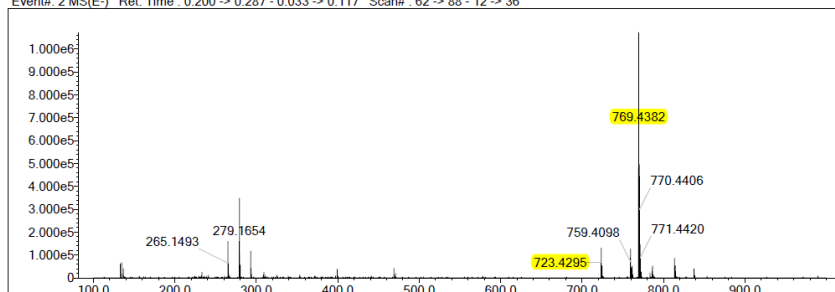
Page 1 of 1

Data File: D:\Recherche\ThalassOMICS\IICIMED\34-SC5A\_2019-10-23.lcd

Elmt	Val.	Min	Max	Elmt	Val.	Min	Max	Elmt	Val.	Min	Max	Use Adduct
H	1	0	300	O	2	0	15	Cl	1	0	3	H
C	4	0	150	F	1	0	3					HCOO
N	3	0	10	S	2	0	3					

Error Margin (mDa): 5.0      DBE Range: -2.0 - 1000.0      Electron Ions: both  
 HC Ratio: unlimited      Apply N Rule: yes      Use MSn Info: yes  
 Max Isotopes: all      Isotope RI (%): 1.00      Isotope Res: 8000  
 MSn Iso RI (%): 75.00      MSn Logic Mode: AND      Max Results: 50

Event#: 2 MS(E-) Ret. Time : 0.200 -> 0.287 - 0.033 -> 0.117 Scan#: 62 -> 88 - 12 -> 36



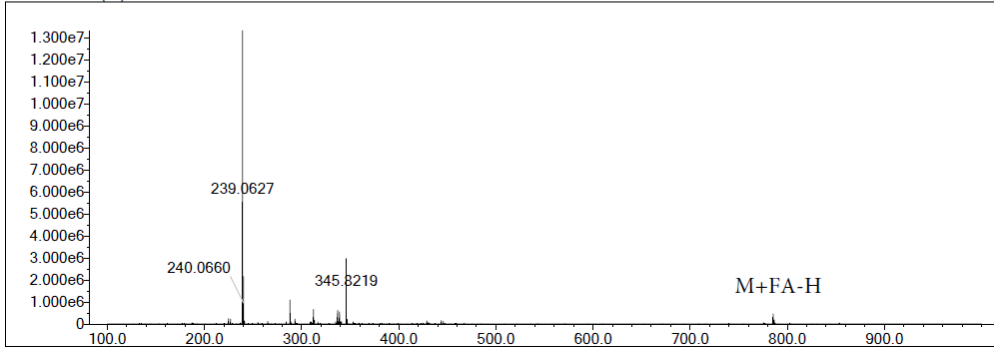
Rank	Score	Formula (M)	Ion	Meas. m/z	Pred. m/z	Df. (mDa)	Df. (ppm)	Iso	DBE
4	100.00	C39 H64 O12	[M+HCOO]-	769.4382	769.4380	0.2	0.26	100.00	8.0

Data File: D:\Recherche\ThalassOMICS\IICIMED\35-SC5B\_2019-10-23.lcd

Elmt	Val.	Min	Max	Elmt	Val.	Min	Max	Elmt	Val.	Min	Max	Use Adduct
H	1	0	300	O	2	0	15	Cl	1	0	3	H
C	4	0	150	F	1	0	3					HCOO
N	3	0	10	S	2	0	3					

Error Margin (mDa): 5.0      DBE Range: -2.0 - 1000.0      Electron Ions: both  
 HC Ratio: unlimited      Apply N Rule: yes      Use MSn Info: yes  
 Max Isotopes: all      Isotope RI (%): 1.00      Isotope Res: 8000  
 MSn Iso RI (%): 75.00      MSn Logic Mode: AND      Max Results: 50

Event#: 2 MS(E-) Ret. Time : 0.207 -> 0.240 Scan#: 64 -> 74



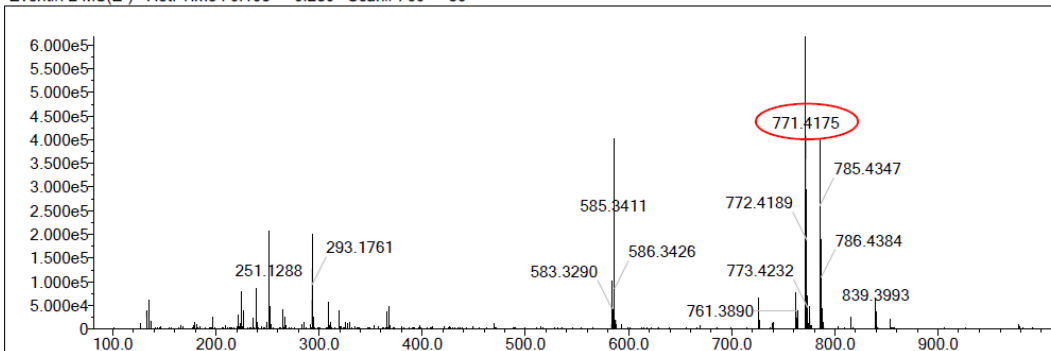
Rank	Score	Formula (M)	Ion	Meas. m/z	Pred. m/z	Df. (mDa)	Df. (ppm)	Iso	DBE
18	75.09	C39 H64 O13	[M+HCOO]-	785.4337	785.4329	0.8	1.02	75.13	8.0

Data File: C:\LabSolutions\Data\Data for all - MMS\Thalassomics\IICIMED\Data\2019-10-23\36-SC5C\_2019-10-23.lcd

Elmt	Val.	Min	Max	Elmt	Val.	Min	Max	Elmt	Val.	Min	Max	Elmt	Val.	Min	Max	Use Adduct
H	1	0	250	F	1	0	0	S	2	0	0	Br	1	0	0	H
2H	1	0	0	Na	1	0	0	Cl	1	0	3	I	3	0	0	HCOO
C	4	1	100	Mg	2	0	0	Ca	2	0	0					CH3O
N	3	0	10	Si	4	0	0	Ti	2	0	0					H2
O	2	0	50	P	3	0	0	Fe	2	0	0					

Error Margin (ppm): 10      DBE Range: 0.0 - 20.0      Electron Ions: both  
 HC Ratio: 0.0 - 5.0      Apply N Rule: yes      Use MSn Info: no  
 Max Isotopes: all      Isotope RI (%): 1.00      Isotope Res: 8000  
 MSn Iso RI (%): 5.00      MSn Logic Mode: AND      Max Results: 100

Event#: 2 MS(E-) Ret. Time : 0.193 -> 0.280 Scan#: 60 -> 86



Rank	Score	Formula (M)	Ion	Meas. m/z	Pred. m/z	Df. (mDa)	Df. (ppm)	Iso	DBE
7	97.19	C38 H62 O13	[M+HCOO]-	771.4175	771.4172	0.3	0.39	97.19	8.0



Data File: C:\LabSolutions\Data\Data for all - MMS\Thalassomics\ISCIIMED\Data\2019-11-04\37-SC5AcA\_2019-11-04.lcd

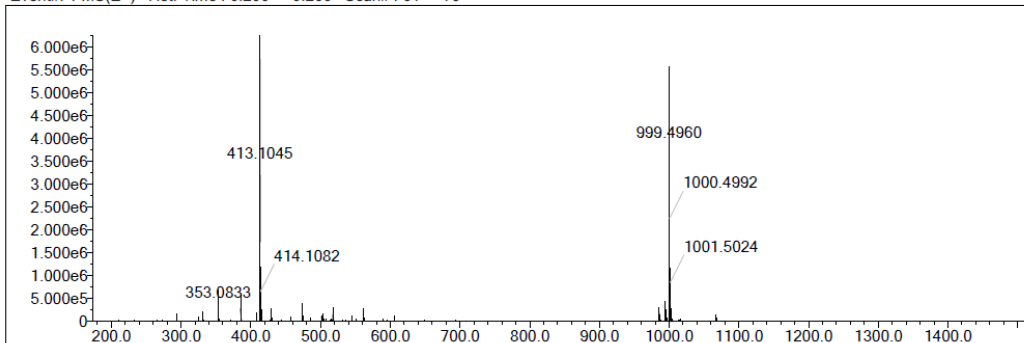
Elmt	Val.	Min	Max	Elmt	Val.	Min	Max	Elmt	Val.	Min	Max	Elmt	Val.	Min	Max	Use Adduct
H	1	0	150	F	1	0	0	S	2	0	0	Br	1	0	0	H
2H	1	0	0	Na	1	0	0	Cl	1	0	3	I	3	0	0	Na
C	4	1	100	Mg	2	0	0	Ca	2	0	0					
N	3	0	100	Si	4	0	0	Ti	2	0	0					
O	2	0	50	P	3	0	0	Fe	2	0	0					

Error Margin (ppm): 10  
 HC Ratio: 0.0 - 5.0  
 Max Isotopes: all  
 MSn Iso RI (%): 5.00

DBE Range: 0.0 - 20.0  
 Apply N Rule: yes  
 Isotope RI (%): 1.00  
 MSn Logic Mode: AND

Electron Ions: both  
 Use MSn Info: no  
 Isotope Res: 8000  
 Max Results: 100

Event#: 1 MS(E+) Ret. Time : 0.200 -> 0.260 Scan# : 61 -> 79



Rank	Score	Formula (M)	Ion	Meas. m/z	Pred. m/z	Df. (mDa)	Df. (ppm)	Iso	DBE
3	93.50	C51 H76 O18	[M+Na] <sup>+</sup>	999.4960	999.4924	3.6	3.60	100.00	14.0

Data File: C:\LabSolutions\Data\Data for all - MMS\Thalassomics\ISCIIMED\Data\2019-11-04\38-SC5AcB\_2019-11-04.lcd

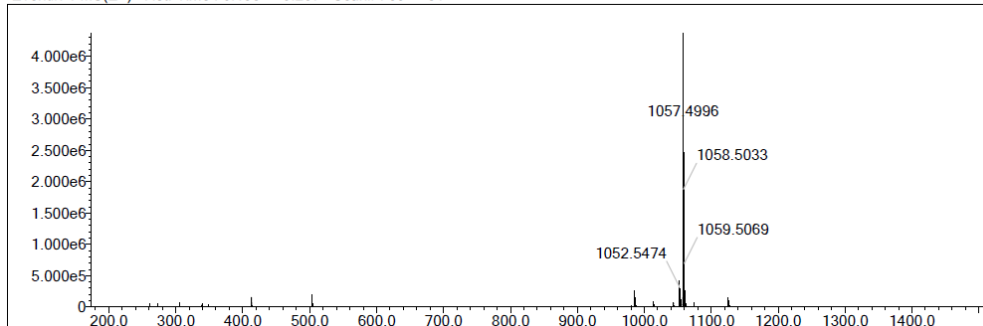
Elmt	Val.	Min	Max	Elmt	Val.	Min	Max	Elmt	Val.	Min	Max	Elmt	Val.	Min	Max	Use Adduct
H	1	0	150	F	1	0	0	S	2	0	0	Br	1	0	0	H
2H	1	0	0	Na	1	0	0	Cl	1	0	3	I	3	0	0	Na
C	4	1	100	Mg	2	0	0	Ca	2	0	0					
N	3	0	100	Si	4	0	0	Ti	2	0	0					
O	2	0	50	P	3	0	0	Fe	2	0	0					

Error Margin (ppm): 10  
 HC Ratio: 0.0 - 5.0  
 Max Isotopes: all  
 MSn Iso RI (%): 5.00

DBE Range: 0.0 - 20.0  
 Apply N Rule: yes  
 Isotope RI (%): 1.00  
 MSn Logic Mode: AND

Electron Ions: both  
 Use MSn Info: no  
 Isotope Res: 8000  
 Max Results: 100

Event#: 1 MS(E+) Ret. Time : 0.193 -> 0.267 Scan# : 59 -> 81



Rank	Score	Formula (M)	Ion	Meas. m/z	Pred. m/z	Df. (mDa)	Df. (ppm)	Iso	DBE
1	95.31	C53 H78 O20	[M+Na] <sup>+</sup>	1057.4996	1057.4979	1.7	1.61	96.79	15.0

Data File: C:\LabSolutions\Data\Data for all - MMS\Thalassomics\ISCIIMED\Data\2019-11-04\39-SC5AcC\_2019-11-04.lcd

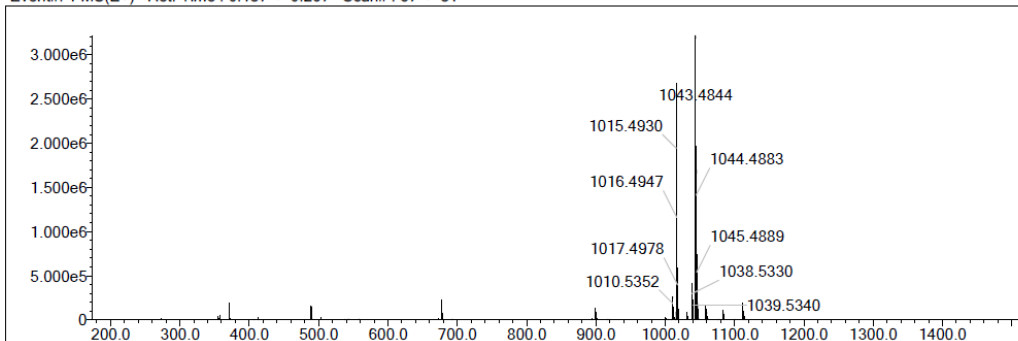
Elmt	Val.	Min	Max	Elmt	Val.	Min	Max	Elmt	Val.	Min	Max	Elmt	Val.	Min	Max	Use Adduct
H	1	0	150	F	1	0	0	S	2	0	0	Br	1	0	0	H
2H	1	0	0	Na	1	0	0	Cl	1	0	3	I	3	0	0	Na
C	4	1	100	Mg	2	0	0	Ca	2	0	0					
N	3	0	100	Si	4	0	0	Ti	2	0	0					
O	2	0	50	P	3	0	0	Fe	2	0	0					

Error Margin (ppm): 10  
 HC Ratio: 0.0 - 5.0  
 Max Isotopes: all  
 MSn Iso RI (%): 5.00

DBE Range: 0.0 - 20.0  
 Apply N Rule: yes  
 Isotope RI (%): 1.00  
 MSn Logic Mode: AND

Electron Ions: both  
 Use MSn Info: no  
 Isotope Res: 8000  
 Max Results: 100

Event#: 1 MS(E+) Ret. Time : 0.187 -> 0.267 Scan# : 57 -> 81



Rank	Score	Formula (M)	Ion	Meas. m/z	Pred. m/z	Df. (mDa)	Df. (ppm)	Iso	DBE
3	97.22	C52 H76 O20	[M+Na] <sup>+</sup>	1043.4844	1043.4822	2.2	2.11	100.00	15.0

## APPENDIX B

Certificate of attendance as oral communicator in the Journée Recherche 2019 at  
the Université de Nantes



UFR DES SCIENCES PHARMACEUTIQUES  
EA 2160 - MMS  
MER MOLECULES SANTE

Pr. Olivier GROVEL  
*Professor of pharmacognosy*  
Faculty of Pharmacy  
*Vice-Dean for Research*  
Research group Sea, Molecules and Health, MMS – EA2160  
*Head of Marine Fungi Group*  
Faculty of Pharmaceutical and Biological Sciences  
University of Nantes  
9, rue Bias BP61112  
44035 Nantes cedex 1  
email : olivier.grovel@univ-nantes.fr

### CERTIFICATE OF ATTENDANCE

This is to certify that Guillermo NUNEZ MOJICA has attended the seminar entitled « Journée Recherche 2019 de l'UFR des Sciences Pharmaceutiques et Biologiques de l'Université de Nantes » given the 21st of November 2019 in Nantes, France.

During this conference, Guillermo NUNEZ MOJICA was invited to give an oral presentation of his research works entitled "Antifungal steroid saponins from *Solanum chrysotrichum*, an interesting source for antibacterial natural products and derivatives".

Nantes,

June 19<sup>th</sup> 2020

Vice-Doyen Recherche et Valorisation  
Faculté de Pharmacie de Nantes

Professeur Olivier GROVEL

Pr Olivier Grovel

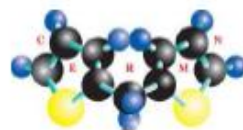


Secrétariat  
Faculté de Pharmacie - 9, rue Bias - BP 59506 - 44035 NANTES-CEDEX 01 - FRANCE  
☎Fax: 02-53-48-41-06  
Laboratoires  
ISOmer - Campus Sciences - 2 rue de la Houssinière - BP 92206 - 44322 NANTES Cedex 3

## APPENDIX C

Certificate of attendance as oral communicator in the Young Research Fellow

Meeting 2020 at the Université de Caen Normandie

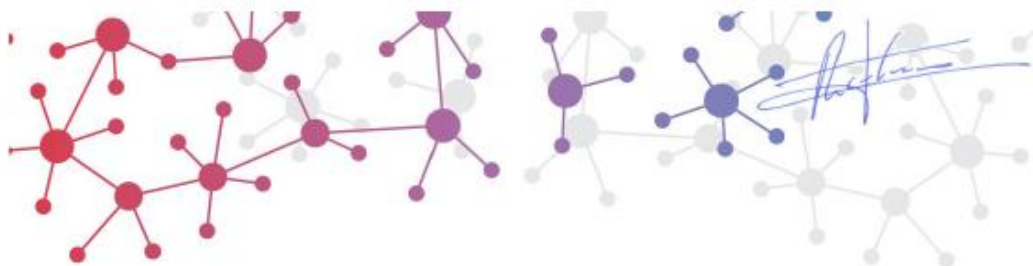


### Certificate of Attendance

This is to certify that Guillermo Núñez Mojica attended the 27th Young Research Fellow Meeting held in Caen, France on January 29 – 31, 2020 and presented an oral communication entitled « Antibacterial and antimycobacterial activities of extracts and steroid saponins from *Solanum chrysotrichum* ».

On behalf of the organising committee.

Prof. Christophe Rochais



## APPENDIX D

Front page of the publication derived of the thesis work

Author's personal copy

Medicinal Chemistry Research  
https://doi.org/10.1007/s00044-020-02648-8

MEDICINAL  
CHEMISTRY  
RESEARCH

ORIGINAL RESEARCH



### Antimicrobial and antileishmanial activities of extracts and some constituents from the leaves of *Solanum chrysotrichum* Schldl

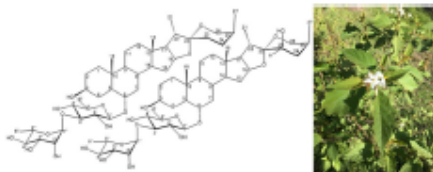
Guillermo Núñez-Mojica<sup>1</sup> · Verónica M. Rivas-Galindo<sup>2</sup> · Elvira Garza-González<sup>3</sup> · Luis D. Miranda<sup>4</sup> · Adriana Romo-Pérez<sup>4</sup> · Fabrice Pagniez<sup>5</sup> · Carine Picot<sup>5</sup> · Patrice Le Pape<sup>5</sup> · Marc-Antoine Bazin<sup>5</sup> · Pascal Marchand<sup>5</sup> · María del Rayo Camacho-Corona<sup>6</sup>

Received: 3 August 2020 / Accepted: 6 October 2020  
© Springer Science+Business Media, LLC, part of Springer Nature 2020

#### Abstract

Three organic extracts were prepared from the leaves of *Solanum chrysotrichum* Schldl. From the methanol extract were isolated two new steroidal saponins (1, 2), and three known compounds (3, 4, and 5). The new saponins were elucidated as 6- $\alpha$ -O- $\alpha$ -L-rhamnopyranosyl-(1  $\rightarrow$  3)- $\beta$ -D-quinovopyranosyl-(25S)-5 $\alpha$ -spirostan-3 $\beta$ -ol (1) and 6- $\alpha$ -O- $\alpha$ -L-rhamnopyranosyl-(1  $\rightarrow$  3)- $\beta$ -D-quinovopyranosyl-(23R,25S)-5 $\alpha$ -spirostan-3 $\beta$ ,23 $\beta$ -ol (2). The structural elucidation of compounds was performed by analysis of 1D and 2D NMR spectral data and HRMS. Antibacterial activity was displayed by the hexane and CH<sub>2</sub>Cl<sub>2</sub> extracts against carbapenem-resistant *Pseudomonas aeruginosa* (MIC = 250  $\mu$ g/mL) and carbapenem-resistant *Acinetobacter baumannii* (MIC = 125  $\mu$ g/mL). The known saponin (3) was the only compound active against bacteria, showing activity against all the gram-positive bacteria (MIC = 12.5  $\mu$ g/mL). Antitubercular activity was observed only for the hexane extract (MIC = 250  $\mu$ g/mL). The antifungal and antileishmanial activities were determined for the steroidal saponins, but they were devoid of antifungal activity at the concentrations tested. Antileishmanial activity was shown only by the saponin (1) (IC<sub>50</sub>: 21.64  $\pm$  1.21  $\mu$ g/mL).

#### Graphical Abstract



**Keywords** *Solanum chrysotrichum* Schldl · Solanaceae · Steroidal saponins · Antimicrobial · Antileishmanial

**Supplementary information** The online version of this article (<https://doi.org/10.1007/s00044-020-02648-8>) contains supplementary material, which is available to authorized users.

✉ Pascal Marchand  
pascal.marchand@univ-nantes.fr

✉ María del Rayo Camacho-Corona  
maria.camacho@uanl.edu.mx

<sup>1</sup> Facultad de Ciencias Químicas, Universidad Autónoma de Nuevo León, Av. Universidad S/N, Ciudad Universitaria, CP, 66451 San Nicolás de los Garza, Nuevo León, México

<sup>2</sup> Facultad de Medicina, Universidad Autónoma de Nuevo León, Av. Madero S/N, Col. Mitas Centro, CP, 64460 Monterrey, Nuevo León, México

<sup>3</sup> Servicio de Gastroenterología Hospital Universitario Dr. José Eleuterio González, Universidad Autónoma de Nuevo León, Av. Gonzalitos y Madero S/N, Col. Mitas Centro, CP, 64460 Monterrey, Nuevo León, México

<sup>4</sup> Instituto de Química, Universidad Nacional Autónoma de México, Circuito Exterior s/n, Ciudad Universitaria, C.P., 04510 Coyocacán, Ciudad de México, México

<sup>5</sup> Cibles et Médicaments des Infections et du Cancer, Université de Nantes, IICiMed, EA 1155, F-44000 Nantes, France

Published online: 21 October 2020

Springer